2069

VTT RESEARCH NOTES

VTT TIEDOTTEITA

Carey J. Simonson

Moisture, Thermal and Ventilation Performance of Tapanila Ecological House

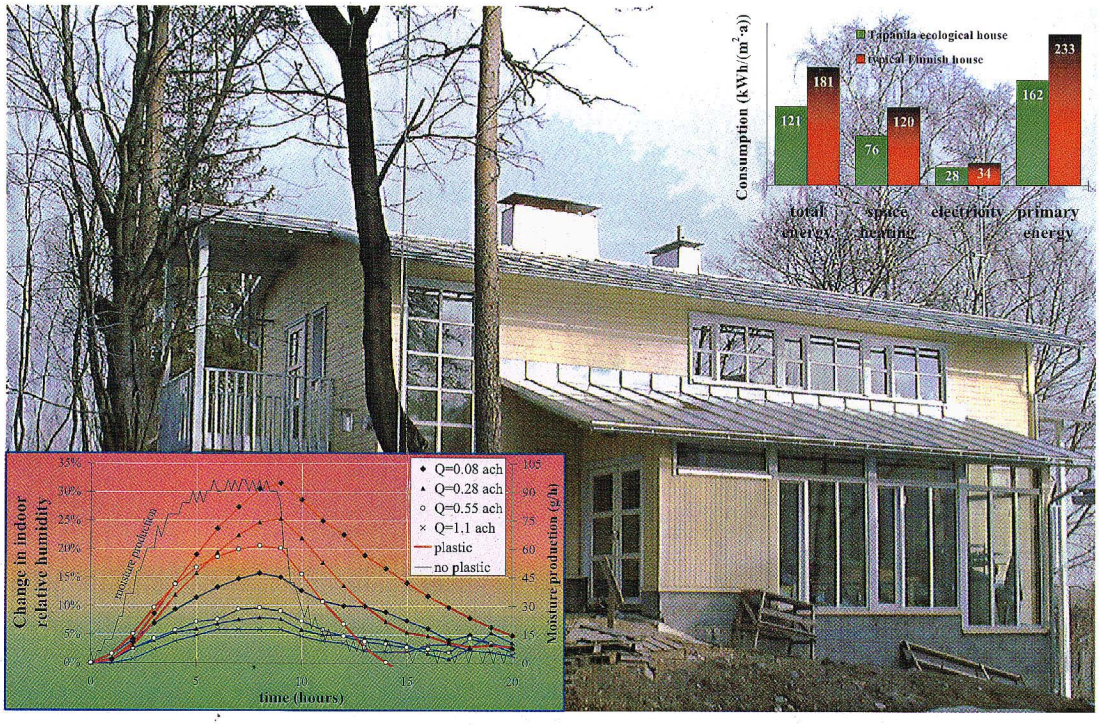

TECHNICAL RESEARCH CENTRE OF FINLAND

ESPOO 2000

VTT TIEDOTTEITA – MEDDELANDEN – RESEARCH NOTES 2069

Moisture, Thermal and Ventilation Performance of Tapanila Ecological House

Carey J. Simonson

VTT Building Technology

TECHNICAL RESEARCH CENTRE OF FINLAND
ESPOO 2000

ISBN 951–38–5796–2 (soft back ed.)
ISSN 1235–0605 (soft back ed.)

ISBN 951–38–5798–0 (URL: http://www.inf.vtt.fi/pdf/)
ISSN 1455–0865 (URL: http://www.inf.vtt.fi/pdf/)

JULKAISIJA – UTGIVARE – PUBLISHER

Valtion teknillinen tutkimuskeskus (VTT), Vuorimiehentie 5, PL 2000, 02044 VTT
puh. vaihde (09) 4561, faksi (09) 456 4374

Statens tekniska forskningscentral (VTT), Bergsmansvägen 5, PB 2000, 02044 VTT
tel. växel (09) 4561, fax (09) 456 4374

Technical Research Centre of Finland (VTT), Vuorimiehentie 5, P.O.Box 2000, FIN–02044 VTT, Finland
phone internat. + 358 9 4561, fax + 358 9 456 4374

VTT Rakennustekniikka, Rakennusfysiikka, talo- ja palotekniikka,
Lämpömiehenkuja 3, PL 1804, 02044 VTT
puh. vaihde (09) 4561, faksi (09) 455 2408

VTT Byggnadsteknik, Byggnadsfysik, fastighets- och brandteknik,
Värmemansgränden 3, PB 1804, 02044 VTT
tel. växel (09) 4561, fax (09) 455 2408

VTT Building Technologgy, Building Physics, Building Services and Fire Technology,
Lämpömiehenkuja 3, P.O.Box 1804, FIN–02044 VTT, Finland
phone internat. + 358 9 4561, fax + 358 9 455 2408

Technical editing Leena Ukskoski

Otamedia Oy, Espoo 2001

Simonson, Carey J. Moisture, Thermal and Ventilation Performance of Tapanila Ecological House [Tapiolan ekotalon ilmanvaihto sekä lämpö- ja kosteustekninen toimivuus]. Espoo 2000. Technical Research Centre of Finland, VTT Tiedotteita – Meddelanden – Research Notes 2069. 141 p. + app. 5 p.

Keywords test houses, residential buildings, ecological houses, moisture, ventilation, indoor climate, heat transfer, small houses, energy consumption, indoor air quality, thermal comfort, space heating, airtightness

Abstract

The research presented in this report demonstrates the moisture, thermal and ventilation performance of a recently built ecological house in the Tapanila district of Helsinki, Finland. The single-family house (gross floor area of 237 m^2 including the basement and porch) has a well-insulated (250 mm in the walls and 425 mm in the roof) wooden frame with no plastic vapour retarder. A natural ventilation system provides outdoor ventilation and district heating and a wood-burning fireplace provide space heating. The space heating energy consumption was measured to be 76 kWh/(m^2·a) of which 29% was provided by wood. For comparison, Finnish houses typically consume 120 kWh/(m^2·a) or nearly 60% more energy for space heating. If the building envelope of Tapanila ecological house had been insulated according to the building code, the space heating energy consumption is expected to be 40% higher. The total energy consumption (121 kWh/(m^2·a)) and electricity consumption (28 kWh/(m^2·a)) were quite low. As a result, the total primary energy consumption was only 162 kWh/(m^2·a), while the primary energy consumption in typical Finnish houses is over 40% higher. However, the outdoor ventilation rate provided by the natural ventilation system tended to be lacking (i.e., less than the required value of 0.5 ach) even though the measured CO_2 concentrations were generally below 1000 ppm when the bedroom doors were open. Extrapolating the measured ventilation data shows that the ventilation rate is expected to be about 0.45 ach (10% below the required value) in the winter and about 0.25 ach (50% of required value) in the summer when the windows are closed. When the windows are open in the summer, the outdoor ventilation rate will be higher.

The moisture performance of the building envelope was good and the risk of mould growth low. In addition, the moisture transfer between the envelope and indoor air was measured to significantly influence the indoor humidity. At a ventilation rate of 0.5 ach, the results show that a porous building envelope can decrease the maximum humidity in a bedroom during the night by up to 20% RH, which may double the number of occupants satisfied with thermal comfort and perceived air quality. Furthermore, the minimum indoor humidity in the winter can be increased by about 10% RH, which is also important in cold climates. These results show that it is possible to build a house with a porous and vapour permeable envelope that is moisture physically safe and improves the indoor climate.

Simonson, Carey J. Moisture, Thermal and Ventilation Performance of Tapanila Ecological House [Tapiolan ekotalon ilmanvaihto sekä lämpö- ja kosteustekninen toimivuus]. Espoo 2000. Valtion teknillinen tutkimuskeskus, VTT Tiedotteita – Meddelanden – Research Notes 2069. 141 s. + liitt. 5 s.

Avainsanat test houses, residential buildings, ecological houses, moisture, ventilation, indoor climate, heat transfer, small houses, energy consumption, indoor air quality, thermal comfort, space heating, airtightness

Tiivistelmä

Julkaisussa esitettävässä tutkimuksessa selvitettiin Helsingin Tapanilassa hiljattain rakennetun ekotalon kosteus- ja lämpösuorituskykyä sekä ilmanvaihtoa. Kyseisessä omakotitalossa (kerrosala 237 m^2 mukaan lukien kellarikerros ja kuisti) on hyvin eristetty (250 mm eristettä seinissä ja 425 mm yläpohjassa) puurunko ilman muovista kosteussulkua. Talossa on painovoimainen ilmanvaihtojärjestelmä, se on liitetty kaukolämpöverkkoon ja siinä on takka. Mitattu tilojen lämmitysenergiankulutus oli 76 kWh/(m^2·a), josta energiasta 29 % tuli puusta. Vertailun vuoksi mainittakoon, että suomalaisten talojen tilojen lämmitysenergiankulutus on tavallisesti 120 kWh/(m^2·a) eli lähes 60 % enemmän. Mikäli Tapanilan ekotalon rakennusvaippa olisi eristetty rakentamismääräysten mukaisesti, arvioitu tilojen lämmitysenergiankulutus olisi noin 40 % suurempi. Kokonaisenergiankulutus (121 kWh/(m^2·a)) ja sähkönkulutus (28 kWh/(m^2·a)) olivat melko alhaisia. Tämän takia primäärinen kokonaisenergian-kulutus oli vain 162 kWh/(m^2·a), kun primäärinen energiankulutus tavallisessa suomalaisessa talossa on yli 40 % suurempi. Painovoimaisen ilmanvaihtojärjestelmän ilmanvaihtuvuus oli kuitenkin jonkin verran puutteellinen (eli alhaisempi kuin ohjearvo, 0,5 1/h), vaikkakin mitatut CO_2-pitoisuudet olivat yleensä alle 1000 ppm, kun makuuhuoneen ovi oli auki. Mitattujen ilmanvaihtoarvojen ekstrapolointi osoittaa, että ilmanvaihtuvuuden voidaan olettaa olevan noin 0,45 1/h (10 % alle ohjearvon) talvella ja noin 0,25 1/h (50 % ohjearvosta) kesällä ikkunoiden ollessa suljettuna. Ikkunoiden ollessa auki kesällä ilmanvaihtuvuus on suurempi.

Rakennusvaipan kosteussuorituskyky oli hyvä ja homekasvun riski alhainen. Lisäksi mitatulla kosteuden siirtymisellä vaipan ja sisäilman välillä oli huomattava vaikutus sisäilman kosteuteen. Kun ilmanvaihtuvuus on 0,5 1/h, mitatut tulokset osoittavat, että huokoinen rakennusvaippa voi yön aikana alentaa makuuhuoneen maksimikosteutta jopa 20 % r.h., mikä voi kaksinkertaistaa niiden asukkaiden määrän, jotka ovat tyytyväisiä lämmityksen miellyttävyyteen ja havaittuun ilmanlaatuun. Lisäksi, sisäilman minimikosteutta voidaan talvella kasvattaa noin 10 % r.h., mikä on myös tärkeä näkökohta kylmässä ilmastossa. Nämä tulokset osoittavat, että on mahdollista rakentaa talo, jossa on huokoinen, vesihöyryn läpäisevä vaippa ja joka on kosteusteknisesti turvallinen ja sisäilmanlaatua parantava.

Preface

The research project “Tapanila Ecological House” has been funded by the Ministry of the Environment. The research results from this project are presented in this report and the planning and construction of the house are presented in a separate report, “Tapanila Ecological House 97 – Planning and Building” written in Finnish by Ilkka Romo (Romo, 2001). Pauli Savolainen initiated construction of Tapanila Ecological house in September 1997 and sold the house to Olli and Jaana Hallamaa in October 1998.

The chair of the research project steering group was Aila Korpivaara, chief architect, (Ministry of the Environment) and the secretary was Ilkka Romo, M.Sc., (IR-Kehitys and Confederation of Finnish Construction Industries). Other steering group members during the project were: Esko Kukkonen, Anja Leinonen and Raimo Ahokas of the Ministry of the Environment; Erkki Kokko, Carey Simonson and Markku Virtanen of VTT Building Technology; Bruno Erat of Ekosolar Oy; and Olli Hallamaa and Pauli Savolainen as building owners.

Research was performed at VTT Building Technology and the project managers were Carey Simonson and Erkki Kokko. Erkki Kokko planned the research project and helped interpret the results, while Carey Simonson managed the execution of the project. Timo Collanus, Hannu Hyttinen and Reijo Saloranta performed field measurements and Mikael Salonvaara and Tuomo Ojanen performed the numerical simulations presented in sections 3.2.2, 3.3.2 and 4.2.

Espoo, December 2000

Carey Simonson

Contents

List of Symbols

a	empirical coefficient in the acceptability equation (equation (2))
ach	air changes per hour [1/h]
b	empirical coefficient in the acceptability equation (equation (2))
C	concentration of gas (volume fraction) [ppm] or general constant
CO_2	carbon dioxide
CO_2-i	carbon dioxide sensor i (i=1, 2 or 3)
Cp	wind pressure coefficient [-] or specific heat capacity [J/(kg·K)]
C_{stack}	coefficient for stack effect [Pa·K]
C_{wind}	coefficient for wind pressure [$Pa \cdot s^2/m^2$]
D_{ab}	binary diffusion coefficient of gas a through gas b [m^2/s]
$D_{x,air}$	diffusion coefficient of a gas in air [m^2/s]
D_w	liquid moisture diffusivity [m^2/s]
g	acceleration due to gravity [m/s^2]
H	enthalpy of air [kJ/kg]
h	height between the inlet and outlet [m]
HVAC	heating ventilating and air conditioning
K	moisture permeability [s]
k	thermal conductivity [W/(m·K)] or constant
kd	permeability of a building material to water vapour [kg/(s·m·Pa)]
kd_x	permeability of a material to gas x (such as CO_2 or SF_6) [kg/(s·m·Pa)]

M	molecular weight [kg/kmole]
n	exponent for flow equation
n_{50}	leakage rate at a pressure difference of 50 Pa [ach]
P	pressure [atm or Pa]
PAQ	perceived air quality
PD	percent dissatisfied
P_v	partial pressure of water vapour [Pa]
Q	total outdoor ventilation rate (including forced ventilation and infiltration) [ach or L/s]
$Q^*_{diffusion}$	the fractional increase in effective ventilation due to diffusion through the envelope
Q^*_{SF6}	relative difference between the effective ventilation rate for CO_2 and SF_6
Q_{code}	ventilation rate specified in the national building code of Finland – D2 (1987) (i.e., 0.5 ach) [ach]
Q_{eff}	effective ventilation rate or air change rate [ach]
$Q_{eff,no\,plastic}$	effective ventilation rate without plastic [ach]
$Q_{eff,plastic}$	effective ventilation rate when the room is covered with plastic [ach]
Q_{forced}	forced ventilation rate or forced air change rate [ach]
q_M	mass flux [kg/(m^2·s)]
R	specific gas constant of air [J/(kg·K)]
$\tilde{R}$	universal gas constant [J/(kg·K)]
R^*	ratio of internal to external vapour diffusion resistance

R^2	regression coefficient
$R_{d,in}$	internal vapour diffusion resistance [$m^2 \cdot Pa \cdot s/kg$]
$R_{d,out}$	external vapour diffusion resistance [$m^2 \cdot Pa \cdot s/kg$]
RH	relative humidity
RH-i	relative humidity sensor i (i=1, 2 or 3)
S	source term [L/h]
SF_6	sulphur hexaflouride gas or sensor
T	temperature [C or K]
t	time [h]
T-i	temperature sensor i (i=1, 2 or 3)
T_{wall}	surface temperature of the wall
u	moisture content [kg/kg or kg/m^2]
u_{max}	maximum moisture content at each measurement location
v	air or wind speed [m/s]
V	volume [L]
VOC	volatile organic compound (C6 – C16)
W_s	absolute humidity at saturation [g/kg]

Greek letters

ρ	density [kg/m^3]
Δ	difference

$\Delta\phi$	change in indoor relative humidity after the humidity source is turned on
$\Delta\phi_{max}$	maximum increase in indoor humidity during the night
ΔP	pressure difference [Pa]
ΔQ_{eff}	difference between the effective ventilation rate with and without plastic [ach]
ΔT	temperature difference between indoor air and the internal surface of the wall [C]
ΔW	difference between indoor and outdoor humidity [g/kg]
ϕ	relative humidity
ϕ_o	initial indoor relative humidity when occupants enter the room
θ	relative concentration of tracer gas

subscripts

a	gas a
air	air
ave	average
b	gas b
corrected	corrected value after calibration
e	exhaust air
i	internal room air
in	indoor conditions
indoor	indoor conditions

m	referring to material m
measured	measured value
o	initial condition, condition when occupants enter the room or condition at dry state
out	outdoor conditions
outdoor	outdoor conditions
s	supply air
stack	stack effect
v	water vapour
w	liquid water
wind	wind pressure
x	referring to gas x

1. Introduction

In Finland, 40% of primary energy is used in the building sector (Statistics Finland, 1996) and, therefore, any reduction in building energy consumption can have a significant impact on the national and global energy consumption and carbon dioxide (CO_2) production. Regulating the indoor temperature and relative humidity (RH) in buildings (usually between 19°C and 26°C and 30% RH and 60% RH) is important, but energy intensive, and accounts for about 25% of primary energy use and over 50% of the energy used in buildings. Well designed heating, ventilating and air-conditioning (HVAC) systems add or remove heat and moisture from occupied spaces of buildings and provide an acceptable indoor climate in many climates. However, in many hot and humid climates, conventional air conditioning units are unable to meet the latent load and the relative humidity exceeds the often recommended value of 60% to 70% RH (ASTM, 1994, ANSI/ASHRAE Standard 55-1992 and ANSI/ASHRAE Standard 62-1989). This has led to the growing application of heat and moisture transfer devices which can reduce the latent load on air conditioning units (Besant and Simonson, 2000, Harriman et al., 1999, Rengarajan et al., 1996 and Nimmo et al., 1993). With these devices, it is possible to provide an acceptable indoor climate in even hot and humid climates. Nevertheless, there is a desire to develop more passive and less energy intensive methods of moderating the indoor environment. The passive method investigated in this report uses the moisture (and thermal) storage capacity of the building envelope (and components) to damp the increase in indoor humidity (and temperature) caused by indoor sources. The main focus will be on moisture storage because thermal storage has been the focus of many previous investigations (e.g., Lamberg et al., 2000, Kosny et al., 1998, Braun, 1990, Ruud et al., 1990 and Gray et al., 1988).

Passive methods of moderating the indoor environment are gaining popularity because they are energy conscience and environmentally friendly. In hot and humid climates, passive methods could help to reduce the peak cooling demand thereby reducing the required capacity of cooling units and electrical demand charges. In more moderate climates, where air conditioning is seldom or never used, these passive methods may make it possible to provide an acceptable indoor climate during hot periods without the need of air conditioning. In cold climates, such as Finland, passive methods could help control the occupant induced diurnal variations in indoor humidities, which are often moderated by providing outdoor ventilation air. This is important because recent research by Fang et al. (1998a and b) has shown that outdoor ventilation rates could be decreased if a moderate enthalpy is maintained in spaces (provided the minimum ventilation for health is satisfied) (Toftum and Fanger, 1999). Therefore, passive methods of moderating the indoor environment can provide benefits in many climates.

Past research has shown that thermal storage is more important in warm climates than in cold climates and that moisture storage is needed in conjunction with thermal storage to moderate the indoor humidity in hot and humid climates (Kamel et al., 1991). In addition, the ability of buildings to damp changes in temperature is much greater than their ability to damp changes in humidity (Padfield, 1998) even though humidity control can be extremely important as will be discussed in section 1.1. There is a need for significant research, development and application in this area (Virtanen et al., 2000).

As discussed by Virtanen et al. (2000), current methods of predicting the indoor humidity are lacking because they neglect moisture adsorption and desorption by building materials and furnishings, even though several researchers have shown sorption effects to be significant (Plathner and Woloszyn, 2000, Woloszyn et al., 2000, Simonson and Salonvaara, 2000, Salonvaara and Simonson 2000, Salonvaara et al., 2000, Plathner et al., 1998, Padfield, 1998, Tsuchiya and Sakano, 1993 and Teischinger, 1990). In these research works, both simple and detailed models as well as laboratory and field experiments have been applied. There are numerous simplified models which assume a uniform moisture content in a thin material layer (Duforestel and Dalicieux, 1994, El Diasty et al., 1993, Jones, 1993, Tsuchiya and Sakano, 1993, Ten Wolde, 1992, Cunningham, 1992 and Kerestecioglu et al., 1990). However, there are only a few detailed models that include the distribution of moisture within materials and the interaction between indoor air (Salonvaara, 1998 and Harderup, 1998) or the interaction between indoor air and HVAC systems (Plathner and Woloszyn, 2000 and Woloszyn et al., 2000). The research in this report will focus on interactions between indoor air and building materials using the model of Salonvaara (1998).

Many measurements have been carried out on the properties of building materials, such as vapour permeability and sorption isotherm (IEA, 1991), but there is a general lack of data that quantifies the rate of moisture transfer, especially for surface coatings and furnishings. Typically, environmental chamber tests have been used to measure the rate of moisture storage of various components when exposed to step changes in humidity (Salonvaara and Kokko, 1999, Plathner et al., 1999, Padfield, 1998 and Rudd, 1994). Some field measurements, other than the one presented in this report, have been reported by Teischinger (1990), Tsuchiya and Sakano (1993) and Plathner et al. (1998). These tests have shown the potential of building envelopes and components to store moisture, but more measurements are needed to confirm the effect of materials on indoor climate and to verify numerical models. Therefore, one of the key purposes of this research is to measure the moisture transfer between indoor air and the building envelope in an existing building.

In addition to a comfortable indoor environment, it is important for buildings to have low levels of contaminants (volatile organic compounds (VOC's), radon, dust, bacteria,

mould, odours, etc.), which are important for indoor air quality (IAQ) and occupant health (Sundell, 1996). Since occupants and buildings produce carbon dioxide (CO_2), VOC's and other gases, which affect the quality of indoor air, outdoor ventilation is necessary (ANSI/ASHRAE Standard 62-1989 and National Building Code of Finland – D2, 1987). Typically outdoor ventilation rates are set with the assumption that the building envelope and furniture are sources of contaminants. However, for carefully selected components, it is possible that the building envelope and furniture can act as contaminant sinks and actually improve the indoor air quality. If a building envelope is made from porous materials, the diffusion of pollutant gases through the envelope can reduce the indoor concentration of pollutants. Therefore, it may be possible to provide a comparable indoor environment with a lower outdoor ventilation rate when a permeable and porous building envelope is applied. Also, since the perception of IAQ is closely linked to the humidity of indoor air, moisture transfer between the indoor air and building structures, could reduce the needed ventilation rate. Reducing the ventilation rate could have a significant impact on energy consumption because the energy required to condition ventilation air typically constitutes 20 to 40% of the thermal load (ASHRAE, 1997).

In most cases, adequate ventilation can provide good IAQ, but the indoor temperature and relative humidity have an important effect on comfort and IAQ as well (section 1.1). Indoor temperatures are often specified assuming that the building is equipped with mechanical heating, ventilating and air conditioning systems, but recent research has shown that occupants in naturally ventilated buildings adapt to their environment and can accept (and, in fact, prefer) a larger range of indoor temperature (Brager and de Dear, 2000). During cold weather, occupants of naturally ventilated buildings accept cooler indoor temperatures and during hot weather, they accept warmer indoor temperatures. This finding is based on the analysis of 21 000 sets of data from 160 different office buildings on four continents. Therefore, there is strong evidence that naturally ventilated buildings can provide acceptable IAQ and comfort, while greatly reducing energy consumption. The energy required to provide outdoor ventilation air can be further reduced by applying energy recovery devices and natural ventilation systems (Enai et al., 2000).

Currently, there is a rising demand for sustainable low-energy housing that has a limited impact on the environment and provides occupants with excellent indoor air quality and climate. The subject of this report, Tapanila ecological house, is a house that fulfils these criteria, but there are several others in Finland as well (Laine and Saari, 1998 and Leppänen, 1998). The unique aspect of Tapanila ecological house is that it employs several passive systems for controlling the indoor climate and IAQ.

Tapanila ecological house is a 2-storey wooden frame house located in Helsinki, Finland and insulated with 250 mm (walls) and 425 mm (roof) of wood fibre insulation. The house has no plastic vapour retarder to permit diffusion mass transfer between indoor air and the porous building envelope. District heat and a wood-burning fireplace provide heating, while a natural ventilation system provides outdoor ventilation. The thick insulation is intended to keep energy consumption low, whereas the porous envelope and natural ventilation systems are examples of passive methods of controlling the indoor climate and IAQ. Therefore, Tapanila ecological house is a low-energy house that employs several passive systems to moderate the indoor environment. The research in this report will focus on quantifying the performance of these passive systems as well as the moisture, thermal and ventilation performance of the building as a whole.

1.1 Importance of Humidity on Occupants and Buildings

Even though conditioning indoor air is energy intensive, as discussed above, it is very important because research has shown that the both the indoor climate and IAQ can influence comfort, health and productivity (Wargocki et al., 1999, Seppänen et al., 1999 and Wyon, 1996). Therefore buildings with a good indoor environment are necessary for a healthy, productive and prosperous society because people spend 90% of their time indoors. An important, but often neglected, indoor environmental parameter is humidity and currently building designers and occupants consider indoor humidity to be of small importance for a successful design because temperature is easier to sense, quantify and comprehend. Nevertheless, research has shown that the indoor relative humidity is extremely important and significantly affects: thermal comfort (Toftum et al., 1998a and b, Berglund, 1998, ANSI/ASHRAE Standard 55-1992 and Fanger, 1982), the perception of IAQ (Fang et al., 1998a and b), occupant health (Clausen et al., 1999, Cooper-Arnold et al., 1997, Dales et al., 1991, and Green, 1985), the durability of building materials (Viitanen, 1996, Ojanen and Kumaran, 1996 and ASTM, 1994) and energy consumption (Besant and Simonson, 2000, and Harriman et al., 1999 and 1997). One of the main focuses of the research in this report is moisture transfer between indoor air and structures.

1.1.1 Thermal Comfort

Research has shown that the indoor humidity has a large effect on indoor climate and indoor air quality and several thermal comfort standard exist (e.g., ISO 7730-1994 and ANSI/ASHRAE 55-1992 with Addendum 55a-1995), which include relative humidity as a parameter affecting thermal comfort. Tuomaala and Piira (2000) have developed a new application that that can calculate the predicted mean vote and the percent

dissatisfied (PD) with given indoor conditions based on ISO 7730-1994. Using the application of Tuomaala and Piira (2000), the solid lines in Figure 1 represent the percent dissatisfied with the indoor thermal conditions at various temperatures and relative humidities assuming: a metabolic rate of 1.2 met (filing, seated in office), a clothing factor of 1 clo (long sleeve shirt, fitted trousers, suit jacket), an air speed is 0.1 m/s and a mean radiant temperature equal to the air temperature. The dissatisfaction here is assumed to be caused by general thermal discomfort, which is warm or cool discomfort for the body as a whole. Local thermal discomfort, on the other hand, arises when one part of the body is warmer or colder than another. Local thermal discomfort is generally due to temperature gradients or drafts in a space, but can also be due to high skin humidity or insufficient cooling of the mucous membranes in the upper respiratory tract Toftum et al. (1998a and b).

Recent experimental work by Toftum et al. (1998a and b) has focused specifically on humidity. They show that at thermal neutrality, high humidity can result in an unacceptably high level of skin humidity or insufficient cooling of the mucous membranes in the upper respiratory tract. The measurements quantify the upper limits of indoor air humidity to avoid uncomfortably humid skin and warm respiratory discomfort and demonstrate that the limits for respiratory discomfort are usually more restrictive than the limits for humid skin. Toftum et al. (1998b) studied the response of 38 subjects exposed to 14 combinations of temperature (20°C to 29°C) and humidity (6 to 19 g/kg) ranging from 20°C and 45% RH to 29C and 70% RH. Unpolluted air from a climate chamber was led to a sampling box where the subjects evaluated the air three or four inhalations after positioning their head inside the box. Based on the response of the subjects, Toftum et al. (1998b) developed the following correlation, which quantifies PD with warm respiratory comfort:

$$PD = \frac{100}{1+\exp\left[-3.58+0.18\left(30-T\right)+0.14\left(42.5-0.01P_v\right)\right]} \quad (1)$$

where T is the air temperature (C) and P_v is the water vapour pressure (Pa). The broken lines in Figure 1 represent the percent dissatisfied with respiratory cooling at various temperatures and relative humidities, while the solid lines represent the percent dissatisfied with general thermal comfort.

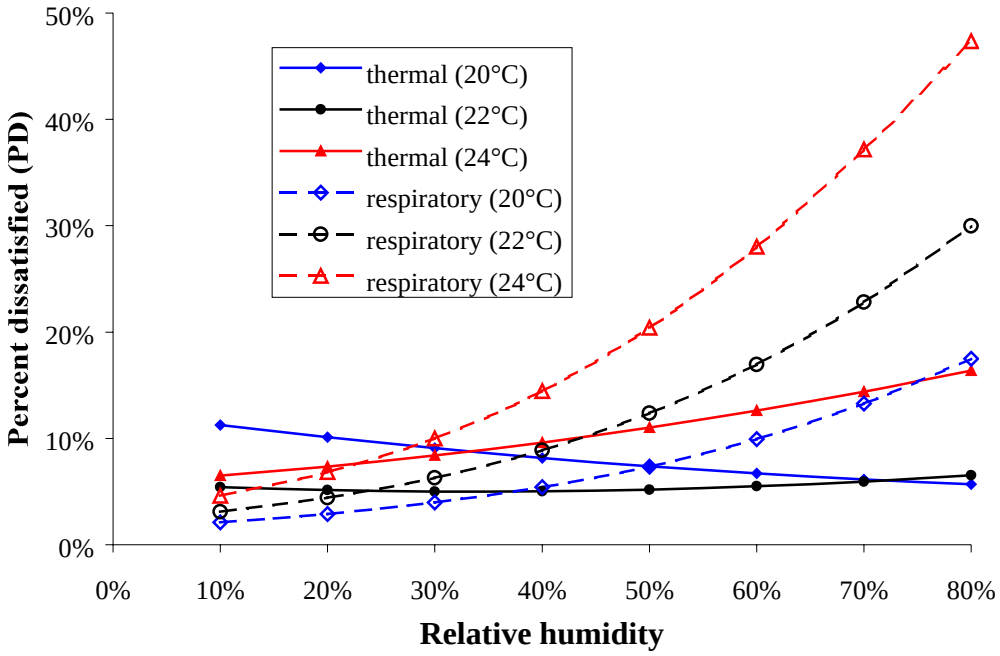

Figure 1. Percent dissatisfied with general thermal comfort and warm respiratory comfort at various temperatures and relative humidities.

Figure 1 shows a significant influence of humidity on the percentage of dissatisfied occupants, especially at warmer indoor temperatures. For example, increasing the humidity from 40% RH to 60% RH at a temperature of 24°C, doubles the percent dissatisfied with warm respiratory comfort (PD=14% at 24°C & 40% RH and PD=28% at 24°C & 60% RH) and increases the percent dissatisfied with general thermal comfort by a third (PD=10% at 24°C & 40% RH and PD=13% at 24°C & 60% RH).

The results in Figure 1 show that as the relative humidity increases the percent dissatisfied with respiratory cooling always increases, but the percent dissatisfied with general thermal comfort increases or decreases depending on the air temperature. When the air temperature is cool (20°C), PD for general thermal comfort decreases with increasing humidity, but when the air temperature is warm (24°C), PD for general thermal comfort increases with increasing humidity. When the temperature is 22°C, PD for general thermal comfort is nearly independent of the relative humidity. Figure 1 also shows that at low humidities the thermal comfort model predicts a higher PD than the respiratory cooling model, but the trend reverses at higher humidities. The humidities at which the models predict the same PD are approximately: 50% RH at 20°C, 25% RH at 22°C and 25% RH at 24°C. Since those who feel general thermal discomfort may also feel local thermal discomfort, the percentage dissatisfied are not additive (ANSI/ASHRAE Standard 55-1992). Even though PD with general and local comfort are not directly comparable, Figure 2 presents the maximum PD for each temperature and humidity.

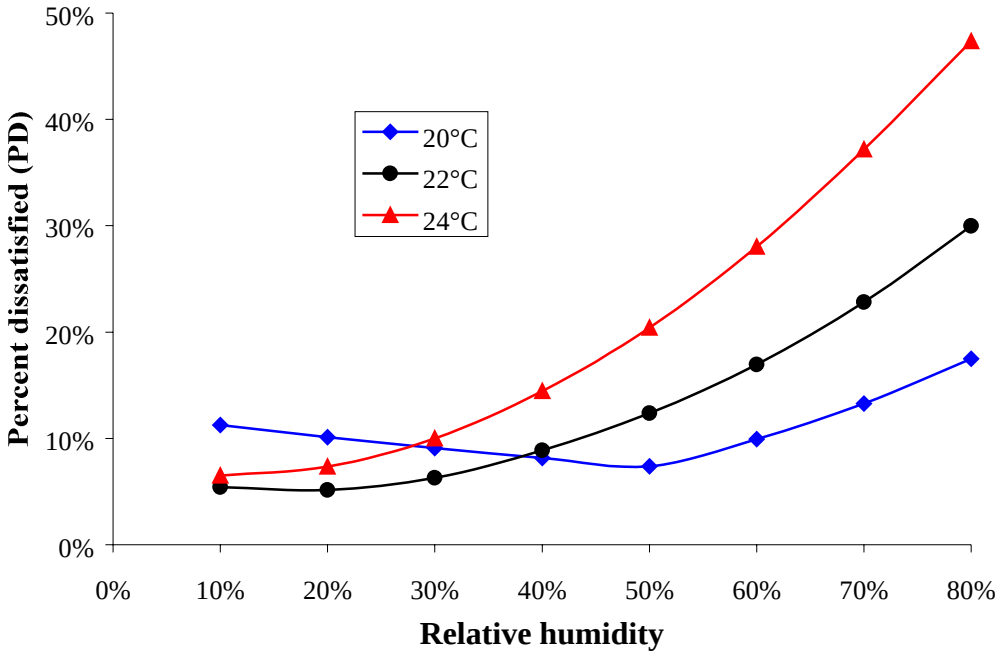

Figure 2. Maximum percent dissatisfied with general thermal and warm respiratory comfort at various temperatures and relative humidities.

1.1.2 Perceived Indoor Air Quality

Toftum et al. (1998b) and Fang et al. (1998a) demonstrate that the humidity of indoor air affects perceived indoor air quality. Fang et al. (1998a) conducted laboratory tests where 40 subjects were facially exposed to air supplied through a diffuser and asked the following question: "Imagine that during your daily work you would be exposed to the air from the diffusers. How acceptable is the air quality?" The subjects assessed the acceptability of polluted and unpolluted air at different temperatures and humidities and the results showed that the acceptability and perceived quality of indoor air are linearly related to the enthalpy. Fang et al. (1998a) provide an equation to calculate the acceptability of air as follows:

$$\text{Acceptability} = aH + b \ , \tag{2}$$

where H is the enthalpy of the air (kJ/kg) and a and b are coefficients, which are determined experimentally. Since acceptability is linear related to enthalpy, air is more acceptable (has a higher perceived quality) at low enthalpies. As the enthalpy increases, the acceptability decreases. Fang et al. (1998a) note that at a certain level of enthalpy (~70 kJ/kg or 28°C and 70% RH), the air is perceived as unacceptable regardless of the pollution level. This shows that occupants will perceive the IAQ to be better at lower humidities (in fact enthalpies), which means that ventilation rates could be decreased

notably by maintaining a moderate enthalpy in spaces. Figure 3 presents the acceptability of clean air (a=–0.033 and b=1.662) and air polluted with carpet (a=–0.023 and b=0.966) and sealant (a=–0.013 and b=0.263) under loading 2 conditions described by Fang et al. (1998a). Figure 3 shows that as the temperature and humidity increase (enthalpy increases), the acceptability decreases for all pollution sources and the importance of the pollution source decreases. Above 24°C and 55% RH, the air is unacceptable regardless of the pollution source.

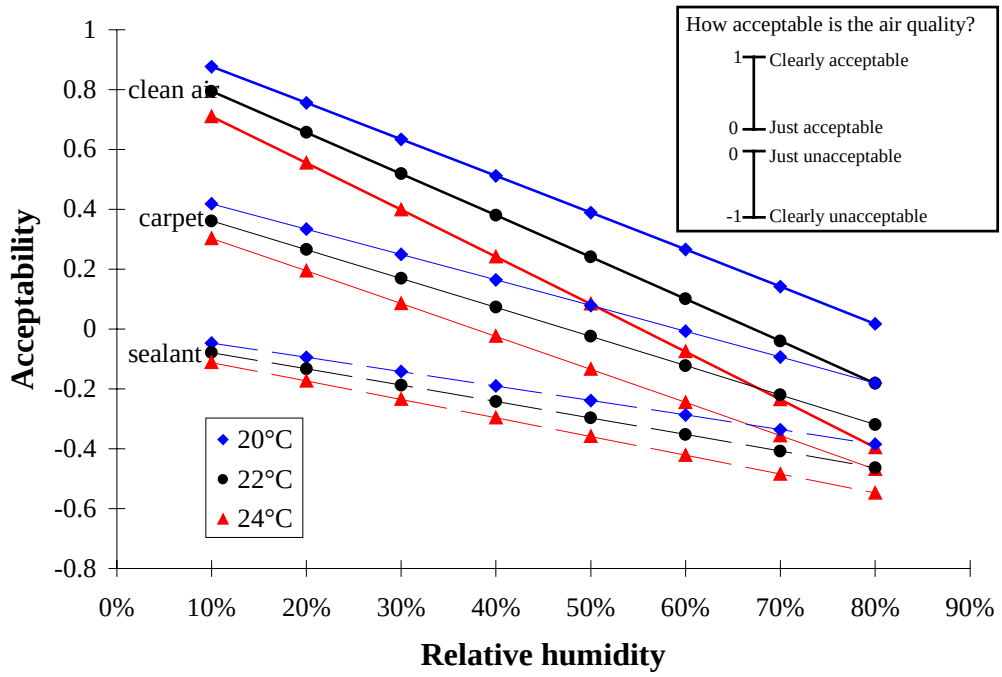

Figure 3. The acceptability of indoor air as a function of relative humidity for different temperatures and pollution sources.

The relative importance of temperature and humidity on perceived air quality (PAQ) can be directly compared using Figure 3. For example, clean air at 20°C and 60% RH has nearly the same acceptability as clean air at 24°C and 40% RH (in fact the former is slightly higher). This means that if the air temperature in a room increases from 20°C to 24°C (ΔT=4°C), the acceptability of the air will remain nearly constant provided the relative humidity decreases from 60% RH to 40% RH (ΔRH=20%). Therefore, a temperature change of 1°C is approximately equivalent to a humidity change of 5% RH. This means that if the temperature increases by 1°C, the humidity must be decreased by 5% RH to keep the same acceptability. On the other hand, if the temperature decreases by 1°C, the humidity of the air is allowed to increase by 5% RH and the acceptability will still be similar.

The effect of humidity on PAQ is typically greater than the effect of humidity on thermal sensation. For example, Toftum et al. (1998b) state that changing the air

temperature by 1°C has the same effect on acceptability, freshness and thermal comfort as changing the vapour pressure by 121, 130 and 231 Pa respectively. This means that at 22°C, changing the relative humidity by 10% RH has a similar effect on PAQ and thermal sensation as changing the temperature by 2.2°C and 1.1°C respectively. Therefore, according to these results, humidity is about twice as important for PAQ than for thermal comfort.

If we consider a cooling system that removes heat from a space, but does not remove moisture unless condensation occurs, such as radiant cooling without dehumidification in the ventilation system (Olesen, 2000, Simmonds, et al., 2000 and Olesen, 1997), the importance of humidity is very clear. Figure 4 shows the sensible cooling of air in a room (i.e., no change in absolute humidity) from 29°C and 50% RH to 23°C (process $\overline{AB}$) and from 25°C and 60% RH to 20°C (process $\overline{ab}$). These processes are expected to significantly increase thermal comfort and productivity (Seppänen and Vuolle, 2000 and Wyon, 2000). Nevertheless, Figure 4 shows that the same change in enthalpy of air can be achieved by simply reducing the humidity by 10% RH and keeping the temperature constant (processes $\overline{AC}$ and $\overline{ac}$). Since PAQ is a function of enthalpy, the acceptability of the air after either process (cooling or dehumidifying) is expected to be the same. Here a change in humidity of 10% RH at constant temperature is equivalent to a change in temperature of 5 or 6°C at constant absolute humidity.

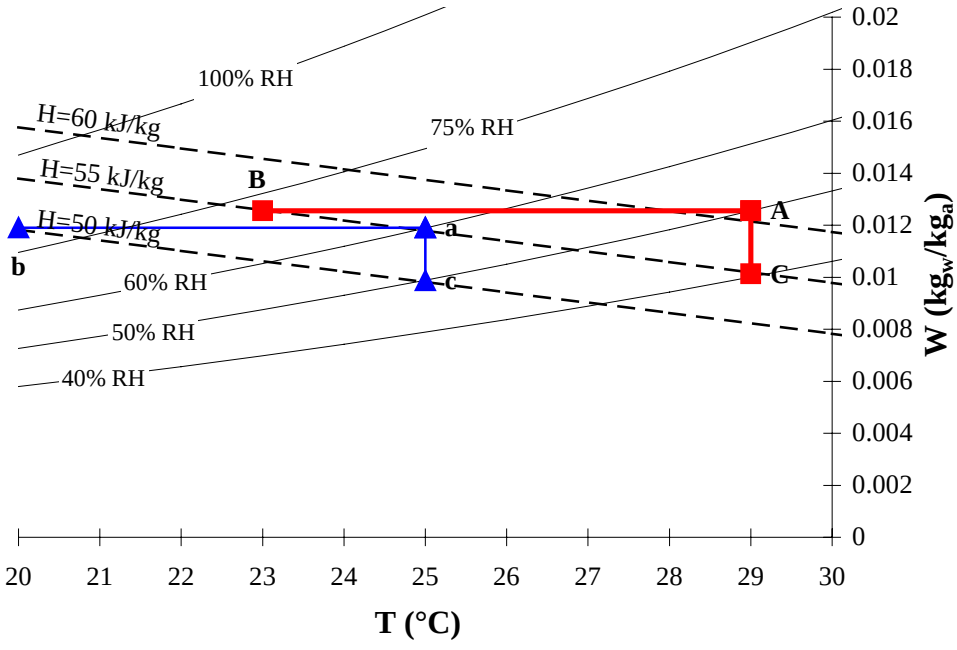

Figure 4. Sensible cooling and dehumidification process lines on the psychrometric chart showing the importance of humidity on enthalpy.

1.1.3 Other Factors

In addition to affecting comfort and IAQ, indoor humidity affects many other parameters as shown in Figure 5.

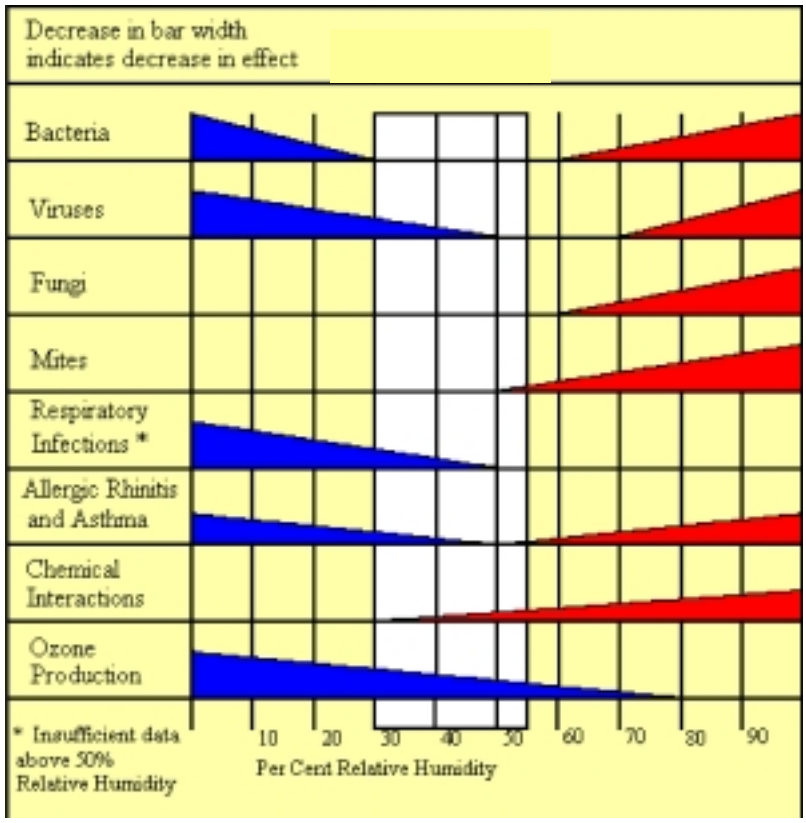

Figure 5. The effect of humidity on several health and IAQ parameters showing that a favourable range of indoor humidity is between 30% RH and 55% RH (ITS, 1999).

Figure 5 shows that a low humidity is needed to reduce the effect of some parameters, while a high humidity is needed to reduce the effects of others. The indoor humidity should be kept below 60% RH to 70% RH to curb the growth of fungi and mites (ASTM, 1994 and Viitanen, 1996) and above 30% RH to reduce respiratory infections (ASHRAE, 1997). For example, research by Green (1985) has shown that increasing the relative humidity from 20% RH to 40% RH in schools, located in cold dry regions, can reduce absenteeism and upper respiratory infections by 50%.

Moisture transfer is important in energy analysis and is termed latent energy. It is most significant in warm moist regions, where the latent load often makes up over 50% of the annual cooling load. Mechanical cooling is the most common method of controlling humidity in buildings, but is very energy intensive. The energy required to remove moisture is a scientific fact that is often under appreciated and not well known. For example, the ideal cooling of air from 30°C and 60% RH to 25°C and 50% RH requires

over 4 times as much energy as cooling air from 30°C to 25°C with no change in moisture level. Moisture also affects energy consumption because it can decrease the thermal resistance of building envelopes by 5 to 10%, which is important during heating, but less important during cooling.

1.2 Objectives

Previous research has shown that indoor humidity has a significant effect on thermal comfort, perceived air quality and other factors and that building materials have the potential to moderate indoor humidity. As a result, one of the main purposes of this report is to present measurements of moisture transfer between indoor air and a porous building envelope in an existing building (Tapanila ecological house) during controlled experiments and during normal occupation. To enhance this moisture transfer, Tapanila ecological house has no plastic vapour retarder and therefore another objective is to measure the moisture performance of a building with no plastic vapour retarder in a cold climate. Other aims are to measure the performance of the natural ventilation system and the energy consumption of Tapanila ecological house. Each chapter in this report presents results and analysis to fulfil the following objectives:

- Chapter 2: to measure the airtightness of Tapanila ecological house;
- Chapter 3: to investigate heat and mass transfer between structures and indoor air;
- Chapter 4: to determine the moisture performance of a building envelope that has no plastic vapour retarder;
- Chapter 5: to evaluate the performance of the natural ventilation system; and
- Chapter 6: to measure and simulate the energy consumption of Tapanila ecological house.

2. Building Description and Airtightness

This chapter briefly describes the materials and construction of Tapanila ecological house, which was designed by Bruno Erat, architect of Ekosolar Oy. More detailed construction information can be found in Romo (2001). Tapanila ecological house is built on a 665 m^2 lot (39.8 m x 16.7 m) in the Tapanila district of Helsinki, Finland. The two-storey house has a full basement and an unheated porch and has a gross floor area (kerrosala) of 237 m^2 and a total volume (rakennustilavuus) of 720 m^3. The floor area (huoneistoala) and volume of the living space is 178 m^2 and 470 m^3, including the basement. All ventilation and infiltration results in this report will be based on the internal volume of 470 m^3, while the energy consumption will be normalised with the gross heated floor area and volume. Figures 6 to 9 contain pictures of the exterior and interior of the completed house. As can be seen in these figures, the triple pane windows are concentrated on the south façade to take advantage of solar heat gains in the winter and to provide natural lighting to the house.

Figure 6. South and west façades of Tapanila ecological house.

Figure 7. North façade of Tapanila ecological house.

Figure 8. Dining room in Tapanila ecological house (Riikka Kostiainen).

Figure 9. Second floor open area in Tapanila ecological house (Riikka Kostiainen).

To optimise the use of natural lighting the house, has been designed with an open layout as shown in Figure 10, Figure 11 and Figure 12. The natural lighting from the south-facing windows can reach nearly every room in the house except those in the basement. The occupants have found this natural lighting to be a very pleasing aspect of the house. The main rooms in the house are: a living room, dining area, kitchen, 4 bedrooms, 2 bathrooms, a sauna and an large enclosed porch on the south side. The house also has a second-floor balcony on the east and west sides of the house. Figure 12 shows the location of the test room, which is the focus of many of the tests in this report.

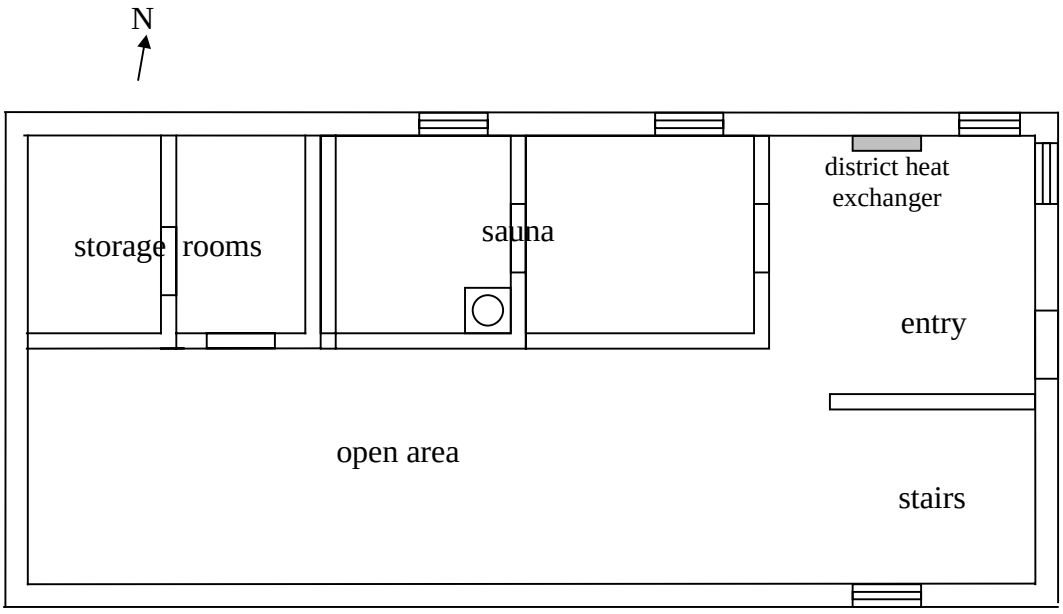

Figure 10. The basement floor plan.

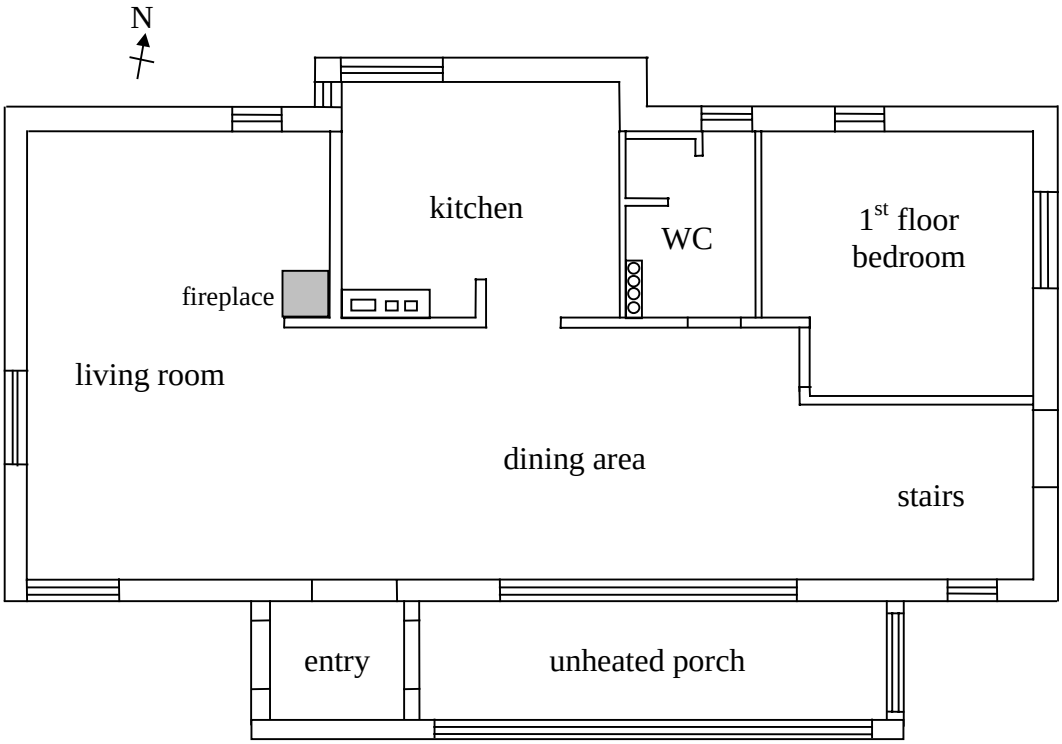

Figure 11. The first storey floor plan.

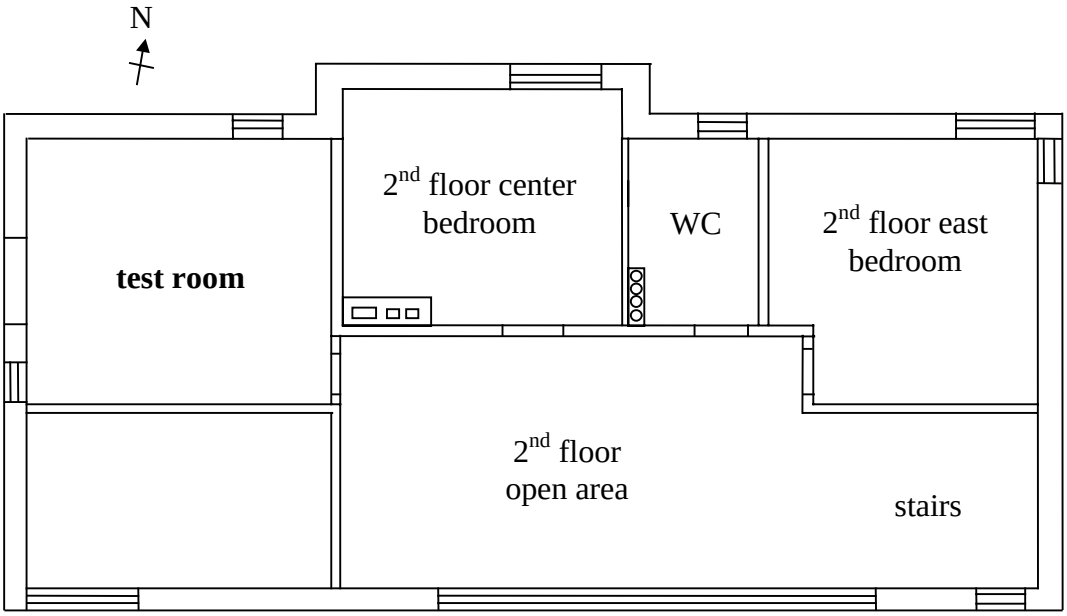

Figure 12. The second storey floor plan.

2.1 Building Materials

For the most part, natural and ecological materials have been used throughout Tapanila ecological house. Wood and wood based materials and ecological finishings have been

used extensively and plastic materials have been limited. To permit the diffusion of water vapour and other gases through the envelope, diffusion permeable coatings are applied and no plastic vapour retarder is used. The insulation material is wood fibre insulation and the thickness is 250 mm in walls and 425 mm in the roof (Figure 13), giving a wall U-value of 0.16 W/(m²·K) and a roof U-value of 0.10 W/(m²·K).

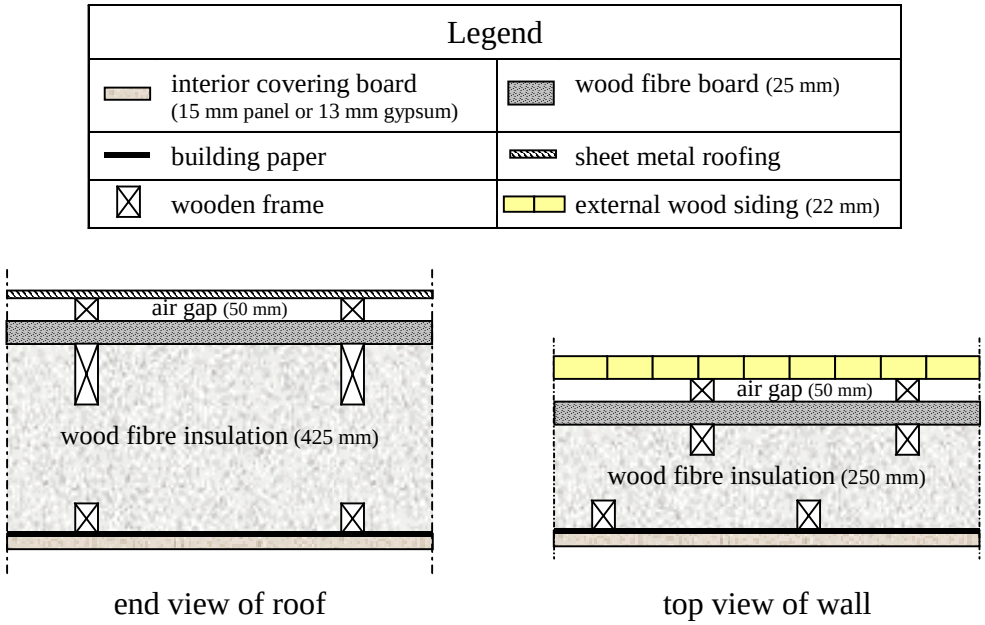

Figure 13. Roof and wall construction.

2.2 Building and Test Room Airtightness

A building with poor airtightness may have uncontrolled airflow through the building envelope, which can lead to problems related to: moisture, thermal comfort, energy consumption, ventilation performance and noise. Therefore, it is important to construct buildings with minimal airflow through the building envelope. The intention of Tapanila ecological house was to build a house that allows mass transfer by molecular diffusion, but not by convection (airflow). To minimise convection mass transfer (airflow) through the envelope, the house is well sealed with building paper and the tightness of the building envelope was measured. In addition, the airtightness of the test room was measured to confirm that the air leakage through the envelope is small during the mass transfer tests described in Chapter 3. Another purpose of the airtightness measurement is to ensure that the make-up ventilation air comes from outside when air is exhausted from the test room during the mass transfer tests. The tightness of the envelope is important because the purpose of the mass transfer tests is to investigate diffusion mass transfer rather than convection mass transfer.

The airtightness of the whole house and the test room were measured with a lower pressure indoors than outdoors, resulting in infiltration airflow (Charlesworth, 1988). A variable-speed fan was ducted through a 5 mm thick, high-density wood fibre board that was sealed in a basement window during the tightness measurement of the whole house and in the door connecting the test room and the house during the tightness measurement of the test room. A calibrated orifice plate was used to measure the flow rate of air exhausted from the house and test room. In all tests, the natural ventilation supply vents were removed and sealed with tape. During the test of the whole house, the chimney and exhaust vents were sealed with polyethylene plastic and tape on the roof and the door leading to the storage rooms in the basement was sealed. All windows and external doors were closed during the pressure tests, but typically were not sealed with tape to represent the conditions during the mass transfer test and actual use. Measurements were also performed in the test room with the balcony door and windows sealed to determine their leakage characteristics.

During the tightness measurement of the whole house, the pressure difference across the building envelope was measured on both the first and second floors. The measured pressure differences on the first floor were only slightly higher (usually less than 3 Pa) than the pressure difference on second floor, indicating good mixing. During the measurement in the test room, the main door of the house was kept open to minimise pressurisation of the house. The pressure difference between the house and outdoors was typically less than 1 Pa. The results of the airtightness test are summarised in Figure 14.

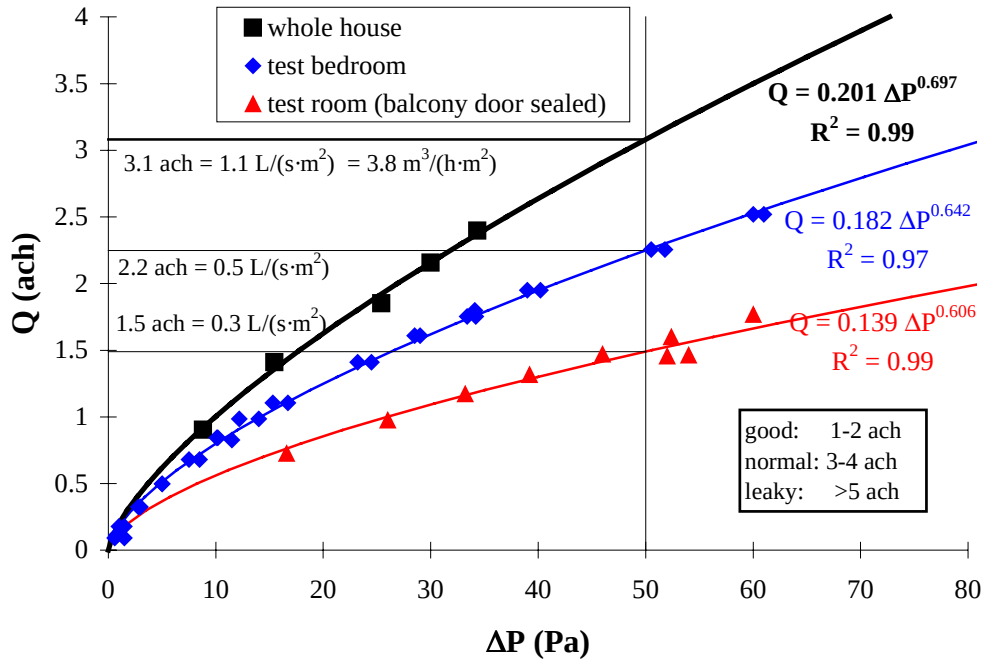

Figure 14. Airtightness of Tapanila ecological house and one test bedroom.

During the pressure test it was noticed that the main leakage paths were the front door of the house and the balcony door in the test room. There was another balcony door in the house, but it appeared to leak less than the balcony door in the test room. The sun porch was considered to be external to the house for the pressure test because it was not totally complete at the time of the test. The pressure in the sun porch was closer to the outdoor pressure than the indoor pressure. When the indoor pressure was 15 Pa lower than the outdoor pressure, the sun porch was 5 Pa higher than the outdoors. The pressure in the sun porch was higher than outside because it was located on the leeward side of the house.

The results in Figure 14 show that Tapanila ecological house is moderately airtight and that the test room has less air leakage than the whole house, especially when the balcony door is sealed with tape. At an underpressure of 50 Pa, the air infiltration through the building envelope is estimated to be 3.1 ach, while the air infiltration into the test room is 2.2 ach and 1.5 ach when the balcony door and windows are unsealed and sealed respectively. This tightness is in the lower range of normal houses in Finland according to the classification of Laine and Saari (1998), which is: good (1–2 ach), normal (3–4 ach) and leaky (>5 ach). This shows that the airtightness of Tapanila ecological house is quite good, especially considering its somewhat complicated structure. Comparing the leakage rate per unit surface area shows that the test room has less than half the airflow per unit surface area (0.5 L/(s·m^2)) than the building as a whole (1.1 L/(s·m^2)). The National Building Code of Canada (NRC, 1995) recommends an airtightness of 0.15 L/(s·m^2) at 75 Pa for buildings when the indoor humidity is less than 27% RH. At 75 Pa, the airtightness of Tapanila ecological house is predicted to be 1.4 L/(s·m^2), which is significantly greater than the recommended value in Canada. Nevertheless, the airtightness is in the range of 1 to 3 x 10^{-5} m^3/(s·m^2·Pa) (0.5 to 1.5 L/(s·m^2) at 50 Pa) as recommended by Uvslokk (1996) and Ojanen (1993).

The airtightness results for the test room show that nearly half of the infiltration air comes through the seals in the balcony door, which was also confirmed with smoke tests. (Sealing the windows with tape had little effect on the leakage.) The exact location of other leakage points was difficult to quantify with smoke because of the low velocities and flow rates. Because the balcony door, windows and ventilation channels are not taped during the mass transfer tests in Chapter 3, these results indicate that during the mass transfer tests most of the ventilation air will be from outdoors, which is desired.

3. Heat and Mass Transfer Between Structures and Indoor Air

In this chapter, the measured and simulated effect of heat and mass transfer between structures and indoor air on the indoor air quality and climate will be presented. The main focus will be on moisture transfer, but the transfer of heat and other gases will be presented as well. The experimental and numerical tests described in sections 3.1, 3.2 and 3.3 will concentrate on the performance of one test room, while the performance of other parts of the house will be presented in sections 3.4 and 3.5.

3.1 Experimental and Numerical Methods

3.1.1 Test Room and Instrumentation

The mass transfer between the building structure and indoor air was studied to investigate the role the building envelope has on the concentration of water vapour, CO_2 and a larger molecule (SF_6) in the indoor air. To permit the diffusion of water vapour and other gases through the envelope, diffusion permeable coatings are applied and no plastic vapour retarder is used in Tapanila ecological house. The mass transfer between the building structure and the indoor air was studied in a second floor bedroom, which is marked as “test room” in the second storey floor plan in Chapter 2 (Figure 12). The test room is nearly square and has two windows and two doors and a volume of 29 m^3 as shown in Figure 15. The north and west walls are exterior walls (250 mm wood fibre insulation) and the south (100 mm wood fibre insulation) and east walls are interior walls. The east wall and the small support wall are made of 140 mm thick brick and coated with plaster and primer. All other walls and the ceiling (425 mm wood fibre insulation) are of wooden frame construction and, at the time of the test, were finished with 13 mm of gypsum board that was plastered and coated with a single coat of paint. The water vapour permeability of the gypsum board coated with plaster and primer is presented in Table 1, which shows that the single coat of paint has no practical impact on water vapour diffusion. The floor has 125 mm of wood fibre insulation and the wooden floorboard is 32 mm thick. The door leading to the interior of the house was not in place at the time of the test, but was covered with a 5 mm thick high-density wood fibre board. During the tests, which were undertaken from May 14, 1999 to May 31, 1999, water vapour, CO_2 and SF_6 were generated in the room and their concentrations monitored for various ventilation rates. Five fans were used to continuously mix the air in the room as shown in Figure 15.

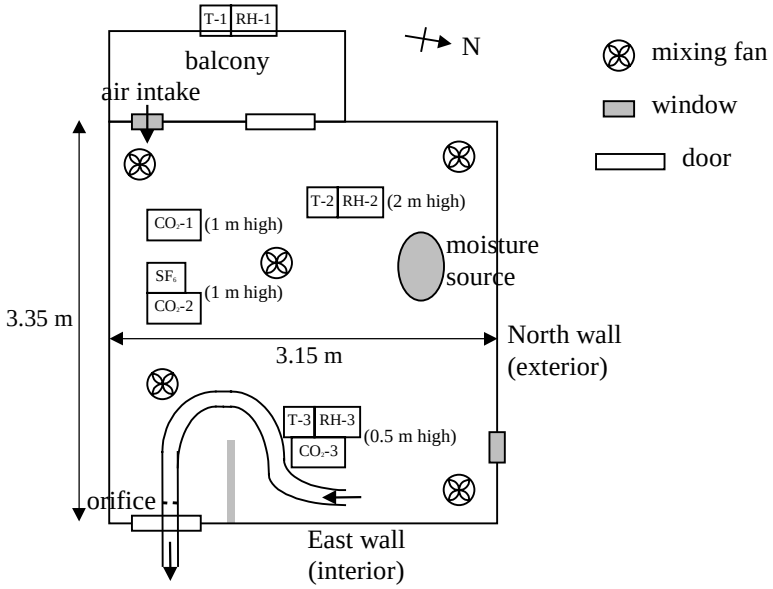

(a) plan view of test room

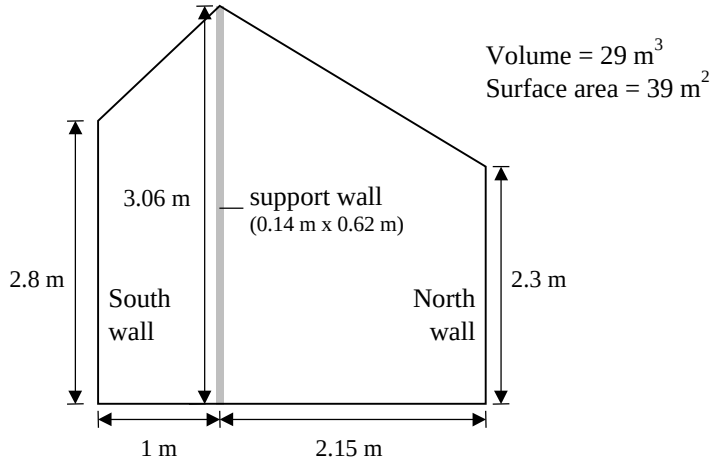

(b) side view of test room

Figure 15. Plan (a) and side view (b) of the test room showing the location of sensors, fans and the humidity generator in the test room.

Table 1. Water vapour permeability of gypsum board coated with plaster and primer.

Material	water vapour permeability [ng/(s·m·Pa)]	water vapour permeance [ng/(s·m^2·Pa)]
gypsum + plaster	13.2	1020
gypsum + plaster + primer	13.2	1020
gypsum (NRC, 1995)	17.4	1340
gypsum (ASHRAE, 1997)	27.1	2090

Figure 15 also shows the location of the temperature, RH, CO_2 and SF_6 sensors. The temperature sensors were thermistors with radiation shields having an accuracy of ±0.3°C. The relative humidity sensors were capacitance type sensors (expected accuracy of ±4% RH) that were calibrated after the tests against salt solutions (prEN 12571, 1999). Figure 16 compares the measured RH and the calibration salt RH for each sensor, where the uncertainty bound for each sensor is assumed to be ±4% RH. The measured values of RH were corrected after the test using the following linear equations:

$$(RH-1)_{corrected} = 0.702(RH-1)_{measured} + 0.163\ , \tag{3}$$

$$(RH-2)_{corrected} = 0.677(RH-2)_{measured} + 0.150\ \text{, and} \tag{4}$$

$$(RH-3)_{corrected} = 0.807(RH-3)_{measured} + 0.224\ . \tag{5}$$

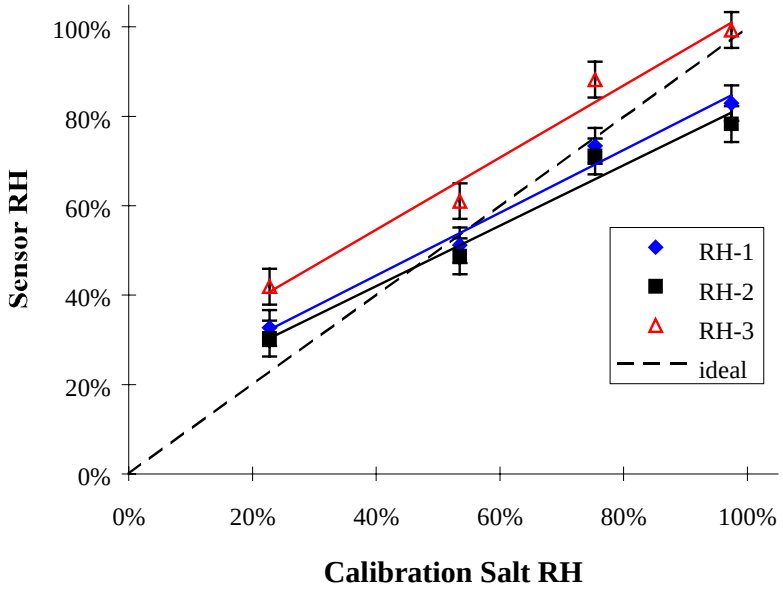

Figure 16. Calibration of the relative humidity sensors after the test.

Figure 16 shows that the linear regression lines are nearly always within the assumed sensor uncertainty of ±4% RH. The regression coefficients (R^2) for equations (3), (4) and (5) were between 0.97 and 0.98, while the standard error for equations (3), (4) and (5) was 3.7%, 4.4% and 5.0% respectively. This indicates that the uncertainty in the corrected relative humidity for individual sensors is slightly greater than ±4% RH. Since two sensors are used to measure the indoor humidity, the accuracy of the average relative humidity will be better than that of the individual sensors. The uncertainty in the average indoor relative humidity, corrected using equations (4) and (5) is expected to be less than ±4% RH. Only corrected values of RH will be presented in this report.

Three different sensors were used to measure the concentration of CO_2 with the most accurate sensor (sensor CO_2-2 in Figure 15) based on the photoacoustic infra-red detection method with an uncertainty of ±3%. This same instrument was also used to measure the concentration of SF_6. The other CO_2 sensors were based on infrared adsorption and are accurate to within ±5%. These sensors were calibrated in-situ against the more accurate photoacoustic device.

As a comparative test, the ceiling, floor and walls of the test room were covered with 0.15 mm (6-mil) polyethylene vapour retarder (except for the external windows and door) as shown in Figure 17. When the room is sealed with plastic, it represents a room with a vapour tight sealing at the interior surface such as a room with a vapour tight paint. By covering the interior surface with plastic, moisture transfer to the building envelope can be nearly eliminated and this permits the quantification of the importance of diffusion mass transfer between the indoor air and the porous building envelope. To minimise the effects of convection mass transfer through the envelope, the room was well sealed with building paper that was located behind the interior board. At an underpressure of 50 Pa, the air infiltration was 1.5 ach and 2.25 ach with the balcony door and windows sealed and unsealed respectively (see Figure 14 in section 2.2).

Figure 17. Sealing the test room with polyethylene plastic.

3.1.2 Numerical Model

The model used for the simulations in this chapter has been developed starting from an existing model that is primarily used for hygrothermal simulations of building envelope parts (LATENITE). The model combines the heat, air, moisture and contaminant balance of indoor air with the hygrothermal performance of the building envelope parts. The conservation equations are solved simultaneously for the indoor air and the structures. The model has been used and presented previously by Salonvaara (1998), Salonvaara and Kokko (1999) and Kokko et al. (1999).

A detailed model description of the LATENITE version 1.0 hygrothermal model is given by Hens and Janssens (1993), Salonvaara and Karagiozis (1994) and only a brief overview is presented here. The moisture transport potentials used in the model are moisture content and vapour pressure; for energy transport, temperature is used. The porous media transport of moisture (vapour and liquid) through each material layer is considered strongly coupled to the material properties (i.e., the sorption-suction curves). The corresponding moisture fluxes are decomposed for each phase and are treated separately. The moisture transfer equation, including liquid and vapour transfer, is

$$q_M = -kd(u,T)\,\nabla P_v - \rho_o D_w(u,T)\,\nabla u + v_{air}\rho_v + K\rho_w g \ , \qquad (6)$$

where q_M is the mass flux (kg/(m^2·s)), kd is the vapour permeability (kg/(s·m·Pa)), u is the moisture content (kg/kg), T is the temperature (°C), P_v is the partial pressure of water vapour (Pa), ρ_o is the dry density of the porous material (kg/m^3), D_w is the liquid moisture diffusivity (m^2/s), v_{air} is the velocity of air (m/s), ρ_v is the density of water vapour (kg/m^3), K is the moisture permeability (s), ρ_w is the density of liquid water (kg/m^3) and g is the acceleration of gravity (m/s^2). The most important term in the moisture transfer equation, for the conditions in this report, is the first term. Here the moisture transfer is assumed to follow Fick's law, which states that moisture transfer is proportional to the vapour pressure gradient.

Energy and moisture conservation equations are coupled via phase changes of water (latent heat of evaporation, freezing of liquid). Indoor air is handled by assuming perfect mixing within the room. Time dependent heat, moisture and contaminant sources can be given as input.

The water vapour permeability (kd) and other moisture properties (D_w and K) of typical building materials can be found in several references (ASHRAE, 1997, Kumaran, 1996 and Karagiozis et al., 1994) allowing the solution of equation (6) for moisture flow. To solve equation (6) for the diffusion of other gases through building envelopes, the permeability of building materials to these gases is needed. Only recently have

measurements been done on the diffusion of other gases through building materials (Kirchner et al, 1999). Nevertheless, the diffusion of gases through other gases is well known and is termed the binary diffusion coefficient. The binary diffusion coefficient of gas a through gas b (D_{ab}) can be calculated using the empirical correlation of Fuller, Schettler and Giddings, which can be found in Reid et al. (1958):

$$D_{ab} = \frac{10^{-3} T^{1.75} \sqrt{(M_a + M_b)/(M_a M_b)}}{\left[(V_a)^{1/3} + (V_b)^{1/3} \right]^2} \ , \tag{7}$$

where T is the absolute temperature (K), M is the molecular weight (kg/kmole), P is the pressure (atm) and V is the diffusion volume. Using equation (7), the diffusion coefficient of the three gasses of interest (H_20, CO_2 and SF_6) can be calculated using air as gas b. The diffusion coefficient ratios are

$$\frac{D_{SF_6,air}}{D_{H_2O,air}} = 0.37 \text{ and } \frac{D_{CO_2,air}}{D_{H_2O,air}} = 0.62 \ . \tag{8}$$

With these diffusion coefficients, the permeability of a gas through air ($kd_{x,air}$) can be calculated using

$$kd_{x,air} = \frac{D_{x,air} M_x}{\tilde{R} T} \ , \tag{9}$$

where $D_{x,air}$ is the binary diffusion coefficient of gas x through air (m^2/s), M_x is the molecular weight of gas x (kg/kmole), $\tilde{R}$ is the universal gas constant (8314.5 J/(kg·K)) and T is the temperature (K).

Using the permeability of gas x through air ($kd_{x,air}$) and the permeability of water vapour through air (kd_{air}), the water vapour permeability data of a certain building material (kd_m) can be extrapolated for use with other gases using the following equation:

$$kd_{x,m} = kd_m \left(\frac{kd_{x,air}}{kd_{air}} \right) , \tag{10}$$

where $kd_{x,m}$ is the permeability of gas x (e.g., CO_2 or SF_6) through material m (e.g., gypsum, wood, or insulation). For the transport of CO_2 and SF_6 through airtight building envelopes, it is assumed that there is only diffusion mass transfer (i.e., no liquid of convection transport) and therefore $kd_{x,m}$ is the only material property needed in the mass transfer equation (6).

3.2 Tracer Gas Tests

The importance of indoor air free of contaminants is well known and providing outdoor ventilation is often used to dilute these contaminants. However, reducing the concentration of indoor contaminants is also possible by diffusion through porous building envelopes. The purpose of this section is to quantify the effect of gas diffusion through a permeable and porous building envelope.

3.2.1 Experimental Results

In order to investigate the diffusion of tracer gases through the building envelope, gases with both a small (CO_2 – 44 kg/kmole) and larger (SF_6 – 146 kg/kmole) molecular weight were added to the room until a high concentration was reached (~2500 ppm CO_2 and ~100 ppm SF_6). The decay of CO_2 and SF_6 were monitored for different forced ventilation rates ranging from 0 ach to 1 ach. The equation describing the mass balance of a tracer gas in a ventilated room is

$$QC_s + \frac{S}{V} = QC_e + \frac{dC_i}{dt} \ , \tag{11}$$

where Q is the ventilation rate (ach), S is the source term (L/h), V is the volume of the room (L), C is the concentration of the gas (volume fraction) and subscripts s, e and i refer to the supply, exhaust and internal room air respectively. It is important to note that Q in equation (11) represents the total outdoor ventilation rate, which includes forced ventilation and infiltration. Equation (11) can be solved for this application by neglecting the source term, assuming that C_s is constant and assuming a well mixed zone (i.e., $C_e = C_i = C$) to give

$$\theta = \frac{C - C_s}{C_o - C_s} = e^{-Q_{eff}t} \ , \tag{12}$$

where θ is the relative concentration of tracer gas, Q_{eff} is the effective ventilation rate or air change rate (ach), t is time (h), and subscript o refers to the concentration in the room at time t = 0. The effective ventilation rate includes the effect of diffusion through the building envelope.

By curve fitting equation (12) to the measured concentration of CO_2 and SF_6, the effective ventilation rate (Q_{eff}) can be calculated. The uncertainty in Q_{eff} determined in this manner depends on the sensor accuracy and the uncertainty in the supply or background concentration of the gas (C_s). Since the house is not located near a busy

street it can be assumed that C_s is quite constant during the tests, nevertheless most tests were run until $C = C_s$ so the value of C_s could be determined more accurately. Based on the data presented in Ekberg and Kraenzmer (1998), the expected uncertainty in the calculated values of Q_{eff} is about ±3%. The effective ventilation rates compared to the forced ventilation rates are presented in Table 2 and Figure 18.

Table 2. Effective ventilation rates at various sensor locations for different forced ventilation rates.

Q_{forced}	Q_{eff} (without plastic) (ach)				Q_{eff} (with plastic) (ach)			
(ach)	CO_2-1	CO_2-2	CO_2-3	SF_6	CO_2-1	CO_2-2	CO_2-3	SF_6
0.00	0.20	0.20	0.17	0.13	0.08		0.08	
0.26	0.37	0.36	0.34	0.31	0.30	0.30	0.27	0.29
0.55	0.64	0.64	0.58	0.59	0.58		0.51	
1.10	1.14	1.06	0.96	1.05				

Figure 18 and Table 2 show that sensor 1 has the highest effective ventilation rate, followed by sensor 2 and then by sensor 3. This is logical because, sensor 1 is closest to the fresh air inlet and sensor 3 is the farthest. The difference between the different sensors is small for low forced ventilation rates, indicating good mixing in the room. However, as the forced ventilation increases, the difference increases, indicating that the zone is less well mixed at a forced ventilation rate of 1 ach. For forced ventilation rates up to 0.55 ach, the effective ventilation rate is greater than the forced ventilation rate when the room is not covered with plastic.

When the inside surface of the room is covered with plastic, the effective and forced ventilation rates are nearly equal except when the forced ventilation rate is 0. In this case, the effective ventilation rate is 0.08 ach, which indicates that there is a leakage rate of 0.08 ach even with no forced ventilation and the ventilation channels sealed with tape. Using the equation presented in Figure 14 of section 2.2, an infiltration rate of 0.08 ach is expected at a pressure difference of 0.3 Pa. This agrees with pressure difference measurements across the envelope which were measured to fluctuate between ±2 Pa.

(a)

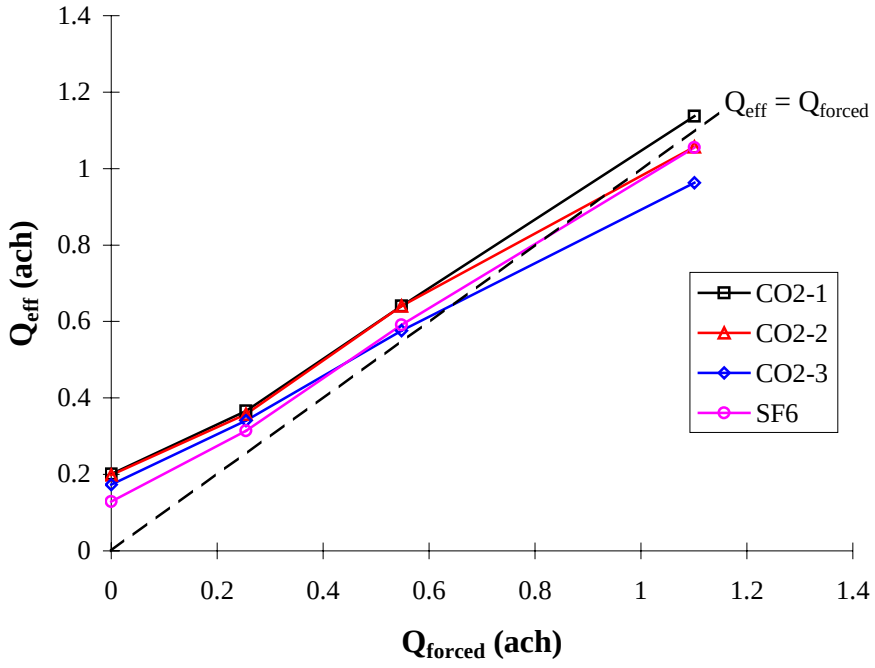

(b)

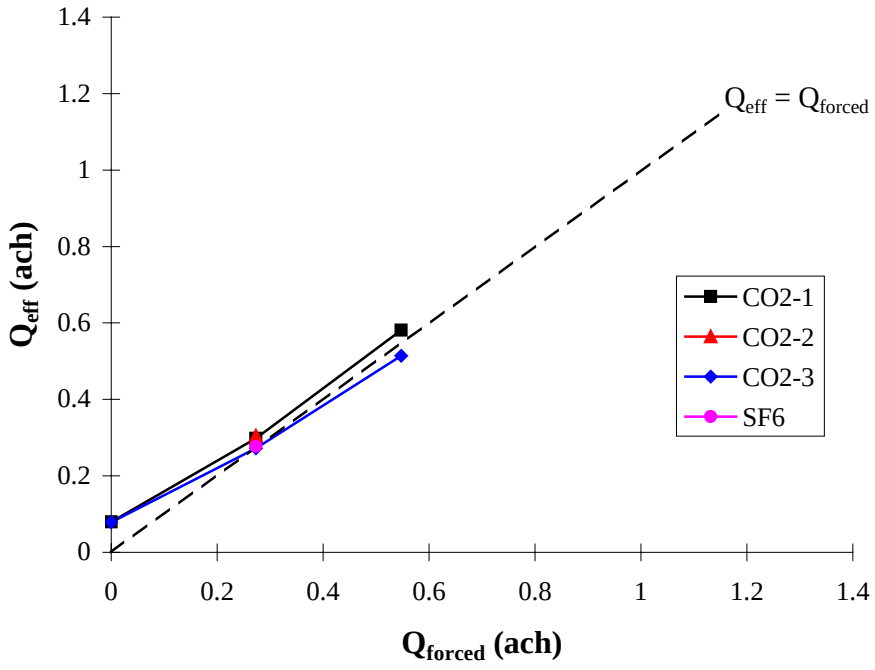

Figure 18. Effective ventilation rate verses forced ventilation rate for CO_2 and SF_6 without plastic (a) and with plastic (b).

As noted in equation (11), Q represents the total outdoor ventilation rate, which includes forced ventilation and infiltration. Since the effective ventilation rate when the room is covered with plastic ($Q_{eff,plastic}$) most closely represents the total outdoor ventilation rate (Q), it will be assumed that

$$Q = Q_{eff\,,\,plastic} = Q_{forced} + Q_{infiltration} \quad . \tag{13}$$

It can be assumed that the difference between the effective ventilation rate with and without the plastic covering represents the effective ventilation rate due to diffusion through the room envelope. Therefore, the fractional increase in effective ventilation due to diffusion through the envelope ($Q^*_{diffusion}$) can be calculated as follows:

$$Q^*_{diffusion} = \frac{\Delta Q_{eff}}{Q} = \frac{Q_{eff\,,no\ plastic} - Q}{Q} = \frac{Q_{eff\,,no\ plastic} - Q_{eff\,,\,plastic}}{Q_{eff\,,\,plastic}} \quad . \tag{14}$$

Again the total ventilation rate (Q) is assumed equal to $Q_{eff,plastic}$, which is the effective ventilation rate with plastic, and $Q_{eff,no\ plastic}$ is the effective ventilation rate without plastic. Figure 19 presents values of $Q^*_{diffusion}$ and ΔQ_{eff} for both tracer gases.

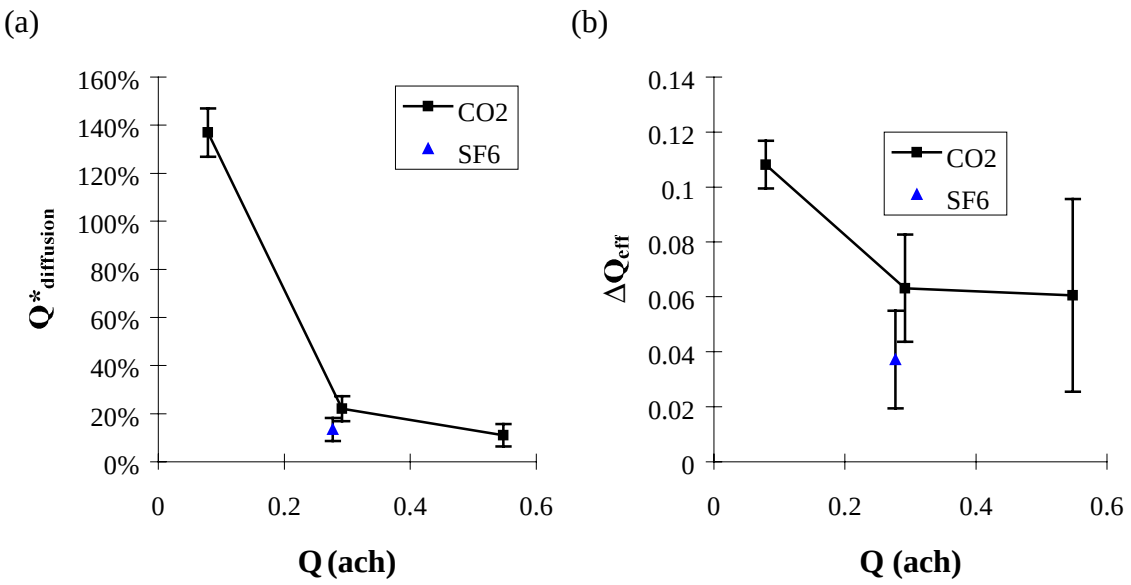

Figure 19. Relative (a) and absolute (b) increase in the effective ventilation rate due to diffusion through the building envelope. The error bars represent the 95% uncertainty limits.

Figure 19(a) shows that the diffusion through the envelope can be relatively important when the ventilation rate is low and the relative importance of diffusion decreases as the ventilation rate increases. However, as shown in Figure 19(b), the absolute increase in effective ventilation rate is quite limited and is usually less than 0.1 ach. When the total ventilation rate (Q) is 0.08 ach (Q_{forced} = 0), the diffusion of CO_2 through the envelope is 140% greater than the ventilation due to air leakage. At total ventilation rates of 0.28 ach and 0.55 ach, the effective ventilation rate is 22% and 11% greater respectively due to diffusion of CO_2 through the envelope. The only measured value of $Q_{eff,plastic}$ for SF_6 is with a forced ventilation rate of 0.25 ach. In this case, $Q^*_{diffusion}$ = 13% for SF_6

compared to 22% for CO_2. These results show that the diffusion of CO_2 (44 kg/kmole) through the walls has a noticeable impact on the effective ventilation rate, however, the diffusion of SF_6 (146 kg/kmole) has a limited effect. Since the diffusion of SF_6 is likely more representative of the diffusion of volatile organic compounds (VOC's) and other pollutants (e.g., toluene C_7H_8 – 92 kg/kmole), these results show that the increased ventilation due to the diffusion of indoor air contaminants is likely limited in practical houses, especially when there is adequate ventilation. The results also show that CO_2 concentration may not be a good representation of effective ventilation rates or indoor air quality in an ecological house because of diffusion through the building envelope. However, since the absolute increase in ventilation rate is usually less than 0.1 ach in Tapanila ecological house, indoor CO_2 concentrations are a useful representative of indoor air quality and ventilation rate and will be used in section 3.5.

To further demonstrate that CO_2 has a higher diffusion rate than SF_6, Figure 20 compares the relative depletion of CO_2 and SF_6 as a function of time using sensor CO_2-2, which is the sensor that measures the concentration of SF_6.

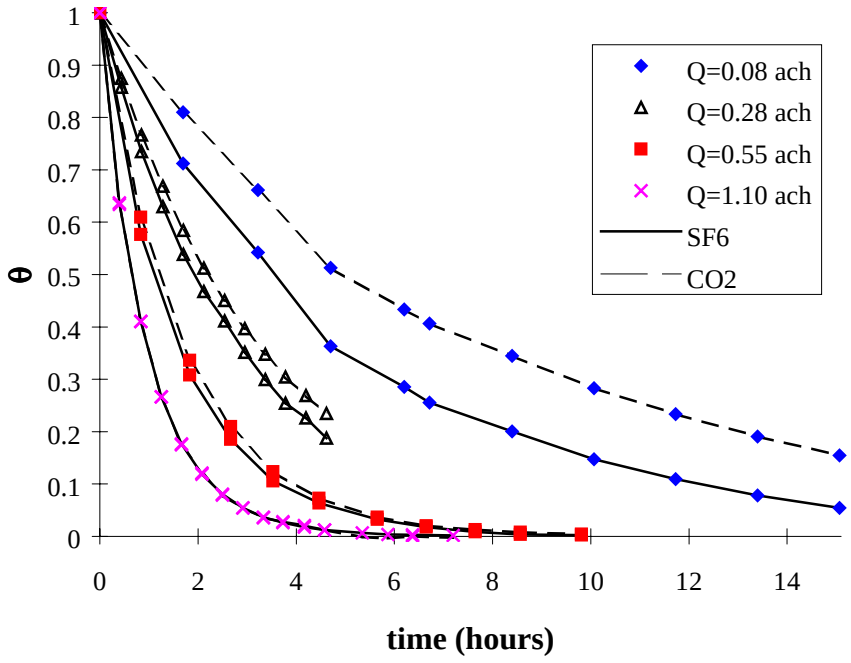

Figure 20. The relative depletion of SF_6 and CO_2 using sensor CO_2-2.

Figure 20 shows that the relative concentration of CO_2 decreases significantly faster than SF_6 for low ventilation rates. As the ventilation rate increases, the difference between the relative concentration of CO_2 and SF_6 decreases. At a ventilation rate of 1.1 ach, there is no noticeable difference between the two curves. This can be seen more clearly in Figure 21, which compares the effective ventilation rates for the two gases

and the relative difference between the effective ventilation rate for CO_2 and SF_6 (Q^*_{SF6}) calculated (again using the sensor CO_2–2) as

$$Q^*_{SF6} = \frac{Q_{eff,no\ plastic}(CO_2 - 2) - Q_{eff,no\ plastic}(SF_6)}{Q_{eff,no\ plastic}(CO_2 - 2)} \quad . \tag{15}$$

The effective ventilation rate for SF_6 is 35%, 12%, 8% and 0% lower than the effective ventilation rate for CO_2 when the ventilation rate is 0.08, 0.28, 0.55 and 1.1 ach respectively. This means that if the ventilation rate is determined by measuring the decay of a tracer gas, the measured ventilation rate will be 8% higher when the tracer is CO_2 than when the tracer gas is SF_6 for a ventilation rate near design.

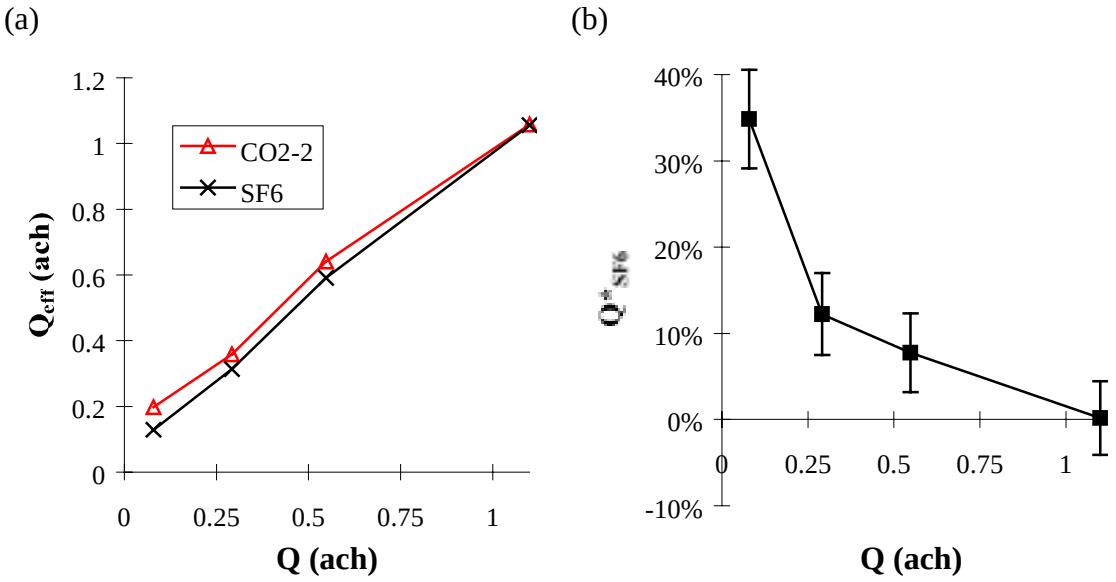

Figure 21. The effective ventilation rate for CO_2 and SF_6 (a) and the relative difference between the effective ventilation rates (b). The results are for the sensor that measures both CO_2 and SF_6 (i.e., CO_2–2).

3.2.2 Numerical Results

Figure 22 presents the measured and simulated relative concentrations of CO_2 and SF_6 as a function of time. The simulated values are calculated using the numerical model LATENITE, which is described in section 3.1.2. The measured and simulated results show good agreement in all cases. Figure 22 also demonstrates the importance of diffusion for low outdoor ventilation rates. For example, if the concentration of CO_2 in a room goes to 2000 ppm and the outdoor CO_2 concentration and ventilation rate are 380 ppm and 0.08 ach, respectively, Figure 22 (a) shows that the CO_2 concentration will decrease to 1000 ppm in less than 6 hours when there is no plastic. However for the same conditions with plastic, the CO_2 concentration will take more than 12 hours to

decrease to 1000 ppm. Comparing Figure 22 (a) and Figure 22 (b) shows that SF_6 decays significantly slower than CO_2 at low ventilation rates.

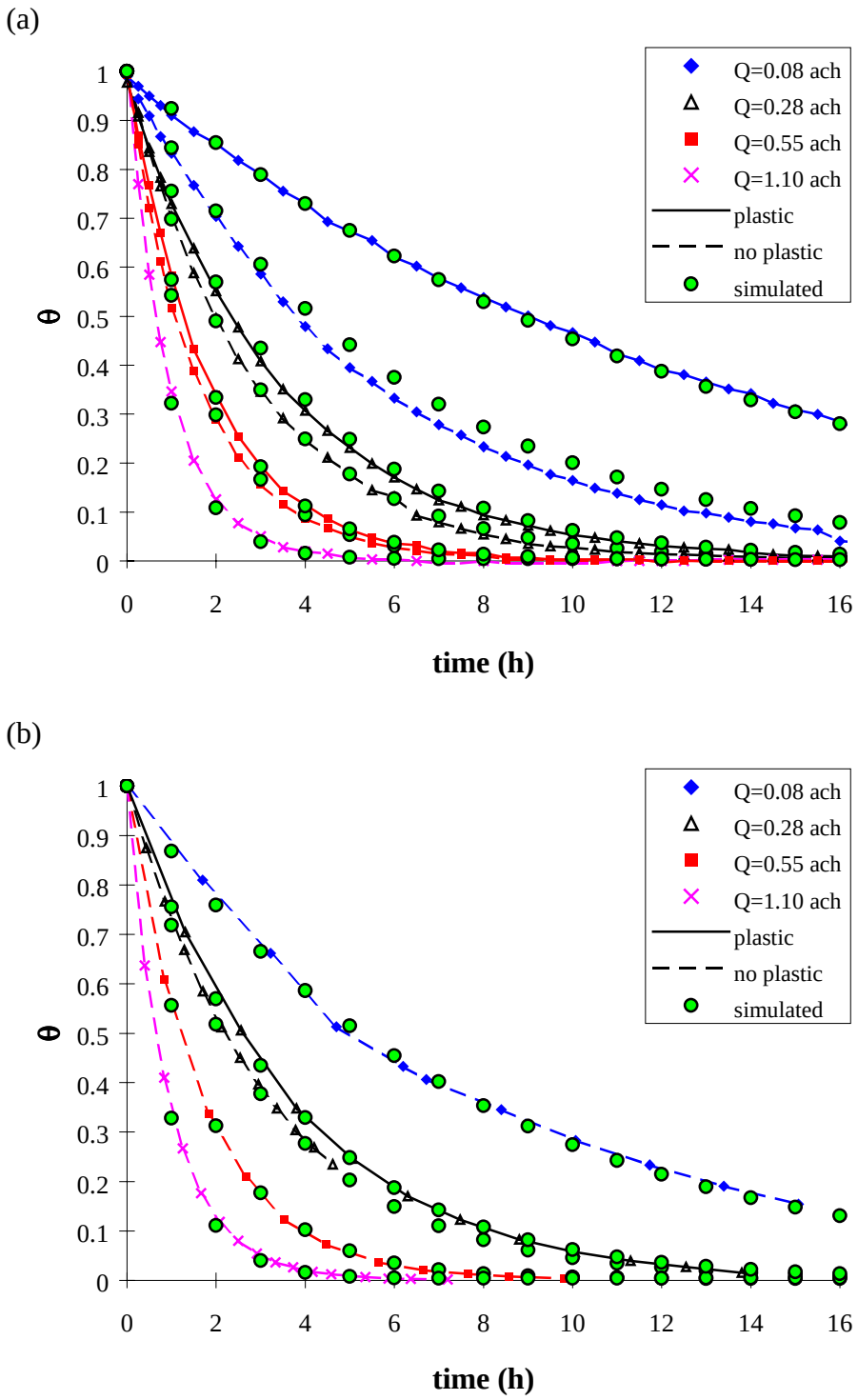

Figure 22. Comparison of measured and simulated relative concentrations of CO_2 (a) and SF_6 (b) for various total ventilation rates with plastic (solid lines) and without plastic (broken lines).

The binary diffusion coefficient for SF_6 is 59% of the binary diffusion coefficient for CO_2 as can be seen from equation (8). Calculating the effective ventilation rates from the numerical results in Figure 22 reveals that the effect of diffusion on the effective ventilation rate can be directly linked to the magnitude of the diffusion coefficient. In each case the ratio $(Q_{eff}-Q)/Q$ for SF_6 is approximately 59% of that for CO_2.

3.3 Water Vapour Tests

As noted in section 1.1, indoor humidity affects thermal comfort, perceived air quality (PAQ) and many other factors. Indoor humidity is often controlled by mechanical cooling equipment and outdoor ventilation. However, vapour permeable building envelopes with moisture storage capacity could also be applied to control indoor humidity levels. The purpose of this section is to quantify the impact of moisture transfer between indoor air and building structures on the humidity of indoor air.

3.3.1 Experimental Results

In the experimental tests, water vapour was generated during the night using an electric humidifier and an electric timer. The mass of water in the humidifier was measured every 10 minutes and the moisture production calculated. Figure 23 presents the moisture production (hourly average) during the test.

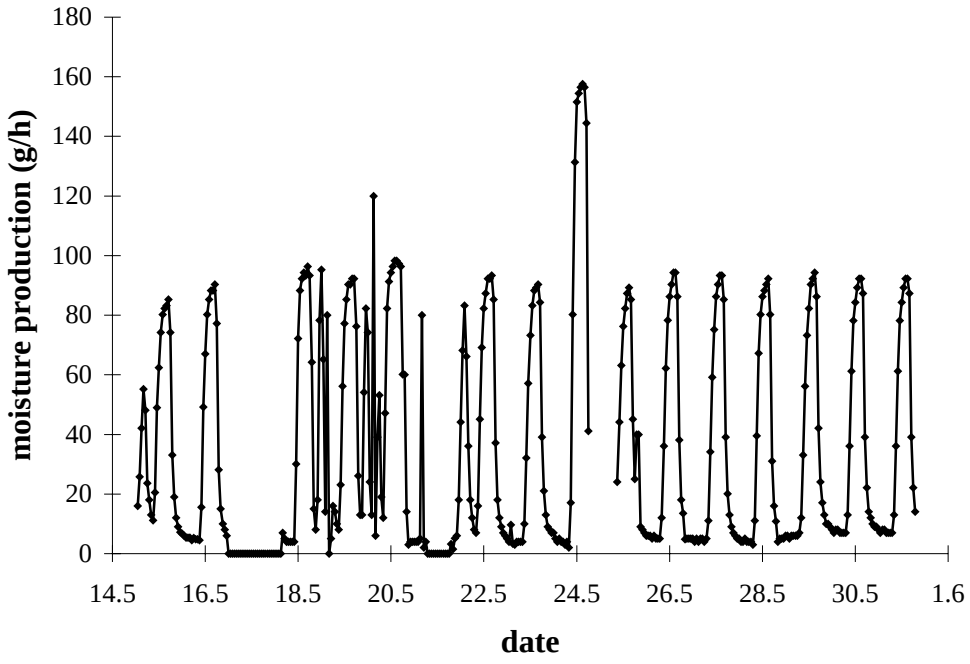

Figure 23. Moisture production in the test room.

The results in Figure 23 demonstrate that the moisture production was quite similar during each day of the test. On some days, however, the humidity generator was accidentally turned on during the day for an hour or two. In these few cases, the average humidity generated during the day was on average 20 to 30 g/h. During one night (May 17) the humidity generation was off because there was a power failure in the test room. During another night (May 24), the moisture production was increased to a peak value of nearly 160 g/h (average of 150 g/h for 8 hours) to see the effect of greater moisture production. Figure 24, shows the moisture production in more detail during a two day test period (26.5 to 28.5) and includes the associated latent energy production.

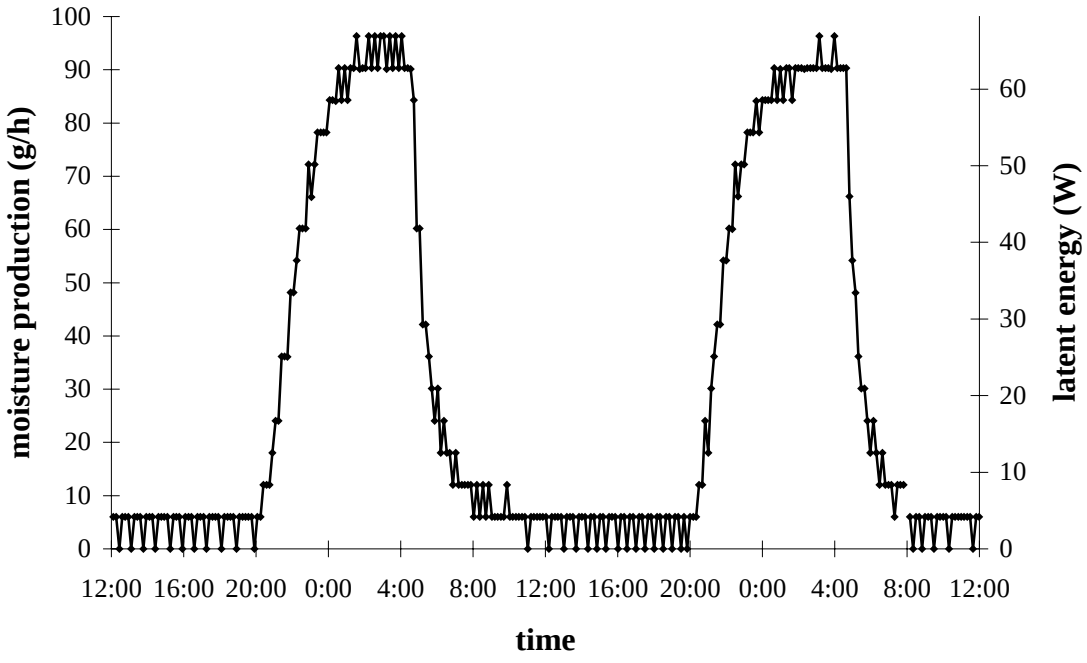

Figure 24. Moisture and latent energy production from 26.5 to 28.5.

Figure 24 shows that it generally took 4 hours for the moisture production to reach a constant value of 90 g/h, which was kept constant for another 4 hours. After this, the timer cut the power to the humidity generator and the moisture production decayed to less than 10 g/h in slightly less than 4 hours. When the humidity generator is off during the day some evaporation occurs from the humidity generator, but the average evaporation is rate is only 5 g/h. The average moisture production during the night is 58 g/h for 12 hours, which corresponds to 87 g/h for a typical 8 hour occupancy. The moisture production is equivalent to two adults occupying the room for 8 hours each night and producing 30 W of latent energy each. This is likely slightly higher than expected for a sleeping adult because ASHRAE (1997) indicates that 30 W of latent energy would be produced, for example, by a person seated at a theatre. No values for sleeping adults are presented in ASHRAE (1997), but the metabolic rate for sleeping

people (0.8 met) is 80% of the metabolic rate for seated and quiet people (1.0 met) (ASHRAE/ANSI Standard 55-1992).

The temperature of the room and outdoor air were measured during the test and are presented in Figure 25. The outdoor temperature during the test varied from –10°C to +20°C and the average outdoor temperature was 11°C. The indoor temperature in Figure 25 is the average of the temperature measured with sensor T-2 (positioned at a height of 2 m) and sensor T-3 (positioned at a height of 0.5 m) as shown in Figure 15. The difference between the temperature sensors was, on average, less than 0.1°C, with peak values of about 0.5°C. The indoor temperature was usually quite high (average of 27°C) during the test because of the heat produced by the five mixing fans (~20 W each), computer (~100 W) and gas analysers (~100 W). (At an average outdoor temperature of 11°C, it is expected that 300 to 400 W of heat is needed to keep the indoor temperature at 27°C depending on the ventilation rate.) The indoor temperature also varied somewhat (range of 24°C to 30°C) because there was no cooling in the room.

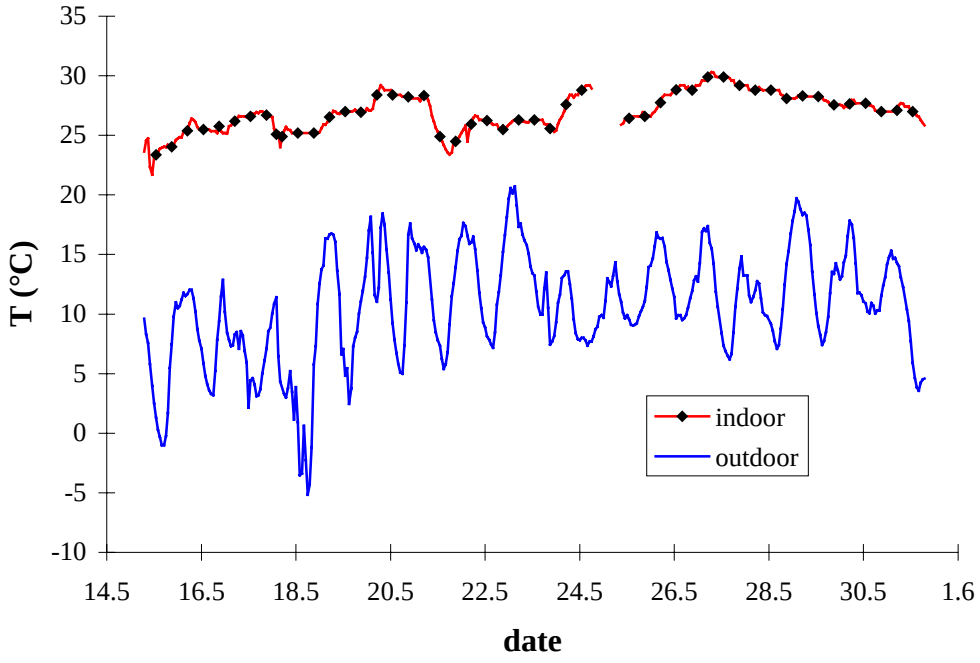

Figure 25. Indoor and outdoor temperatures during the test.

To compare different ventilation rates with and without a plastic vapour retarder, Figure 26 contains the measured indoor and outdoor absolute humidity as a function of time for the entire measurement period. Each day shows an increase in humidity during the night followed by a decrease during the day. On some days, the measured results show additional peaks and valleys due to inadvertent moisture production or temporarily higher ventilation rates.

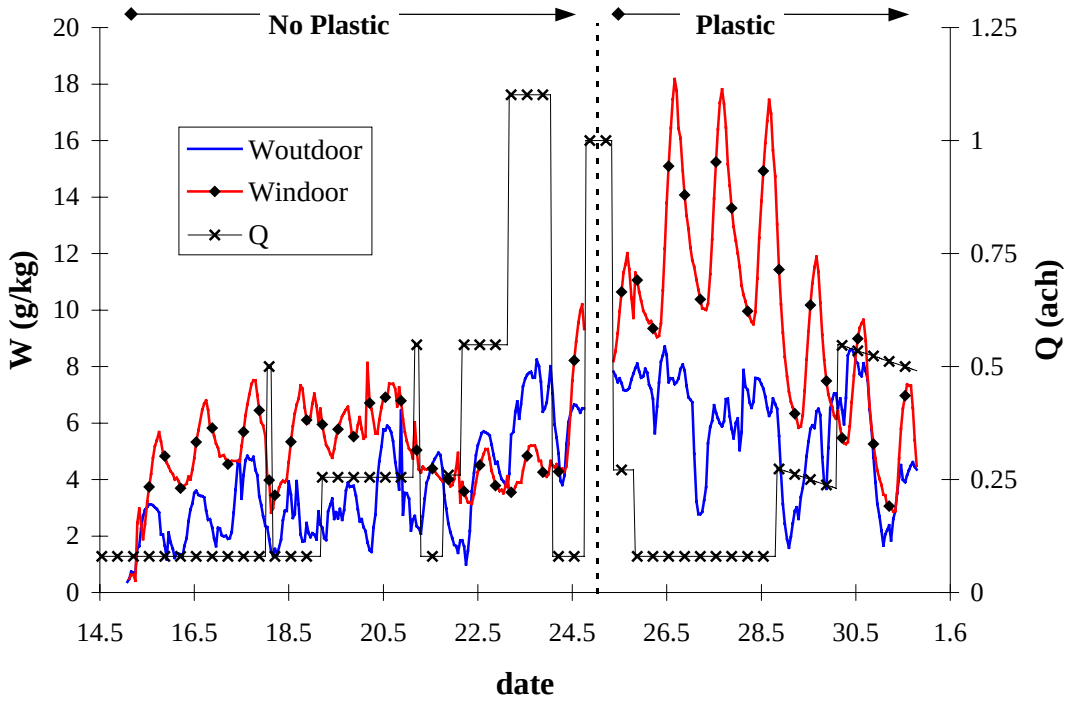

Figure 26. Measured outdoor and indoor absolute humidity and total ventilation rate (forced ventilation + infiltration) during the test.

The results in Figure 26 clearly show that the increase in humidity is significantly greater for the tests with plastic than for the tests without plastic, especially when the total ventilation rate is low. During most of the test, the indoor humidity is greater than the outdoor humidity. This can be seen more clearly in Figure 27 which presents the difference between indoor and outdoor humidity (ΔW), where

$$\Delta W = W_{indoor} - W_{outdoor} \ . \qquad (16)$$

The most noticeable occurrence of $W_{outdoor} > W_{indoor}$ (i.e., $\Delta W < 0$) is on May 23. During May 23, the outdoor humidity increases by about 4 g/kg and the indoor humidity increases by only 1 g/kg even though the ventilation rate is high (1.1 ach). During this rapid increase in outdoor humidity, the measured results show that the absolute humidity indoors remains below the outdoor level. This may be due to the adsorption of moisture in the porous building envelope, but since the ventilation rate is quite high, it is suspected that the level of the measured humidity (or temperature) is too low and that W_{indoor} will not be significantly below $W_{outdoor}$ when the ventilation rate is 1 ach. The simulation results presented in section 3.3.2 (Figure 35) tend to confirm this.

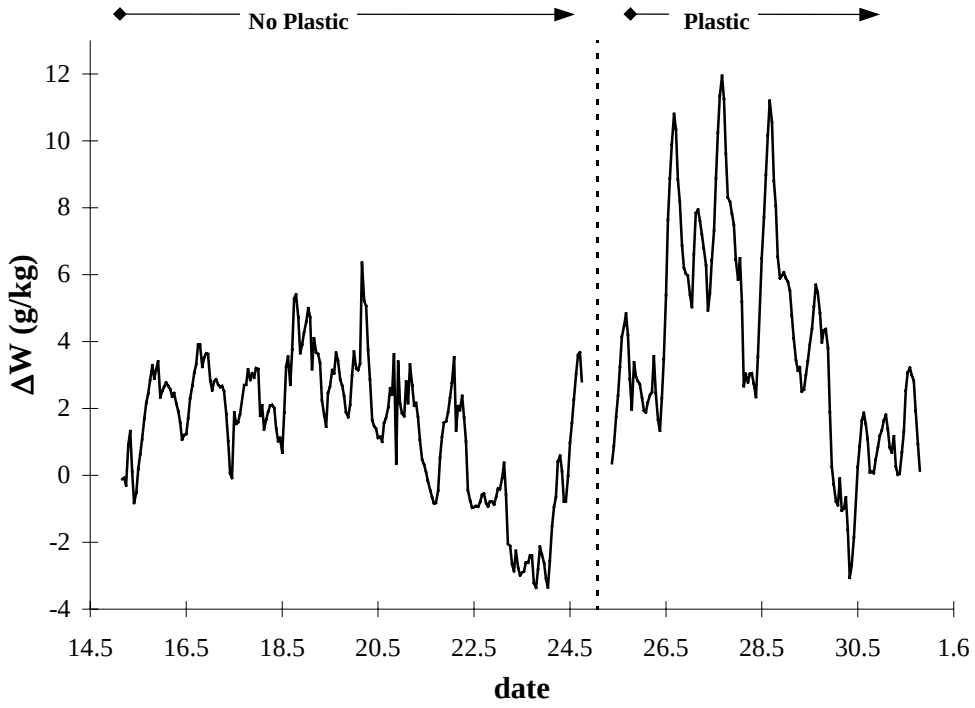

Figure 27. Difference between indoor and outdoor absolute humidity.

The average measured relative humidity during the test are presented in Figure 28, where

$$\phi = average(RH-1, RH-2) \ . \qquad (17)$$

The results Figure 28 are very similar to the results of absolute humidity in Figure 26 and show that the indoor RH is effected by the ventilation rate and whether the there is a plastic coating or not. By focusing on the measurement during the first four days of the test when there was no forced ventilation (total ventilation rate estimated to be 0.08 ach) and no plastic coating, it is evident that the increase in relative humidity is quite constant during each night (Figure 29).

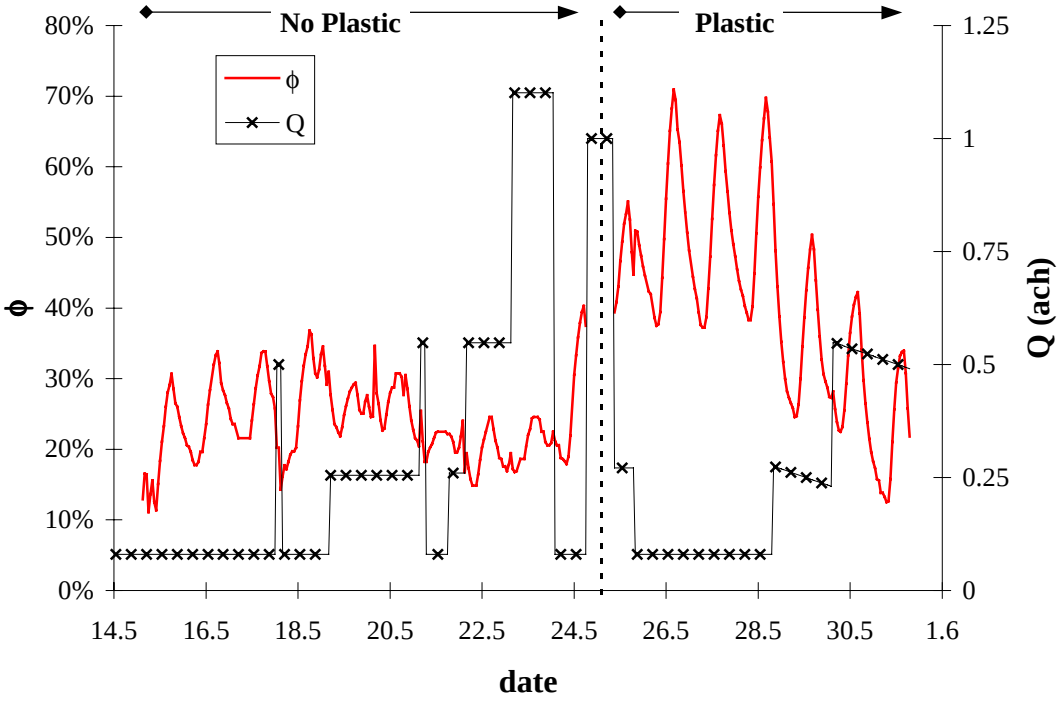

Figure 28. Measured average indoor relative humidity during the test.

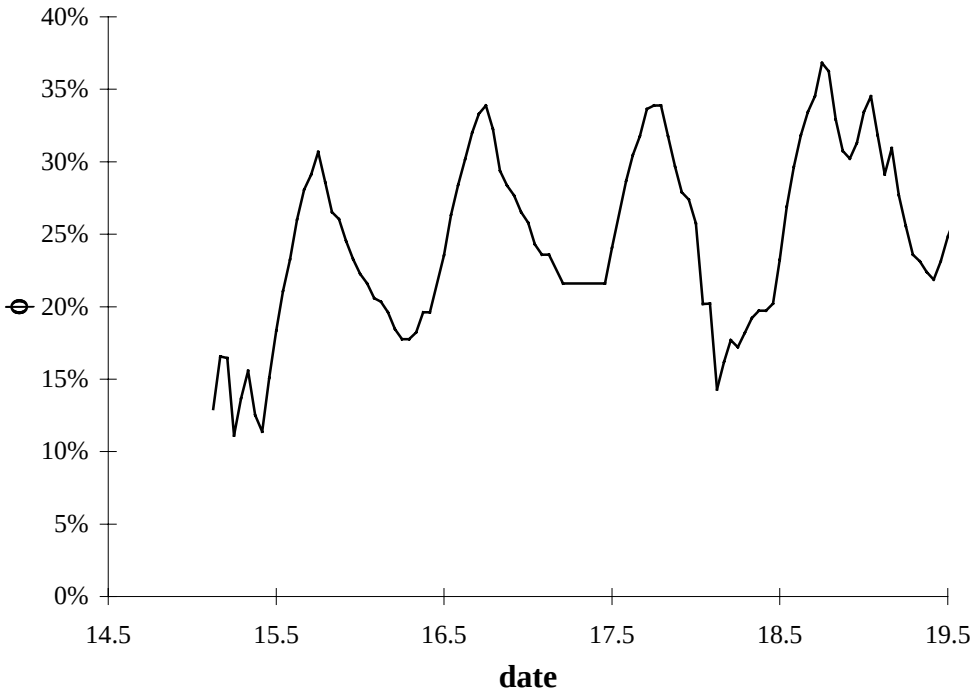

Figure 29. Average indoor relative humidity for the case where there is no forced ventilation (Q≈0.08 ach) and no plastic covering.

The sorption characteristics of most building materials are non-linear, with the slope of the sorption curve increasing with relative humidity. This means that as the indoor

relative humidity increases, the moisture storage potential of the materials per unit change in relative humidity increases. Therefore, at higher indoor relative humidities, the building envelope will tend to have a greater effect on the indoor humidity. This trend can be seen in Figure 30, where the change in relative humidity of the room ($\Delta\phi$) as a function of time after the humidity source was turned on is presented. The value of $\Delta\phi$ is calculated as follows:

$$\Delta\phi = \phi - \phi_o \ , \qquad (18)$$

where ϕ_o is the initial indoor relative humidity, which is the relative humidity in the room when the humidity generator is turned on. As expected, Figure 30 shows that the increase in RH is the greatest during the night of May 15, which has the lowest initial RH, and the increase in RH is the lowest during the night of May 17, which has the highest initial RH. Nevertheless, the increase in relative humidity during each night is quite similar when the ventilation rate is constant and therefore $\Delta\phi$ is used to compare different ventilation rates with and without a plastic vapour retarder in Figure 31. For the cases where several days had the same ventilation rate the average value of $\Delta\phi$ for these days is presented in Figure 31. Once again the ventilation rates in Figure 31 represent the total ventilation rate including the measured forced ventilation and the estimated infiltration according to equation (13). As noted in section 3.2.1, when there is no forced ventilation, infiltration was the most noticeable and seemed to be about 0.08 ach.

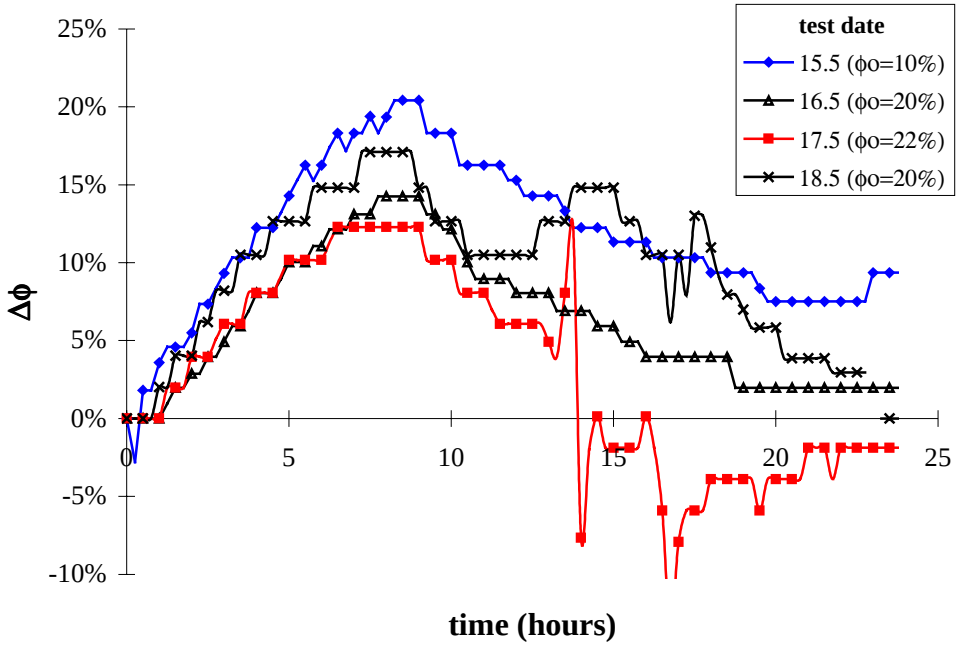

Figure 30. Change in relative humidity in the test room after the humidity generator is turned on for 4 nights with Q=0.08 ach and no plastic covering.

During the day (i.e., time > 8 hours), the value of $\Delta\phi$ in Figure 30 show significant scatter. The reason for this is that, during the day, the room was entered to check the experiment and perform other tests. For example, on May 17 two people entered the test room at 12:30 in the afternoon, which is about 13.5 hours after the humidity generator had been turned on. The people remained in the room for half an hour with the doors and windows closed while they prepared for a tracer gas test. During this short time, the relative humidity in the room increased by 8% RH. At 13:00 (time = 14 hours), the occupants left the room and ventilation rate was increased to 1 ach to facilitate a tracer gas test. As a result, the relative humidity decreased very rapidly and remained very low for the rest of the day, even though the ventilation rate was maintained for only 3 hours. Since the conditions in the room were not kept constant during the day due to other testing constraints, the measurement results are not directly comparable during this time. However, during the night, when moisture was being generated, the test conditions were controlled and the results are therefore comparable.

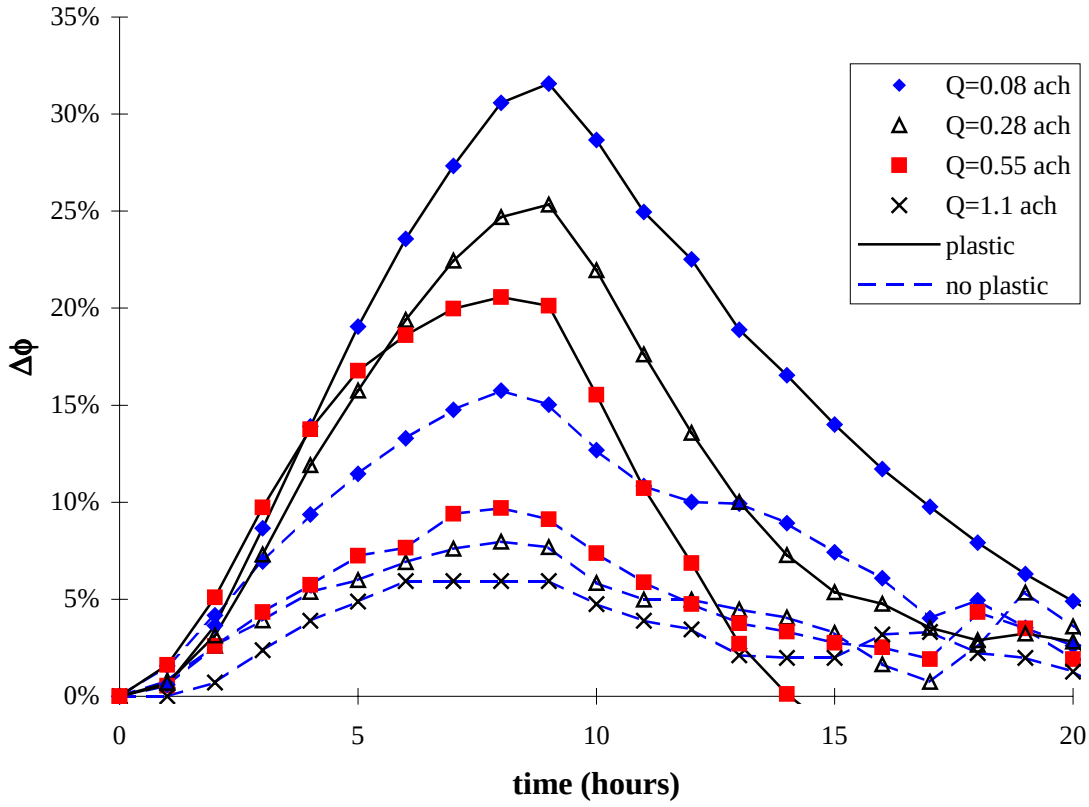

Figure 31. Change in relative humidity in the test room after the humidity generator was turned on for different ventilation rates with and without plastic.

The results in Figure 31 show that the increase in relative humidity is significantly greater for the tests with plastic than for the tests without plastic. In fact, the increase in relative humidity is greater when Q = 0.55 ach with plastic than when Q = 0.08 ach without plastic. This shows that, for these test conditions, the sorption of water vapour

in the porous envelope has a greater effect on the increase in indoor humidity during the night than ventilating the room with 0.55 ach (near design). With a ventilation rate of 0.08 ach, the maximum increase in humidity ($\Delta\phi_{max}$) is twice as large when the room is covered with plastic ($\Delta\phi_{max}$ = 32% with plastic and $\Delta\phi_{max}$ = 16% without plastic) as shown in Figure 32. When the forced ventilation rate is 0.25 ach and 0.55 ach, the decrease in the maximum humidity due to sorption is 18% RH and 12% RH respectively. The average difference between $\Delta\phi_{max}$ with and without plastic is 15% RH at 27°C. At these conditions there would be nearly twice as many people dissatisfied with the humidity conditions when the room is covered with plastic than when it is not (see Figure 1 in section 1.1.1). Figure 32 also contains extrapolated values of $\Delta\phi_{max}$ to a temperature of 22°C. The extrapolation assumes that the temperature indoors is 27°C and that, if the temperature was 22°C, the increase in absolute humidity would be the same as measured. Therefore, $\Delta\phi_{max}$ at 22°C is calculated as follows:

$$\Delta\phi_{\max}(22^{\circ}C) = \Delta\phi_{\max}(27^{\circ}C)\frac{W_s(27^{\circ}C)}{W_s(22^{\circ}C)} \tag{19}$$

where W_s is the absolute humidity at saturation. At 27°C, W_s = 22.7 g/kg and at 22°C, W_s = 16.7 g/kg. At an indoor temperature of 22°C, the average difference between $\Delta\phi_{max}$ with and without plastic is therefore expected to be 21% RH. With Q = 0.08 ach and an indoor temperature of 22°C, $\Delta\phi_{max}$ during the night is expected to be 43% RH with plastic and 21% RH without plastic. Even at a ventilation rate of 0.55 ach (22°C), $\Delta\phi_{max}$ is 28% RH with plastic, while it is only 13% without plastic. These results clearly show the influence moisture transfer to the walls has on the indoor relative humidity for these tests.

Most of the results in Figure 31 and Figure 32 show, as expected, that $\Delta\phi$ decreases as the ventilation rate increases. When the room is not covered with plastic, however, $\Delta\phi$ is greater when Q = 0.55 ach than when Q = 0.28 ach. This is possibly due to the non-linear sorption effects because the initial humidity is 22% RH for Q = 0.28 and only 15% RH for Q = 0.55 as shown in Table 3. It may also be due to slightly higher temperatures at a lower ventilation rate. Nevertheless, the main reason for this is likely that the humidity ratio of the outdoor air is greater than the humidity ratio of the indoor air when Q = 0.55 ach. As a result, the ventilation air is actually increasing the humidity in the room rather than decreasing it, as is the case in the other tests. Figure 33 displays that $W_{outdoor}$ is less than W_{indoor} during the 0.28 ach test (19.5 and 20.5), but $W_{outdoor}$ is greater than W_{indoor} during the 0.55 ach test (22.5). As a result, $W_{outdoor}$ is greater than W_{indoor} during the first part of the 0.55 ach test and the ventilation increases the moisture content of the room, rather than decreases as is the case with most other test conditions.

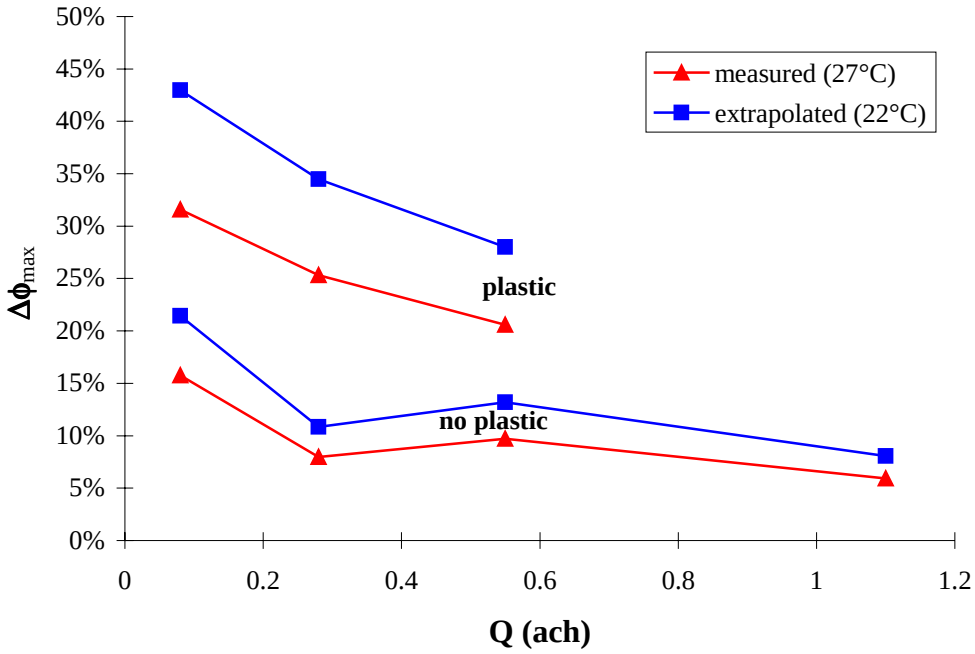

Figure 32. Maximum increase in relative humidity during the night measured during the tests with an average temperature of 27°C and extrapolated to 22°C.

Table 3. Initial relative humidity when the humidity generator was turned on for each ventilation rate with and without plastic.

	without plastic				with plastic		
Q (ach)	0.08	0.28	0.55	1.1	0.08	0.28	0.55
ϕ_o	18%	22%	15%	19%	38%	25%	17%

Since the conditions are not exactly the same for each test, the data in Figure 31 and Figure 32 are somewhat limited. Therefore, to supplement these measurements, the LATENITE numerical model is applied in the next section to compare different ventilation rates and to extrapolate these results to other test conditions.

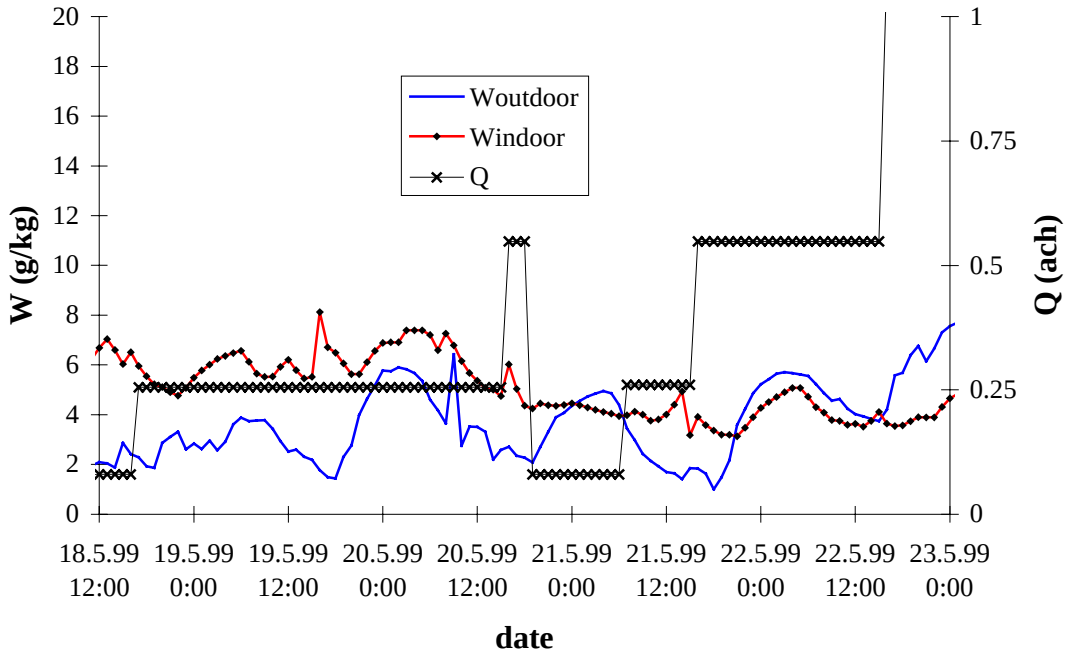

Figure 33. Measured indoor and outdoor humidity ratios during the 0.28 ach and 0.5 ach test without plastic.

To compare the effect of a higher moisture production rate, Figure 34 presents $\Delta\phi$ for 8-hour average moisture production rates of 90 g/h and 150 g/h. These results are for no forced ventilation and no plastic coating. The increase in humidity during the night is 16% RH for the 90 g/h test and 22% RH for the 150 g/h test. The ratio of moisture generation rates is 1.7, while the ratio of $\Delta\phi_{max}$ is 1.4. However, the indoor temperature is nearly 3°C higher when the moisture production is higher, which means that the relative humidity will increase less for the same change in absolute humidity. The average indoor temperatures during the 90 g/h tests and the 150 g/h test are 25.4°C and 28.2°C respectively, giving a ratio of saturation absolute humidities of 1.2. By modifying $\Delta\phi_{max}$ according to equation (19), the ratio of $\Delta\phi_{max}$ at a common temperature becomes 1.7, which is the same as the ratio of moisture production rates. It appears from these results that when values of $\Delta\phi_{max}$ are correlated to a common temperature, the response of the room is quite linear. This is believed to be the case because the differences between the outdoor and indoor absolute humidity are similar for both cases and the initial relative humidity for both tests are nearly the same (average of 18% RH for the 90 g/h tests and 19% RH for the 150 g/h test). Therefore, it may be possible to obtain a correlation where $\Delta\phi_{max}$ at a common temperature is a linear function of the moisture production rate. Since there is only one measurement with a different moisture production rate, this is left to future work.

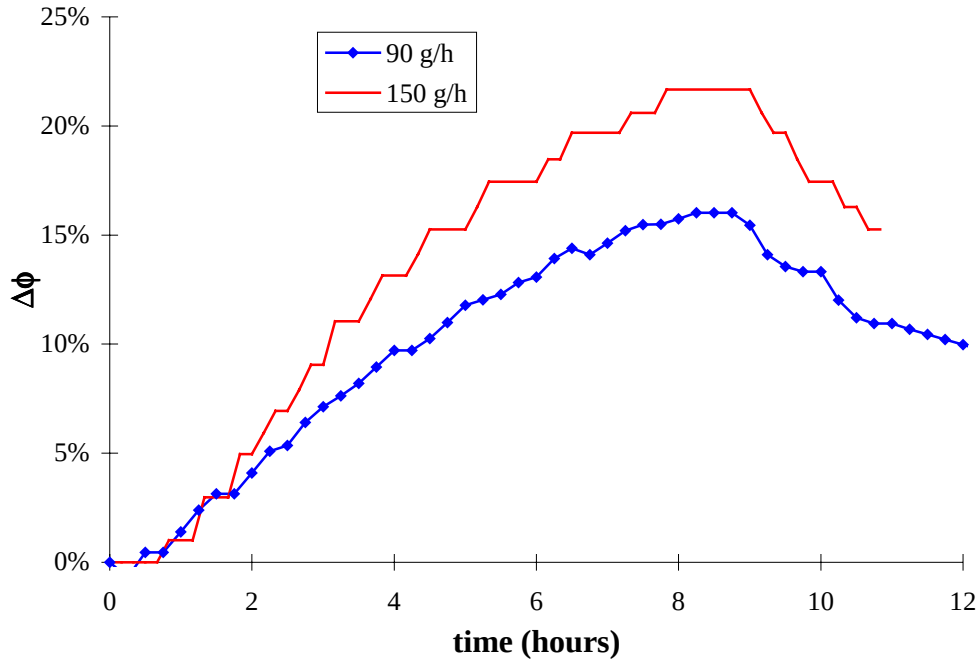

Figure 34. Comparison of the $\Delta\phi$ for different average moisture production rates for Q=0.08 ach and no plastic.

3.3.2 Numerical Results

Since simultaneous heat and mass transfer between building envelopes and indoor air is complicated and expensive to measure in laboratory and field experiments, a numerical model is important in understanding and extrapolating experimental results. However before using the model for extrapolation, it is important to compare the model with measured results. For this comparison, the measured moisture production in the room and ventilation rate were used as input to the numerical model. The boundary conditions for the exterior walls were the measured outdoor temperature and relative humidity. Due to lack of information, the boundary conditions for the interior walls were simplified and a constant temperature (21°C) and relative humidity (32%) were set to represent conditions in the rest of the rooms in the house. This value of 32% RH at 21°C corresponds to the average vapour pressure outdoors, which was approximately 800 Pa. The property data of the building materials listed in Table 4 were taken mainly from the database of property data included in the LATENITE simulation program (Karagiozis et al., 1994) and are given in Appendix A. In addition to the envelope parts, a thermal conductance of 2 W/K was used to represent the heat transfer through the two windows and the balcony door.

Table 4. Envelope areas, boundary conditions and material layers.

Envelope part and boundary condition	Area (m^2)	Material layers
ceiling (external)	11.1	13 mm gypsum board, building paper, 425 mm wood fibre insulation, 25 mm porous wood fibre board
supporting wall	3.8	140 mm brick with plaster (impermeable and adiabatic conditions in the middle at 70 mm)
east wall (interior)	6.8	140 mm brick with plaster
north wall (external)	6.3	13 mm gypsum board, building paper, 250 mm wood fibre insulation, 25 mm wood fibre board
west wall (external)	5.4	13 mm gypsum board, building paper, 250 mm wood fibre insulation, 25 mm wood fibre board
south wall (interior)	9.4	13 mm gypsum board, 100 mm wood fibre insulation, 13 mm gypsum board
floor (interior)	10.6	32 mm wooden floor board, 125 mm wood fibre insulation

Figure 35 contains the indoor vapour pressure as a function of time for the whole measured period. The measured and calculated results match each other very well. The calculated increase in vapour pressure during the night closely follows the measured values. During some of the days, the measured results show additional peaks and valleys due to inadvertent moisture production or temporarily higher ventilation rates and the simulation results track these well. The largest disagreement between the measured and calculated results occurs during a 2-day period just before adding the plastic on the interior surfaces. As discussed in section 3.2.1 (Figure 27), it is suspected that the level of the measured humidity (or temperature) is too low because the outdoor humidity became much higher than the indoor humidity during these days. In the case when the room was covered with polyethylene foil, some sorption of moisture was found to exist. When the relative humidity increases in the room, the surfaces covered with plastic adsorb moisture and the effect is noticeable. The values for surface adsorption were taken from IEA (1991) where surface adsorption on polyethylene foil was found to be 0.0021 kg/m^2 (in the range of 0 to 100% RH) in an experimental study.

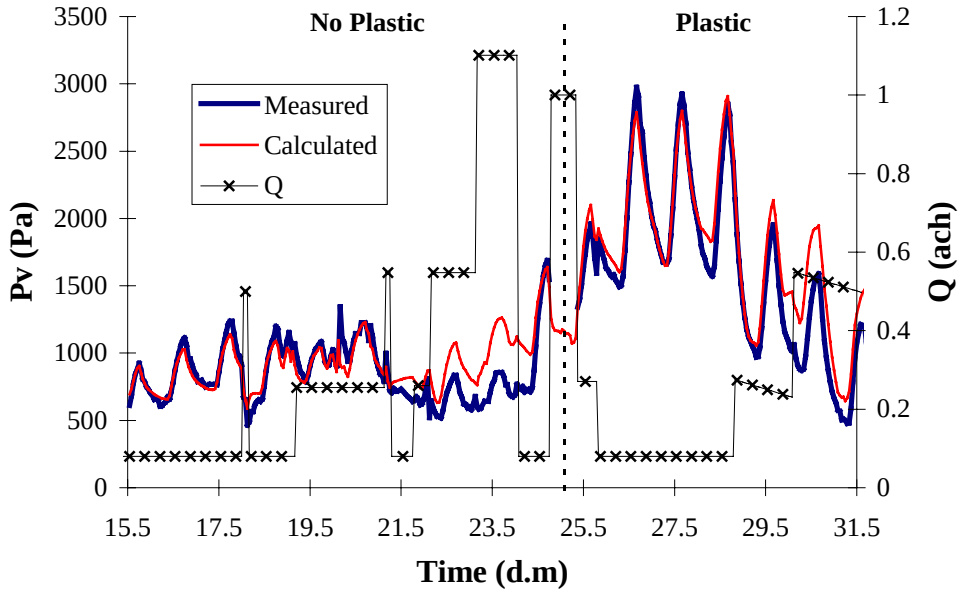

Figure 35. Measured and calculated indoor vapour pressure during the test.

In order to expand the results to other weather conditions, the thermal and hygric performance of the test bedroom was calculated for a winter (January) and summer (July) month in Helsinki, Finland. The weather in January is cold and dry and the average and standard deviation of temperature and absolute humidity are –8.5 ± 6.1°C and 1.8 ± 0.9 g/kg. The weather in July is warmer and more humid with monthly average and standard deviation values of 16.0 ± 4.5°C and 6.6 ± 1.5 g/kg. The average relative humidity is 88% RH in January and 78% RH in July. Because the time to reach steady state conditions is quite long for walls with hygroscopic mass, the simulations were started 3 months before the investigated period in order to avoid initial moisture content effects. The room represented a bedroom with two adults producing a total of 90 W of sensible heat and 60 g/h of moisture (42 W of latent heat) for nine hours per night. The mid-plane of interior walls were made impermeable and adiabatic, because it is assumed that the rest of the house has similar ventilation rates and moisture and heat sources as the bedroom. The room was heated to about 21°C in January, but there was no heating or cooling in July.

Figure 36 and Figure 37 present the calculated average, minimum and maximum relative humidity and temperature of indoor air at various ventilation rates during July and January, respectively. Each figure compares the case where the interior paint is vapour tight and allows essentially no moisture transfer to the structure (solid line) with the case where the paint is vapour permeable and has no effect on the moisture transfer to the structure (dashed line). The purpose of these tests is to compare the case where moisture transfer occurs between indoor air and the building envelope with the case where no moisture transfer occurs. It is important to note that the tests do no represent

the effect of real paints. In addition, the ventilation rate was kept constant in each simulation, which is not exactly what would exist in real buildings – opening doors, or windows would temporarily increase the ventilation rate.

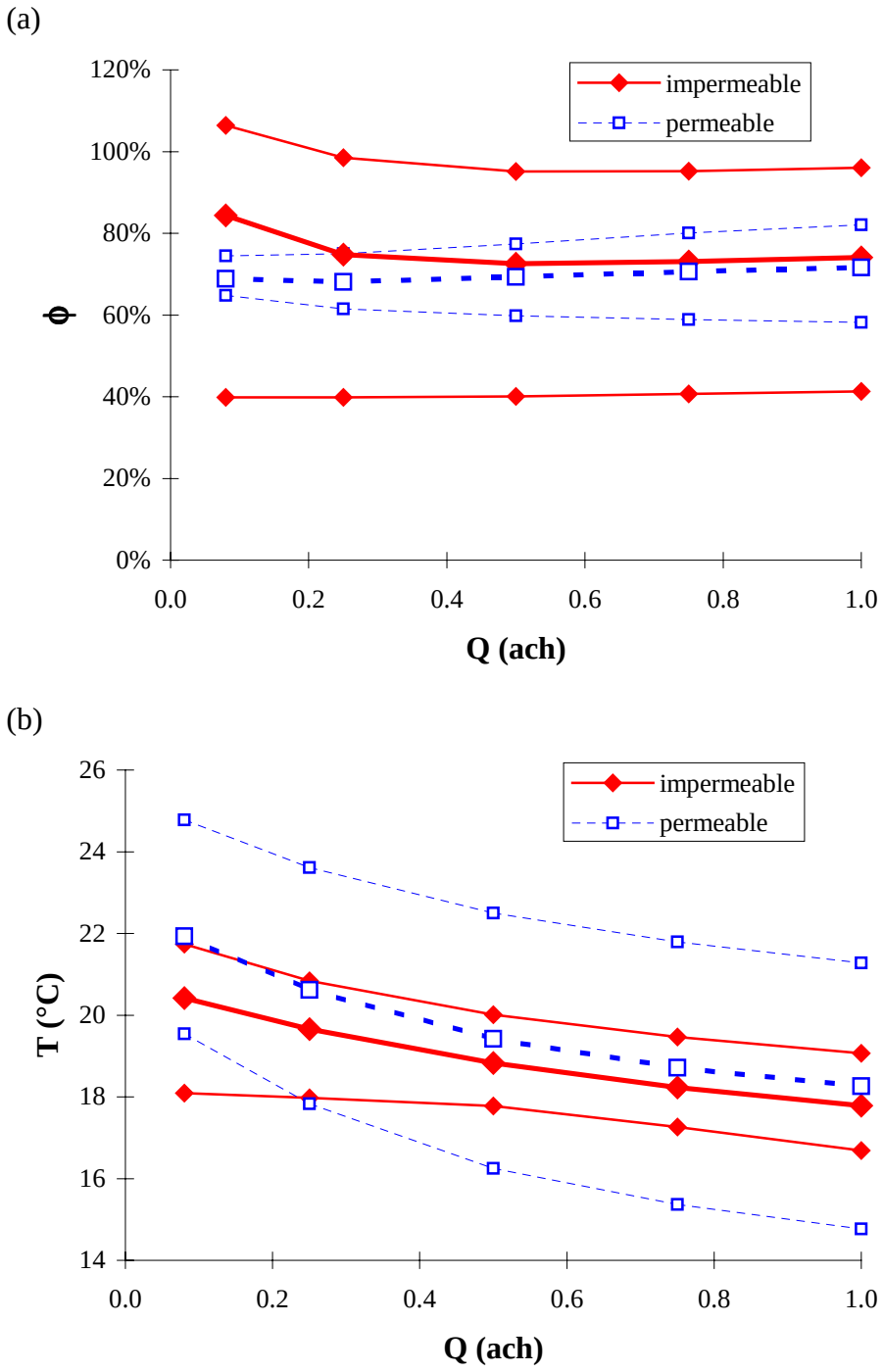

Figure 36. Calculated average (thick lines), minimum and maximum relative humidity (a) and temperature (b) of indoor air in July as a function of ventilation rate. The solid lines are for a room with vapour tight paint and the dashed lines are for a room with vapour permeable paint.

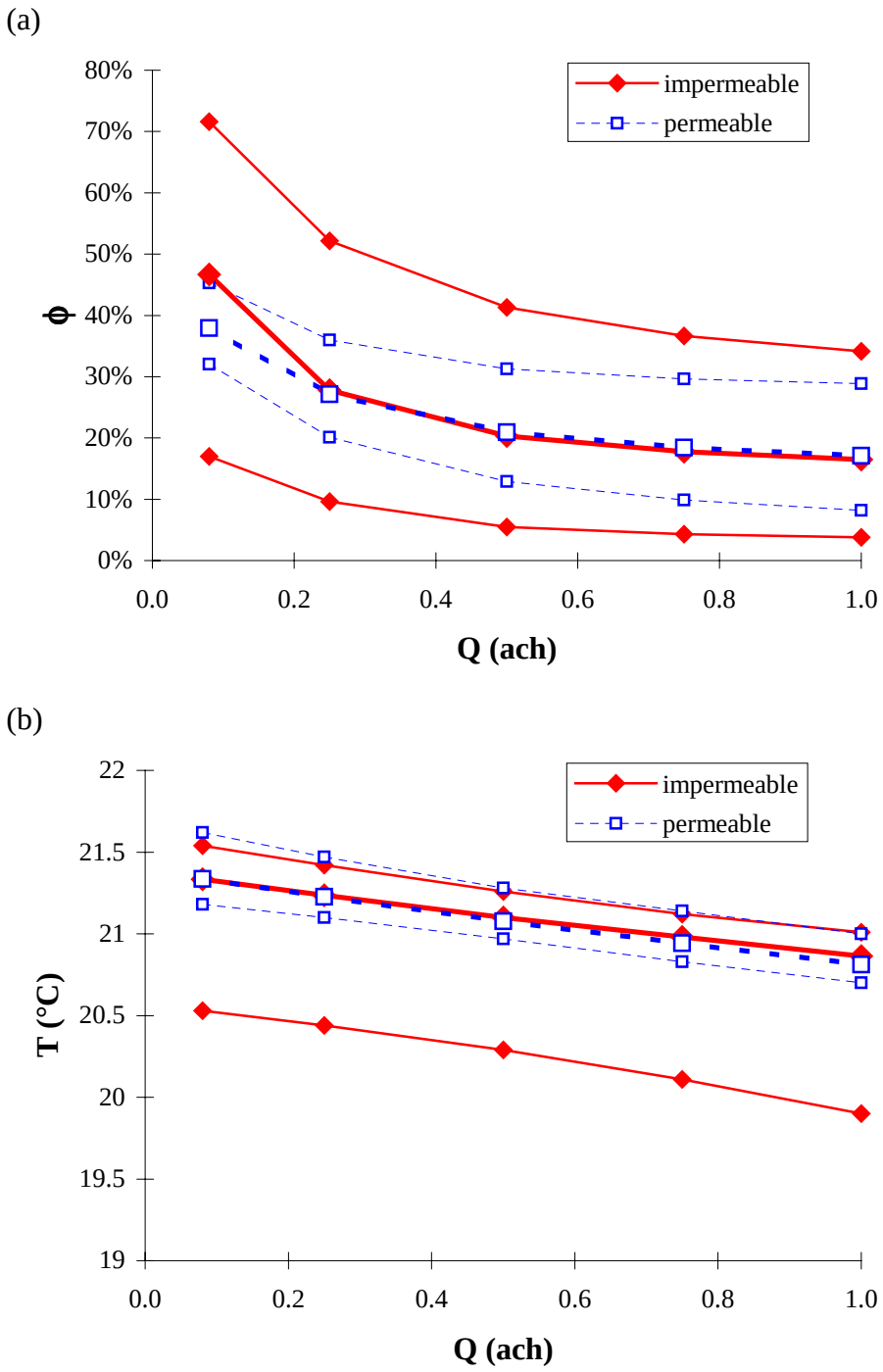

Figure 37. Calculated average (thick lines), minimum and maximum relative humidity (a) and temperature (b) of indoor air in January as a function of ventilation rate. The solid lines are for a room with vapour tight paint and the dashed lines are for a room with vapour permeable paint.

The results in Figure 36 and Figure 37 show that walls without a vapour retarder at the internal surface and with vapour permeable materials allow vapour to diffuse through the building envelope, which will lower the humidity in the indoor air for low

ventilation rates, especially during the summer months. As a result, even the maximum humidity for the permeable case is less than the average humidity for the impermeable case when the ventilation rate is low (0.08 ach). The average indoor relative humidity is significantly lower in January than in July and, typically, the average humidity is slightly higher in the case where an impermeable paint prevents moisture transfer between the indoor air and the structures. At a ventilation rate 0.08 ach, the difference between the average humidity in the permeable and impermeable case is 9% RH in January and 16% RH in July, while the difference reduces to 1% RH in January and 3% RH in July at a ventilation rate of 0.5 ach.

The fluctuation of indoor humidity is greater in the impermeable case, but the fluctuation of indoor temperature is greater in the permeable case. The fluctuations in temperature are due to the coupling of heat and moisture transfer. When moisture is adsorbed in the structure, heat is released and the room temperature will increase slightly and, similarly, when moisture is desorbed from the structure, the room temperature will decrease slightly. The indoor temperature is generally warmer during the night and cooler during the day in the permeable case than in the impermeable case. The average temperature in January is the same in both cases, but the average temperature in July is 0.5 to 1.5°C higher in the permeable case depending on the ventilation rate. The ventilation rate also affects the level of indoor temperature and humidity. As Q increases, ϕ and T both typically decrease, but ϕ sometimes increases as Q increases in July and T is nearly independent of the ventilation rate in January because of the heating system.

The difference between the maximum and minimum relative humidities is always smaller for the permeable test case than for the impermeable test case, which shows that the hygroscopic mass is damping the changes in indoor humidity. This effect is most noticeable at low ventilation rates, but is significant at high ventilation rates as well. For all ventilation rates, the permeable test case shows lower maximum humidities in the summer and higher minimum humidities in the winter than the impermeable test case. During July, with a ventilation rate of 0.08 and 0.5 ach, the maximum humidity in the permeable case is respectively 32% RH and 18% RH lower than in the impermeable case. In January, with a ventilation rate of 0.5 ach, the minimum humidity is 7% RH greater in the permeable case than in the impermeable case.

It is important to note that Figure 36 shows a maximum humidity greater than 100% RH when the ventilation rate is 0.08 ach. This is a numerical value that would not occur in practice because condensation would occur on the interior surfaces of the room. This anomaly occurs because the simulation model includes the vapour resistance of the interior surface in the convective mass transfer coefficient. Therefore in the impermeable case, the convective mass transfer coefficient is very low and the moisture

transfer to the surface of the room is very slow and humidities above 100% are possible. This phenomenon could be more correctly accounted for in the model by separating the convective mass transfer coefficient and the surface resistance. To accomplish this, the interior surface of the wall would be treated as a separate node that is connected to the indoor air through the convective mass transfer coefficient and then this surface node would be connected to the rest of the wall through the resistance of the interior coating. This would allow surface condensation to occur even when the indoor coating has a high vapour resistance and would help keep the indoor humidity below 100% RH. However, during normal conditions when the indoor humidity is below 100% RH, this improved model would have essentially no effect on the results.

One disadvantage of the permeable case is that the average humidity is lower in the permeable case than in the impermeable case during the winter when the ventilation rate is low (i.e., less than 0.25 ach). Nevertheless, the average humidity is within an acceptable range in both cases. Another disadvantage of the permeable case is that the maximum summer temperatures are higher (2°C at 0.5 ach). Since the maximum indoor temperature is 2°C higher and the maximum humidity is 18% RH lower (at 0.5 ach) in the permeable case, the permeable case is expected to have a higher PAQ, but a similar thermal comfort as the impermeable case (section 1.1 showed that a 10% RH change is similar to a 2.2°C and 1.1°C temperature change for PAQ and thermal comfort respectively). The increase in temperature in the summer is due to phase energy that is released when moisture is adsorbed in the building envelope. On the other hand, when moisture is desorbed from the envelope, energy is required and this can have a cooling effect. The simulation results show this effect to be important for ventilation rates above 0.25 ach. The next section will address this issue with measurements.

3.4 Fluctuation of Indoor Temperature

In this test, the effect of solar radiation on the indoor temperature is investigated for north and south facing rooms in the house. The purpose of the test is to determine the ability of a wooden frame structure with hygroscopic material to damp the effect of solar radiation. The idea is that when solar radiation increases the indoor temperature, the relative humidity will decrease and moisture will be released from the building envelope. Since energy is required to desorb the moisture from the building envelope, this phase change will have a cooling effect on the room and increase the apparent thermal capacitance of the structure.

During the test presented in this section, the occupants were asked to keep the external windows and doors closed so the temperature could fluctuate freely in the house. This, of course, is not a true test of the performance of a naturally ventilated house, which

will need additional ventilation through open window in the summer. Tapanila ecological house is quite well protected from summer solar radiation and solar direct radiation passes through the windows for only short periods. The test was run from August 13, 1999 to August 31, 1999 and Figure 38 shows the indoor and outdoor temperature as well as the temperature of the external surface of the house on the north and south sides. The north side surface temperature is nearly equal to the air temperature, which varies between 5°C and 20°C. The south side surface temperature, on the other hand, is affected by the solar radiation and can be up to 20°C warmer than the air temperature. The temperature of the south surface of the house shows that most of the days were sunny, but there were a few cloudy days near the end of the test. The indoor temperature during the test varied between 20°C and 23°C.

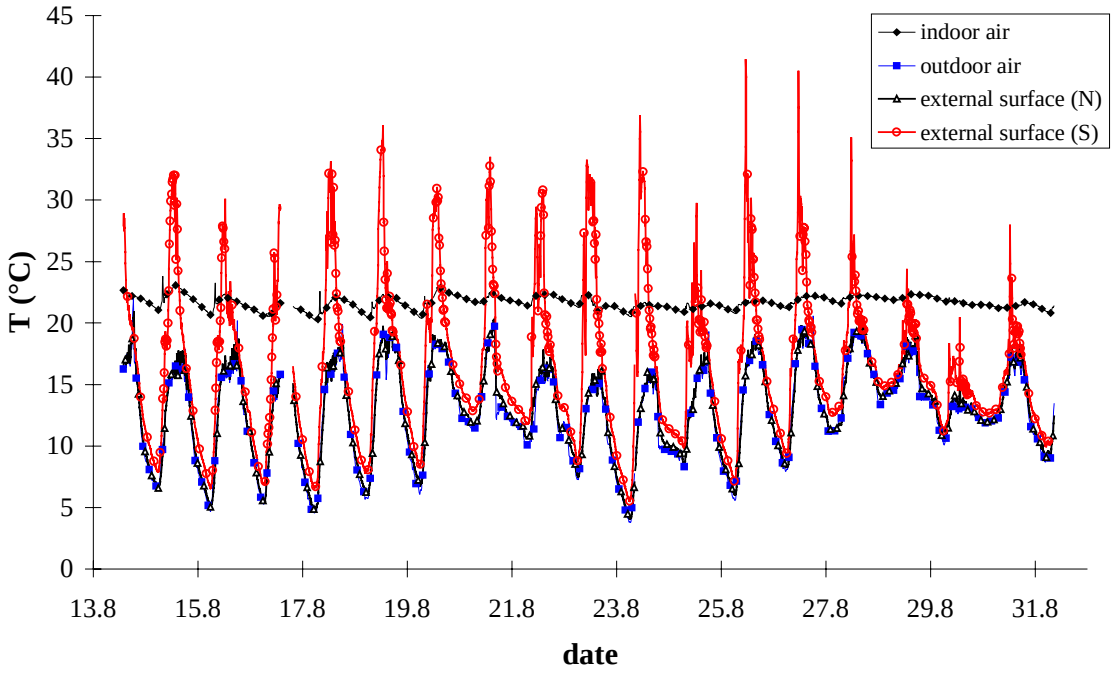

Figure 38. Temperature of outdoor air, north and south external surfaces and indoor air during the test.

During the test, the inside surface temperatures in the north-east bedroom on the first floor and the open area on the south side on the second floor were also measured. The sensors were placed on the floor, the external wall and for reference on the brick that formed an interior wall as shown in Figure 39. At each location, the sensors were positioned at a height of 0.5m and 1.5 m, but the average temperature will be presented because the difference between the two values was typically less than 0.5°C.

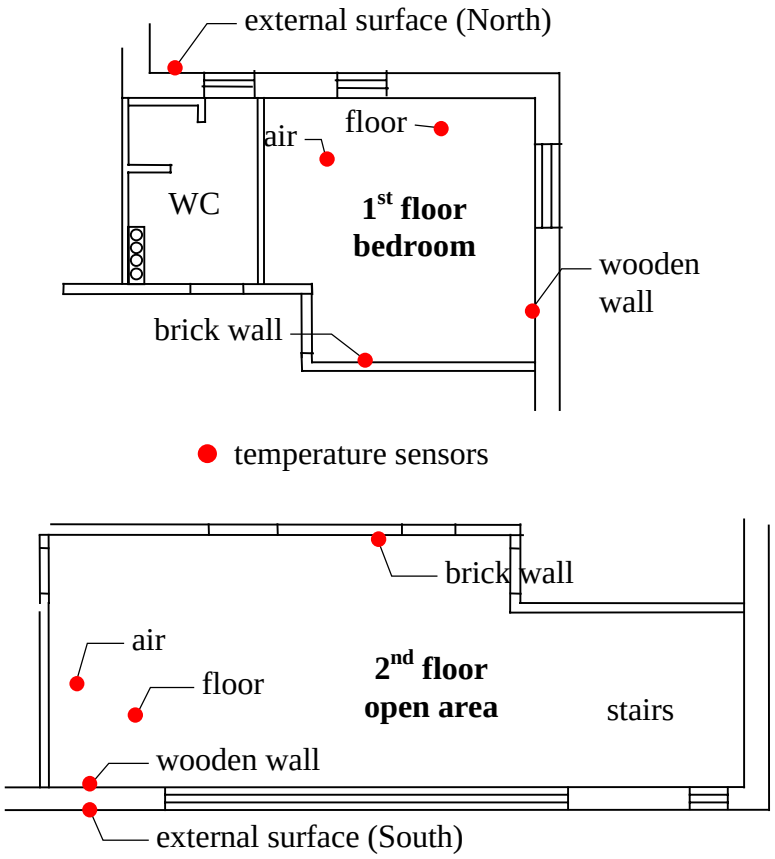

Figure 39. Location of the temperature sensors in the north and south rooms.

To show the variation in indoor surface and air temperatures, both sunny and cloudy days have been chosen for comparison. In both cases, the outdoor temperature is about the same and the main difference is the amount of solar radiation. The average of the external wooden panel temperature and the indoor air temperature on the north and south sides together with the outdoor temperature are presented in Figure 40. The effect of solar radiation is quite clear in Figure 40.

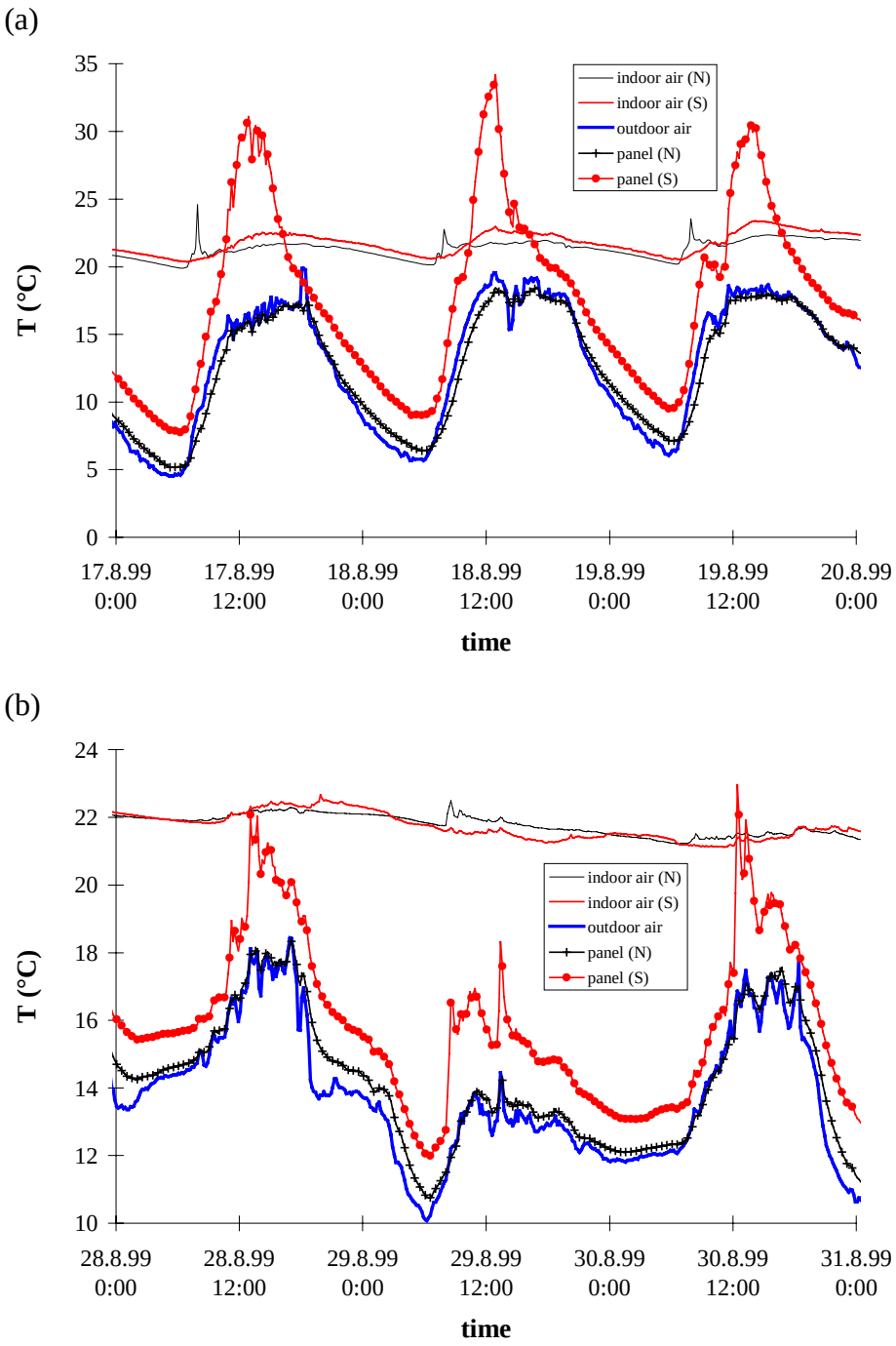

Figure 40. Temperature of outdoor air, north and south wood panel and indoor air during a sunny day (a) and a cloudy day (b).

Figure 41 and Figure 42 present the fluctuation of the indoor and surface temperatures for the north and south rooms on the sunny and cloudy days. In the south room, the temperature of the floor and wooden frame wall closely follow the temperature of the indoor air and show little thermal capacitance effect. The brick, on the other hand, is up to 0.8°C cooler than the indoor air during the afternoon and up to 0.8°C warmer during the night on the south (sunny day). The wooden wall is a maximum of 0.6°C warmer

and only 0.3°C cooler than the indoor air. During the cloudy days on the south side, the brick wall is almost always warmer than the air. This is likely because of the stored energy from the previous sunny days.

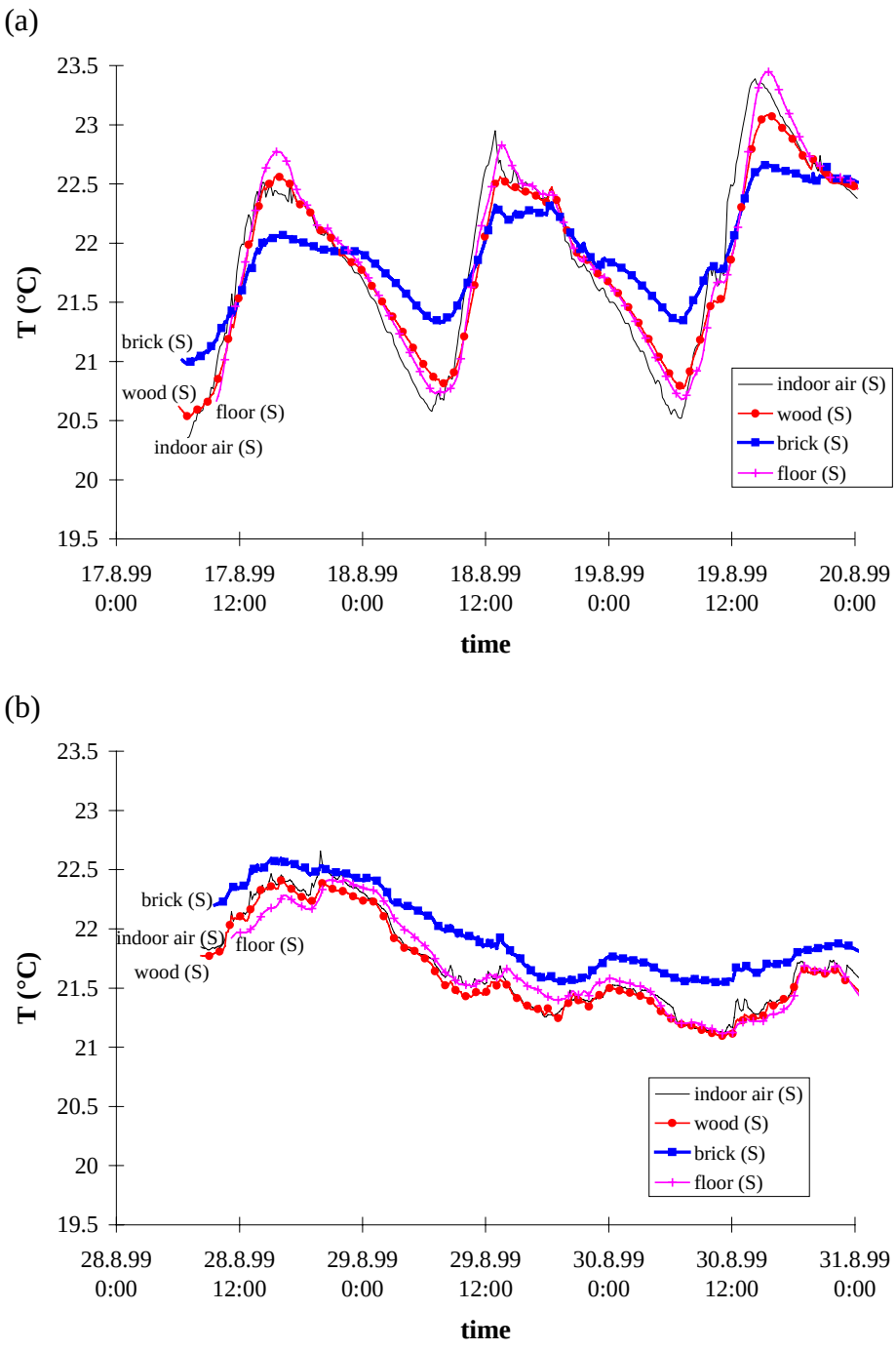

Figure 41. Indoor air and internal surface temperatures for the south room on sunny (a) and cloudy (b) days.

On the north side (Figure 42), the temperature of the wooden wall is always less than the temperature of the indoor air because it is continuously cooled by the outdoor air.

Even though the outdoor air cannot cool the brick wall because it is an interior wall, the brick wall is often colder than the wooden wall. These results can be seen more clearly in Figure 43 where the temperature difference between the various walls and the air are presented, where

$$\Delta T = T_{wall} - T_{indoor,air} \ . \tag{20}$$

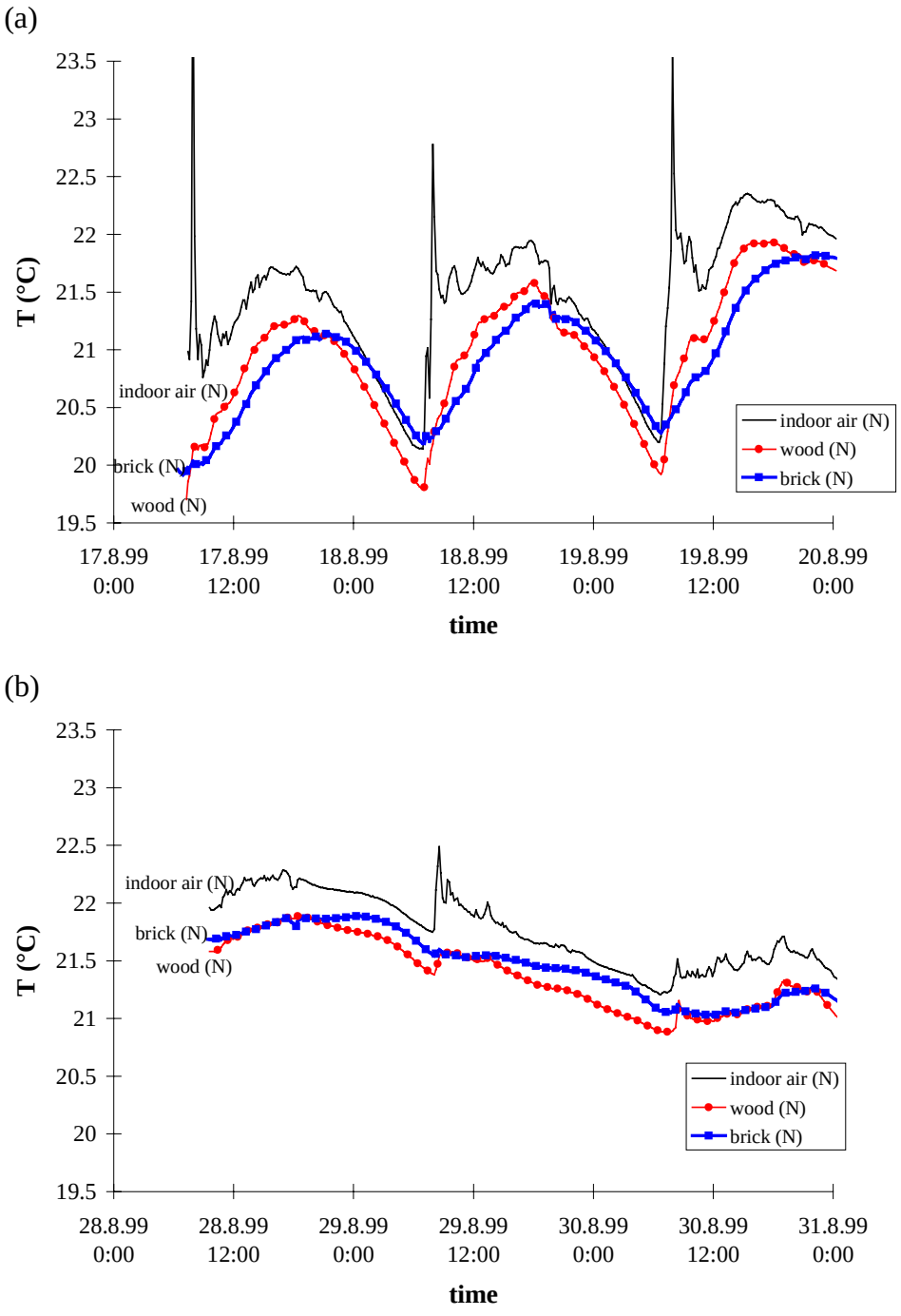

Figure 42. Indoor air and internal surface temperatures for the north room on sunny (a) and cloudy (b) days.

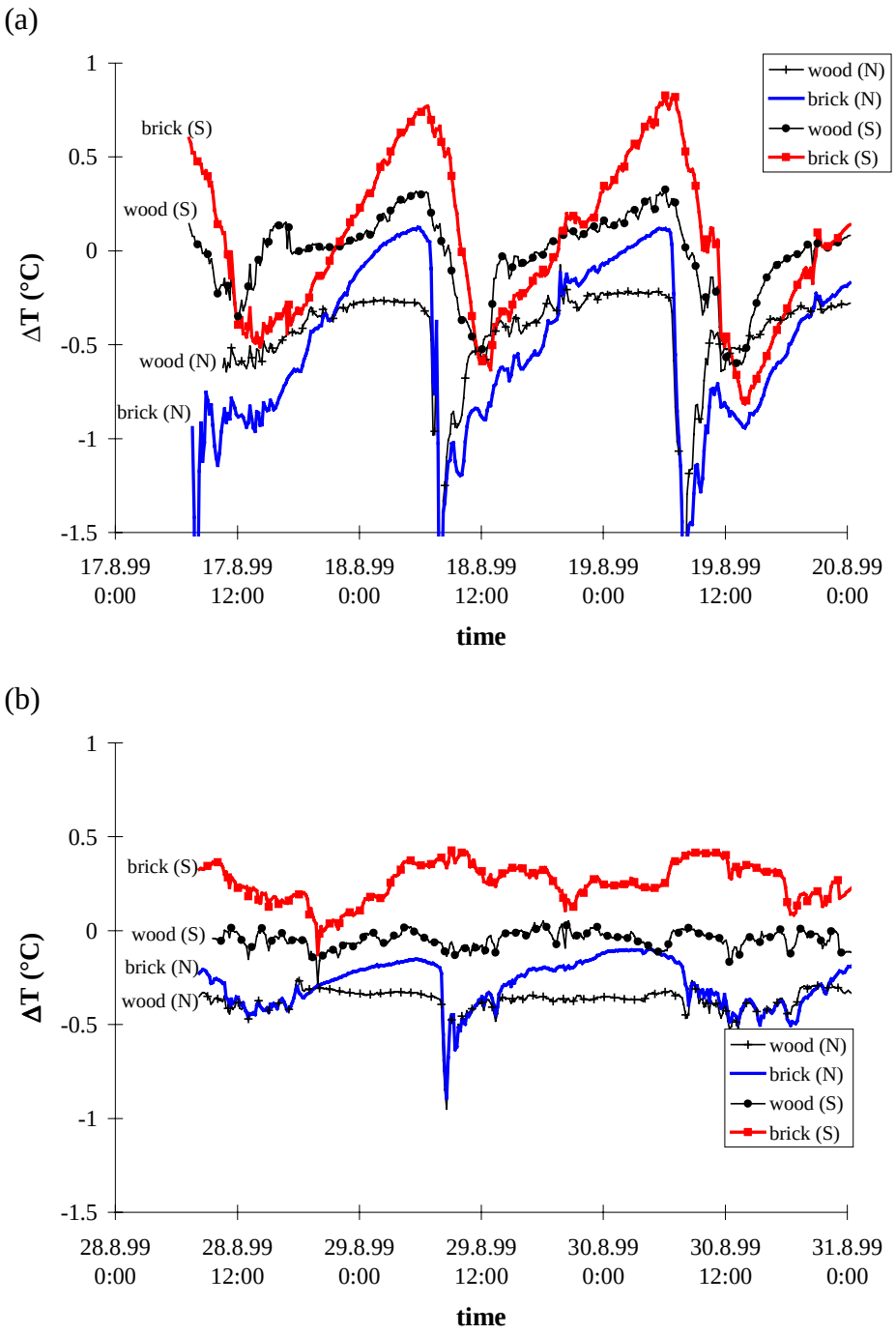

Figure 43. Temperature difference between the surface of the walls and indoor air during sunny (a) and cloudy (b) days.

Figure 43 clearly shows that the temperatures of the wooden wall follow the indoor air temperature quite closely. This can also be seen in Figure 44 where the frequency distribution of ΔT is presented for the entire 18 day test period. The wooden wall on the north and south sides show frequency peaks at $\Delta T = -0.4°C$ and $\Delta T = -0.1°C$ respectively. The values of ΔT for the brick walls show much more scatter, indicating a thermal capacitance effect.

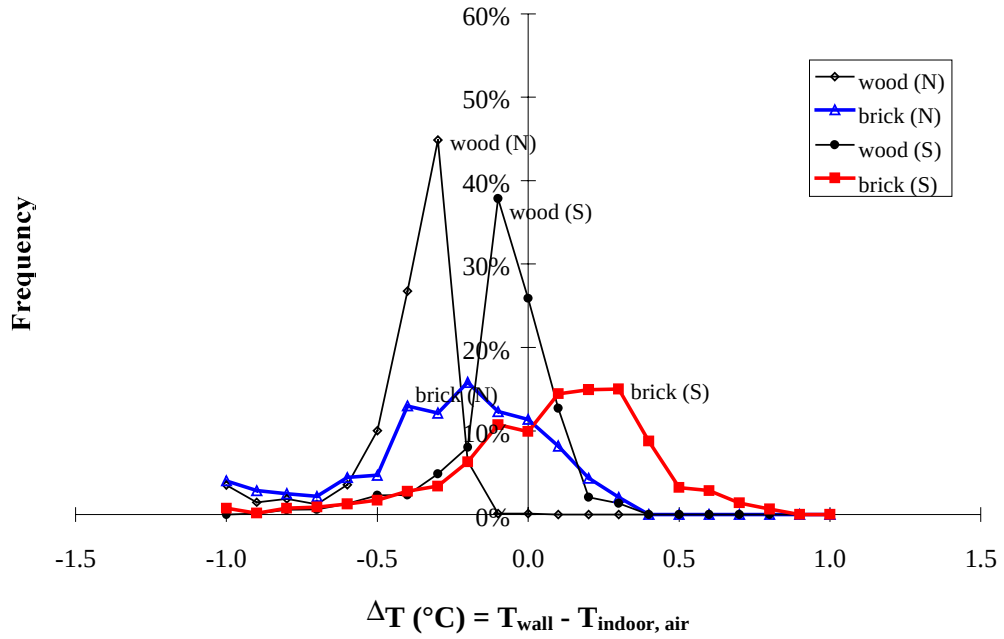

Figure 44. Frequency of temperature differences between the walls and the indoor air during the entire test.

One interesting result from these measurements can be seen on 25.8.99, which is the day when the temperature of the south facade is the highest. The measured temperatures on this day are given in Figure 45 and show that the indoor temperature rises quite rapidly from 21°C to 22°C (8:00 to 11:00). At this time, the indoor air temperature remains quite constant even though the external wooden panel temperature is quite high. These results indicate that the windows of the house may have been opened to increase the ventilation rate and cool the house. Discussion with the house owners tended to confirm this, which shows that opening the windows has a strong effect on the ventilation rate and consequently the indoor thermal conditions.

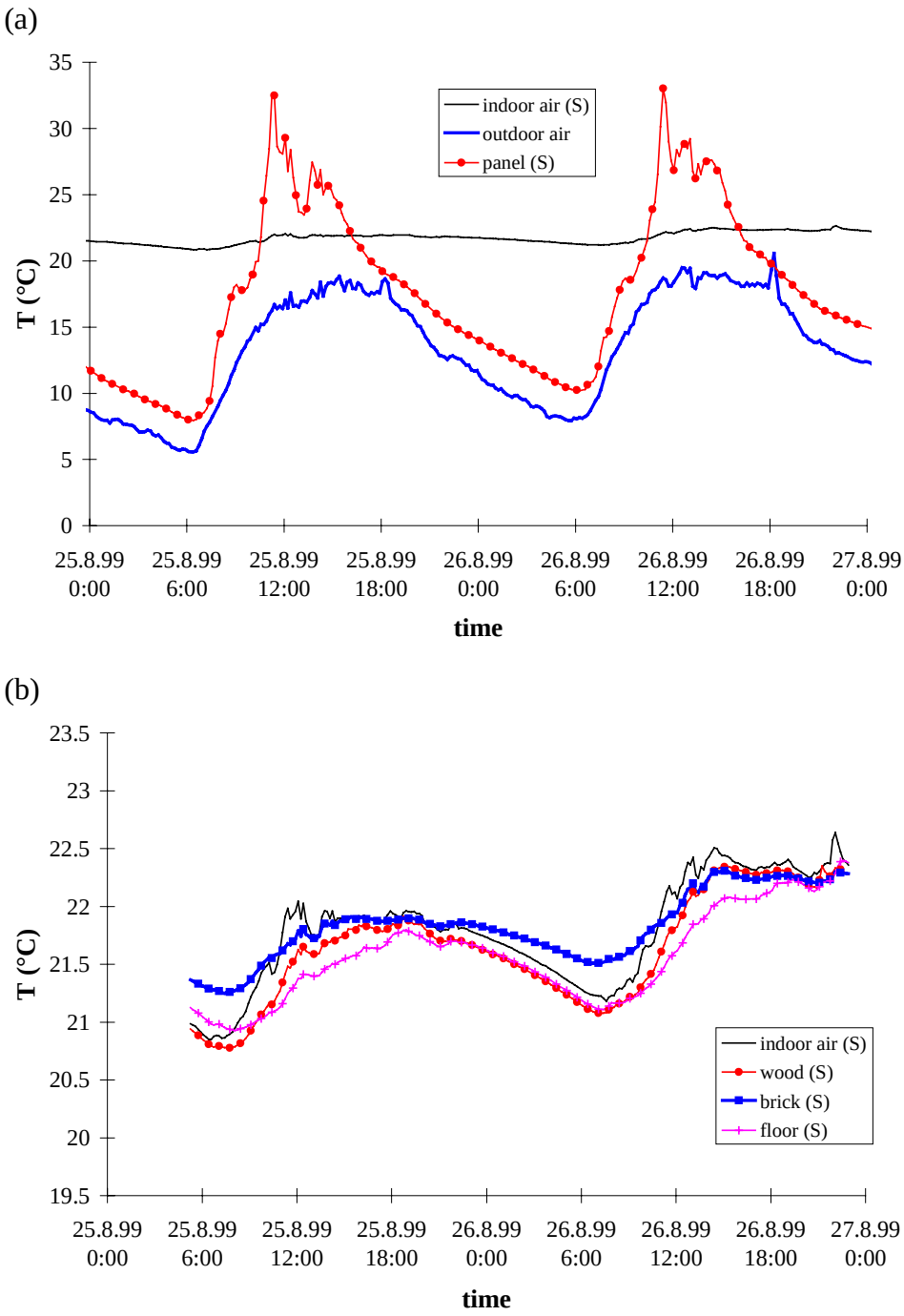

Figure 45. Temperatures of the outdoor air and wooden panel (a) and the indoor air and surfaces of the south room (b) when the windows are likely open during the day.

3.5 Measurements during Occupation

All of the previous tests presented in this chapter have been controlled in some way and do not necessary reflect how Tapanila ecological house will perform during normal occupation. Therefore, the purpose of this section is to present the indoor temperature,

relative humidity and concentration of CO_2 when the occupants of the house are uninhibited by experimental protocol. The measurement locations are shown in the house floor plans in Figure 46. The test room is the same second floor bedroom that was studied in sections 3.1, 3.2 and 3.3 and the open area of the second floor is the same as the south room studied in section 3.4. The first floor measurement location is in an opening located between the kitchen and the living room.

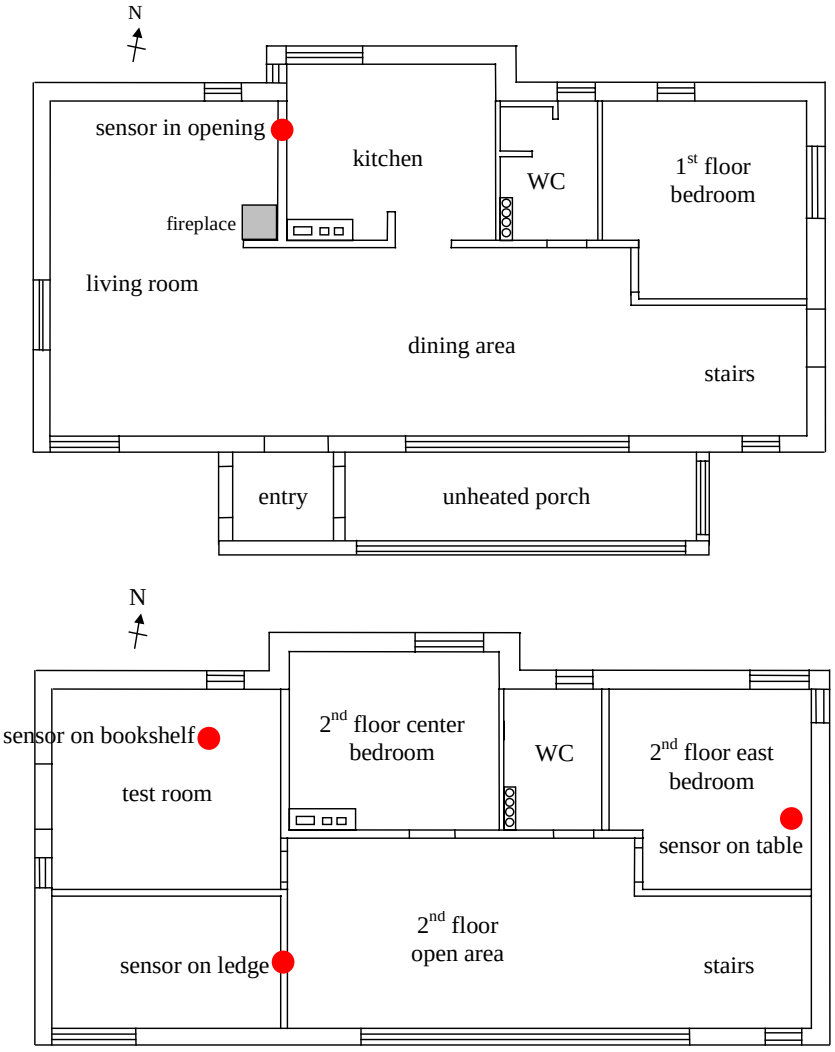

Figure 46. Location of CO_2, temperature and relative humidity sensors for the measurements during occupation.

3.5.1 Carbon Dioxide

Carbon Dioxide is a dangerous contaminant only at concentrations of 30000 ppm to 50000 ppm, but is often used as a surrogate for other occupant-generated contaminants (Janssen, 1994 and ANSI/ASHRAE Standard 62-1989). People at an activity level of

1.2 met produce 5 ml/s, which means that the steady-state indoor concentration of CO_2 can be calculated as follows,

$$C = \frac{QC_s + 5000}{Q} , \quad (21)$$

where Q is the ventilation rate is L/s and C_s is the outdoor concentration of CO_2 in ppm. At a ventilation rate of 7.5 L/s per person and an outdoor CO_2 concentration of 300 ppm, the indoor CO_2 concentration will be 1000 ppm. Therefore, indoor CO_2 concentrations below 1000 ppm are recommended and often indicate that the ventilation rate is satisfactory. Since the outdoor concentrations near Tapanila ecological house were measured to be nearly 400 ppm, a steady-state indoor concentration of CO_2 of 1650 ppm will indicate an outdoor ventilation rate of 4 L/s per person as required in the National Building Code of Finland – D2 (1987). If the average indoor concentration of CO_2 throughout the entire house is less than 800 ppm, then the air change rate for the house will satisfy the requirement in the National Building Code of Finland – D2 (1987) (i.e., 0.5 ach). Based on this, the measured CO_2 concentrations in Figure 47 indicate that the ventilation rate in the open area of the second floor is satisfactory because the CO_2 concentrations are always below 1650 ppm and generally below 800 ppm.

Figure 47 shows that the peak CO_2 concentration during the night is usually less than 800 ppm and the maximum CO_2 concentration is 1130 ppm, which is clearly acceptable. This means that the general ventilation rate in Tapanila ecological house is adequate and that there is likely good IAQ. The owners of the house have personally commented on the good IAQ in the house. It is interesting to note that one of the highest concentration peaks occurs on February 19, which was the night before most of the family left for a holiday. During the following week, only the father was at home and the CO_2 concentrations reflect this with measured values usually less than 400 ppm.

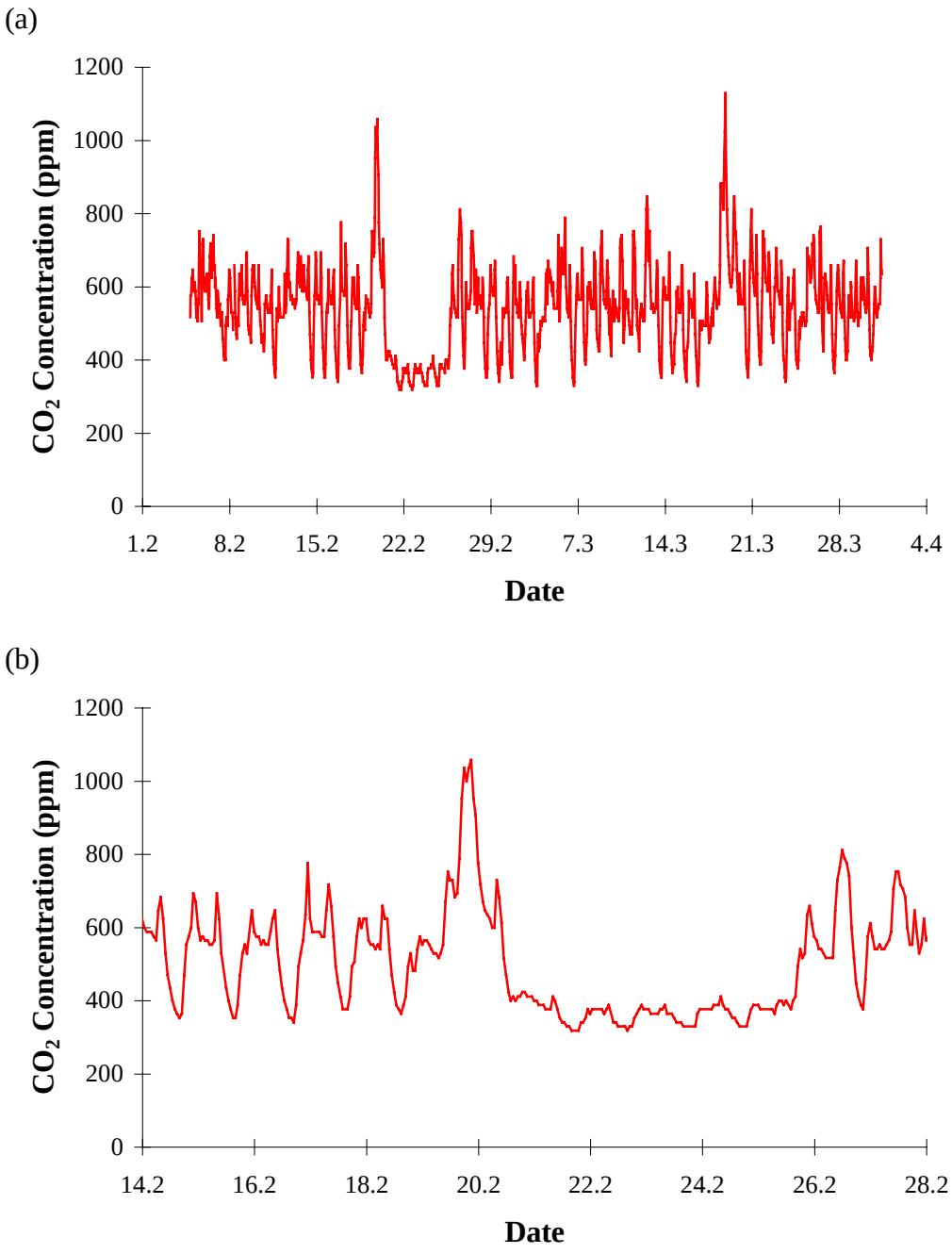

Figure 47. Measured concentrations of CO_2 in the second floor open area during February and March (a) and during a two-week period in February (b).

Even though the whole house ventilation and IAQ are acceptable, certain parts of the house may have poorer IAQ. The most likely place of problems is the second floor test room because the occupant likes to keep the bedroom door closed. There is no exhaust vent in this room, so the ventilation rate is expected to be severely limited when the door is closed, even though there is a crack below the door (~10 mm). As a result, the CO_2 concentration was as high as 1800 ppm as shown in Figure 48, which contains the measured CO_2 concentration in the test room during October to December.

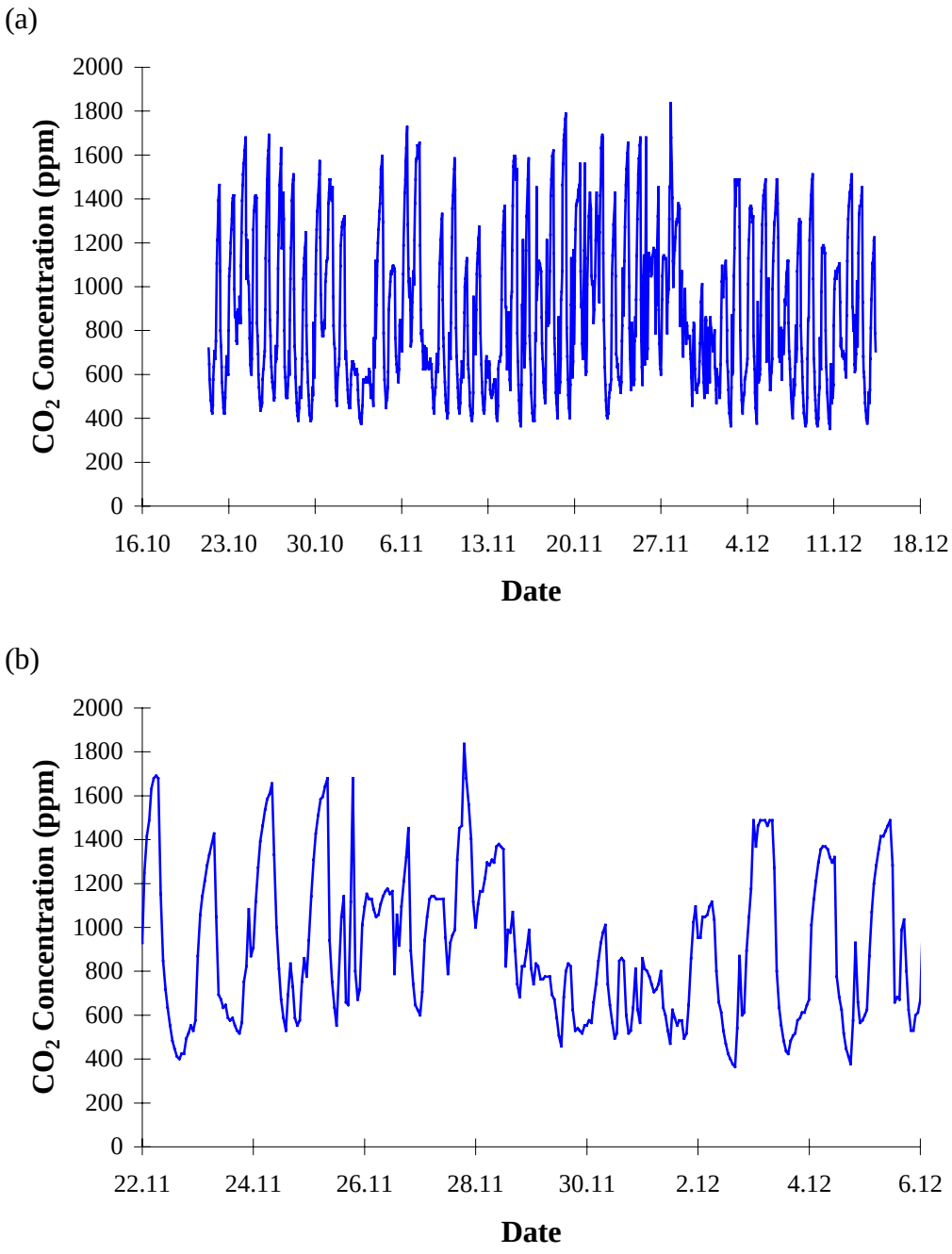

Figure 48. Measured concentrations of CO_2 in the second floor test room from October to December (a) and during a two-week period (b).

Figure 48 shows that the CO_2 concentration increases to about 1400 to 1600 ppm most nights and then decreases to about 400 to 600 ppm the next day. Using equation (21), the peak CO_2 concentrations indicate that the ventilation rate for the test room is about 4 L/s (0.5 ach for the test room). The CO_2 concentrations measured during the day in the test room are similar to the values measured in the open area (Figure 47). This shows that there is adequate mixing in the house during the day. It is also interesting to note that the CO_2 concentration remains below 1000 ppm from 29.11 to 2.12, indicating that

the bedroom door was left open these nights. When the door is open, the IAQ and ventilation rate appear to be significantly better than when the door is closed. Figure 49 compares the CO_2 concentration when the test room door is suspected to be open and closed.

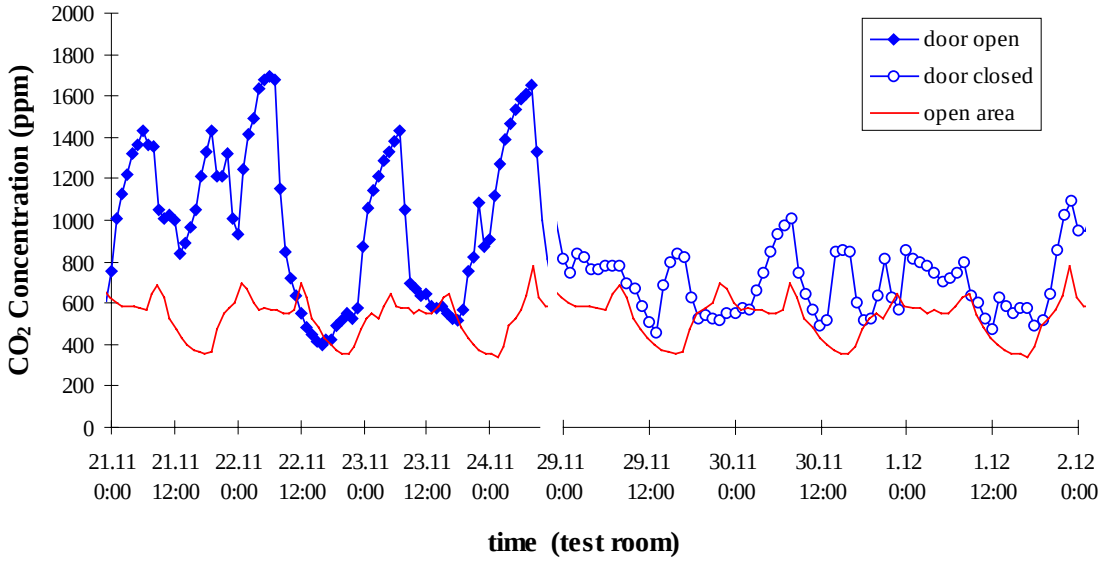

Figure 49. Concentration of CO_2 in the test room during a three-day period when the test room door is suspected to be open and closed. For comparison the concentration in the open area from 14.2 to 17.2 is included.

The concentrations of CO_2 were also measured during the summer and are presented in Figure 50. The results show that the concentrations of CO_2 in the living room and the first floor bedroom are usually between 400 ppm and 600 ppm, which are similar to those measured in the second floor open area during the winter (Figure 47). The measured concentrations are lower in the first floor bedroom than in the second floor bedrooms, even though there are two occupants in the first floor bedroom, because the occupants of the first floor bedroom keep the door and windows nearly always open. To compare the effect of having the bedroom doors open and closed, the bedroom doors were initially open for a few nights and then closed for a few nights as is evident in Figure 50. The peak concentration of CO_2 during the night was much lower when the bedroom doors were open and the measured concentrations of CO_2 were similar in both the test room and the east bedroom (both rooms have one occupant). Figure 50 shows that, during the summer, the CO_2 concentrations in the bedrooms have maximum values between 1400 and 1800 ppm when the doors are closed and between 800 ppm and 1000 ppm when the doors are open. These results are quite similar to those measured during the winter (Figure 48 and Figure 49), indicating that the actual ventilation rate in the summer is quite comparable to that in the winter. The reason for this is that the windows are often open in the summer.

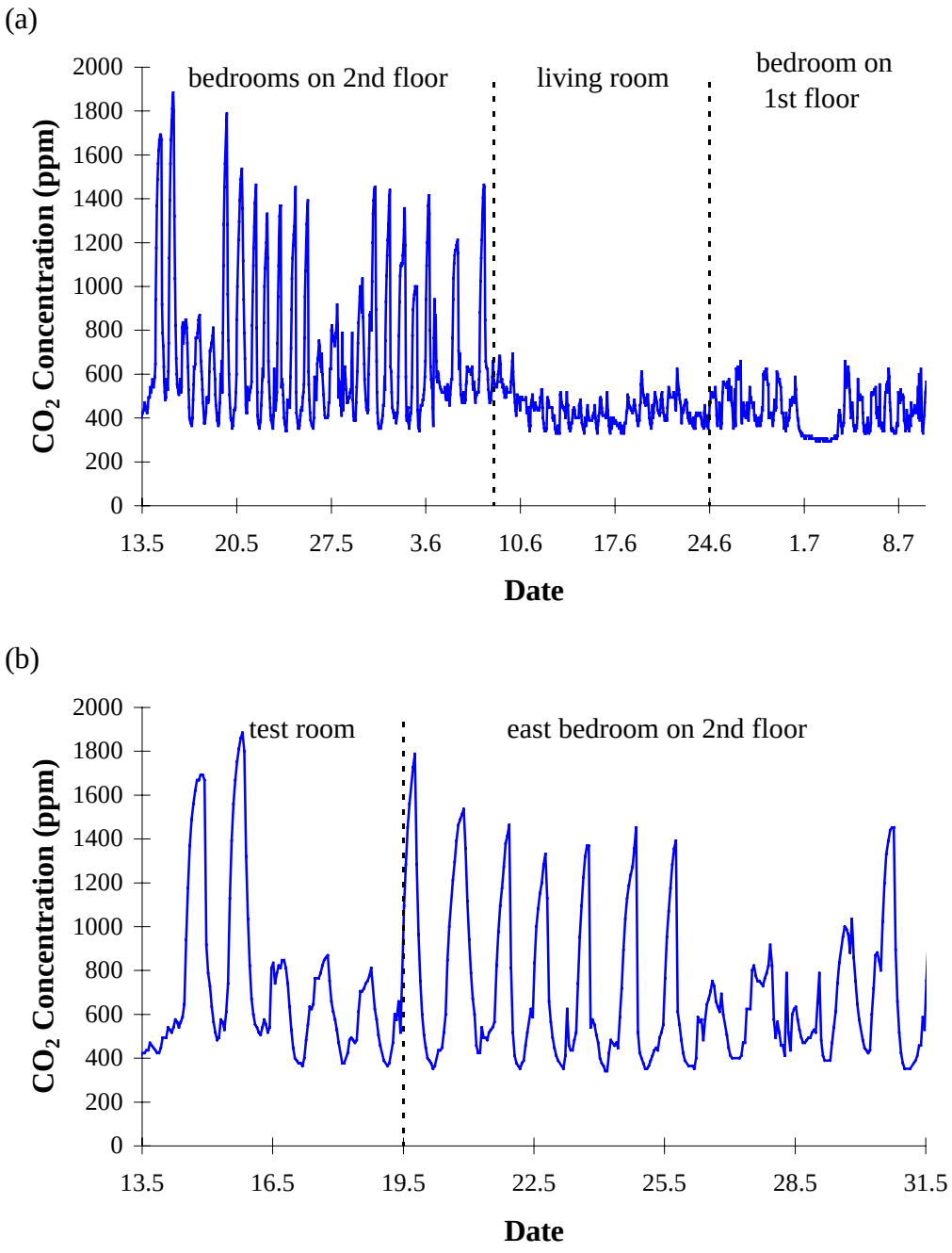

Figure 50. Measured concentrations of CO_2 in various rooms of Tapanila ecological house during the summer (a) and in two bedrooms during May.

3.5.2 Temperature

A moderate indoor temperature is also important for indoor comfort. To determine the indoor temperature in the summer and winter, the indoor temperature was measured for three months in each season. Figure 51 compares the measured indoor and outdoor temperatures where the indoor temperature is the average of all measurement locations.

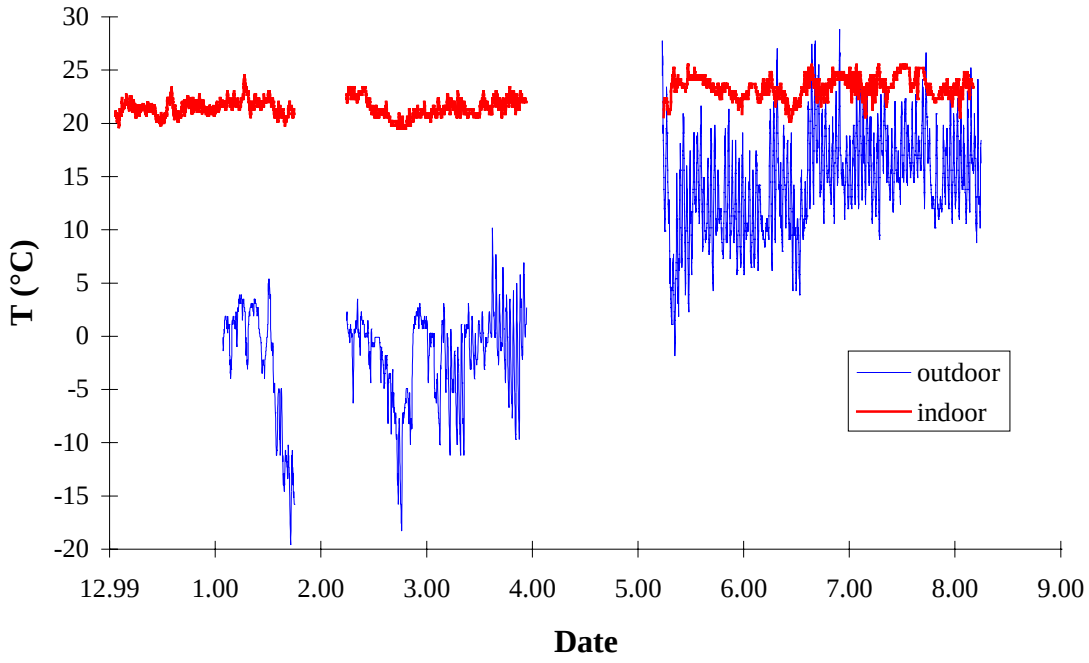

Figure 51. Indoor and outdoor temperatures measured at various times during the year.

The results in Figure 51 demonstrates that the indoor temperature is typically between 20°C and 23°C in the winter and between 22°C and 25°C in the summer. The measured temperatures indicate that the thermal climate is satisfactory for most of the time, except for some hot periods in the summer when the indoor temperature slightly exceeds 25°C. The owners of the house have also attested to this.

The difference between the temperature on the first and second floors and the temporal variation of indoor temperature can be seen more clearly in Figure 52. The difference between the first and second floor temperature is usually less than 1°C and the temperature on the first floor is greater than the temperature on the second floor. The reason for this somewhat unexpected result is that the temperature sensor on the first floor was located quite near the fireplace (Figure 46). The heat from the fireplace is clearly warming this temperature sensor and the temperature difference between the first and second floors is greater just after wood burning. This location is likely slightly warmer than the rest of the first floor, but the uniformity of temperature appears to be quite good.

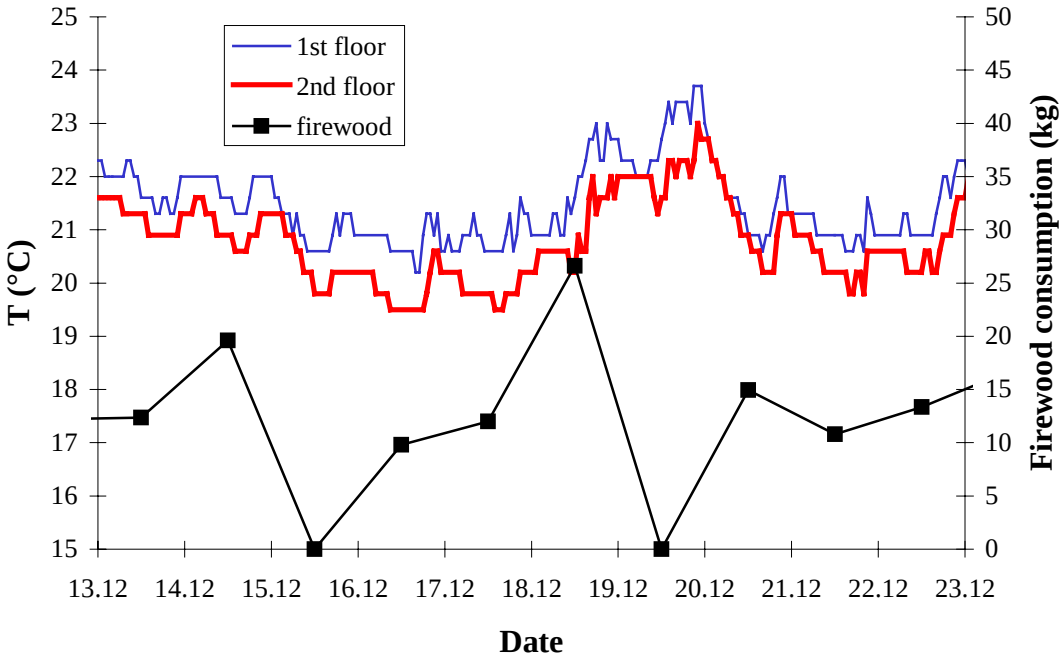

Figure 52. First and second floor temperatures and firewood consumption.

The transient change in indoor temperature after wood is burned in the fireplace is interesting to note in Figure 52. For example, on 18.12 over 25 kg of wood is burned in the fireplace increasing the indoor temperature by nearly 2°C. The temperature remains high for two days before cooling. After cooling, more wood is burned in the fireplace. These results show that it is possible to keep a good indoor temperature while burning wood for heat.

3.5.3 Relative Humidity

The relative humidity in the indoor air was measured during two months in the winter and summer and the results are in Figure 53. The average humidity in the winter was 21% RH with a standard deviation of 3% RH. In the summer, the average humidity was 30 % RH with a standard deviation of 7% RH.

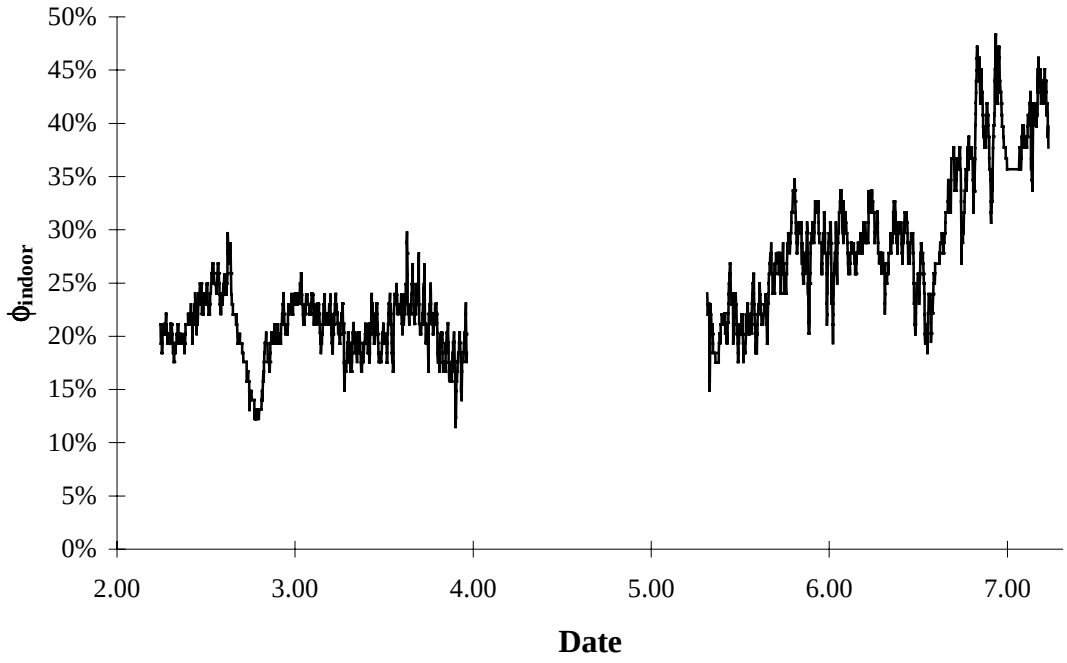

Figure 53. Measured relative humidities in the test room and second-floor open area during February to March and May to June.

In the winter, the humidity in the test room is slightly higher than in the second floor open area as shown in Figure 54. This is logical because the occupant of the test room usually keeps the door closed, which will decrease the ventilation rate and reduce the removal of moisture. The humidity in the house is quite stable during the winter except near the end of February when 4 of the 5 occupants left for a vacation. During the week vacation, the humidity decreases to nearly 10% RH. After the occupants return, the indoor humidity increases again.

The humidity in the summer shows more fluctuations, because one of the sensors was moved between different rooms together with the CO_2 sensor described in section 3.5.1 (Figure 50). The highest humidity values are measured near the end of June in the first floor bedroom, which is occupied by two adults. At this time the outdoor temperature is also quite high as can be seen in Figure 51.

Diurnal fluctuations in the indoor humidity can be seen Figure 54, which contains the indoor humidity during a two-week period in the winter and summer. During the summer, the humidity sensor was located in various rooms with open or closed doors and the concentration of CO_2 is also included in Figure 56(b) to show when the bedroom door is open or closed. A high concentration of CO_2 indicates that the door is closed and a low concentration of CO_2 indicates that the door is open. The maximum increase in humidity during the night ($\Delta\phi_{max}$) is nearly the same in the winter and summer, but is clearly influenced by the position of the bedroom door.

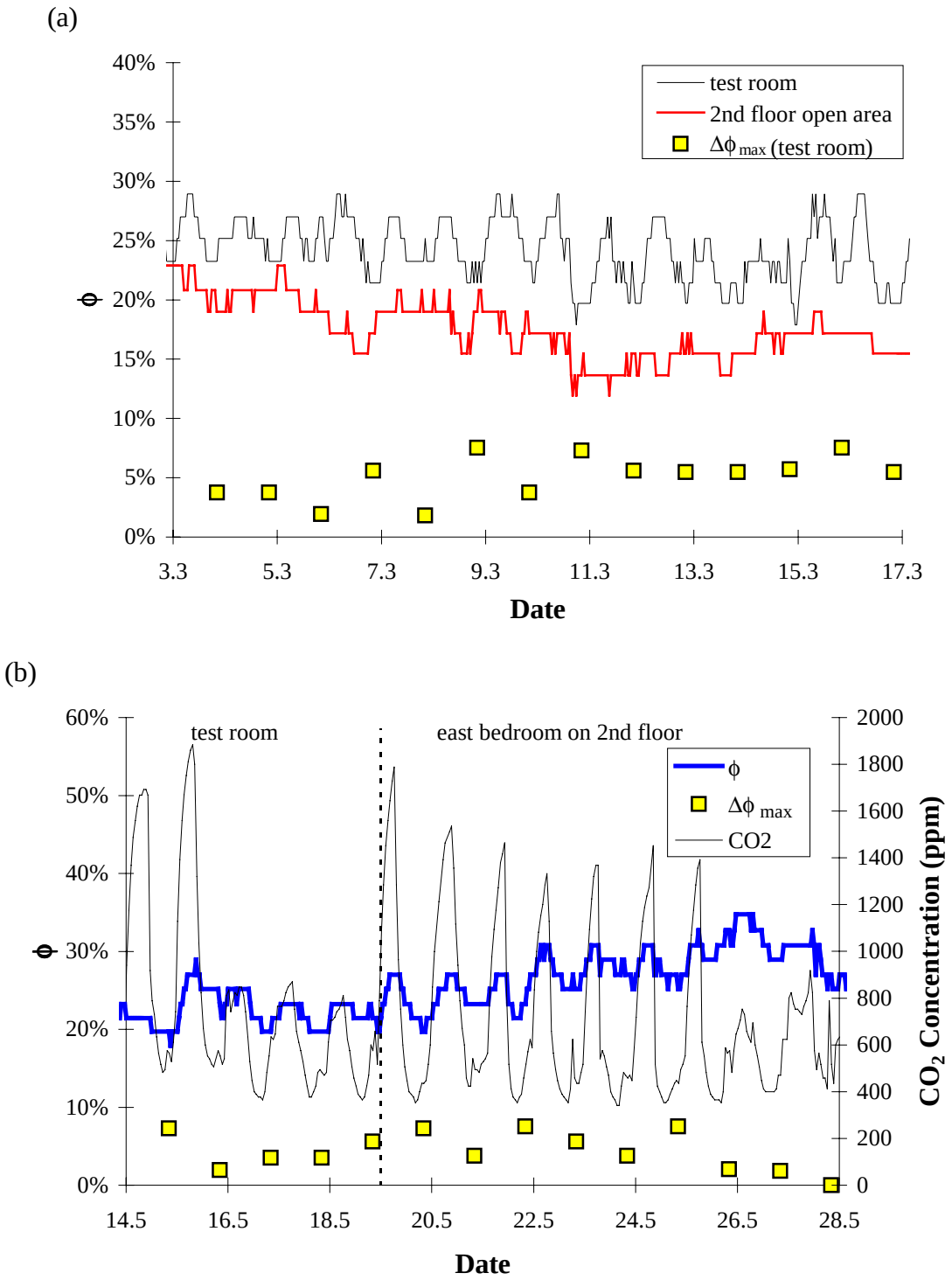

Figure 54. Indoor relative humidity during two weeks of occupation, showing the increase in relative humidity during the night for winter (a) and summer (b) conditions. The measured CO_2 concentrations are shown in the summer to indicate when the bedroom doors are open (high concentration) and closed (low concentration).

The diurnal fluctuations in indoor humidity are evident in Figure 54, especially in the bedrooms when the doors are closed. The relative humidity increases during the night

and decreases the following day. Since the relative humidity sensor was located in the test room for nearly 2 months during the winter (8.2.00 to 4.4.00), the maximum increase in humidity during the night ($\Delta\phi_{max}$) is presented as a frequency diagram in Figure 55. Here the indoor humidity at 20:00 is used as ϕ_o.

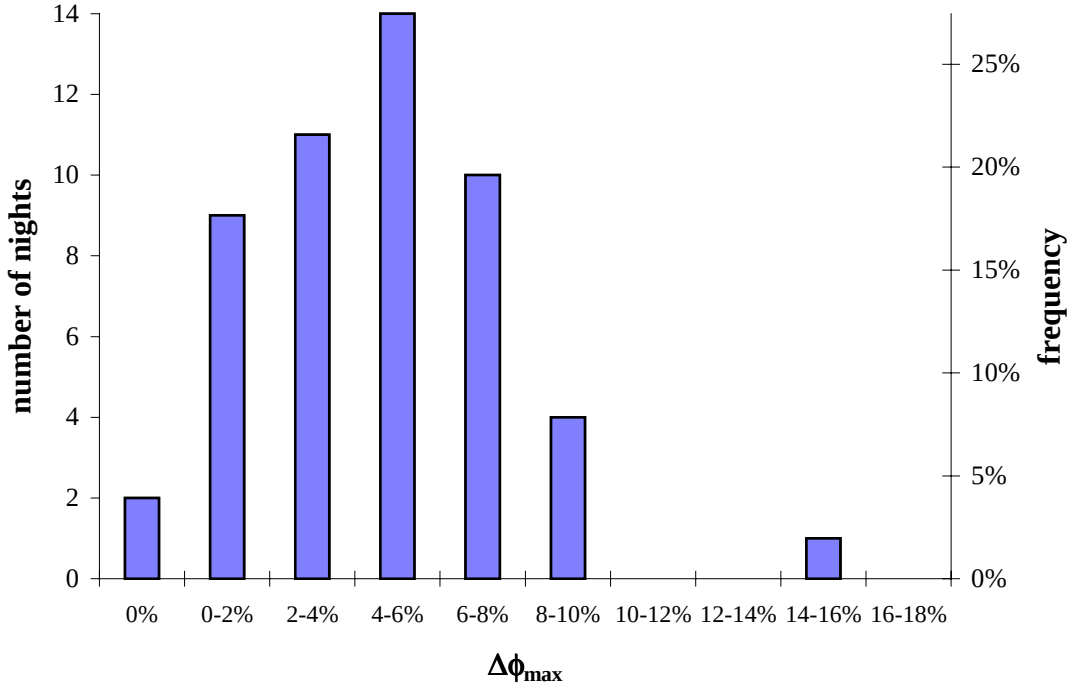

Figure 55. Frequency distribution of maximum increase in relative humidity during the night in the test room from 8.2.00 to 4.4.00.

Figure 55 shows that during 2 nights the increase in humidity during the night was 0% RH (i.e., there appeared to be no occupant in the room, or the outdoor humidity decreased significantly). The maximum value of $\Delta\phi_{max}$ is 14.6% RH, but $\Delta\phi_{max}$ is greater than 10% RH during only one night. The most common value of $\Delta\phi_{max}$ is between 4% and 6% RH, which occurred 14 out of 51 nights or 27% of the time. The average value of $\Delta\phi_{max}$ is 5.1% RH and the standard deviation is 2.8% RH. To compare the results in Figure 55 to those measured during the controlled experiments in section 3.3.1, the ventilation of the test room must be estimated. Since the average temperature during the measurement time was –2°C, the expected ventilation rate of the house is about 0.35 to 0.4 ach (see Table 6 or Figure 75 in Chapter 5). However, since the test room door is often closed, the ventilation rate in the test room will be significantly lower and likely about 0.25 ach. From Figure 32 in 3.3.1, the value of $\Delta\phi_{max}$ is about 10% to 15% RH at a ventilation rate of 0.25 ach. Considering that there is only one occupant in the furnished bedroom during normal occupation (in the experimental test of section 3.3.1, two occupants were simulated in the unfurnished room), the experimental results are quite comparable to the results measured during occupation.

Since the humidity sensor was moved between bedrooms in the summer, the frequency distribution for a single room is not meaningful, however, the summer measurements can be used to show the difference between having the bedroom door open or closed (Figure 56). In Figure 56 the value of $\Delta\phi_{max}$ has been normalised by the number of people in the room because the 1st floor bedroom has two occupants, while the rest of the bedrooms have one occupant. The average value of $\Delta\phi_{max}$ is 3.4% RH (standard deviation of 3.1% RH) when the bedroom door is open and is 5.2% RH (standard deviation of 2.2% RH) when the bedroom door is closed.

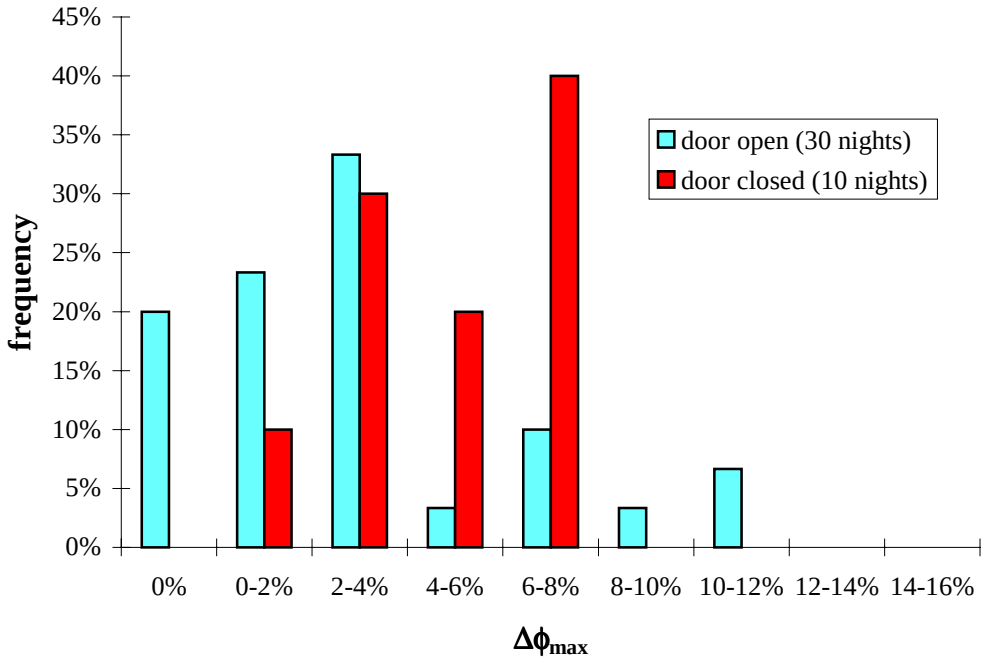

Figure 56. Distribution of maximum increase in relative humidity during the night in the summer showing the effect of an open or closed bedroom door.

3.5.4 Comparison with Other House

An interesting comparison between the CO_2 and humidity levels and fluctuations between Tapanila ecological house and a more conventional house was possible because the sensors were at the home of a VTT technician before they were placed in Tapanila ecological house. The CO_2 and RH sensors were located in the master bedroom of the technician's house (called other house here), where there were two occupants. In the Tapanila ecological house, the CO_2 sensor was located in the second floor open area and the RH sensor was located in the second floor test room. The other house has a mechanical exhaust ventilation system that is expected to have an air change rate less than 0.5 ach (about 0.3 to 0.4 ach). The house was built in the 1978 and has 150 mm of fiberglass insulation and a plastic vapour retarder. Figure 57 presents the

concentration of CO_2 and relative humidity, showing when the sensor was placed in Tapanila ecological house.

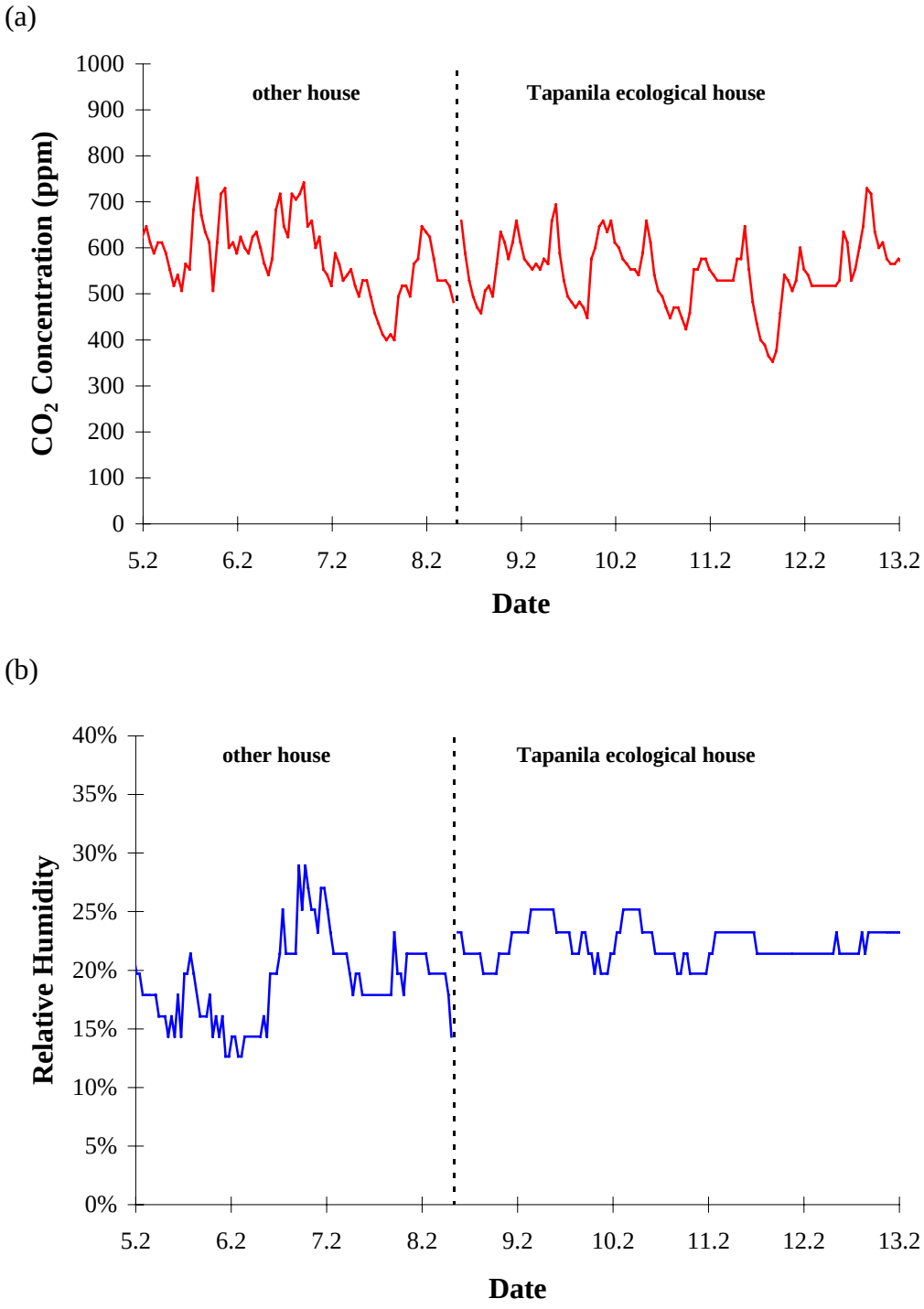

Figure 57. Concentration of CO_2 (a) and relative humidity (b) measured in Tapanila ecological house and another house.

Figure 57 shows that the concentration of CO_2 is very similar in the both houses, but the relative humidity is significantly different. Since the concentration of CO_2 reflects the outdoor ventilation rate per person, these results indicate that the ventilation rate per person in both houses is similar and adequate because the concentration is below 1000 ppm. The average relative humidity in both houses is also similar (~20% RH), but the increase in humidity during the night is clearly smaller in Tapanila ecological house. The increase in RH (in Tapanila ecological house) is about 4% RH each day, while the other house shows values as high as 16% RH. These results are difficult to compare directly because there is one occupant in the test room of Tapanila ecological house and two occupants in the master bedroom of the other house. Furthermore, the ventilation rate in the test room of Tapanila ecological house is likely about 0.25 ach, whereas the ventilation rate in the other house is possibly 0.3 to 0.4 ach. Nevertheless, the results show an important difference between the houses, with the measurements from Tapanila ecological house being closer to the results without plastic in Figure 31 of section 3.3.1 and the measurements from the other house being closer to the results with plastic.

3.6 Summary

The measured and simulated results presented in this chapter show that mass transfer between indoor air and a porous building envelope can affect the indoor concentration of CO_2, SF_6 and water vapour, which can improve the indoor air quality and climate. The diffusion of gases through the building envelope significantly increases the effective ventilation rate for poorly ventilated rooms, but only moderately increases the effective ventilation rate for well ventilated rooms. The measurements showed that the diffusion of CO_2 through the envelope increases the effective ventilation rate by as much as 140% for a low ventilation rate (0.08 ach) and by about 10% when the ventilation rate is near design (0.5 ach). However, the diffusion of CO_2 is greater than the diffusion of a gas with a larger molecule like SF_6 and the effective ventilation rate for SF_6 was measured to be from 35% (at 0.08 ach) to 8% (at 0.55 ach) lower than the effective ventilation rate for CO_2. The measured and simulated results showed good agreement.

The results in this chapter demonstrate that moisture transfer between indoor air and the building envelope has a significant influence on the indoor humidity for both poorly and well ventilated rooms. In the experiments, the sorption of water vapour in the bedroom walls reduced the peak humidity during the night by 15% RH at an average temperature of 27°C, which corresponds to 21% RH at 22°C. This lower humidity is significant and could possibly double the number of occupants satisfied with the indoor climate. The maximum increase in humidity during the night was 32% RH and 21% RH with plastic and 16% RH and 10% RH without plastic, when the ventilation rate was 0.08 and 0.55

ach respectively. This shows that, for these conditions, moisture transfer has a greater effect on the increase in indoor humidity during the night than increasing the outdoor ventilation rate from 0.08 ach to 0.55 ach because the increase in humidity was greater at a ventilation rate of 0.55 ach with plastic than at a ventilation rate of 0.08 ach without plastic. It is important to note that, in addition to affecting the increase in humidity during the night, ventilation also affects the level of indoor humidity as well as the indoor temperature and indoor air quality.

To expand on the experimental results, a numerical model is validated with the measurements and applied to investigate water vapour transfer and sorption for different weather conditions. These results show that water vapour transfer is very important during warm weather and can reduce the maximum indoor relative humidity in July by up to 30% RH when the ventilation rate is very low (0.08 ach), which would significantly improve comfort. When the ventilation rate is near design (0.5 ach), the maximum humidity in the permeable case is 18% RH lower than in the impermeable case. In January, with 0.5 ach, the minimum humidity is 7% RH greater in the permeable case than in the impermeable case. These numerical results complement the experimental results and show that the moisture capacity of the building envelope can damp the variations in indoor humidity during both summer and winter conditions. However, the effect of individual materials was not identified. In addition to reducing the maximum humidity in the summer and winter, moisture storage in building envelopes can, in fact, help avoid very low relative humidity in indoor air by releasing the stored moisture during dry outdoor conditions. The main disadvantage of the permeable case is that the average temperature in July is 0.5 to 1.5°C higher than in the impermeable case.

The porous walls in Tapanila ecological house can adsorb and desorb a significant amount of water vapour and the resulting phase change energy may increase the apparent thermal mass of the structure. Fluctuations of indoor temperature due to solar radiation were measured and the ability of the hygroscopic wooden frame structure to damp the effect of solar radiation was analysed. The results showed that the temperature of the lightweight walls in Tapanila ecological house followed the indoor temperature quite closely. There appeared to be little increase in thermal capacitance of the walls.

The final section in this chapter presents CO_2, temperature and humidity measurements during normal occupation. These results helped confirm the controlled experiments and numerical simulation. The CO_2 concentrations in the house were generally below 1000 ppm when mixing was possible, however when mixing was poor (such as when bedroom doors were closed), the CO_2 concentration approached 2000 ppm. These confirms that CO_2 diffusion alone is not enough to keep the concentration of CO_2 to an acceptable level. The indoor temperature was satisfactory and varied between 20°C and

25°C and was found to be quite uniform, despite the natural ventilation system and wood-burning fireplace.

The average measured relative humidity in Tapanila ecological house was 21% RH in the winter and 30% RH in the winter and summer. The diurnal fluctuations in indoor humidity were greater in the bedrooms (particularly when the doors were closed) than in the open area of the house. The increase in humidity during the night in the test room, which was occupied by one occupant, was on average 5% RH at an expected ventilation rate of 0.25 ach. These results compare favourably to those measured in the controlled experimental test, where the increase in humidity during the night for two occupants and a similar ventilation rate and temperature is approximately 10% RH to 15% RH.

4. Moisture Performance of the Building Envelope

As shown in Chapter 3, moisture transfer between indoor air and the building envelope can significantly impact the indoor climate. Moisture from indoor air can be stored in a porous building envelope and thereby reduce the peak indoor humidity. Even though this moisture transfer can improve the indoor climate and IAQ, it can be detrimental to the building envelope if it is uncontrolled. It is known that a vapour resistant layer on the inside of an insulated envelope in cold climates is needed to prevent excessive diffusion of water vapour from indoor air into the building envelope. However, the required magnitude of this vapour resistance has been debated in recent years. In this chapter, the moisture performance of building envelopes that have no plastic vapour retarder are analysed with field measurements and numerical simulations. The results show that the diffusion resistance of the internal surface should be greater than the diffusion resistance of the external surface (typically recommended ratio of 3:1 or 5:1), but that the vapour resistance of the vapour retarder can be significantly below that provided by polyethylene and still result in a safe structure, even in cold climates.

Moisture accumulation in building envelopes due to the convection and diffusion of water vapour from indoor air has been and continues to be an important issue, especially in cold climates (ASTM, 1994). Moisture accumulation can degrade the IAQ and building materials through mould growth, rotting, corrosion and other physical or aesthetic damage. To minimise convection moisture transfer, the building envelope should be made airtight and any exfiltration airflow should be very small (Ojanen and Kumaran, 1996). An airtight layer (often called air barrier) reduces air leakage through the building envelope, thereby improving the moisture performance, energy consumption and thermal comfort. Even with an airtight building envelope, the diffusion of water vapour may be significant and therefore it is important to have a layer that is resistant to vapour diffusion on the warm side of an insulated envelope in cold climates. The purpose of this layer (often called vapour barrier or vapour retarder) is to reduce the diffusion of moisture from indoor air into the building envelope to such a level that is does not cause problems. Naturally, in cold climates, a very high vapour resistance is safer (i.e., reduces diffusion moisture transfer more) than a very low resistance for an airtight envelope and often polyethylene vapour retarders are recommended and applied in practice. However, since a vapour permeable and porous building envelope can reduce the peak humidity, it may actually be safer than a vapour tight envelope when there are small air leakages through construction defects. Polyethylene also has a very low air permeance and therefore functions as both an air and vapour barrier. Because of its dual function, polyethylene is often specified and the safety of envelopes with air and vapour barriers other than polyethylene is often questioned. The purpose of this chapter is to present field measurements from Tapanila ecological house which demonstrate the safety of the structure. The field and numerical

results also illustrate the level of vapour resistance required to keep water vapour diffusion from causing a moisture problem in Finland. In this report, mould growth will be considered to be the most critical moisture concern, where the risk of mould growth depends on the temperature, humidity and time of exposure. Mould growth can occur at temperatures as low as 0°C (requires 100% RH) and humidities as low as 80% RH (requires temperatures greater than 15°C), but requires at least six weeks exposure to these conditions as shown in Figure 58 (Hukka and Viitanen, 1999 and Viitanen, 1996). For pine wood, the moisture content is about 0.16 kg/kg at 80% RH and about 0.28 kg/kg at 100% RH.

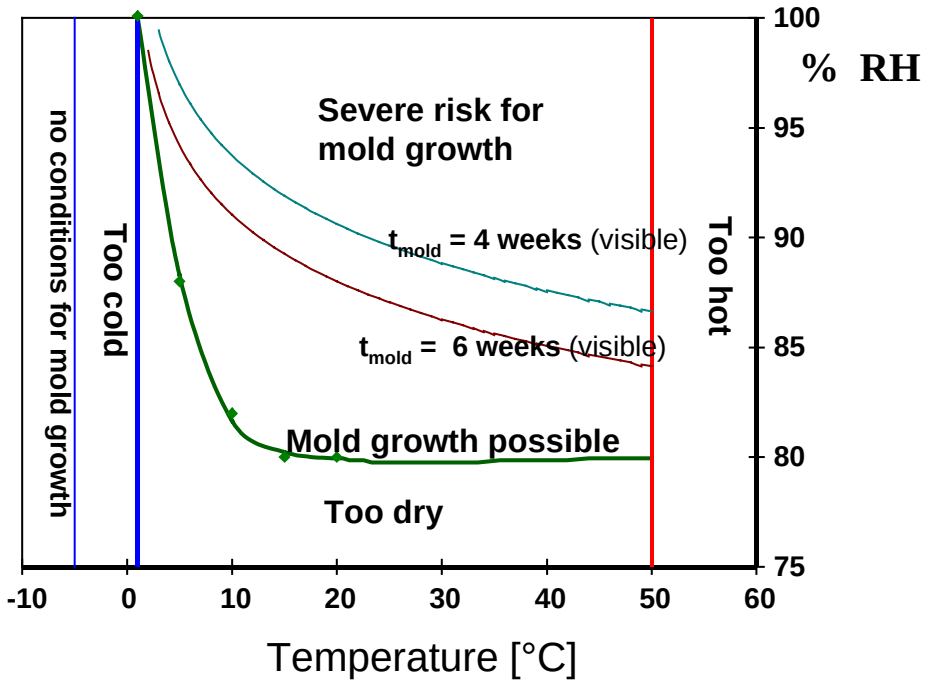

Figure 58. Temperature and humidity conditions necessary for mould growth (Hukka and Viitanen, 1999 and Viitanen, 1996).

4.1 Field Measurements

Tapanila ecological house has no plastic vapour retarder and the ratio of the internal to external vapour resistance is about 3 or 4:1 ($1.5 – 3 \times 10^9$ to $0.5 – 1.0 \times 10^9$ $m^2 \cdot Pa \cdot s/kg$ depending on humidity). To minimise convection mass transfer through the envelope, the house is well sealed with building paper. The air leakage through the envelope (excluding window and door seals) in one room was measured to be 1.5 air changes per hour (0.3 L/s per m^2 of surface area) at an underpressure of 50 Pa as shown in section 2.2 (Figure 14).

The moisture content of the wooden frames in the walls and roof were measured using electric resistance moisture pins near the interior and exterior sides of the envelope as shown in Figure 59. To obtain the greatest spread in moisture content, the moisture pins were located as close as practical (~15 mm) to the internal and external covering boards. The moisture content of the roof was measured on the north and south sides of the sloped roof (1:3) and in the north, south and east walls. The moisture content of the walls were measured near the top (200 mm from the ceiling) and near the bottom (200 mm from the floor). Only the walls on the first floor were measured. In all, 32 moisture pins were monitored and the uncertainty of the measured moisture content is expected to be ±0.02 kg/kg.

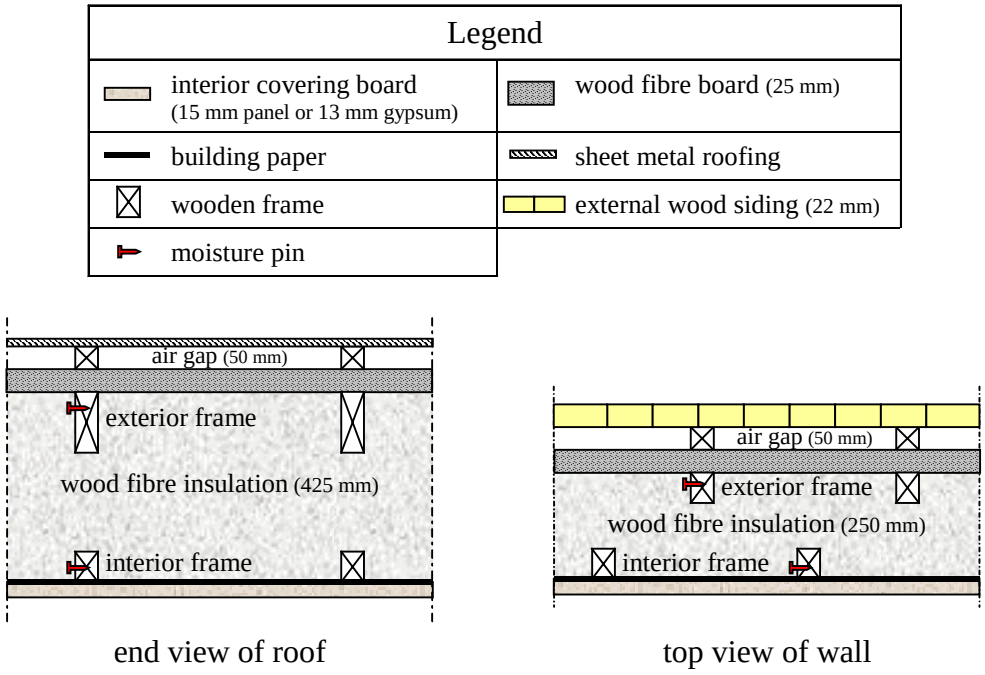

Figure 59. Roof and wall construction showing the location of moisture pins.

Even though there are many moisture measurements, only the maximum moisture content (u_{max}) at each location will be presented because this is the most important value when assessing moisture performance and the risk of mould growth. Table 5 lists the measurement locations and Figure 60 presents the measured results. When analysing the data, it was noticed that the moisture content was most significantly affected by the frame in which the moisture pins were located (i.e., internal or external frame). The moisture content on the north and south sides of the roof were very similar and are not presented separately. The exterior frame in the north and south walls, on the other hand, had slightly different moisture contents and are shown separately.

Table 5. Measurement locations and nomenclature.

Structure	Location	Nomenclature	number of moisture pins
Roof	external frame	Roof,e	8
Roof	internal frame	Roof,i	8
North wall	external frame	Wall,e (N)	4
South wall	external frame	Wall,e (S)	2
All walls	internal frame	Wall,i	8

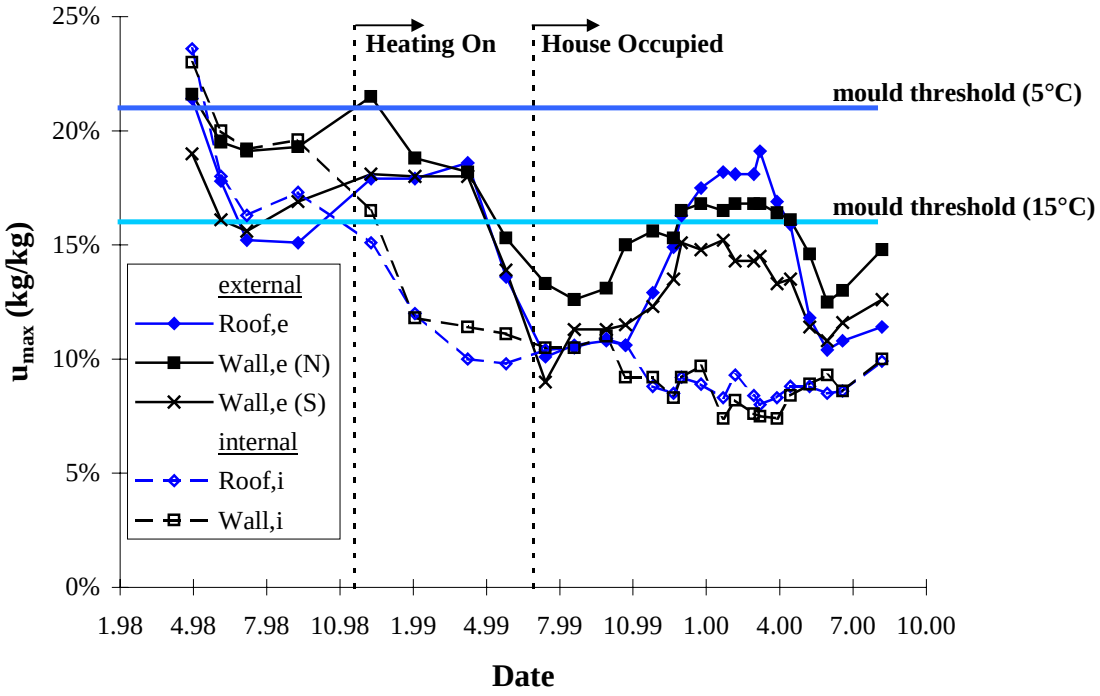

Figure 60. Maximum moisture content of the interior and exterior frames in the roof and walls.

The results in Figure 60 show that the moisture content was quite high (>20% by mass) when the moisture pins were installed in April 1998. Most of the construction dried below the mould threshold (80% RH, 0.16 kg/kg and 15°C) during the first summer, but the exterior frame of the north wall (Wall,e (N)) and the interior frame of all walls (Wall,i) had moisture contents as high as 0.19 kg/kg. Heating began in October 1998 and the interior frames dried to about 0.10 kg/kg during the first winter. The maximum moisture content of the external frames were between 0.18 kg/kg and 0.22 kg/kg during the first winter, but the house was not occupied. During the second summer, all the measurements were below the mould growth threshold (15°C) and the maximum moisture contents were between 0.13 kg/kg and 0.10 kg/kg. These results show that the

initial construction moisture dries after about two years. Since the measured moisture content during the second winter and spring are important because the house is occupied, these measurements are shown on an expanded scale in Figure 61.

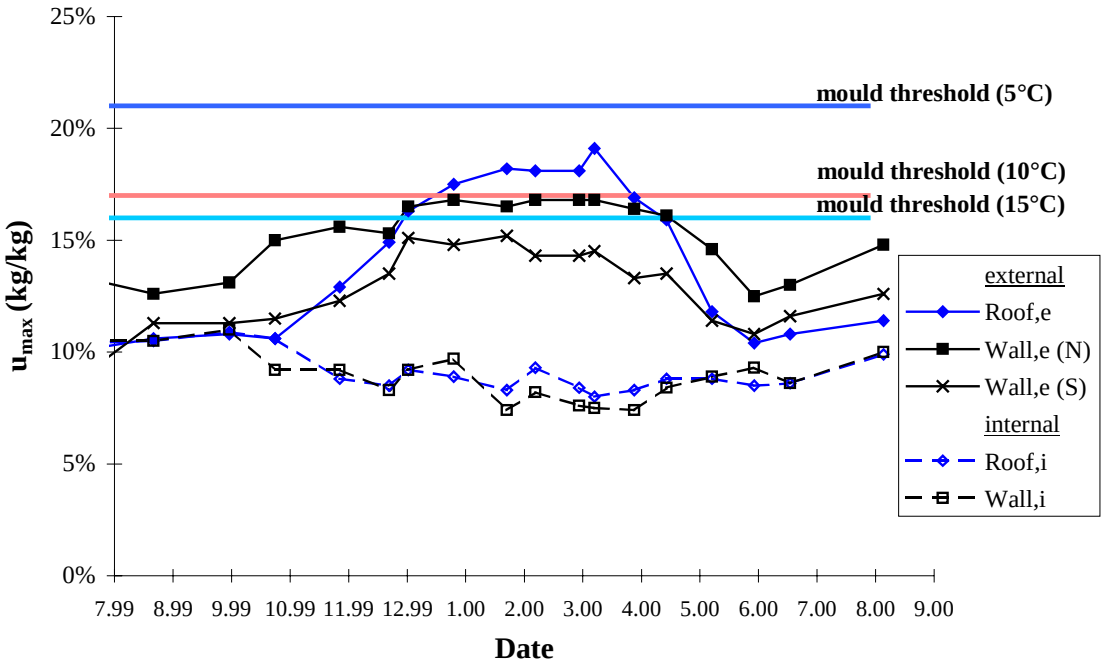

Figure 61. Maximum moisture content during the second winter and following summer.

The results in Figure 61 show that the internal frames remain dry, while the external frames accumulate moisture such that the maximum moisture contents in the roof, north wall and south wall are 0.19 kg/kg, 0.17 kg/kg and 0.15 kg/kg respectively. Since these maximum moisture contents are between the 15°C and 5°C mould thresholds, the temperature at the measurement points is critical. Figure 62 (a) shows that the temperature at the location of the maximum moisture content was between 0 and 6°C greater than the outdoor temperature and did not exceed the threshold for mould growth at the time of the moisture content measurement. Other temperature sensors positioned near the other external measurement points were 2 to 12°C greater than the outdoor temperature, depending on the solar radiation as shown in Figure 62 (b). It is important to note that the temperatures in Figure 62 are the measured temperatures at the time of the moisture content measurement, which was always during the day. Therefore, these values do not reflect the average temperature for the measurement period. Considering that the average temperature in Helsinki was about –3°C when the moisture content is above the mould threshold (January to March), the average temperature at the points of maximum moisture content will be below 5°C and mould growth is unlikely. The average temperature in Helsinki during January to March of the typical year used for energy calculations (1979) is –7 °C. This indicates that the winter of 1999–2000 was slightly milder. The moisture content will be slightly higher during a colder winter.

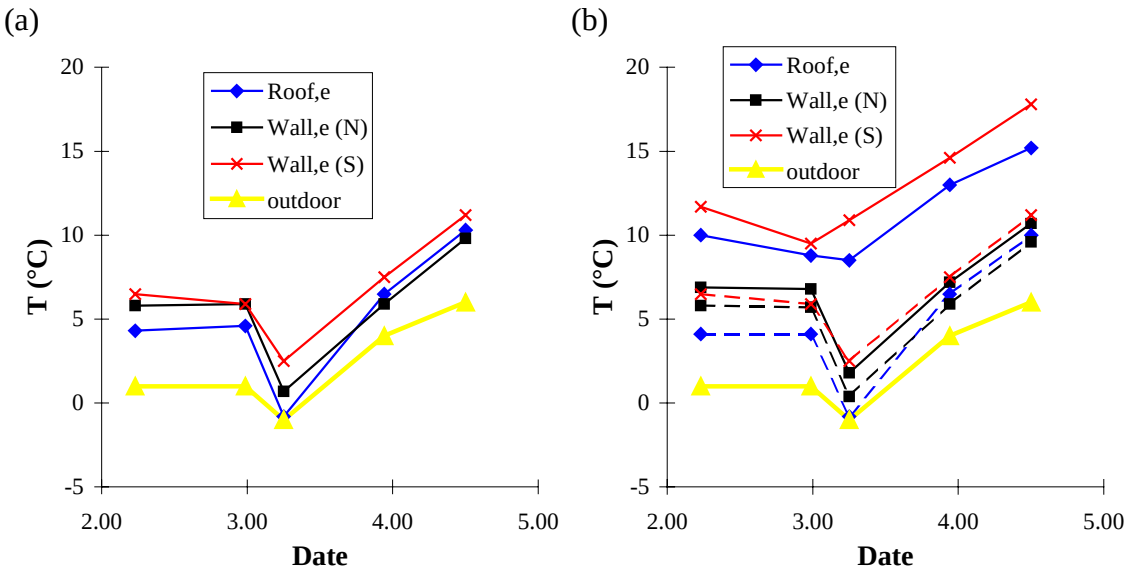

Figure 62. Measured temperature at the location of the maximum moisture content (a) and maximum (solid lines) and minimum (broken lines) temperatures (b) in each wall at the time of the moisture content measurement. These measurements were taken during the day and do not reflect the average temperature during the measurement period.

Figure 60 and Figure 61 also demonstrate some interesting features and one is that the initial moisture dries faster from the roof than from the walls during the first summer. Another is that the initial moisture content in the south wall dries faster than in the north wall and the moisture content of the external frame in the south wall is almost always a few percent by mass lower than the moisture content of the north wall. This is likely due to the drying caused by solar radiation. The moisture content of the east wall (not presented) is nearly always between the moisture content of the north and south wall and is quite close to the values for the south wall. It is also important to note that the roof has a slightly lower maximum moisture content than the walls during the summer, but a slightly higher maximum moisture content during the winter. The lower moisture content during the summer is likely due to higher solar radiation and the higher moisture content in the winter is likely a result of stratification of temperature and humidity in the house. These results show that the critical moisture point is likely the exterior frame in the north wall or the exterior frame in the roof.

4.2 Numerical Results

To supplement the field results, numerical results will be presented which demonstrate the moisture accumulation and drying of a wall with various internal and external water vapour resistances. These results were originally presented by Kokko et al. (1999) and were summarised by Simonson and Ojanen (2000). The analysis is made on a simple

one-dimensional wall that has no framing members but only mineral wool insulation and internal and external vapour resistances (Figure 63). This wall has a safety factor because the moisture capacity is lower than in actual walls and the thermal resistance of the external board is neglected (Ojanen, 1998 and Ojanen et al., 1997). The wall is perfectly airtight (i.e., no convection) and is subject to the boundary conditions shown in Figure 64. Initially the insulation is dry and the simulation starts on September 1.

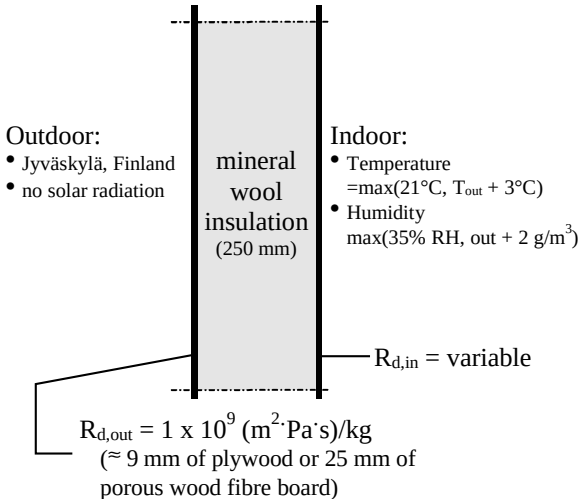

Figure 63. Wall construction and boundary conditions used in the numerical studies.

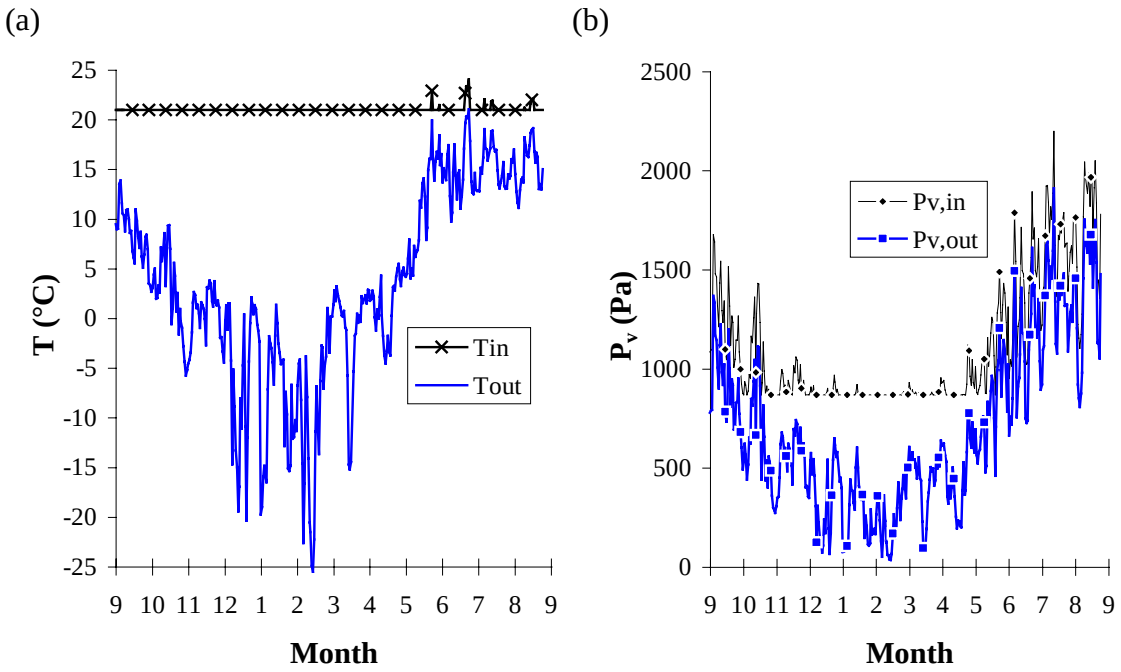

Figure 64. Temperature (a) and vapour pressure (b) boundary conditions used in the numerical studies.

The numerical model TCCC2D, which solves transient heat, air and moisture transport in building structures, is applied in this study. Details of TCCC2D can be found in the literature (ASTM, 1994 and Ojanen and Kohonen, 1995). The moisture content of the insulation and the external surface temperature are given in Figure 65 for different values of internal resistance. The external resistance is always 1 x 10^9 (m^2·Pa·s)/kg, which corresponds to about 9 mm of plywood or 25 mm of porous wood fibre board and the ratio of internal to external vapour diffusion resistance (R*) is defined as

$$R^* = \frac{R_{d,in}}{R_{d,out}} \quad . \tag{22}$$

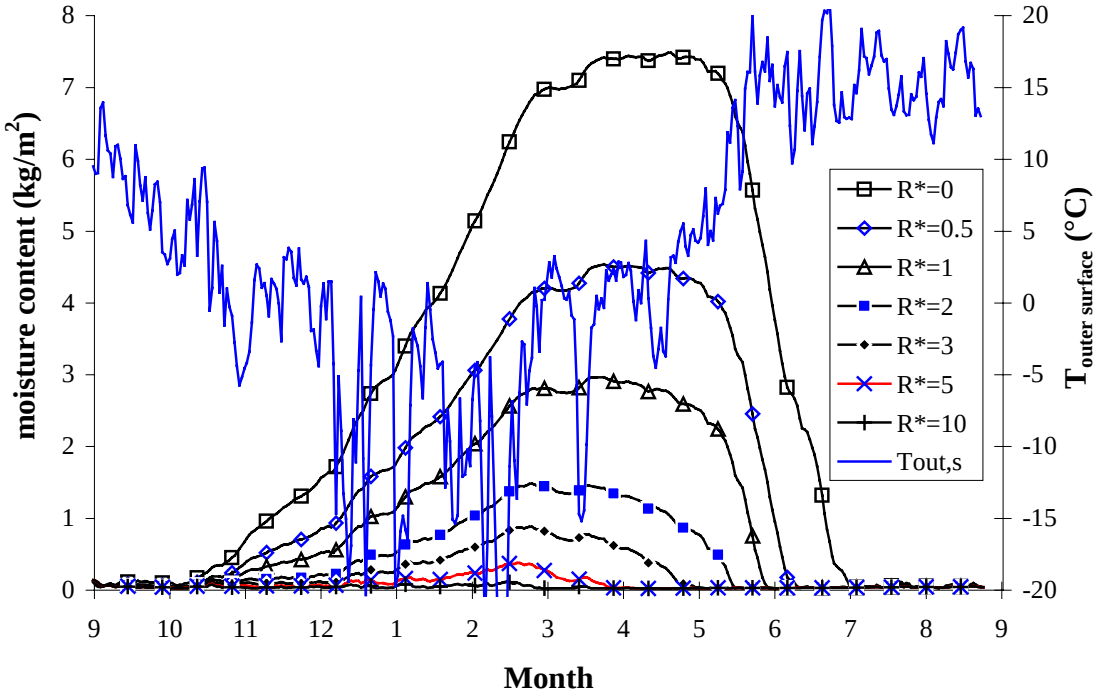

Figure 65. Moisture content of the 150 mm thick insulation and the corresponding daily average outdoor surface temperature.

The results in Figure 65 show that the moisture that accumulates in the winter dries during the summer regardless of the ratio of internal to external vapour resistance. However, as R* decreases, the maximum moisture content and drying time increase. When R* is less than 1, the moisture content of the insulation is high when the outdoor surface temperature warms to the point where it is always above 0°C (end of April), which means that mould growth is likely. If a plastic vapour retarder is applied ($R_{d,in} \approx 5$ x 10^{11} (m^2·Pa·s)/kg and R* = 500), essentially no moisture will accumulate in this ideal wall, yet with an internal resistance that is 100 times smaller than plastic ($R_{d,in}$ = 5 x 10^9 (m^2·Pa·s)/kg and R* = 5), the maximum moisture content in the winter is 0.4 kg/m^2 of wall area. If all this moisture accumulated in 10 mm of wood (density of 450 kg/m^3), the

increase in moisture content during the winter would be 0.09 kg/kg. Considering that the moisture content after summer is about 0.12 kg/kg (Figure 60 and Figure 61), the peak moisture content in 10 mm of wood is expected to be 0.21 kg/kg during the winter when R* = 5. The field measurements in Figure 60 and Figure 61 (R* ≈ 3 to 4) show similar maximum moisture contents during the winter. Figure 65 shows that, when R* = 5, the moisture will dry before the daily average temperature becomes consistently above 0°C.

Since mould does not grow when the temperature is below 0°C, moisture accumulation during the winter is permitted, provided it dries before the temperature gets too high in the spring. To demonstrate the drying of this ideal wall, the time that mould growth at the outdoor surface is possible (i.e., above the critical temperature for mould growth (0°C to 15°C) and above the corresponding critical relative humidity (80% to 100% RH)) is presented in Figure 66.

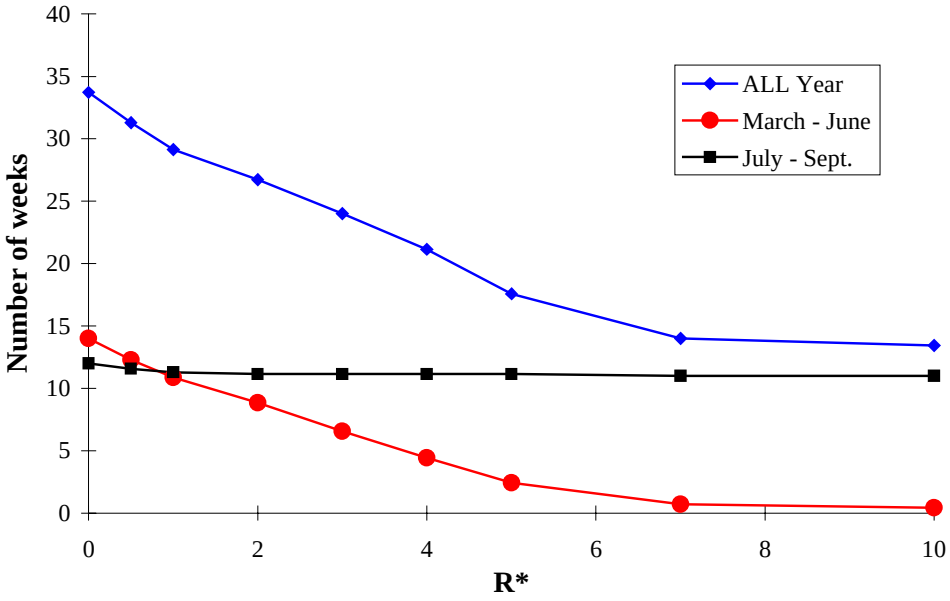

Figure 66. Number of weeks that the outdoor surface is warm enough to permit mould growth for various ratios of internal to external vapour diffusion resistances.

The results in Figure 66 show that number of weeks during the year where mould growth is possible is quite high for all values of R*. However, as described by Hukka and Viitanen (1999), the activity of mould will tend to decrease during dry periods, which means that the total time during the year when mould growth is possible may not be a good measure of the performance of a structure. Therefore, Figure 66 contains results for the drying period of the structure, which is from March to June. March is the time when the daily average temperature begins to exceed 0°C (Figure 64) and June is the time when drying is complete and the moisture content will reach a minimum (Figure 61). During the time from July to September mould growth is possible,

regardless of the value of R* and these results will not be studied here because the field measurements in section 4.1 clearly indicate that the moisture content will be below the critical value during this time. The simulation results show higher humidities in the summer compared to the measured results because solar radiation is neglected in the simulated results. As pointed out by Simonson (1994), neglecting solar radiation can have a large influence on the moisture performance of wooden buildings, even in Finland.

Figure 66 demonstrates that as R* decreases, the number of weeks that mould growth is possible increases during the drying period of March to June. Since several weeks of exposure is usually needed to initiate mould growth as shown in Figure 58 (Hukka and Viitanen, 1999 and Viitanen, 1996), the results for the drying period show that a value of R* greater than 3 is likely acceptable. The results during the drying period (March to June) also demonstrate that increasing R* beyond 7 has no impact on the risk of mould growth. This indicates that for R* > 7, the relative humidity of the outdoor surface is likely a result of the outdoor humidity and not caused by vapour diffusion from indoors. These results confirm that plastic is not needed to reduce moisture diffusion from indoor air to a safe level for moisture growth. It is important to note that some materials will suffer physical damage if the moisture content is high when the temperature cycles above and below freezing and other materials fail due to corrosion or warping. These are not considered here.

4.3 Summary

The measured and simulation results presented in this chapter show that a building without a plastic vapour retarder can have good moisture performance in a cold climate. The field measurements from Tapanila ecological house show that the initial moisture dries after the second summer and that the moisture content in the winter is not excessively high to prevent rapid drying in the spring and summer. The numerical results show that the drying of the wall depends on the internal vapour diffusion resistance. The results show that the indoor vapour diffusion resistance should be greater than the outdoor vapour diffusion resistance by a factor of at least 3:1 to keep mould growth to a minimum. However, increasing the vapour diffusion resistance of the indoor surface beyond 7 times the outdoor resistance has essentially no effect on vapour diffusion. This chapter concentrates on the water vapour diffusion and its affect on mould growth. The results are applicable only if convection is eliminated, the initial moisture content of the building envelope is low and other failure mechanisms are not important. Furthermore, if there is a small airflow through construction defects, it is possible that a construction with a low internal vapour resistance may be safer than one with a high internal vapour resistance because the peak humidity is lower in the former.

5. Performance of the Natural Ventilation System

The results presented in section 3.5 indicate that generally the ventilation system is able to keep the indoor concentration of CO_2 below 1000 ppm, which indicates that the ventilation system is performing adequately. The purpose of this section is to measure the ventilation rate of the house during different seasons.

5.1 Natural Ventilation System and Measurements

Supply air to the house is provided through vents located in the upper window frame or in the exterior wall above the hot water radiators as shown in Figure 67. The occupants can control both types of supply vents and the duct shaped supply vents in the exterior wall are seldom open, particularly in the winter because the occupants find that this creates a cold draft on the floor. During the tests, the position of each supply vent was noted, but not adjusted, to reflect the setting desired by the occupants. To determine the effect of adjusting the supply opening, a separate test was carried out (section 5.2.2). This test showed that adjusting the supply openings has a limited effect on the ventilation rate.

Figure 67. Supply vents located in the window frame (a) and exterior wall (b).

The natural ventilation exhaust vents are located in the open areas of the house. There are 2 vents in the basement, 1 on the first floor and 1 one the second floor. In addition, the bathrooms, sauna and kitchen have exhaust vents with an exhaust fan. Each exhaust vent is ducted individually to the roof of the house to reduce the potential of exhaust air returning to the house through some other exhaust vent. As a result there are numerous ducts on the roof of the house (Figure 68).

Figure 68. Chimneys and natural ventilation exhaust ducts on the roof.

To determine the ventilation performance of the house, the exhaust airflow rate was measured using a flow nozzle and an anemometer as shown in Figure 69. The exhaust flow rate could be measured by placing the flow nozzle directly over the exhaust vent for all locations except for the kitchen fume hood and one exhaust vent in the basement. The flow rate through the kitchen fume hood was measured by fitting an adapter of polyethylene plastic between the flow nozzle and the fume hood. It was not possible to measure the flow rate through one of the exhaust vents in the basement because it was partially covered by a bookshelf. Since the bookshelf covered only about 10% of the exhaust vent, it was assumed that the flow rate was equal to the flow rate through the other exhaust vent in the basement.

The flow nozzle was an AM300 flow nozzle and the flow anemometers were GGA-65P and GGA-26 from ALNOR. The flow rate is calculated by multiplying the measured velocity with a constant, according to

$$Q = k\ v = 5.8\ v\ , \qquad (23)$$

where Q is the flow rate is L/s, k is the constant (L/m) and v is the measured air speed (m/s). The uncertainty in measured flow rate is expected to be ±10%. The flow rate through each exhaust vent was measured separately and the flow rate of the exhaust fans was also measured. The exhaust flow rate through the fireplace and sauna chimneys was estimated with a velocity traverse of the chimneys near the roof. The fireplace and

sauna dampers were closed during this measurement and therefore the flow rate was quite small and the associated uncertainty is therefore quite high (~±25%). During the measurements, all external windows and doors were closed, all bedroom doors were open and all bathroom doors were closed. Before and after the measurement of the exhaust flow rates, which took about 2 hours, the pressure difference between indoors and outdoors was measured in several locations on both the first and second floors. In addition, the outdoor temperature and the wind speed and direction were measured. The wind speed was measured on the roof of the house.

Figure 69. Measuring the exhaust flow rate.

5.2 Results

The performance of the natural ventilation system was measured five times from March to June 2000. The measured pressure differences between indoor and outdoor air on the windward and leeward sides of the house and the measured exhaust flow rates during the March 10 test are presented in Figure 70. Also included in Figure 70 is the outdoor temperature, wind speed, the ventilation rate in air changes per hour (ach) and L/s per person (L/(s·p)) and the pressure difference across the building envelope. In Figure 70 and throughout this report, the pressure difference (ΔP) is calculated as

$$\Delta P = P_{outdoor} - P_{indoor} \qquad (24)$$

and therefore a positive value of ΔP means the house is at a lower pressure than outdoors (i.e., underpressure).

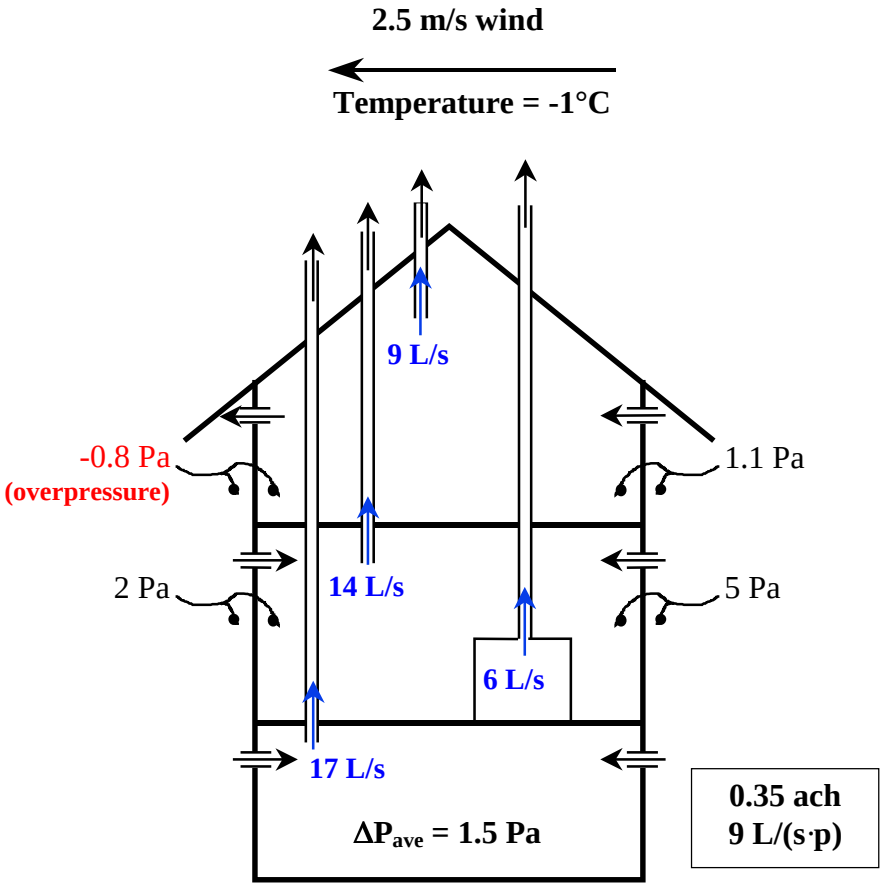

Figure 70. Flow and pressure distribution during the test on March 10, 2000.

Figure 70 shows a significant distribution of pressure and flow. As expected, the pressure difference between indoors and outdoors is greater (~3 Pa) on the windward side of the house than on the leeward side and greater (~3 Pa) on the first floor than on the second floor. The house is generally at a lower pressure than outdoors, but there is a region of slight overpressure in the second floor on the leeward side.

The ventilation rate of the house on March 10, 2000 is 0.35 ach, which corresponds to 10 L/(s·person). The National Building Code of Finland – D2 (1987) states that 4 L/s of outdoor air per occupant must be supplied to non-smoking spaces, but the air change rate of rooms of normal height shall not be less than 0.5 ach. The ventilation rate per person is satisfied, but the air change rate is 30% lower than the required value. For comparison the proposed ASHRAE Standard 62.2P, Ventilation and acceptable indoor air quality in low-rise residential buildings, (Sherman, 1999) requires a ventilation rate of about 0.4 ach for a house such as Tapanila ecological house. The measured ventilation rate is only about 10% below the proposed ASHRAE Standard.

The distribution of outdoor ventilation air is also important and Figure 70 shows that the second floor has a lower exhaust ventilation rate than the basement and first floor. This

may be a problem because there are three occupants that sleep upstairs, which means that the local ventilation rate is only 3 L/(s·person). When the bedroom doors are open, however, there appears to be adequate mixing in the house as explained in section 3.5.

The pressure and flow distributions for the remaining tests are presented in Figure 71 and show a similar distribution as in Figure 70.

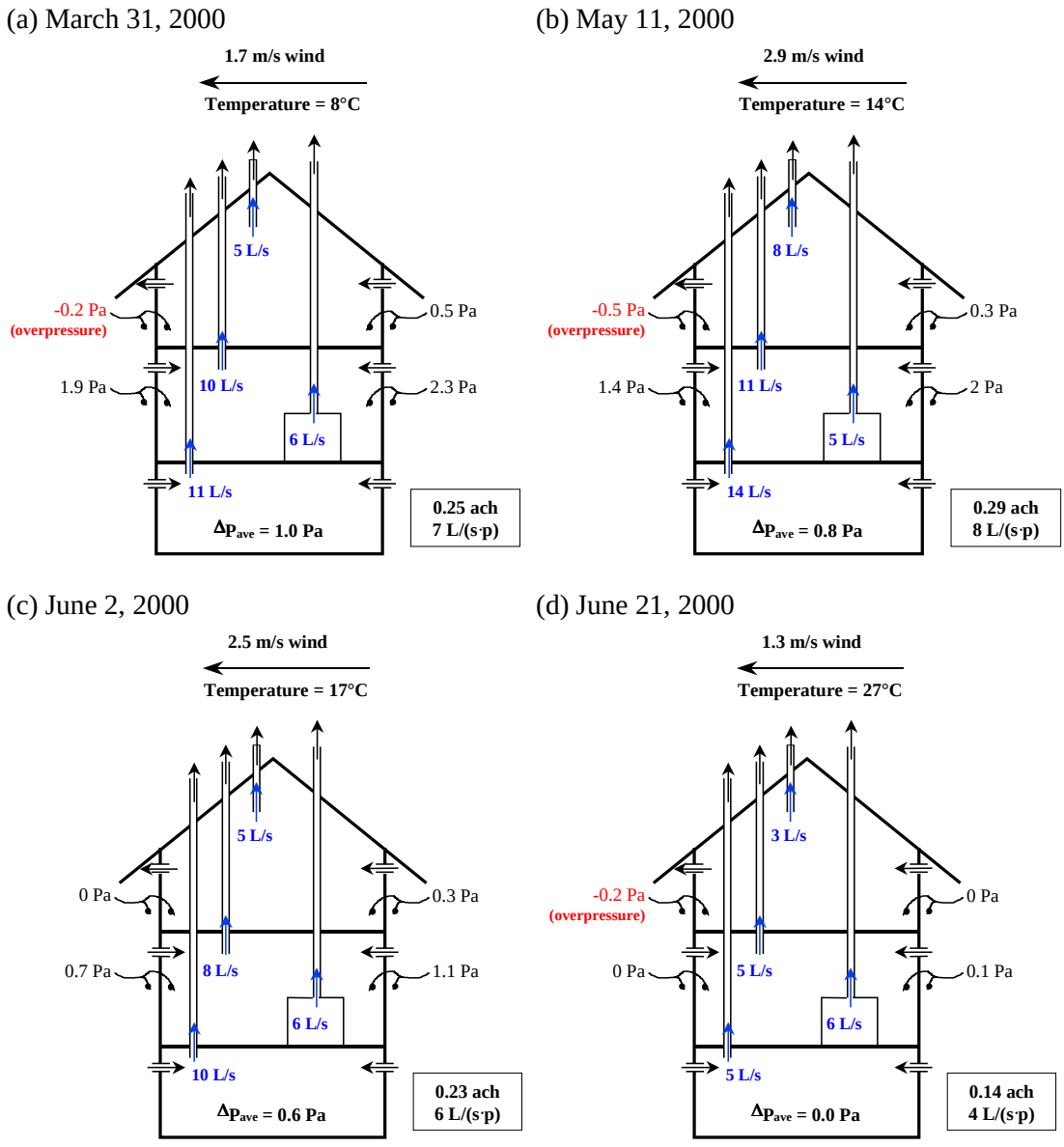

Figure 71. Flow and pressure distributions during the ventilation tests.

The measured results are summarised in Table 6 and Figure 72 for each test. The data covers a range of temperatures from –1°C to 27°C and wind speeds from 1.3 m/s to 2.9 m/s and the ventilation rate varies between 0.35 ach and 0.14 ach (10 L/(s·person) to 4 L/(s·person)). All the measured ventilation rates in Table 6 and Figure 72 are below the

required air change rate of 0.5 ach in the National Building Code of Finland – D2 (1987), even though the ventilation rate per person is satisfactory (i.e., 4 L/(s·person)).

Table 6. Temperatures, wind velocities, pressure differences and ventilation rate measured during the ventilation tests.

Test date	T_{out} (°C)	T_{in} (°C)	wind velocity (m/s)	ΔP_{ave} (Pa)	Q (ach) & (L/s·p)
March 10, 2000	–1.3	22	2.5 (N-NE)	1.5	0.35 (9)
March 31, 2000	7.5	22	1.7 (SW)	1.0	0.25 (7)
May 11, 2000	13.5	24	2.9 (NW)	0.8	0.29 (8)
June 2, 2000	17	22	2.5 (S-SW)	0.6	0.23 (6)
June 21, 2000	27	24	1.3 (SE)	0.0	0.14 (4)

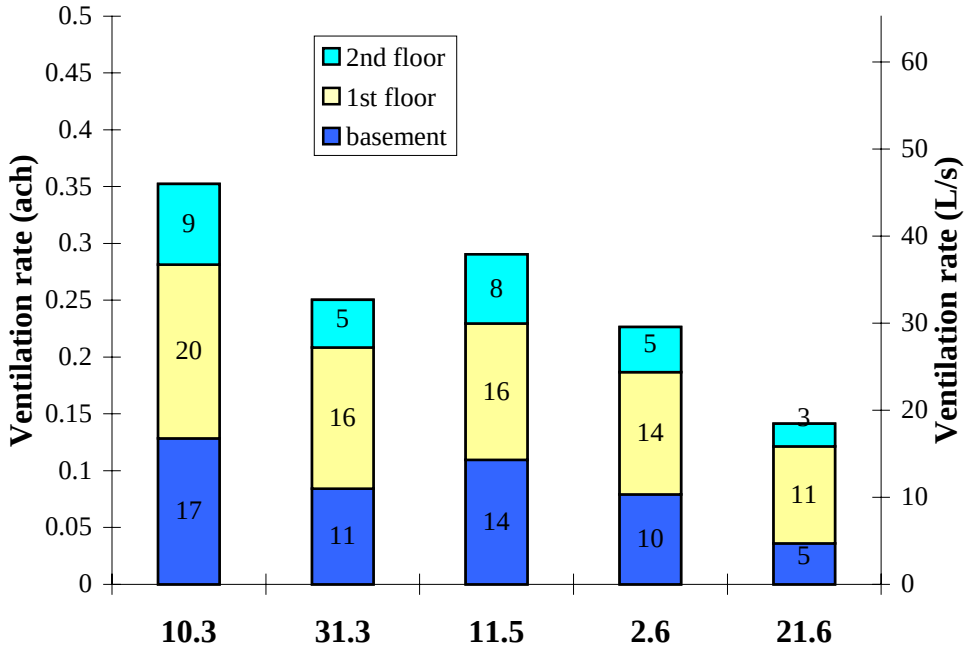

Figure 72. Measured ventilation rates for each test showing the distribution between the three storeys.

5.2.1 Mechanical Exhaust Flow Rates

In addition to continuous ventilation, the National Building Code of Finland – D2 (1987) gives guide values for the exhaust rate from bathrooms, kitchens and saunas as

follows: bathroom with shower 15 L/s, bathroom without shower 10 L/s, kitchen 20 L/s and sauna 2 L/(s·m²) with a minimum of 6 L/s. The exhaust ventilation rate through each exhaust fan was measured on each test day (except for the stove hood in the kitchen, which was measured only on 31.3.00) and the results are given in Figure 73. These results show that the exhaust fans can provide adequate exhaust flow rate from the kitchen and bathrooms. The floor area of the sauna is about 12 m² and therefore the exhaust rate from the sauna should be 24 L/s. The results in Figure 73 show that the flow rate through the sauna exhaust fan is only 30% of the recommended amount. However, the sauna has a fresh air vent under the bench in the steam room, which is intended to be open when the sauna is use. Therefore, when the sauna is in use, there will be significant exhaust flow rate through the wood-burning sauna stove and the exhaust rate is expected to be adequate.

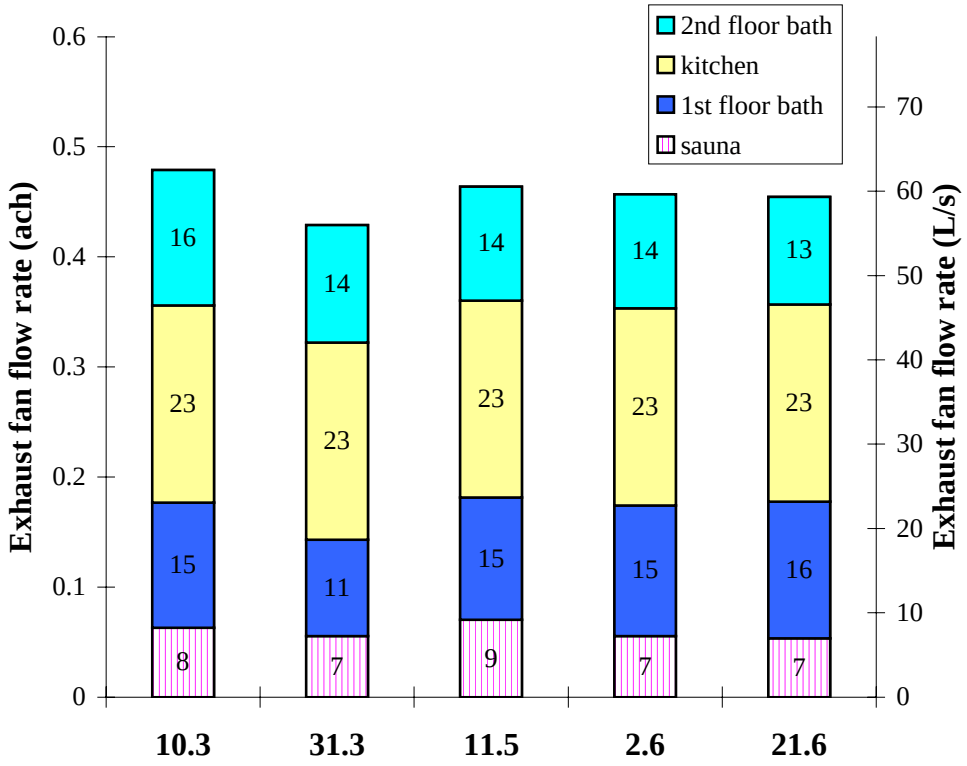

Figure 73. Measured flow rates through the exhaust fans.

5.2.2 Effect of Supply Vent Settings

Since Tapanila ecological house is equipped with two types of supply vents and both are adjustable, a measurement was made to determine the effect of these setting on the ventilation rate. The tests were performed on March 10 and the settings of the vents are presented in Table 7 and the results are in Figure 74. The measurements were performed in sequence from setting 1 to setting 4 and the waiting time before the start of

measurements, after adjusting the supply vents, was 10 minutes after setting 2, 20 minutes after setting 3 and 45 minutes after setting 4. It took 10 to 15 minutes to complete the measurements at each setting.

Table 7. Position of window and wall vents used to study the effect of the supply vent settings.

Setting	Position of window vent	Position of wall vents
setting 1	4 vents open (rest closed)	all closed
setting 2	all closed	all closed
setting 3	all open	all closed
setting 4	all closed	all open

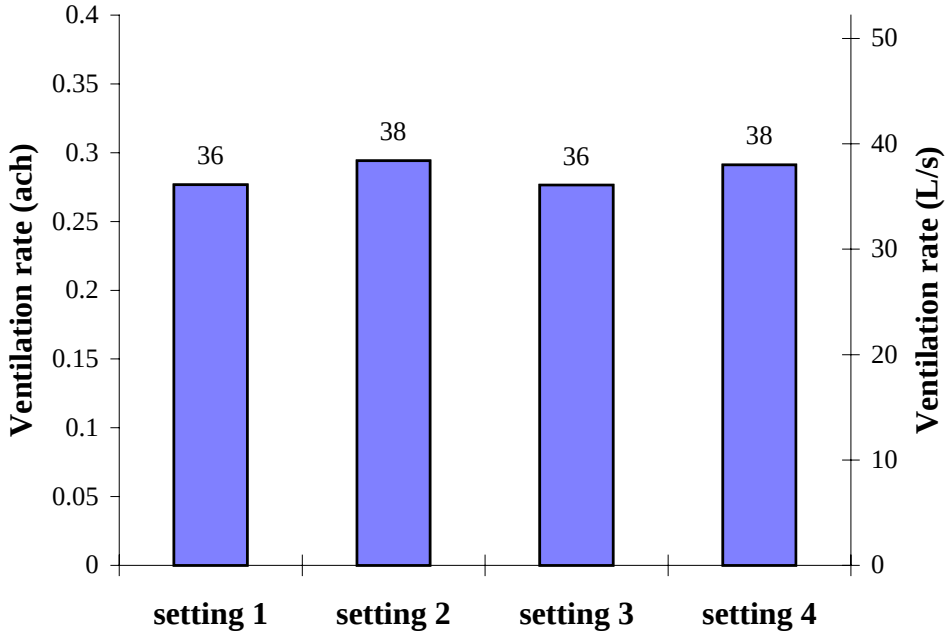

Figure 74. Ventilation rates with supply vent settings as given in Table 7.

Figure 74 shows that the ventilation rate is nearly the same regardless of the supply vent settings. This is likely due to the fact that when the supply vents were closed they did not seal tightly. The wall vents were intended to close completely, but in practice they did not. Similarly, the window vents allow significant airflow even when they are closed. Another possible reason for the small effect of the supply vent settings is that infiltration through the building envelope will increase as the supply vents are closed. At the average measured pressure of 1.5 Pa, the infiltration is expected to be about 0.25

ach (Figure 14 in section 2.2) therefore it is not surprising that adjusting the poorly sealing supply vents has little effect on the ventilation rate. Furthermore, the effect of the supply vent setting may have minimised because the time between the adjustment of the vents and the measurement was less than the time constant of the system.

5.3 Extrapolation

In order to predict the ventilation rate in conditions other than the 5 measurements, a simple model is developed in this section. The model is based on the basic equations for pressure differences due to wind and stack effects (Orme, 1999, Walker and Wilson, 1998, ASHRAE, 1997 and Walton, 1989) and are as follows:

$$\Delta P_{wind} = Cp\frac{\rho v^2}{2} = C_{wind} v^2 \text{ and} \tag{25}$$

$$\Delta P_{stack} = \frac{P}{R}\left(\frac{1}{T_{out}} - \frac{1}{T_{in}}\right)gh = C_{stack}\left(\frac{1}{T_{out}} - \frac{1}{T_{in}}\right), \tag{26}$$

where Cp is the wind pressure coefficient, ρ is the density of air (kg/m^3), v is the wind speed (m/s), P is the absolute air pressure (Pa), R is the specific gas constant of air (J/(kg·K)), T is the absolute temperature (K), g is the acceleration due to gravity (m/s^2), h is the height between the inlet and outlet (m) and subscript out and in refer to the outdoor and indoor temperatures respectively. The total pressure differences between indoors and outdoors is calculated by simple addition superposition of the wind pressure and the stack pressure (Walker and Wilson, 1993) rather than including the interaction of pressure effects given in Walker and Wilson (1998), which was found necessary for a wider range of leakage distributions. The total pressure difference is therefore

$$\Delta P = \Delta P_{wind} + \Delta P_{stack} \tag{27}$$

and the ventilation flow rate uses the standard exponential relation

$$Q = C\Delta P^n , \tag{28}$$

where C and n are constants.

Equations (25) to (28) describe the model used to calculate the outdoor ventilation rate from temperature difference and wind speed. The unknown constants in the equations, that must be determined from the measured data, are C_{wind}, C_{stack}, C and n. By fitting the measured data, the ventilation flow rate can be calculated as

$$Q = 0.125\left(0.07\,v^2 + 3650\left(\frac{1}{T_{out}} - \frac{1}{T_{in}}\right)\right)^{0.602} \quad . \tag{29}$$

Using equation (29), the ventilation rate at various wind speeds and outdoor temperatures can be predicted for Tapanila ecological house by assuming a constant indoor temperature of 22°C (Figure 75). The measured ventilation rates and associated wind speeds are also included in Figure 75 and show that the model fits the experimental data quite well. The main discrepancy is that the model predicts a lower flow rate than that measured when the outdoor temperature is 27°C. This difference can be partly explained by the fact that the uncertainty in the measured ventilation rate is highest for the 27°C test because the ventilation through the chimneys was nearly half of the total ventilation. (As discussed in section 5.1, the uncertainty of the flow rate through the chimney is much higher than the uncertainty of the ventilation rate through the natural ventilation ducts.)

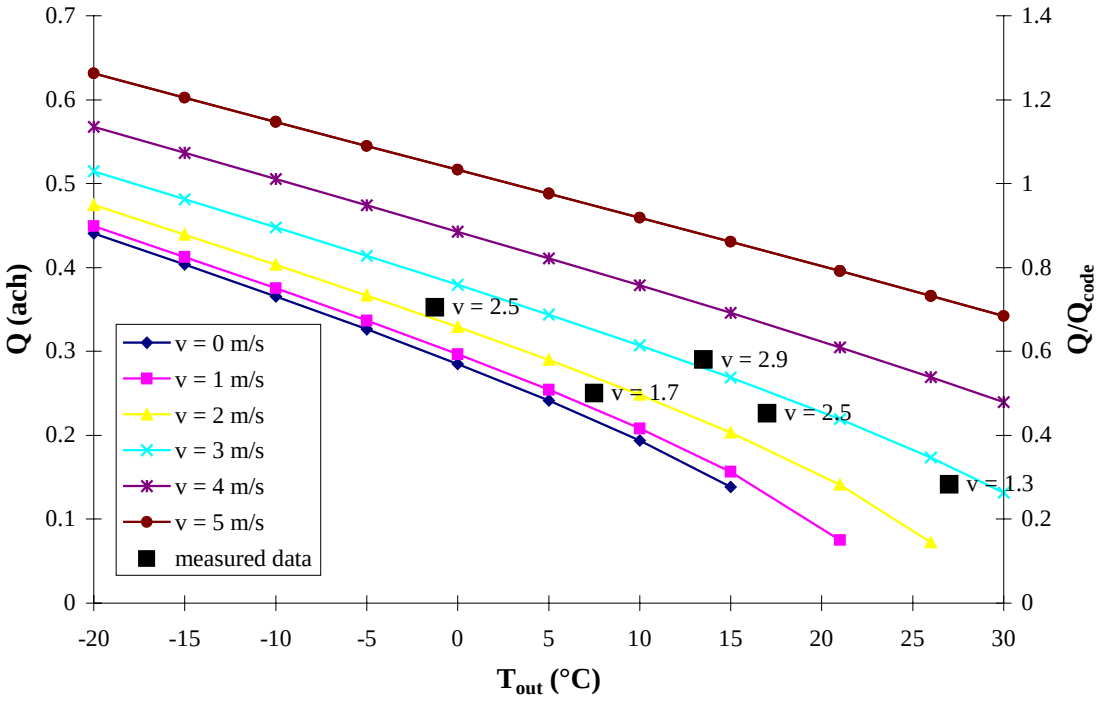

Figure 75. Expected ventilation rate and ratio to the code requirement (i.e., 0.5 ach) for Tapanila ecological house at various outdoor temperatures and wind speeds calculated using equation (29). The measured data are included for comparison.

Figure 75 also includes the ratio Q/Q_{code} where Q_{code} is the ventilation rate specified in the National Building Code of Finland – D2 (1987) (i.e., 0.5 ach). The ratio Q/Q_{code} is often less than 1, which shows that it is quite difficult to meet the building code requirement when the windows are closed, unless the wind velocity is high and the outdoor temperature is low. At a wind speed of 4 m/s, a ventilation rate of 0.5 ach will

be realised when the outdoor temperature is below –10°C. For wind speeds less than 3 m/s, the outdoor temperature must be below –15°C before the ventilation rate is expected to reach 0.5 ach. The results in Figure 75 show that additional ventilation is likely always needed to satisfy the building code when the outdoor temperature is above 0°C. Opening windows or operating the exhaust fans could provide this ventilation.

To estimate the performance of the natural ventilation system during the year, equation (29) is applied using the hourly weather data for Helsinki (1979) and an indoor temperature of 22°C (Figure 76). The average wind speed measured at the weather station was 4 m/s for the whole year, which is slightly higher than the measured wind speeds at Tapanila ecological house. Therefore, the measured wind speed was reduced by 25% to account for the local wind shielding around Tapanila ecological house. Figure 76 also includes the monthly average ventilation rate using the average outdoor temperatures and modified wind speed from Helsinki (1979).

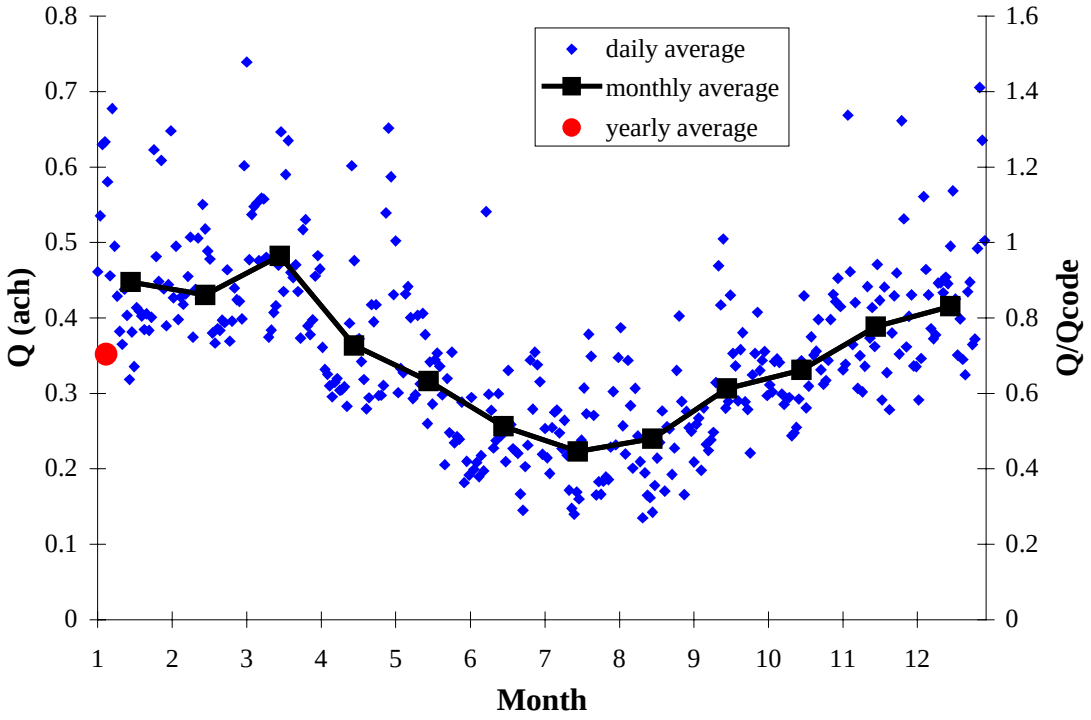

Figure 76. Expected ventilation rate and Q/Q_{code} for Tapanila ecological house using the Helsinki (1979) weather data and reducing the wind speed by 25% to account for local wind shielding.

Figure 76 shows that in the winter (November to March) the daily average ventilation rate varies between 0.3 and 0.7 ach, whereas the monthly average ventilation rate varies between 0.4 and 0.5 ach (80% to 100% of the required value). In the summer (June to August), the ventilation rate often is below 0.25 ach (or 50% of the required value), but

additional ventilation by opening windows is possible at this time. Using the assumption of a constant wind speed of 3 m/s, the ventilation rate at the yearly average temperature of 4.3°C is calculated to be 0.35 ach, which is 70% of the required ventilation rate.

5.4 Summary

The measured ventilation rates through the natural ventilation system in Tapanila ecological house, satisfy the ventilation rate per person (4 L/(s·person) as stated in the National Building Code of Finland – D2 (1987). However, the measured air change rates are below the requirement of 0.5 ach. Using the measured data, an equation was developed to predict the ventilation rate under different conditions. Applying this equation shows that additional ventilation (by opening windows or operating the exhaust fans) is likely always needed to satisfy the building code when the outdoor temperature is above 0°C. At the average yearly temperature in Helsinki (~5°C) and a wind speed of 3 m/s, the ventilation rate of Tapanila ecological house is expected to be 0.35 ach or 30% below the design value. At higher wind speeds and lower temperatures, the ventilation rate will be greater and at lower wind speeds and higher temperatures, the ventilation rate will be lower. As a result, the ventilation rate through the natural ventilation system is expected to be between 0 and 20% below the code value in the winter and about 50% below the code value in the summer. Opening windows in the summer will increase the ventilation rate significantly.

6. Energy Consumption

Tapanila ecological house was designed as a low-energy house with a target space heating energy consumption of 50 kWh/(m^2·a). The insulation is 250 mm thick in the walls (U = 0.16 W/(m^2·K)) and 425 mm in the roof (U = 0.10 W/(m^2·K)). The house is connected to the Helsinki district heating system, which provides space heating through hot water radiators and heat for domestic hot water. A wood-burning fireplace and sauna stove also provide space heating.

The energy consumption of Tapanila ecological house was monitored from August 1999 to August 2000. During this time, the consumption of district heating energy was recorded weekly. The district-heating substation is located in an uninsulated closet against an external wall in the basement. It is assumed that 95% of the delivered district heating energy provides heating and the remaining 5% is lost through the basement wall and uninsulated piping or lost due to unneeded heat during the summer months. The total water consumption was recorded nearly every month and the consumption of hot water was recorded weekly starting in October 1999. The hot water consumption from October 1999 to August 2000 was extrapolated to determine the yearly consumption. The energy required to heat the hot water was calculated assuming that the cold water temperature is constant at 5°C and the hot water supply temperature is 55°C.

The occupants of the house began burning firewood in October 1999 and the mass of consumed firewood was recorded daily. The heating energy from firewood is calculated from the heat value of pine wood, which is 4.15 kWh/kg and 4.2 kWh/kg when the moisture content is 20% and 10% by mass respectively (Työtehoseura, 1997). The moisture content of the firewood used in Tapanila ecological house was measured to be between 12% and 17%. Since the fireplace in the living room is massive and the two dampers in the chimney are nearly always closed after the burning of the wood, it is assumed that a large portion (70%) of this energy provides space heating. The sauna stove, on the other hand, is much less massive and the damper is nearly always open during use, so only 10% of the wood consumed in the sauna is assumed to provide useful space heating. Therefore, the space heating energy obtained from the wood that is burned in the fireplace and sauna stove is assumed to be 3 kWh/kg and 0.4 kWh/kg respectively. In addition, the wood that is burned during the months of June, July and August is assumed to provide no useful space heating. To evaluate the effect of wood burning on energy consumption, no wood was consumed in the fireplace during a two-week period in February 2000.

The consumption of electricity was determined from the electrical meter, which was read by the utility company on May 26, 1999 and May 29, 2000. In addition, the electricity consumption was recorded weekly from May to August 2000. These

measurements indicated that the electricity consumption was quite constant throughout the year. The electricity consumption used outside the house was very small and was not subtracted from the reported values.

Energy consumption is often reported per unit volume or unit floor area. In this report, the gross heated floor area (217 m^2) and volume (665 m^3) will be used to normalise the energy consumption results. The heated floor area and volume are smaller than the gross floor area and volume listed in Chapter 2 because of the two cold-storage rooms in the basement (8 m^2 and 19 m^3) and the unheated porch (12 m^2 and 36 m^3).

6.1 Measured Energy and Water Consumption

The yearly energy and water consumption of Tapanila ecological house is reported in Table 8 and shows that slightly over ¾ of the energy consumed is heat energy. Heat energy is the energy provided by the district heating and wood heating. Figure 77 and Figure 78 compare the energy and water consumption of Tapanila ecological house to two other recently-built low-energy houses in Finland known as ESPI 1 and ESPI 2 (Laine and Saari, 1998) and to typical Finnish houses (Motiva, 1999). The values for typical Finnish houses are from Motiva (1999) and are based on a house with 4 occupants and a gross floor area of 140 m^2. Figure 77 shows that the normalised consumption of energy and water is significantly higher in typical Finnish houses than in Tapanila ecological house. A typical Finnish house consumes 50% more total energy, 58% more heating energy, 25% more electricity, 58% more water and 44% more primary energy than Tapanila ecological house (Figure 78).

Table 8. Yearly energy and water consumption in Tapanila ecological house.

Consumed quantity	Consumption	Normalised consumption
Total energy	26 184 kWh	121 kWh/m^2 or 39 kWh/m^3
Heat energy	20 216 kWh	93 kWh/m^2 or 30 kWh/m^3
Electrical energy	5 968	28 kWh/m^2 or 9 kWh/m^3
Water	127 m^3	70 L/(day·person)
Primary energy	35 135 kWh	162 kWh/m^2 or 52 kWh/m^3

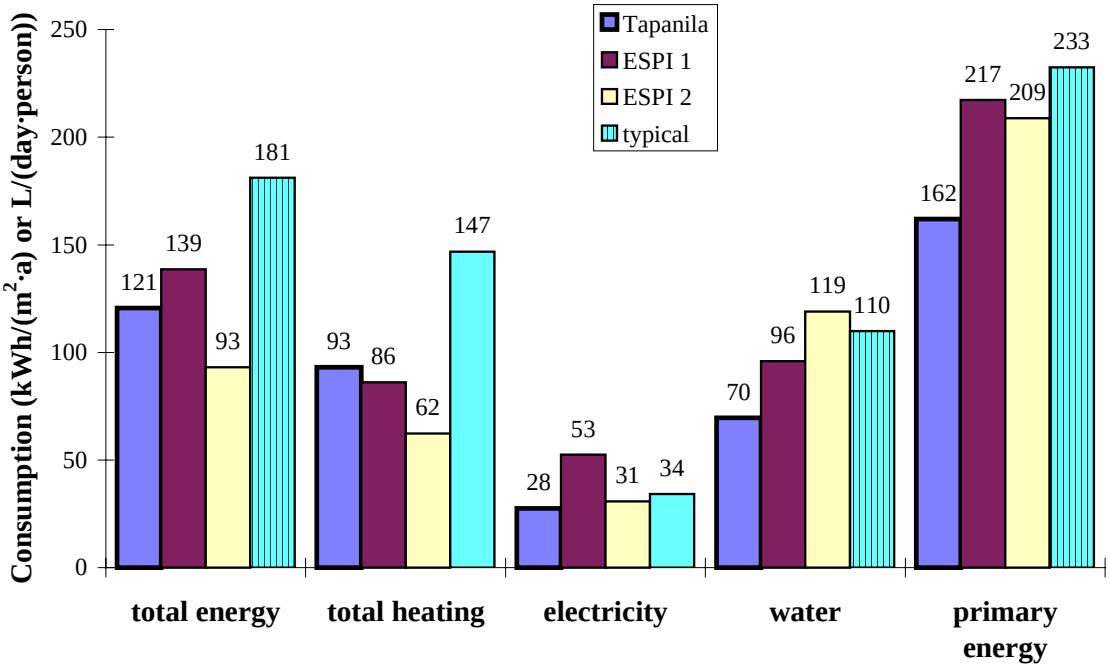

Figure 77. Normalised energy and water consumption in Tapanila ecological house, low-energy houses ESPI 1 and ESPI 2 (Laine and Saari, 1998) and typical Finnish houses (Motiva, 1999).

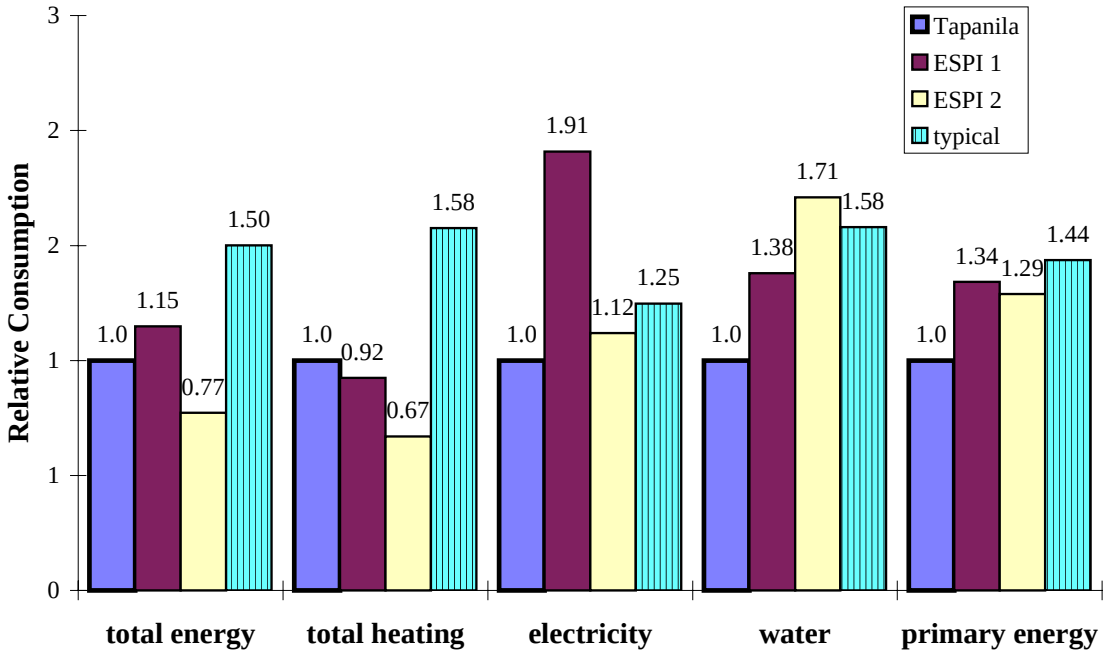

Figure 78. Consumption of energy and water in various houses relative to the consumption in Tapanila ecological house.

Tapanila ecological house uses comparable amounts of total energy and heating energy, but less electricity and water than ESPI 1 and ESPI 2 (Laine and Saari, 1998). The electricity consumption is 28 kWh/(m^2·a) compared to 53 kWh/(m^2·a) and 31 kWh/(m^2·a) for ESPI 1 and 2 respectively and 34 kWh/(m^2·a) for typical Finnish houses. The main reason for the low electricity consumption in Tapanila ecological house is the natural ventilation system. The mechanical ventilation systems in ESPI 1 and 2 houses consumed between 20% and 22% of the total electricity. The low water consumption in Tapanila ecological house (normal usage is about 110 L/(day·person)) attests to the careful water use by the house inhabitants.

To further compare the performance of Tapanila, ESPI 1, ESPI 2 and typical Finnish houses, the primary energy consumption of each house is included in Figure 77 and Figure 78. When calculating the primary energy consumption of these houses, 1 kWh of electricity is assumed to equal 2.5 kWh of primary energy, while 1 kWh of heat energy obtained from wood, oil or district heat is assumed to equal 1 kWh of primary energy. The primary energy results show that Tapanila ecological house consumes the lowest amount of primary energy (ESPI 1, ESPI 2 and typical Finnish houses consume 34%, 29% and 44% more primary energy than Tapanila ecological house respectively).

6.1.1 Heating Energy Consumption

Since heating energy is a large part of the total energy, the distribution of the heating energy is presented in Table 9, Figure 79 and Figure 80, where the heating energy is divided into space heating, water heating and heat losses. As mentioned previously, the water heating was calculated using the measured hot water consumption and an estimated cold water temperature of 5°C and a hot water supply temperature of 55°C. The space heating was determined by subtracting the water heating from the district heating and adding the wood heating. The heat losses in Tapanila ecological house were assumed to be only 5% of the supplied district heat because the district heat exchanger is located in the basement and most of the heat dissipated will heat the house.

Table 9. Yearly heating energy consumption in Tapanila ecological house.

Consumed quantity	Consumption	Normalised consumption
Total heating	20 216 kWh	93 kWh/m^2 or 30 kWh/m^3
Space heating	16 568 kWh	76 kWh/m^2 or 25 kWh/m^3
Water heating	2 881	13 kWh/m^2 or 4 kWh/m^3
Heat losses	767	4 kWh/m^2 or 1 kWh/m^3

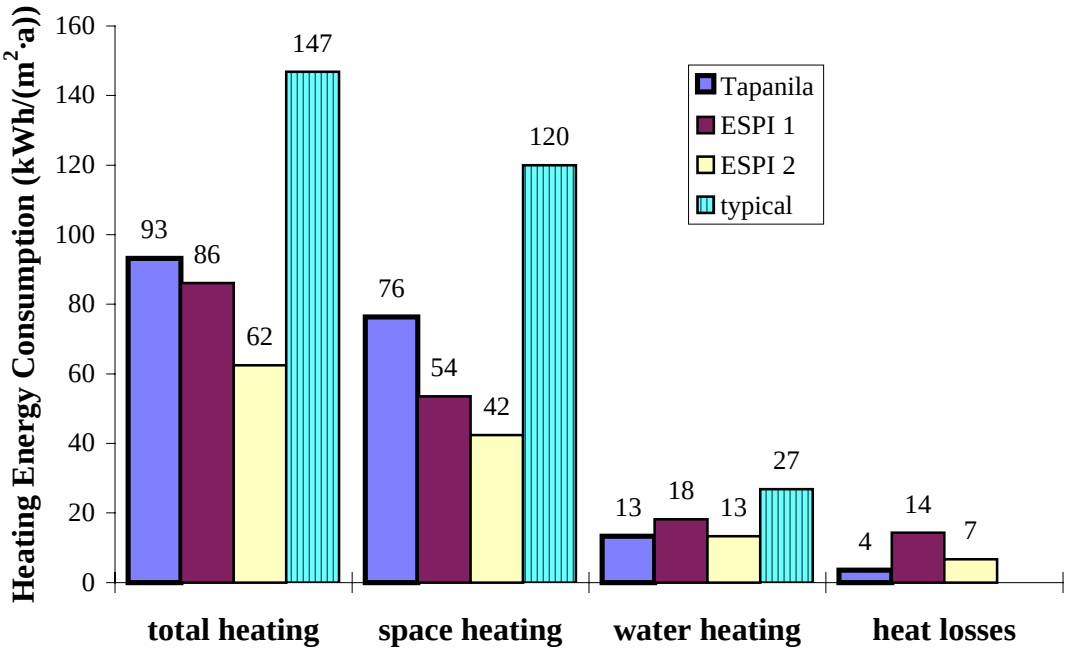

Figure 79. Normalised heating energy consumption in Tapanila, ESPI 1 and 2 (Laine and Saari, 1998) and typical Finnish houses (Motiva, 1999).

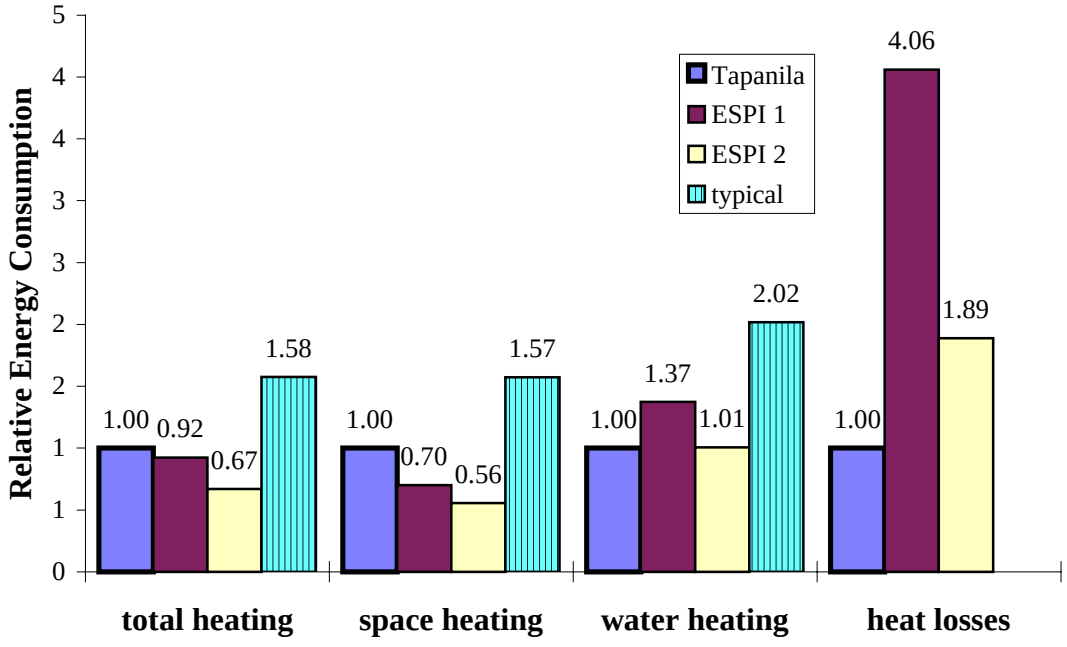

Figure 80. Consumption of heating energy in various houses relative to the consumption in Tapanila ecological house.

Figure 79 and Figure 80 show that the normalised consumption of total heating energy is higher in Tapanila ecological house than in the ESPI houses. ESPI 1 has an 8% lower consumption and ESPI 2 has a 33% lower consumption than Tapanila ecological house.

Similarly, the space heating is 30% lower in ESPI 1 and 44% lower in ESPI 2, but the space heating in typical Finnish houses is 57% higher than in Tapanila ecological house. It is important to note that ESPI 1 and ESPI 2 had significant heat losses because of their heating systems, which were an oil burner and electrically heated water storage tank respectively. The heat losses in ESPI 1 were 27% of space heating energy and in ESPI 2 the heat losses were 16% of the space heating energy, while the heat losses in Tapanila ecological house were only 5% of the space heating energy. Combining the space heating and heat losses gives a total of 80 kWh/(m^2·a) for Tapanila ecological house, 68 kWh/(m^2·a) for ESPI 1 and 49 kWh/(m^2·a) for ESPI 2. The total for the ESPI houses is still the lowest, but only 15% lower in ESPI 1 and 39% lower in ESPI 2 than in Tapanila ecological house (compared to 30% and 44% for space heating alone). The higher space heating in Tapanila ecological house compared to ESPI 1 and 2 is likely due to a combination of the lack of ventilation air heat recovery and the lower electricity consumption in Tapanila ecological house. These effects will be examined in more detail in section 6.2.

The total space heating in Tapanila ecological was measured to be 76 kWh/(m^2·a), which is over 50% higher than that target value of 50 kWh/(m^2·a). However, Tapanila ecological house is quite a large house and a more representative normalisation of heating energy consumption may be the volume of the house given in Figure 81.

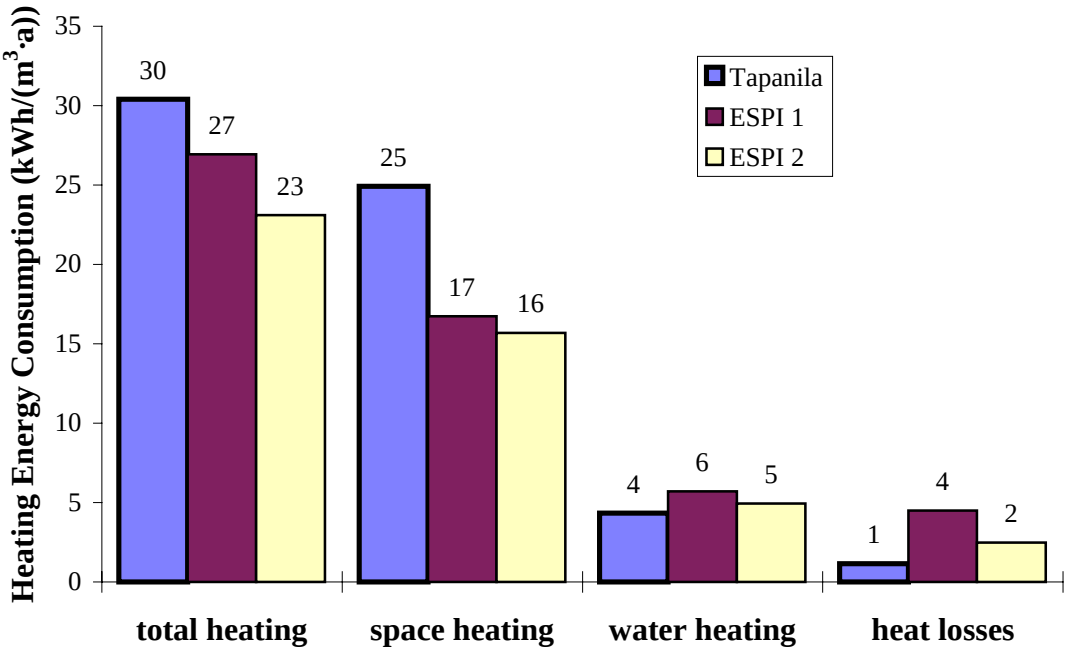

Figure 81. Heating energy consumption normalised by the heated volume of the house.

6.1.2 Consumption of Wood

In the above energy calculations, the space heating energy provided by the wood that is burned in the fireplace and sauna stove was assumed to be 3 kWh/kg and 0.4 kWh/kg respectively as described previously. To evaluate the reliability of this assumption the fireplace was unused for a two week period in February (13.02 to 26.02) as shown in Figure 82.

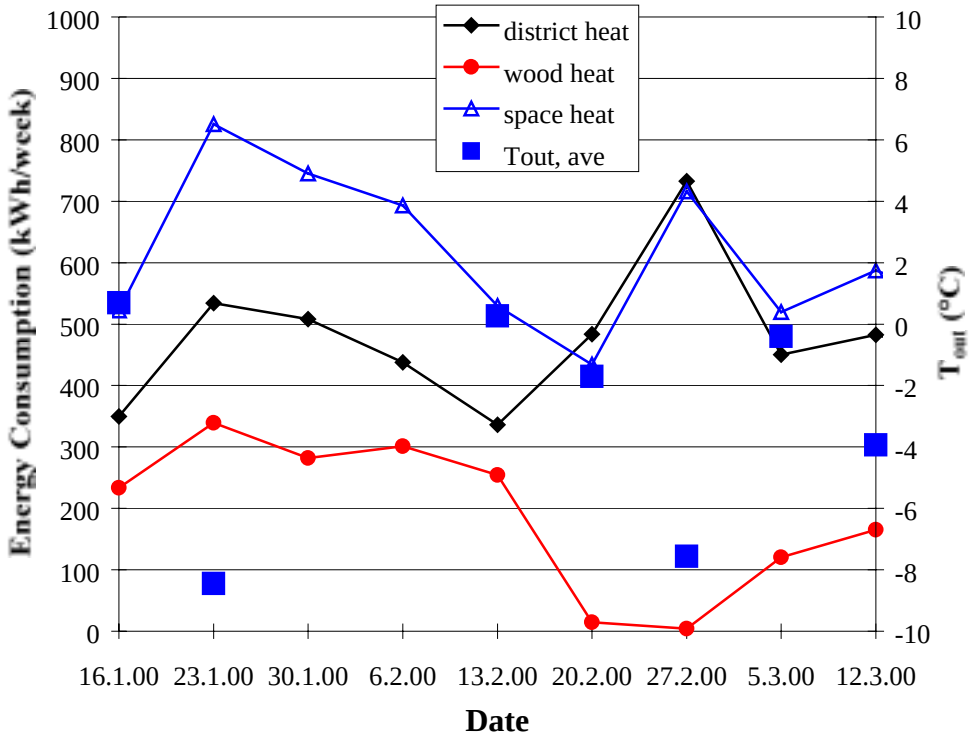

Figure 82. Weekly energy consumption and weekly average outdoor temperature including a two-week period when the fireplace is not used.

The results in Figure 82 show that during the month before the two-week period when the fireplace is not used, the average energy provided by wood burning is nearly 300 kWh/week, which is over 40% of the space heating. During the two weeks that the fireplace is not used, the district heating consumption clearly increases. For the week ending 20.2.00, the consumption of district heating is nearly as great as for the week ending 23.1.00, even though the average outdoor temperature is nearly 7°C warmer for the week ending 20.2.00. When the outdoor temperatures are similar, the energy consumption for space heating is similar whether the fireplace is used or unused. This can be seen more clearly in Table 10 where the space heating energy for weeks with similar average outdoor temperatures are compared when the fireplace is used and unused. These results suggest that the estimated space heating produced by the wood burning is suitable.

Table 10. Comparison of the weekly space and wood heating energy when the fireplace is used and unused during the week.

Week ending	Status of fireplace	$T_{out,ave}$ (°C)	space heating	wood heating
23.01.00	Used	–8.4	826 kWh/week	339 kWh/week
27.02.00	Unused	–7.6	716 kWh/week	4 kWh/week
19.03.00	Used	–0.9	532 kWh/week	147 kWh/week
20.02.00	Unused	–1.7	434 kWh/week	14 kWh/week

Figure 82 showed that a significant fraction of energy is provided by burning wood in Tapanila ecological house. This is further illustrated in Figure 83 where the energy supplied by wood heating per unit heated floor area is presented for Tapanila ecological house and ESPI 1 and ESPI 2. In Tapanila ecological house, 1550 kg and 570 kg of wood were burned in the fireplace and sauna respectively from 21.10.99 to 28.5.00. The total heating energy provided by the fireplace and sauna stove is therefore 4650 kWh and 230 kWh respectively. This accounts for nearly 30% of the space heating.

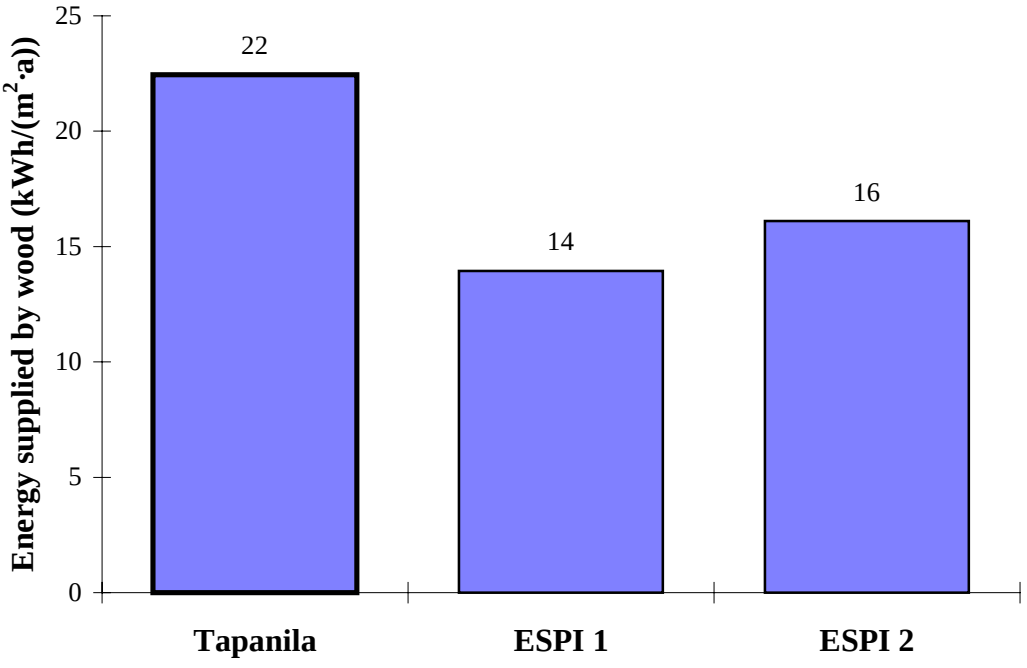

Figure 83. Energy supplied by wood in Tapanila, ESPI 1 and ESPI 2 houses.

6.1.3 Distribution of Energy Supply and Consumption

Figure 84 and Figure 85 present the distribution of energy supplied to the house and the fraction of space heating supplied by district heat and wood. These figures show that wood provides 19% of the total energy and 29% of the space heating, while district heat provides 59% of the total energy and 71% of the space heating. Electricity accounts for 23% of the energy supplied to Tapanila ecological house

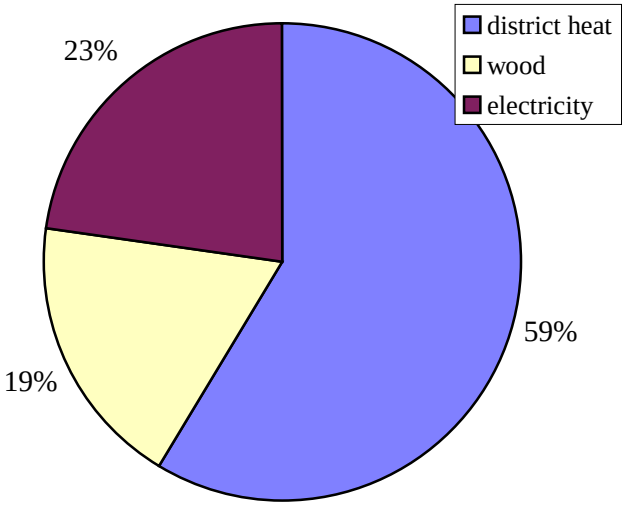

Figure 84. Distribution of energy supplied to Tapanila ecological house from various sources.

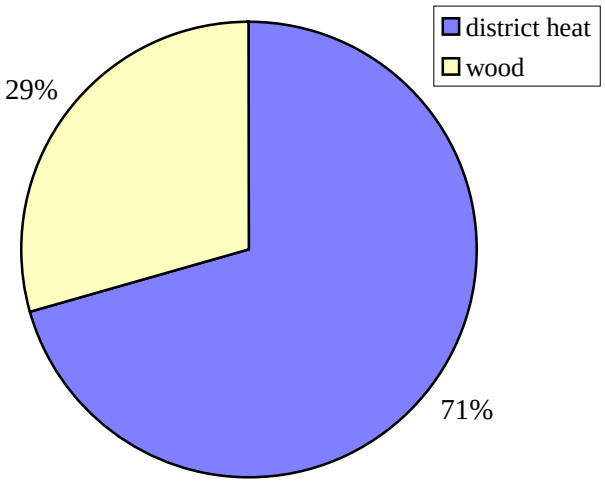

Figure 85. Fraction of space heating energy supplied by district heat and wood.

Figure 86 presents how the heating energy supplied is divided between space heating, water heating and heat losses. Space heating accounts for 82% of the heating energy, water heating accounts for 14% and heat losses account for the remaining 4%.

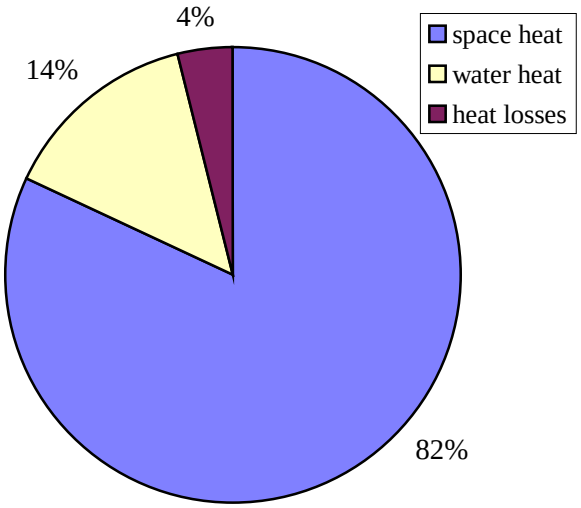

Figure 86. Fraction of heating energy used for space heating, water heating and heat losses.

6.2 Calculated Energy Consumption

In this section, the energy consumption of Tapanila ecological house will be analysed using the WinEtana simulation program. The WinEtana simulation program has been developed at VTT Building Technology for estimating building energy consumption and is described in publications by Kosonen and Shemeikka (1997) and Shemeikka (1997). The program calculates the energy consumption using a single-zone steady-state thermal analysis, which is based on the National Building Code of Finland – D5 (1985) and the prEN 832 (1998). Kalliomäki and Kohonen (1989) have shown the validity of the steady-state method for estimating energy consumption in Finland. WinEtana calculates the heating, electrical and water consumption and peak demands in the building using monthly average outdoor temperatures and assuming a constant indoor temperature. Despite its simplicity, Kosonen and Shemeikka (1997) have shown that, when simulating the IEA BESTEST validation case (Haapala et al., 1995) with reasonable assumptions, the heating energy consumption calculated by WinEtana is similar to that calculated by several transient simulation models.

6.2.1 Input Data

The WinEtana program is particularly useful for Finnish buildings because it contains a database of typical input parameters (U-values, window types, water consumption, electricity consumption, internal gains, air change rates, etc.) for Finnish buildings and Finnish regulations (National Building Code of Finland – C3, 1985; D2, 1987 and D5, 1985). These database values will be used together with the size of Tapanila ecological house when describing a “reference” case for Tapanila ecological house as shown in Table 11. The “reference” case uses the actual window (including French doors) and

wall areas of Tapanila ecological house. Therefore, the "reference" case represents the case where the envelope of Tapanila ecological house is insulated according to the building code and the electricity and water consumption are as in typical Finnish houses of the same size (665 m^3) and occupancy (5 people). Since the area of windows and doors in Tapanila ecological house is 16.4% of the gross heated floor area, which is slightly greater than the 15% required in the National Building Code of Finland – C3 (1985), a case where the window area is 15% of the gross heated floor area is included (i.e., window (15%)). The input data for the actual and database values are listed in Table 12.

Table 11. Source of input data for the energy simulation cases, where "database" means that the data is from the database in WinEtana and "actual" means that the data reflects the as-built Tapanila ecological house.

Case	Surface areas	Water consumption	Electricity consumption	U-values	Ventilation system	Σ(UA) (W/K)
reference	actual	database	database	database	database	185
window (15%)	window area 15% of floor area	database	database	database	database	180
code	actual	actual	actual	database	database	185
actual-MV	actual	actual	actual	actual	database	126
actual-NV	actual	actual	actual	actual	actual	126

Table 12. Input data for the simulations obtained from the WinEtana database ("database") and measurements from Tapanila ecological house ("actual").

Water consumption Database: total: 152 m^3/a, hot water: 53 m^3/a, water heating: 3 070 kWh/a Actual: total: 127 m^3/a, hot water: 50 m^3/a, water heating: 2 880 kWh/a
Electricity consumption Database: household: 4 880 kWh/a, ventilation: 990 kWh/a, other: 1 070 kWh/a Actual: household: 5 570 kWh/a, ventilation: 0 kWh/a, other: 400 kWh/a
Envelope U-values (W/(m^2·K)) Database: walls: 0.28 (0.36 underground), roof: 0.22, floor: 0.36, windows: 1.8 Actual: walls: 0.16 (0.21 underground), roof: 0.10, floor: 0.25, windows: 1.2 (Table 13)
Ventilation system (infiltration of 0.15 ach, total outdoor ventilation of 0.5 ach) Database: mechanical supply and exhaust with 50% heat recovery Actual: natural ventilation system without heat recovery

Table 11 shows that in the code case, the measured water and electricity consumption will be set equal to the measured values, while the thermal performance of the envelope and the ventilation system will be from the database. It is important to note that the measured electricity consumption does not include electricity for the ventilation fans. The WinEtana program will also be used to calculate the actual case where the actual insulation levels (Table 13), which are greater than specified in the building code, are used in the simulation. Actual-MV is the case with a mechanical supply and exhaust ventilation system and actual-NV is the case with natural ventilation. In all cases, a district heating system is used (95% efficiency), the outdoor weather is from Helsinki (1979), the indoor temperature is 22°C, the infiltration rate is assumed to be 0.15 ach (i.e., $n_{50}/20$ – Sherman, 1987) and the total outdoor ventilation rate is 0.5 ach. In addition to the tests in Table 11, a sensitivity analysis of ventilation rate and heat recovery will be presented. This is important because the database uses a mechanical ventilation system with a 50% effective heat recovery system and a ventilation rate of 0.5 ach, while Tapanila ecological house has a natural ventilation system with no heat recovery and a ventilation rate below 0.5 ach.

Table 13. U-value, surface area, description and external boundary conditions for the envelope parts in Tapanila ecological house.

part of building envelope	U-value ($W/(m^2 \cdot K)$)	surface area (m^2)	description	external bounday condition
normal walls	0.16	185	250 mm insulation	ventilated cavity
roof	0.1	72	425 mm insulation	ventilated cavity
basement floor	0.25	62	expanded clay	ground
basement wall	0.27	42	expanded clay	outdoor air
basement wall	0.21	42	expanded clay + insulation	ground
windows	1.2	6.64	triple, low e, argon	North
windows	1.2	2.28	triple, low e, argon	East
windows	1.2	13.98	triple, low e, argon	South
windows	1.2	2.75	triple, low e, argon	West
entry roof	0.3	4.1	125 mm insulation	outdoor air
entry wall	0.18	6.7	160 mm insulation	outdoor air
entry floor	0.25	4.2	~125 mm insulation	crawl space
entry windows	1.8	0.91	triple, clear	South
doors	1.8	5.25	double door, 1 glass	outdoor air
balcony doors	2.2	3.78	double door, 1 glass	outdoor air

The different cases are arranged in such a way that each subsequent case uses increasing actual data from Tapanila ecological house. In this way, the impact of various parameters can be assessed. The difference between the code and reference cases shows the impact of the actual electricity and water consumption on the energy consumption of Tapanila ecological house, while the difference between the window (15%) and reference cases shows the impact of the window area. However, the differences between the hot water consumption, electricity consumption and window areas between these cases are very small as can be seen in Table 11 and Table 12. The difference between the actual-MV case and the code case indicates the impact of the improved building envelope on the energy consumption. Finally, the difference between the actual-NV and actual-MV shows the impact of the natural ventilation system on energy consumption.

6.2.2 Results

The simulated energy consumption for the five different cases compared to the actual consumption measured in Tapanila ecological house are presented in Figure 87 and Figure 88. These results shown that the reference case has a total, space heating and electrical energy consumption of 154 kWh/(m^2·a), 102 kWh/(m^2·a) and 32 kWh/(m^2·a) respectively. This means that if the envelope and equipment in Tapanila ecological house were according to typical Finnish standards, the total, space heating and electrical energy consumption would be greater than that measured in Tapanila ecological house by 28%, 33% and 16% respectively (Figure 88). The reference case has the highest total and space heating energy consumption.

The actual-MV case (actual house, but with mechanical ventilation) has the lowest total and space heating energy consumption (118 kWh/(m^2·a) and 69 kWh/(m^2·a) respectively), but the actual-NV case (actual house with natural ventilation) has the lowest electricity consumption (28 kWh/(m^2·a)). The total, space heating and electrical energy consumption in the actual-MV case are 2% lower, 10% lower and 17% higher than the measured values respectively. The calculated total and space heating energy consumption for the actual-NV case are about 10% higher than the measured consumption because the actual ventilation rate is below the assumed value of 0.5 ach in the simulation.

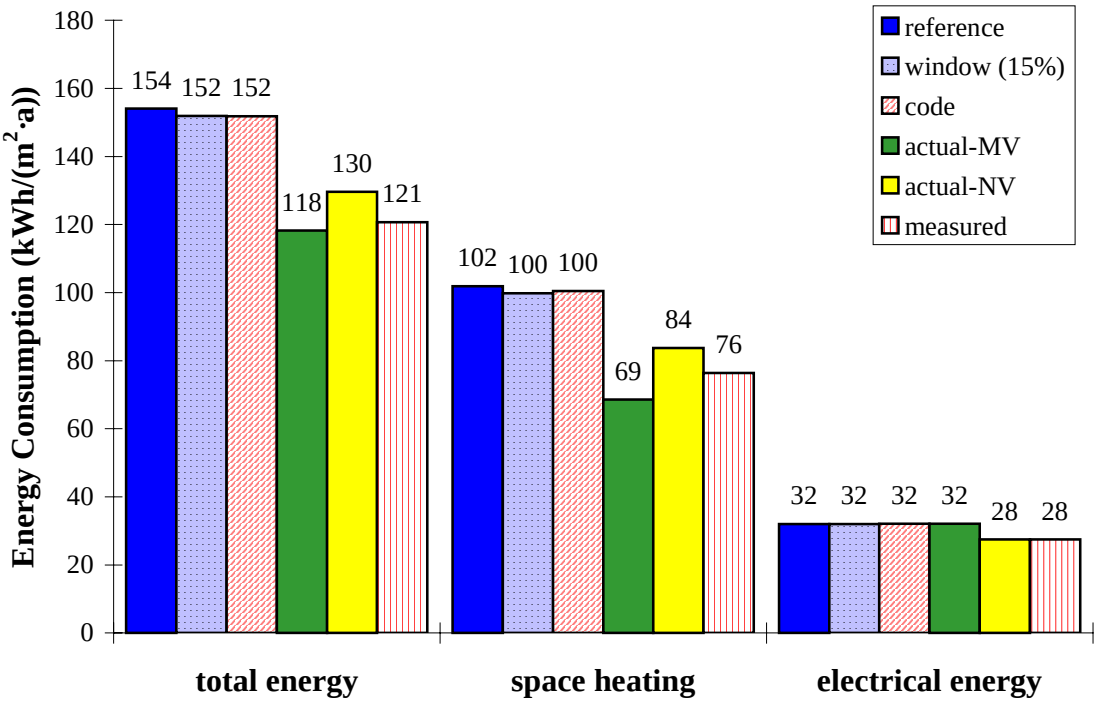

Figure 87. Calculated energy consumption of Tapanila ecological house for the cases listed in Table 11.

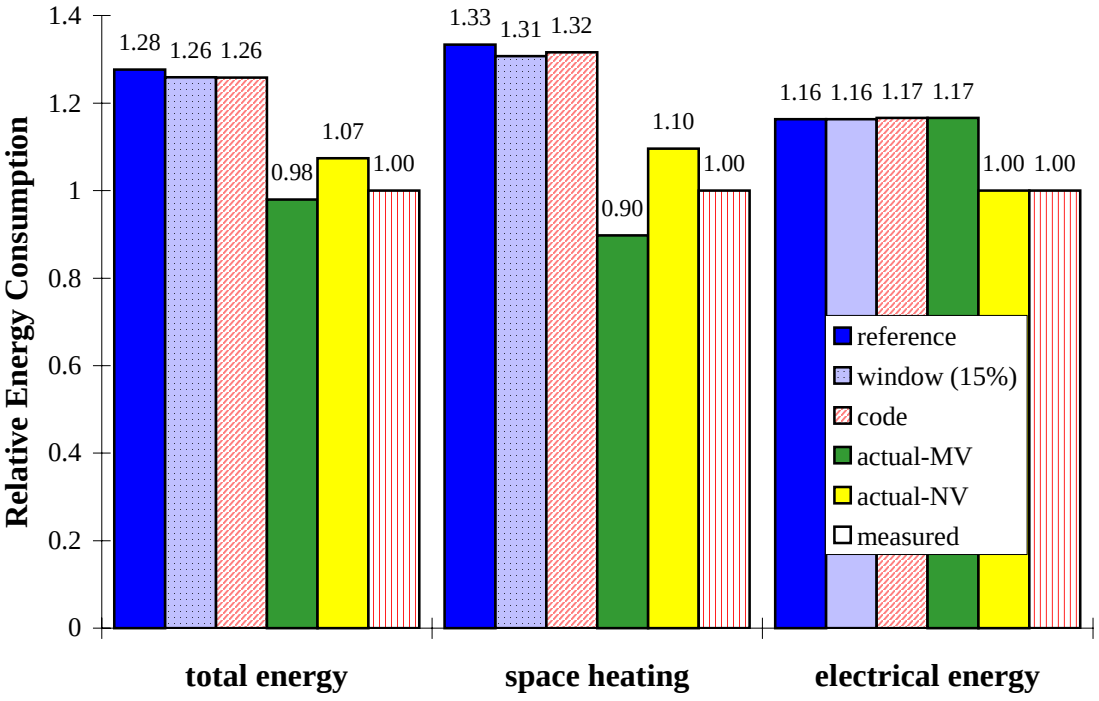

Figure 88. Ratio of calculated to measured energy consumption.

Figure 89 shows the impact of various parameters on the calculated energy consumption. Reducing the window area from 16.4% to 15% of the gross heated floor

area, decreases the energy consumption very little. Similarly, changing the water and electricity consumption from the database to the actual values has a small effect on the energy consumption because the consumption of water and electricity are very similar in both cases. However, if the changes in window area, electricity consumption and water consumption were greater between the database and actual values, the differences would be greater. For example, simulation results show that if the household electricity consumption increased by 10 kWh/(m^2·a), the space heating would decrease by 4.4 kWh/(m^2·a). This is important and shows that increasing the consumption of household electricity can decrease the consumption of space heating energy. Naturally the actual heating required by a house is independent of the electricity consumption, but the typically reported space heating consumption depends on the electricity consumption because the waste heat from electrical appliances is not included in the reported space heating. This is particularly important because electricity is a higher valued energy source than district heat and the production of electrical energy is about 2.5 times more resource intensive than the production of heat energy.

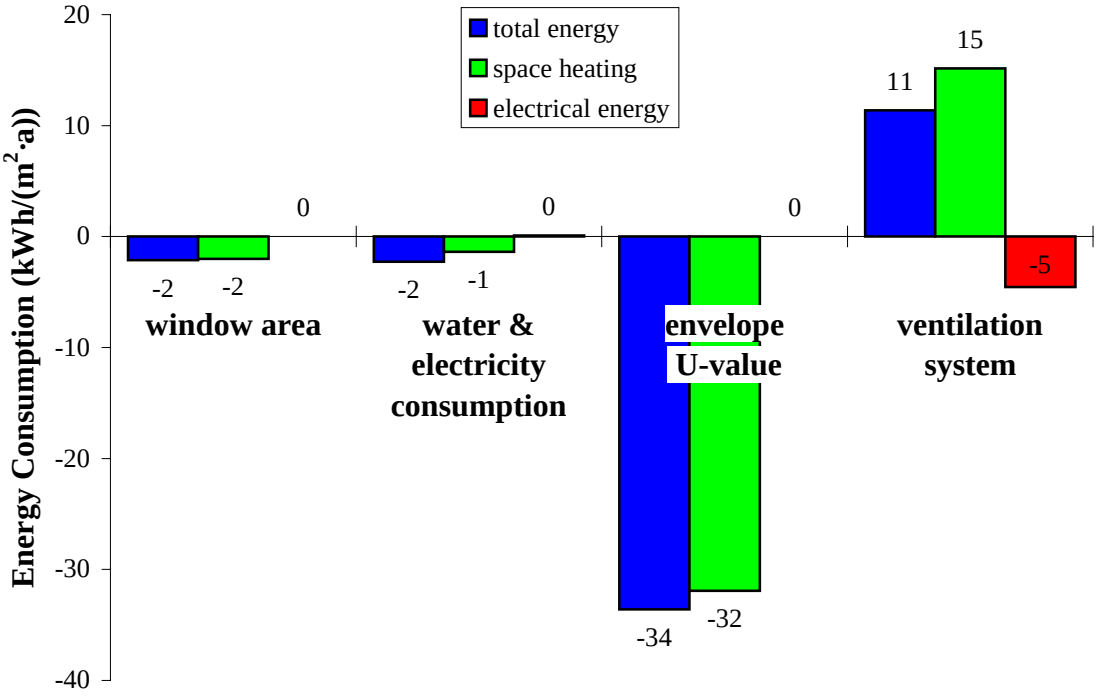

Figure 89. The change in calculated energy consumption when changing various parameters from the database value to the actual value.

Changing the U-value of the envelope from the database value (i.e., building code value) to the actual value (i.e., greater thermal insulation) decreases the total and space heating energy by 34 and 32 kWh/(m^2·a) respectively. Changing the ventilation system from the database system (i.e., mechanical ventilation with heat recovery) to the actual system (i.e., natural ventilation) increases the total and space heating energy by 11 and

15 kWh/(m^2·a) respectively, but decreases the electricity consumption by 5 kWh/(m^2·a). Assuming that 1 kWh of electrical energy requires 2.5 kWh of primary energy, the primary energy consumption of a natural and mechanical ventilation system are quite comparable as shown in Figure 90. This emphasises the importance including total energy consumption (and possible primary energy consumption) when assessing the performance of ecological houses. Space heating energy consumption alone is not an adequate measure of performance.

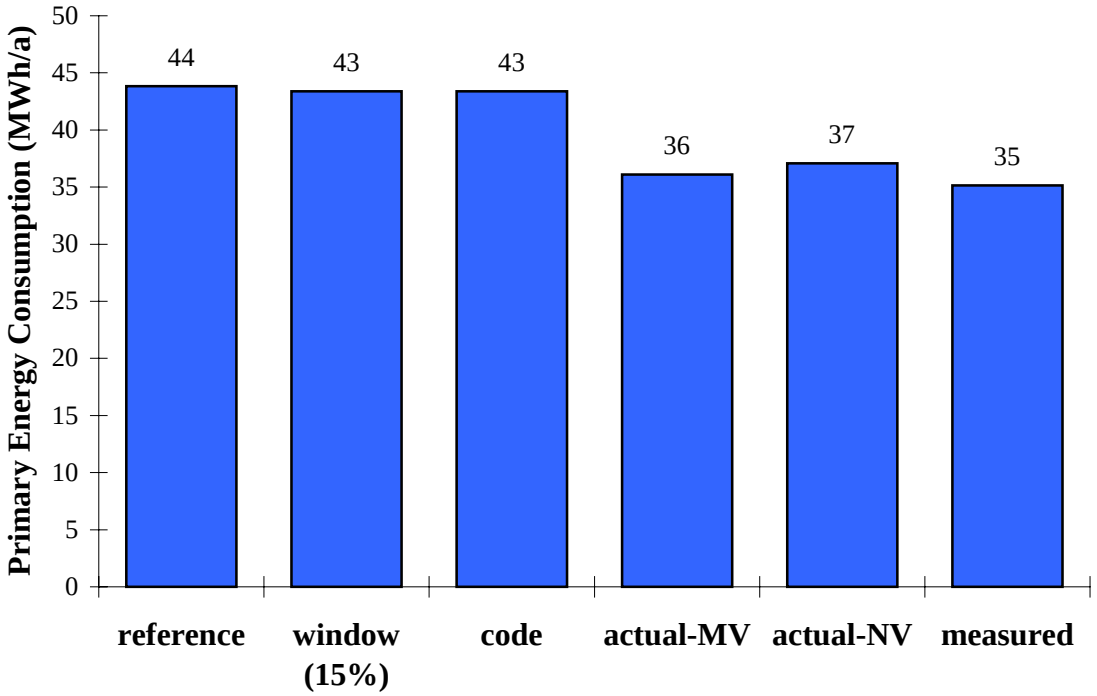

Figure 90. Primary energy consumption of different cases.

The previous results show that the calculated energy consumption for Tapanila ecological house is slightly greater than the measured consumption. This may be a result of slightly warmer outdoor temperatures during the measurements than during the reference year of 1979 because simulation results show that if the average temperature increases by 2°C, the space heating will decrease by 13% (11 kWh/(m^2·a)). Nevertheless, the main reason for the difference between measured and calculated energy consumption is that the ventilation rate in Tapanila ecological house is typically less than 0.5 ach. Figure 91 contains the calculated total energy consumption and space heating energy consumption for the different cases as a function of the ventilation rate. Comparing the actual-NV case to the measured values indicates that the actual ventilation rate is likely about 0.4 ach, which is comparable to that expected in the winter months (see Figure 76 in section 5.3).

The effect of ventilation rate on energy consumption is also evident in Figure 91. As expected, the energy consumption in the actual-NV case is the most sensitive to the ventilation rate because this case has no heat recovery. The increase in total energy consumption for every 0.1 ach increase in ventilation rate is 6.0 kWh/(m²·a) for the actual-MV case and 9.7 kWh/(m²·a) for the actual-NV case. The increase in space heating energy consumption for every 0.1 ach increase in ventilation rate is 4.5 kWh/(m²·a) and 9.2 kWh/(m²·a) for the actual-MV and actual-NV cases respectively, which means that the sensitivity to ventilation rate is double for the case without heat recovery. This means that a house with a 50% effective heat recovery system and a ventilation rate of 0.5 ach will have the same space heating energy consumption as a house with no heat recovery and a ventilation rate of 0.25 ach. Furthermore, a higher ventilation rate is possible with the same total energy consumption when a mechanically ventilated house includes heat recovery. If the heat recovery effectiveness is 50%, the ventilation rate can be 1.8 times higher and if the effectiveness is 70%, the ventilation rate can be 2.7 times higher. It is important to note that these results are based on the WinEtana simulation program, which neglects the fact that the fan energy consumption increases as the heat recovery effectiveness increases. The heat recovery effectiveness has a significant impact on the calculated energy consumption as shown in Figure 92. Here a 10% change in heat recovery effectiveness changes the space heating energy consumption by 3.3 kWh/(m²·a) when the ventilation rate is 0.5 ach.

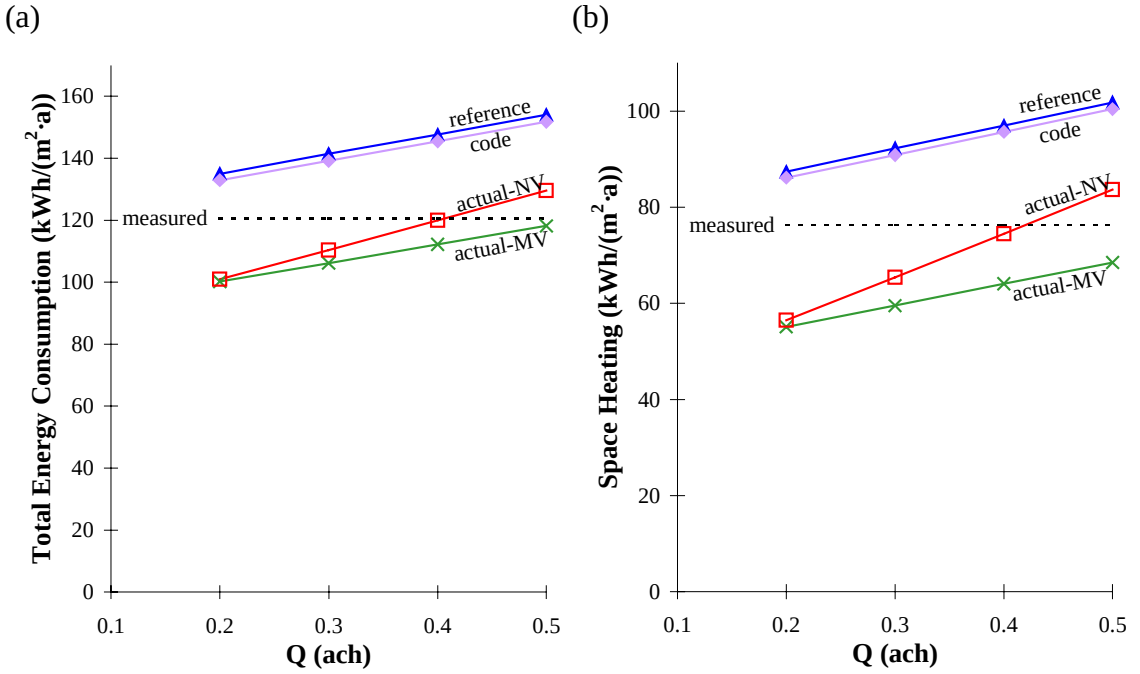

Figure 91. Total (a) and space heating (b) energy consumption as a function of the total outdoor ventilation rate.

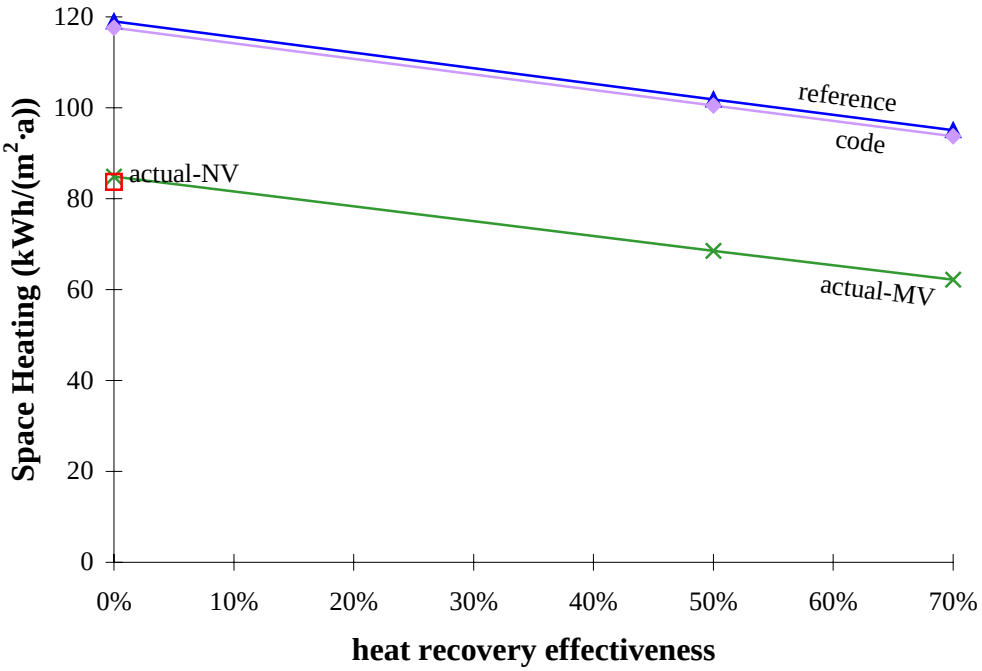

Figure 92. Space heating energy consumption as a function of heat recovery effectiveness for a ventilation rate of 0.5 ach.

6.3 Summary

The results presented in this chapter show that Tapanila ecological house uses significantly less energy than typical Finnish houses. The normalised total energy consumption is 50% higher in typical Finnish houses (181 kWh/(m²·a)) than in Tapanila ecological house (121 kWh/(m²·a)). The natural ventilation system saves electrical energy for fans, but increases the space heating because there is no possibility for heat recovery. As a result, the measured space heating energy consumption (76 kWh/(m²·a)) is significantly greater than the target value (50 kWh/(m²·a)) and the consumption in other single-family low-energy houses in Finland (e.g., ESPI 1 – 54 kWh/(m²·a) and ESPI 2 – (42 kWh/(m²·a)). Nevertheless, typical Finnish houses use nearly 60% more energy for space heating (i.e., 120 kWh/(m²·a)) than Tapanila ecological house. The normalised consumption of electricity in Tapanila ecological house is 28 kWh/(m²·a) (5970 kWh), which is much lower than in ESPI 1 house (53 kWh/(m²·a)) and ESPI 2 house (31 kWh/(m²·a)), while a typical Finnish house consumes 34 kWh/(m²·a). The total energy consumption in Tapanila ecological house is comparable to other low-energy houses. The total normalised energy consumption is 15% higher in ESPI (139 kWh/(m²·a)) and 23% lower in ESPI 2 (93 kWh/(m²·a)) than in Tapanila ecological house. The normalised primary energy consumption is the lowest in Tapanila ecological house, with ESPI 1, ESPI 2 and a typical Finnish house having 34%, 29% and 44% higher primary energy consumption respectively.

The calculated energy consumption using the WinEtana simulation program shows good agreement with the measured data when the ventilation rate is assumed to be 0.4 ach. The results presented in this report show that Tapanila ecological house would have consumed 34 kWh/(m^2·a) more energy (28%) if the building envelope was built according to the current building code. Similarly, the space heating would increase by 32 kWh/(m^2·a) (42%) without the highly insulated envelope. In other words, the space heating is expected to be about 40% higher (~108 kWh/(m^2·a)) if the envelope was insulated according to the building code. Since the well-insulated envelope decreases the heating energy consumption, but has no effect on the electricity consumption, the primary energy consumption is significantly lower with a well-insulated envelope.

Unlike a well-insulated envelope, the natural ventilation system increases the space heating because there is no possibility for heat recovery from the ventilation air, but saves electrical energy because there are no ventilation fans. The natural ventilation system increases the space heating by 15 kWh/(m^2·a) (22%), but decreases the electricity consumption by 5 kWh/(m^2·a) (14%) compared to a mechanical ventilation system with 50% effective heat recovery. Therefore, if Tapanila ecological house had a mechanical ventilation system with heat recovery (50% effective) that provided the same ventilation rate as the natural ventilation system, the space heating consumption is expected to be about 60 kWh/(m^2·a). Even though a house with a mechanical supply and exhaust ventilation system has a lower total energy consumption than a similar house with a natural ventilation system, the primary energy consumption is nearly the same for both systems.

Increasing the ventilation rate and decreasing the heat recovery effectiveness increases the energy consumption. The increase in space heating energy consumption for every 0.1 ach increase in ventilation rate is 2.7, 4.5 and 9.2 kWh/(m^2·a) when the heat recovery effectiveness is 70%, 50% and 0% respectively. At 0.5 ach, a 10% change in heat recovery effectiveness changes the space heating energy consumption by 3.3 kWh/(m^2·a).

7. Conclusions and Future Work

The purpose of this report was to investigate the moisture, thermal and ventilation performance of Tapanila ecological house, with particular focus on the performance of the passive systems for controlling the indoor environment (porous building envelope, natural ventilation system and wood-burning fireplace). The main objectives of this research were addressed in individual chapters and are:

- to investigate heat and mass transfer between structures and indoor air (Chapter 3);
- to determine the moisture performance of a building envelope that has no plastic vapour retarder (Chapter 4);
- to evaluate the performance of the natural ventilation system (Chapter 5); and
- to determine the energy consumption of Tapanila ecological house (Chapter 6).

Each of the above chapters contains a summary that discusses the conclusions of the chapter. In this concluding chapter, the final conclusions of this research are presented and areas of future work are recommended.

7.1 Conclusions

The results in this report show that mass transfer between indoor air and a porous building envelope can be applied to improve the indoor climate and consequently the indoor air quality. The transfer of tracer gases is significant only at low ventilation rates, but moisture transfer is significant for all tested ventilation rates (up to 1 ach). At a design ventilation rate of 0.5 ach, the diffusion of CO_2 and SF_6 increase the effective ventilation rate by about 10% and 5% respectively. On the other hand, the moisture transfer between indoor air and the building envelope can reduce the maximum indoor humidity in the summer by 20% RH and increase the minimum indoor humidity in the winter by 10% RH when the ventilation rate is near design (0.5 ach). Numerical results show that this moisture transfer may increase the temperature in the room by about 2°C because of phase change energy release during adsorption. Nevertheless, the net benefit is positive because research has shown that if the humidity decreases by 5% RH, the indoor temperature can increase by 1°C and the perceived air quality will be the same. Humidity and CO_2 concentration measurements during occupation supported the results obtained from the controlled experiments and numerical model. Temperature measurements during occupation showed temperatures between 20°C and 25°C and indicated that the hygroscopic envelope was unable to significantly damp the effect of

solar radiation. The hygroscopic wooden frame structure performed like a lightweight structure.

The moisture performance of the vapour permeable and porous envelope in Tapanila ecological house was monitored for over 2 years after construction and the measurements indicate that the envelope is moisture physically safe. Numerical simulations demonstrate that the vapour diffusion resistance of the internal surface can be significantly below that provided by polyethylene and still result in a safe structure, even in cold climates. Based on the measurements and simulation, it is recommended that the vapour diffusion resistance of the internal surface be at least 3 to 5 times greater than the diffusion resistance of the external surface. These results are applicable only if convection is eliminated, the initial moisture content of the building envelope is low and other failure mechanisms are not important.

The performance of the natural ventilation system in Tapanila ecological house was analysed by measuring the exhaust flow rates during different conditions, measuring the concentration of CO_2 during the summer and winter and developing an equation to predict the ventilation rate as a function of outdoor temperature and wind speed. The results indicate that the outdoor ventilation rate per person is usually above the requirement of 4 L/(s·person), but below the required air change rate for the house of 0.5 ach. The ventilation rate is expected to be below 0.5 ach whenever the outdoor temperature is above 0°C. At the average yearly temperature in Helsinki (~5°C) and a wind speed of 3 m/s, the ventilation rate of Tapanila ecological house is expected to be 30% below the design value of 0.5 ach when the windows are closed. Since the occupants often keep the windows open in the summer, which increases the ventilation rate, the measured indoor concentration of CO_2 in the summer and winter are quite similar, even though the average ventilation rate through the natural ventilation system is expected to be 0.25 ach in the summer and 0.45 ach in the winter.

Tapanila ecological house was designed as a low-energy house with a target space heating consumption of 50 kWh/(m^2·a). The target was not achieved, but the measured space heating energy consumption (76 kWh/(m^2·a)) was significantly less than in typical Finnish houses, which consume nearly 60% more energy for space heating (i.e., 120 kWh/(m^2·a)). The space heating consumption was higher than the target value because there was no ventilation heat recovery and the household electricity consumption was low in Tapanila ecological house. It is estimated that the space heating energy consumption would have been 40% higher than the measured value (i.e., ~108 kWh/(m^2·a)) if the envelope was insulated according to the building code of Finland. Furthermore, simulation results show that if a house is insulated according to the building code and the household electricity decreases by 10 kWh/(m^2·a), the space heating will increase by 4.4 kWh/(m^2·a). The natural ventilation system allows the

consumption of electricity in Tapanila ecological house (28 kWh/(m^2·a)) to be lower than in typical Finnish houses (34 kWh/(m^2·a) – Motiva, 1999) and other low-energy houses (e.g., ESPI 1 house – 53 kWh/(m^2·a) and ESPI 2 house – 31 kWh/(m^2·a) as reported by Laine and Saari, 1998). The total energy consumption in Tapanila ecological house is 121 kWh/(m^2·a), while the consumption is 15% higher in ESPI 1 (139 kWh/(m^2·a)) and 23% lower in ESPI 2 (93 kWh/(m^2·a)) and 50% higher in typical Finnish houses (181 kWh/(m^2·a)). The primary energy consumption of Tapanila ecological house is only 162 kWh/(m^2·a), while the values in ESPI 1, ESPI 2 and typical Finnish houses are 217, 209 and 233 kWh/(m^2·a) respectively (i.e., 30% to 40% higher). These results show the importance of including total and primary energy consumption when assessing the performance of ecological and low-energy houses.

7.2 Future Work

Research presented and reviewed in this report indicate that moisture transfer between indoor air and structures can significantly influence indoor humidity levels and that many materials are well suited for moisture storage applications. However, the work has not identified which materials (e.g., internal wallboard, insulation or furniture) are the most active in damping the indoor humidity. Future research should concentrate on identifying which building layers are active in moisture transfer with indoor air (Simonson et al., 2001).

Despite the fact that many materials can reduce the indoor humidity in buildings, ventilation rates are often based on the number of people in the space with no consideration that the enthalpy (i.e., temperature and humidity) of the indoor air has a pronounced effect on perceived indoor air quality, which can consequently affect comfort and productivity. Similarly, when architects design and estimate the energy consumption of buildings, thermal storage is often included, but moisture storage is almost never included, even though it can be equally important for energy consumption in warm climates. As a result, future work is needed to promote, demonstrate and research the importance of moisture transfer between building components, indoor air and HVAC systems. Such a holistic view of moisture transfer within buildings will be key to energy-efficient and cost-effective humidity control. Promotion of the importance of moisture transfer will increase designers' and occupants' awareness of moisture issues and result in better designed buildings.

Even though significant research has been done on the topic of whole building hygrothermal performance, there is need for more experimental measurements and numerical studies. Virtanen et al. (2000) have reviewed existing work and identified several areas of future work in this field. Laboratory experiments are needed to identify

the important physical parameters and field experiments are needed demonstrate the performance of different structures and systems in different climates. Current numerical models need to be improved to include the important physics and expanded to include moisture transfer throughout the whole building. These models also need to be validated with measurements, applied in a different climates and used to optimise moisture storage in buildings. There is also a need for user-friendly models or simple design methods for designers and architects. Questions such as how much moisture storage material (mass, area, …) is required per occupant and what type of paint can be applied need to be addressed. Finally, the results from this research must be interpreted with respect to IAQ, comfort, health and energy consumption. Since moisture storage is passive and utilises materials that are, in any case, needed for structural or aesthetic purposes, it can theoretically be applied in any building. The optimal solution and benefits will be different in each climate, but some benefits will be realised in each climate.

The results in this report show that it is possible to have a moisture safe structure in cold climates without a plastic vapour retarder. Nevertheless, additional field measurements would be useful to further demonstrate this, especially in buildings with more occupants or higher moisture loads such as in schools or day cares. Also, future research could focus on verifying whether a porous and vapour permeable envelope is less susceptible to moisture damage due to exfiltration because the peak indoor humidities are lower when applying such an envelope.

Future work arising from the thermal performance analysis would be in the comparison of energy quantity and quality (i.e., exergy analysis as in IEA Annex 37, 2000 and Leskinen and Simonson, 2000). This research could show the importance of using low valued energy such as low temperature district heat or ground-source heat pumps, rather than direct electrical heating. It would also demonstrate the importance of including total and primary energy consumption (rather than only space heating energy consumption) when assessing the performance of ecological and low-energy houses.

Acknowledgements

Financial support from the Finnish Ministry of the Environment has made this project possible. In addition, financial support from the Natural Sciences and Engineering Research Council of Canada (NSERC) in the form of a postdoctoral research fellowship is greatly appreciated. Thanks to all who have helped with the planning and implementation of this research project. Special thanks are extended to Erkki Kokko for planning the research activities, securing finding and helping interpret the results and to Olli and Jaana Hallamaa and their children for patiently co-operating with many intrusive measurements in their home. Also, direction and guidance from the steering group (Aila Korpivaara, Ilkka Romo, Esko Kukkonen, Anja Leinonen, Raimo Ahokas, Erkki Kokko, Markku Virtanen, Bruno Erat, Olli Hallamaa and Pauli Savolainen) and the assistance of Timo Collanus, Mikael Salonvaara, Tuomo Ojanen, Hannu Hyttinen and Reijo Saloranta are appreciated.

References

ANSI/ASHRAE 55a-1995, Addendum to Thermal environmental conditions for human occupancy, ASHRAE, Atlanta.

ANSI/ASHRAE Standard 55-1992, *Thermal environmental conditions for human occupancy*, ASHRAE, Atlanta.

ANSI/ASHRAE Standard 62-1989, *Ventilation for acceptable indoor air quality*, ASHRAE, Atlanta.

ASHRAE, 1997, *Fundamentals handbook*, ASHRAE, Atlanta.

ASTM, 1994, *Moisture control in buildings*, (edited by H.R. Trechsel), ASTM, Philadelphia.

Berglund, L., 1998, Comfort and humidity, *ASHRAE Journal*, **40**(8), 35–41.

Besant, R.W. and Simonson, C.J., 2000, Air-to-air energy recovery, *ASHRAE Journal*, **42**(5), 31–42.

Brager, G.S. and de Dear, R., 2000, A standard of natural ventilation, *ASHRAE Journal*, **42**(10), 21–27.

Braun, J.E., 1990, Reducing energy costs and peak electrical demand through optimal control of building thermal storage, *ASHRAE Trans.*, **96**(2), 876–888.

Charlesworth, P.S., 1988, *Air exchange rate and airtightness measurements techniques – An application guide*, Air Infiltration and Ventilation Centre, Coventry, Great Britain.

Clausen, G., Rode, C., Bornehag, C.-G. and Sundell, J., 1999, Dampness in buildings and health. Interdisciplinary research at the International Centre for Indoor Environment and Energy, *Proceedings of the 5th Symposium on Buildings Physics in the Nordic Countries*, Göteborg, Sweden.

Cooper-Arnold, C., et al., 1997, Moisture and lung disease: Population attributable risk calculations, *Proceedings of the ISIAQ 5th International Conference on Healthy Buildings*, Vol. 1, 213–218.

Cunningham, M.J., 1992, Effective penetration depth and effective resistance in moisture transfer, *Building and Environment*, **27**(3), 379–386.

Dales, R.E, et al., 1991, Adverse health effects among adults exposed to home humidity and mould, *Am. Rev of Respiratory Diseases*. **143**, 505–509.

Duforestel, T. and Dalicieux, P., 1994, A model of hygroscopic buffer to simulate the indoor air humidity behaviour in transient conditions, *Proceedings of European Conference on Energy Performance and Indoor Climate in Buildings*, Lyon, France, Vol. 3, 791–797.

Ekberg, L.E. and Kraenzmer, M., 1998, Determination of ventilation rates by CO_2 monitoring: assessment of inaccuracies, *proceedings of Roomvent 98*, **2**, 461–468.

El Diasty, R., Fazio, P. and Budaiwi, I., 1993, The dynamic modelling of air humidity. Behaviour in a multi-zone space, *Building and Environment*, **19**, 35–51.

Enai, M., Shimada, K., Fukushima, F., Aratani, N. and Bogaki, K., 2000, Evaluation of a ventilation system for a low-energy house, *Proceedings of Cold Climate HVAC2000*, Hokkaido University, 229–236.

Fang, L., Clausen, G. and Fanger, P.O., 1998a, Impact of temperature and humidity on the perception of indoor air quality, *Indoor Air*, **8**, 80–90.

Fang, L., Clausen, G. and Fanger, P.O., 1998b, Impact of temperature and humidity on the perception of indoor air quality during immediate and longer whole-body exposures, *Indoor Air*, **8**, 276–284.

Fanger, P.O., 1982, *Thermal comfort*, Robert E. Krieger Publishing Company, Florida.

Gray, B.F., Johnson, C.A., Schoenau, G.J. and Besant, R.W., 1988, Energy consumption and economic evaluation of thermal storage and recovery systems for a large commercial building, *ASHRAE Trans.*, **94**(1) 412–424.

Green, G.H, 1985, Indoor relative humidities in winter and the related absenteeism, *ASHRAE Trans.*, **91**(1B) 643–653.

Haapala, T., Kalema, T. and Kataja, S. (editors), 1995, Energy Analysis Tests for Commercial Buildings (Commercial Benchmarks), IEA Solar Heating & Cooling Task 12 B, Tampere University of Technology, Tampere, Finland. 66 pages.

Harderup, L.-E., 1998, *Humidity of the indoor air considering non stationary phenomena*, (Luftfuktighet inomhus med hänsyn till icke-stationära fenomen), Lund University, Department of Building Physics, Report number TVBH-3033, Lund, Sweden. (in Swedish)

Harriman, L.G., Plager, D. and Kosar, D., 1997, Dehumidification and cooling loads from ventilation air, *ASHRAE Journal*, **39**(11), 37–45.

Harriman, L.G., Witte, M.J., Czachorski, M. and Kosar, D.R., 1999, Evaluating active desiccant systems for ventilating commercial buildings, *ASHRAE Journal*, **41**(10), 28–37.

Hens, H. and Janssens, A., 1993, *Inquiry on HAMCAT CODES*, International Energy Agency, Heat, Air and Moisture Transfer in Insulated Envelope Parts, Report Annex 24, Task 1, Modeling.

Hukka, A. and Viitanen, H.A., 1999, A mathematical model of mould growth on wooden material, *Wood Science and Technology*, **33**, 475–485.

IEA Annex 37, 2000, Low exergy systems for heating and cooling of buildings, International Energy Agency, Energy Conservation in Buildings and Community Systems, 2000-2003, http://www.vtt.fi/rte/projects/annex37.

IEA, 1991, Annex 14: Condensation and Energy, Energy Conservation in Buildings and Community Systems Programme, Volume 1 Sourcebook, March.

ISO 7730-1994, *Moderate thermal environments – Determination of the PMV and PPD indices and specification of the conditions for thermal comfort*, International Organization for Standardization, Geneva, Switzerland.

ITS, 1999, Information Technology Specialists Inc., The Residential Energy Efficiency Database (designed and created by B. J. Mitchell, M. Ryder and M. Mitchell): Indoor Air Quality – moisture and humidity. http://www.its-canada.com/reed/iaq/chart1.htm.

Janssen, J.E., 1994, The V in ASHRAE: an historical perspective, *ASHRAE Journal*, **36**(8), 126–132.

Jones, R., 1993, Modelling water vapour conditions in buildings. *Building Serv. Eng. Res. Technol.*, **14**(3), 99–106.

Kalliomäki, P. and Kohonen, R., 1989, Calculation of the heat balance of a building. Method and evaluation of reliability of programs (Rakennusten lämpötaseen ratkaisu. Menetelmät ja ohjelmistojen luotettavuuden arvionti), Espoo, *VTT Research Notes*, **1077**, 129 p. + app. 13 p. ISBN 951-38-3628-2 (in Finnish, English abstract)

Kamel, A.A., Swami, M.V., Chandra, S. and Fairey, P.W., 1991, An experimental study of building-integrated off-peak cooling using thermal and moisture ("enthalpy") storage systems, *ASHRAE Trans.*, **97**(2), 240–244.

Karagiozis, A., Salonvaara, M. and Kumaran, K., 1994, LATENITE hygrothermal material property database, IEA Annex 24 Report T1-CA-94/04, Trondheim, Norway.

Kerestecioglu, A.A., Swami, M.V. and Kamel, A.A., 1990, Theoretical and computational investigation of simultaneous heat and moisture transfer in buildings: "effective penetration depth" theory, *ASHRAE Trans*., **96**(1), 447–454.

Kirchner, S., Badey, J.R., Knudsen, H., Meininghaus, R., Quenard, D., Saarela, K., Sallée, H. and Saarinen, A., 1999, Evaluation of VOCs sorption/diffusion capacities of indoor surface materials: proposal of new test procedures, *Proceedings of the 8th International Conference on Indoor Air Quality & Climate, Indoor Air 99*, Edinburgh, 430–435.

Kokko, E., Ojanen, T., Salonvaara, M., Hukka, A. and Viitanen, H., 1999, Moisture physical behaviour of wooden structures (Puurakenteiden kosteustekninen toiminta), Espoo, *VTT Research Notes*, **1991**. 160 p. ISBN 951-38-5499-X, http://www.inf.vtt.fi/pdf/tiedotteet/1999/T1991.pdf. (in Finnish)

Kosny, J., Christian, J.E., Desjarlais, A.O. et al., 1998, Performance check between whole building thermal performance criteria and exterior wall measured clear wall R-value, thermal bridging, thermal mass, and airtightness, *ASHRAE Trans.*, **104**(2), 1379–1389.

Kosonen, R. and Shemeikka, J., 1997, The use of simple simulation tool for energy analysis, *proceedings of Building Simulation '97, 5th International IBPSA conference*, Prague, September 8–10, 369–376.

Kumaran, K., 1996, *Material properties*, IEA Annex 24, Task 3, Final Report, K.U.-Leuven, Belgium.

Laine, J. and Saari, M., 1998, *ESPI low-energy houses* (*ESPI-matalaenergiapientalot*), Espoo, *VTT Research Notes*, **1924**. 75 p. + app. 44 p. ISBN 951-38-5332-2; 951-38-5333-0, http://www.inf.vtt.fi/pdf/tiedotteet/1998/T1924.pdf. (in Finnish)

Lamberg, P., Jokisalo, J. and Sirén, K., 2000, The effects on indoor comfort when using phase change materials with building concrete products, *Proceedings of Healthy Buildings 2000*, Vol. 2, (edited by O. Seppänen and J. Säteri), SIY Indoor Air Information OY. Pp. 751–756.

Leppänen, P., 1998, *The Rannanpelto house Suomusjarvi, Finland*, Technical Research Centre of Finland (internal report).

Leskinen, M. and Simonson, C.J., 2000, Annex 37: Low Exergy Systems for Heating and Cooling of Buildings, Technical report for the IEA ECBCS and ECES Executive Committees, November, 2000. 9 pages.

Motiva, 1999, Energy Information Centre for Energy Efficiency and Renewable Energy Sources, Database. http://www.motiva.fi/tietopankki/asuminen/asu-kulutustietoa.html (in Finnish)

National Building Code of Finland – C3, 1985, *Thermal insulation regulations*, The Ministry of the Environment, Helsinki, Finland.

National Building Code of Finland – D2, 1987, *Indoor climate and ventilation in buildings*, The Ministry of the Environment, Helsinki, Finland.

National Building Code of Finland – D5, 1985, *Calculation of heating power and energy demand of buildings*, The Ministry of the Environment, Helsinki, Finland.

Nimmo, B.G., Collier, R.K. Jr. and Rengarajan, R., 1993, DEAC: Desiccant enhancement of cooling-based dehumidification, *ASHRAE Trans.*, **99**(1), 842–848.

NRC, 1995, *National building code of Canada 1995*, National Research Council of Canada, Ottawa.

Ojanen, T. and Kohonen, R., 1995, Numerical simulation of heat, air and moisture transfer in building structures, *Proceedings of the workshop on mass-energy transfer and deterioration of building components. Models and characterization of transfer properties*, Organized by BRI, Japan & CSTB, France. Pp. 221–239.

Ojanen, T. and Kumaran, K., 1996, Effect of exfiltration on the hygrothermal behaviour of a residential wall assembly, *J. Thermal Insul. and Bldg. Envs.*, **19**(1), 215–227.

Ojanen, T., 1993, Criteria for the hygrothermal performance of wind barrier structures, *Proceedings of the 3rd Symposium of Building Physics in the Nordic Countries*, (edited by B. Saxhof), Thermal Insulation Laboratory, Technical University of Denmark, 643–652.

Ojanen, T., 1998, Improving the drying efficiency of timber frame walls by using exterior insulation, *Thermal Performance of the Exterior Envelopes of Buildings VII*, ASHRAE/DOE/ORNL/BETEC/NRCC/CIBSE Conference, Clearwater Beach, FL. Pp. 155–164.

Ojanen, T., Kokko, E., Salonvaara, M. and Viitanen, H., 1997, Moisture performance of plywood wall structures (Havuvanerirakenteiden kosteusteknisen toiminnan perusteet), Espoo, *VTT Research Notes*, **1870**. 90 p. + app. 2 p. ISBN 951-38-5169-9 (in Finnish)

Olesen, B.W., 1997, Possibilities and Limitations of Radiant Floor cooling, *ASHRAE Trans.*, **103**(1), 42–48

Olesen, B.W., 2000, Low temperature heating and high temperature cooling of buildings using hydronic surface systems, *Proceedings of Healthy Buildings 2000*, Vol. 2, (edited by O. Seppänen and J. Säteri), SIY Indoor Air Information OY. Pp. 635–640.

Orme, M., 1999, Applicable models for air infiltration and ventilation calculations, *Technical Note AIVC*, **51**, Coventry, Great Britain.

Padfield, T., 1998, *The role of absorbent building materials in moderating changes of relative humidity*, Ph.D. thesis in the Department of Structural Engineering and Materials, The Technical University of Denmark, Denmark, http://www.natmus.dk/cons/tp/phd/phd-indx.htm.

Plathner, P. and Woloszyn, M., 2000, Interzonal air and moisture transport in a test house. Experiment and modelling, accepted for publication in *Building and Environment*, June.

Plathner, P., Littler, J. and Cripps, A., 1998, Modelling water vapour conditions in dwellings, *Proceedings of the 3rd International Symposium on Humidity and Moisture*, London, Vol. 2, 64–72.

Plathner, P., Littler, J. and Stephen, R., 1999, Dynamic water vapour sorption: measurement and modelling, *Proceedings of IA99*, **1**, 720–725.

prEN 12571, 1999, *Building materials – Determination of hygroscopic sorption properties*, European Committee for Standardization.

prEN 832, 1998, *Thermal performance of buildings – Calculation of energy use for heating – Residential buildings*, European Committee for Standardization, February, final draft.

Reid, R.C., Prausnitz, J.J. and Sherwood, T.K., 1958, *The properties of gases and liquids*, Third edition, McGraw-Hill Book Company. P. 554.

Rengarajan, K., Shirey, D.B. III and Raustad, R.A., 1996, Cost-effective HVAC technologies to meet ASHRAE Standard 62-1989 in hot and humid climates, *ASHRAE Trans.*, **102**(1), 166–182.

Romo, I., 2001, Tapanila ecological house 97 – planning and building (Tapanilan ekotalo 97 – suunnittelu ja rakentaminen), to be published in *Suomen Ymparisto*, Helsinki (in Finnish).

Rudd, A.F., 1994, Development of moisture storage coatings for enthalpy storage wallboard, *ASHRAE Trans.*, **100**(1), 84–90.

Ruud, M.D., Mitchell, J.W. and Klein, S.A., 1990, Use of building thermal mass to offset cooling loads, *ASHRAE Trans.*, **96**(2), 820–829.

Salonvaara, M. and Karagiozis, A., 1994, Moisture transport in building envelopes using an approximate factorization solution method, *Proceedings of the Second Annual Conference of the CFD Society of Canada*, (edited by J. Gottlieb and C. Ethier), Toronto, Canada, June. Pp. 317–326.

Salonvaara, M. and Kokko, E., 1999, Heat and mass transfer in cellulose fibre insulation structures (Sellukuiturakenteiden lämmön- ja aineensiirtotekninen toiminta), Espoo, *VTT Research Notes*; **1946**. 51 p. ISBN 951-38-5650-X, 951-38-5651-8
http://www.inf.vtt.fi/pdf/tiedotteet/1999/T1946.pdf (in Finnish)

Salonvaara, M., Simonson, C.J. and Kokko, E., 2000, The effect of mass transfer between buildings and indoor air on indoor climate (Rakenteiden ja sisäilman välisen aineensiirron vaikutus sisäilmastoon), Sisäilmastoseminaari 2000 (Finnish Indoor Climate Seminar 2000), *Sisäilmayhdistys raportti* **14.** (Finnish Society of Indoor Air Quality and Climate Report 14). Pp. 353–358 (in Finnish).

Salonvaara, M.H. and Simonson, C.J., 2000, Mass transfer between indoor air and a porous building envelope: Part II – Validation and numerical studies, *Proceedings of Healthy Buildings 2000*, Vol. 3, (edited by O. Seppänen and J. Säteri), SIY Indoor Air Information OY. Pp. 123–128.

Salonvaara, M.H., 1998, Prediction of hygrothermal performance of building envelope parts coupled with indoor climate, *ASHRAE Trans.*, **104**(2), 908–918.

Seppänen, O. and Vuolle, M., 2000, Cost effectiveness of some remedial measures to control summer time temperatures in an office building, *Proceedings of Healthy Buildings 2000*, Vol. 1 (edited by O. Seppänen and J. Säteri), SIY Indoor Air Information OY. Pp. 665–670.

Seppänen, O., Fisk, W. and Mendell, M., 1999, Association of ventilation rates and CO_2-concentrations with health and other responses in commercial and institutional buildings, *Indoor Air*, **9**(4), 226–252.

Shemeikka, J., 1997, *WinEtana 1.0 LT building energy calculation program manual* (R*akennusten energialaskentaohjelman manuaali*), Technical Research Centre of Finland, Espoo. 29 pages. (in Finnish)

Sherman, M., 1987, Estimation of infiltration from leakage and climate indicators, *Energy and Buildings*, **10**(1), 81.

Sherman, M., 1999, Indoor air quality for residential buildings, *ASHRAE Journal*, **41**(5), 26–30.

Simmonds, P., Gaw, W., Holst, S. and Reuss, S., 2000, Using Radiant Cooled Floors to Condition Large Spaces and Maintain Comfort Conditions, *ASHRAE Trans.*, **106**(1), 695–701.

Simonson, C.J. and Ojanen, T., 2000, Moisture performance of buildings with no plastic vapour retarder in cold climates, *Proceedings of Healthy Buildings 2000*, Vol. 3, (edited by O. Seppänen and J. Säteri), SIY Indoor Air Information OY. Pp. 477–482.

Simonson, C.J. and Salonvaara, M.H., 2000, Mass transfer between indoor air and a porous building envelope: Part I – Field measurements, *Proceedings of Healthy Buildings 2000*, Vol. 3, (edited by O. Seppänen and J. Säteri), SIY Indoor Air Information OY. Pp. 117–122.

Simonson, C.J., Salonvaara, M. and Ojanen, T., 2001, Improving indoor climate and comfort with wooden structures, Espoo, *VTT Publications*, **431**. 192 p. + app. 91 p.

Simonson, C.J., 1994, Effect of solar radiation on the moisture content of insulated log houses, *Proceedings of the North Sun'94 Conference*, Glasgow, Scotland, (edited by K. MacGregor and C. Porteous). Pp. 361–366.

Statistics Finland, 1996, Energy statistics 1996. Official Statistics of Finland, *Statistics Finland*, Helsinki. 130 p.

Sundell, J., 1996, What we know, and what don't know about sick building syndrome, *ASHRAE Journal*, **38**(6), 51–57.

Teischinger, A., 1990, Relations between sorption activity of wood and air relative humidity, *Wood*, **45**(9), 249–254, (in Slovak).

Ten Wolde, A., 1992, Ventilation, humidity, and condensation in manufactured houses during winter, *ASHRAE Trans.*, **104**(1), 103–115.

Toftum, J. and Fanger, P.O., 1999, Air humidity requirements for human comfort, *ASHRAE Trans.*, **105**(2), 641–647.

Toftum, J., Jorgensen, A.S. and Fanger, P.O., 1998a, Upper limits for indoor air humidity to avoid uncomfortably humid skin, *Energy and Buildings*, **28**, 1–13.

Toftum, J., Jorgensen, A.S. and Fanger, P.O., 1998b, Upper limits of air humidity for preventing warm respiratory discomfort, *Energy and Buildings*, **28**, 15–23.

Tsuchiya, T. and Sakano, K., 1993, Computer simulation of multi room temperature and humidity variation under variable infiltration conditions, *Proceedings of the 3rd international building performance simulation conference*. Pp. 401–406.

Tuomaala, P. and Piira, K., 2000, A new application for predicting thermal comfort, *Proceedings of Healthy Buildings 2000*, Vol. 2, (edited by O. Seppänen and J. Säteri), SIY Indoor Air Information OY. Pp. 605–610.

Työtehoseura, 1997, Chopped firewood instructions for single-family houses (Pilkeopas omakotitaloille), *Työtehoseura publication*, **357**, KarPrint Ky – Huhmari, (in Finnish).

Uvslokk, 1996, The importance of wind barriers for insulated timber frame constructions, *J. Thermal Insul. and Bldg. Envs.*, **20**, July, 40–62.

Viitanen, H., 1996, *Factors affecting the development of mould and brown rot decay in wooden material and wooden structures. Effect of humidity, temperature and exposure time*, The Swedish University of Agricultural Sciences, Uppsala, Sweden.

Virtanen, M.J., Kunzel, H.M. and Simonson, C.J., 2000, WS10 The effect of wood based materials on indoor air quality and climate, *Healthy Buildings 2000 Workshop Summaries*, Espoo, Finland, (edited by O. Seppänen, M. Tuomainen and J. Säteri), SIY Indoor Air Information OY. Pp. 55–60. http://www.hb2000.org/workshop10.html.

Walker, I.S. and Wilson, D.J., 1993, Evaluating models for superposition of wind and stack effect in air infiltration, *Building and Environment*, **28**(2), 201–210.

Walker, I.S. and Wilson, D.J., 1998, Field validation of algebraic equations for stack and wind driven air infiltration calculation, *Int. J HVAC&R Research*, **4**(2), 119–139.

Walton, G.N., 1989, Airflow network model for element-based building airflow modelling, *ASHRAE Transactions*, **95**(2), 611–620.

Wargocki, P., Wyon, D.P., Baik, Y.K., Clausen, G. and Fanger, P.O., 1999, Perceived air quality, sick building syndrome (SBS) symptoms and productivity in an office with two different pollution loads, *Indoor Air*, **9**(3), 165–179.

Woloszyn, M., Rusaouën, G. and Hubert, J.-L., 2000, Predicting indoor climate using electric analogy estimations of condensation potential, *Proceedings of Healthy Buildings 2000*, Vol. 3, (edited by O. Seppänen and J. Säteri), SIY Indoor Air Information OY. Pp. 165–170.

Wyon, D.P., 1996, Indoor environmental effects on productivity, *Proceedings of IAQ 96 – Paths to better building environments*, (edited by K.Y. Teichman), ASHRAE, Atlanta. Pp. 5–15.

Wyon, D., 2000, Individual control at each workplace: the means and the potential benefits, *Creating the productive workplace*, (edited by D. Clements-Croome), E & FN Spon, London and New York.

Appendix A: Property Data

This appendix presents the property data that is used in the LATENITE simulation model when simulating the performance of the test room in section 3.3.2. The important property data are the sorption isotherm, water vapour permeability and thermal conductivity and these are given for the different materials (gypsum board, building paper, wood fibre insulation, porous wood fibre board, pine wood, brick and plaster) in Figure A1 to Figure A8.

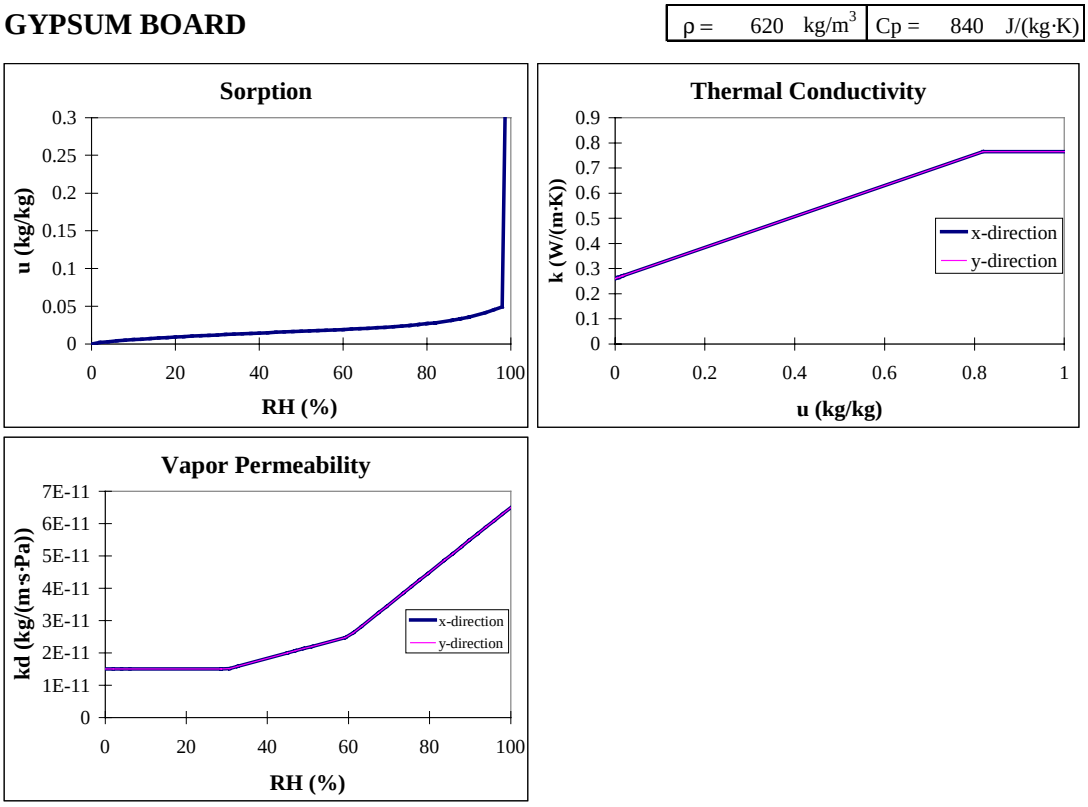

Figure A1. Material properties for gypsum board.

WOOD FIBRE INSULATION

ρ =	30	kg/m^3	Cp =	1400	J/(kg·K)

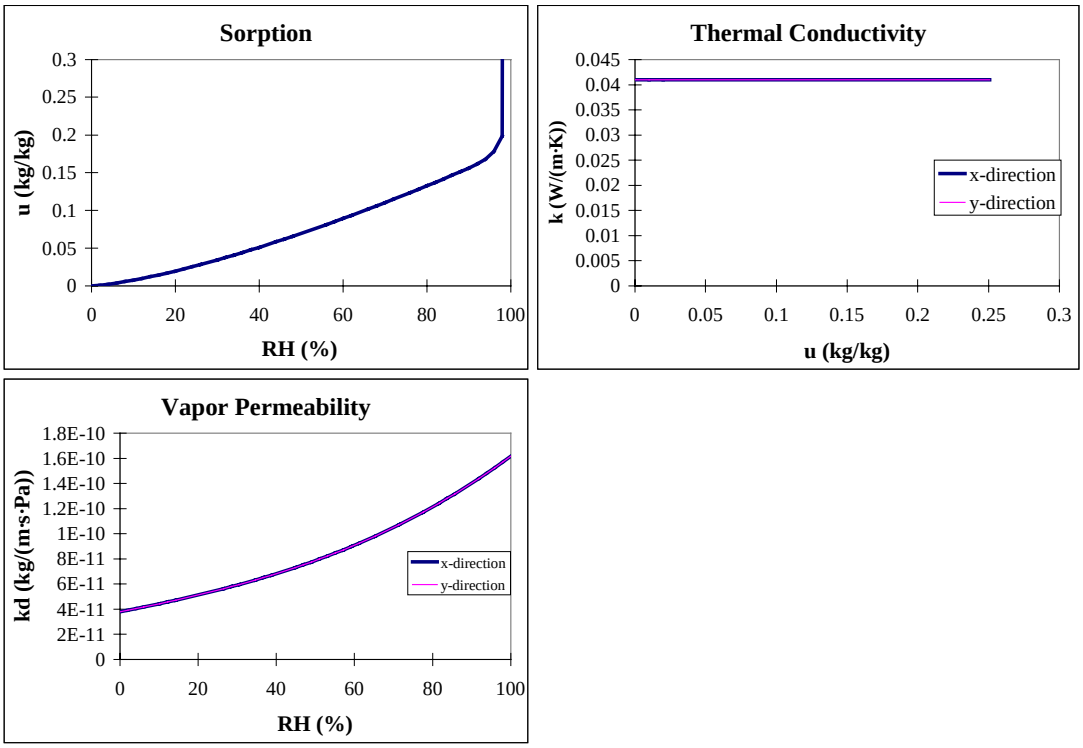

Figure A2. Material properties for wood fibre insulation.

POROUS WOOD FIBRE BOARD

ρ =	310	kg/m^3	Cp =	2100	J/(kg·K)

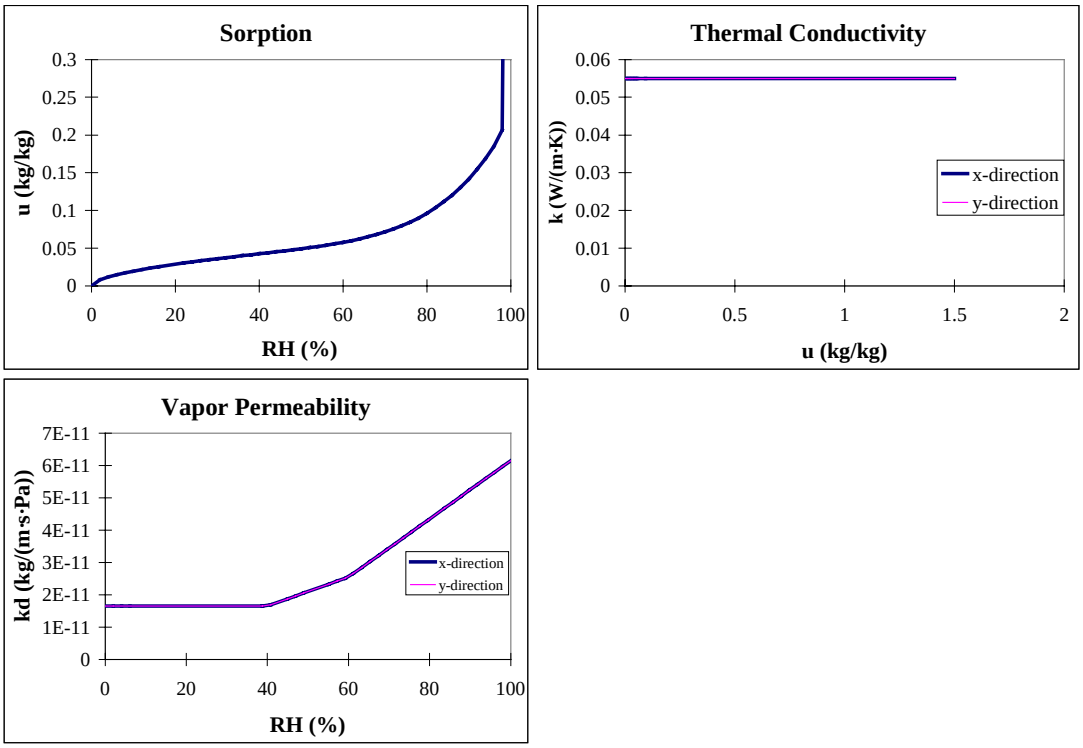

Figure A3. Material properties for porous wood fibre board.

PINE WOOD

ρ =	425	kg/m^3	Cp =	2390	J/(kg·K)

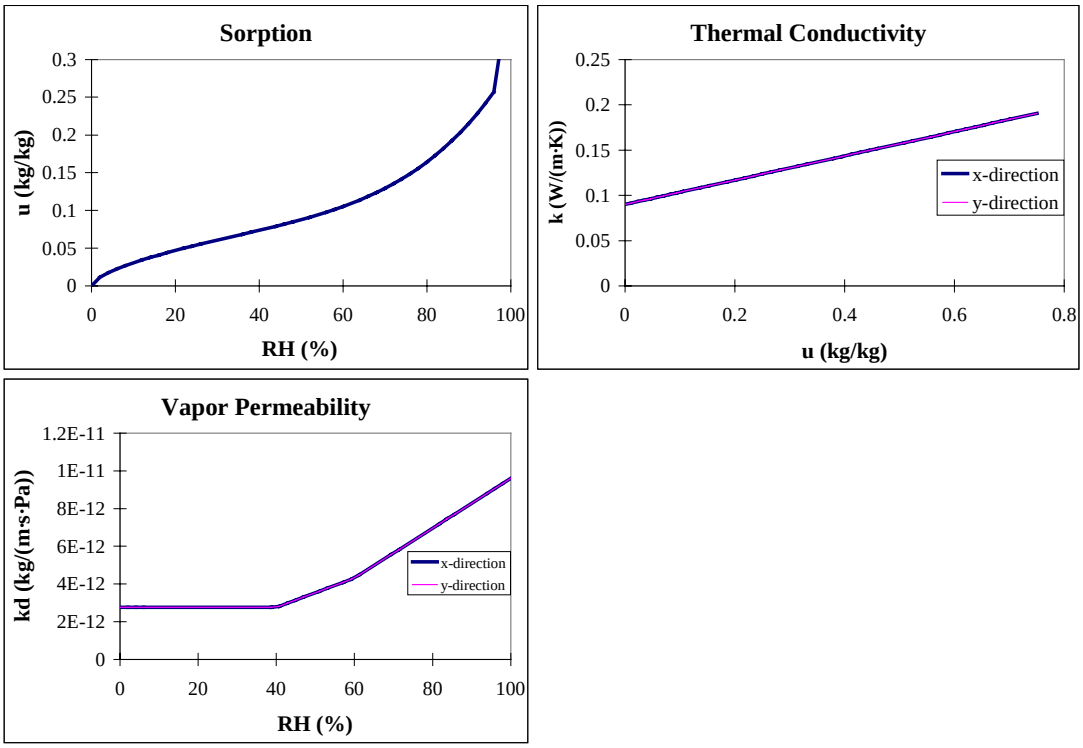

Figure A4. Material properties for pine wood.

BUILDING PAPER

ρ =	840	kg/m^3	Cp =	1256	J/(kg·K)

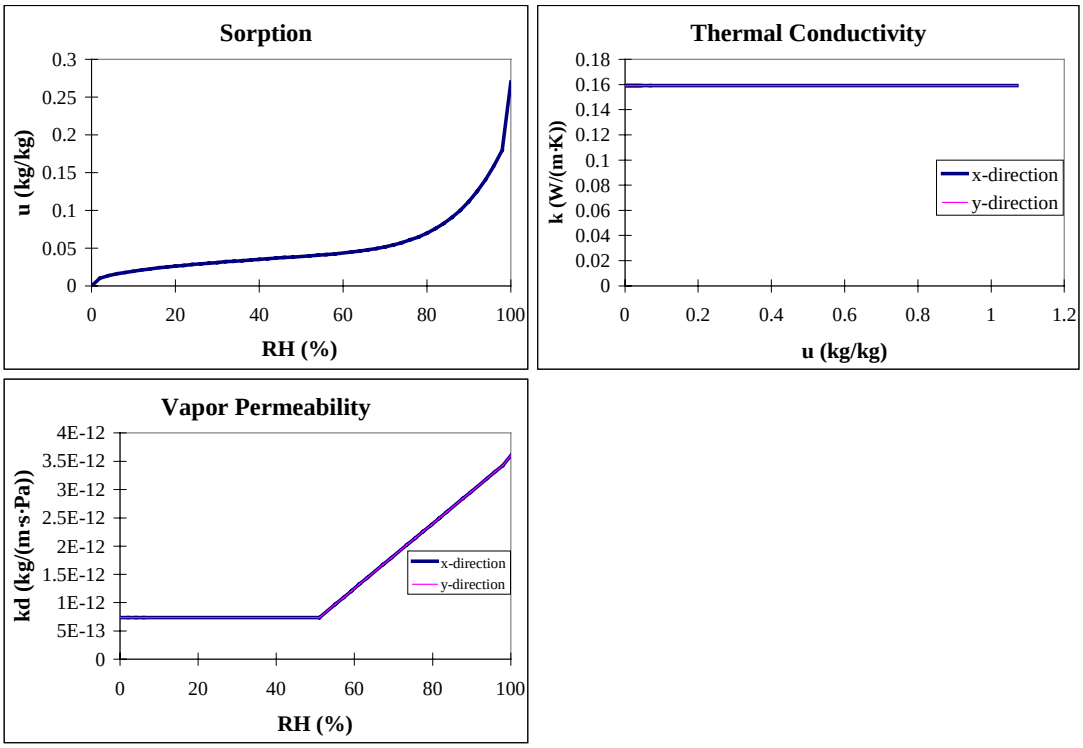

Figure A5. Material properties for building paper.

POLYETHYLENE SHEET 6-MIL

ρ =	840	kg/m^3	Cp =	1256	J/(kg·K)

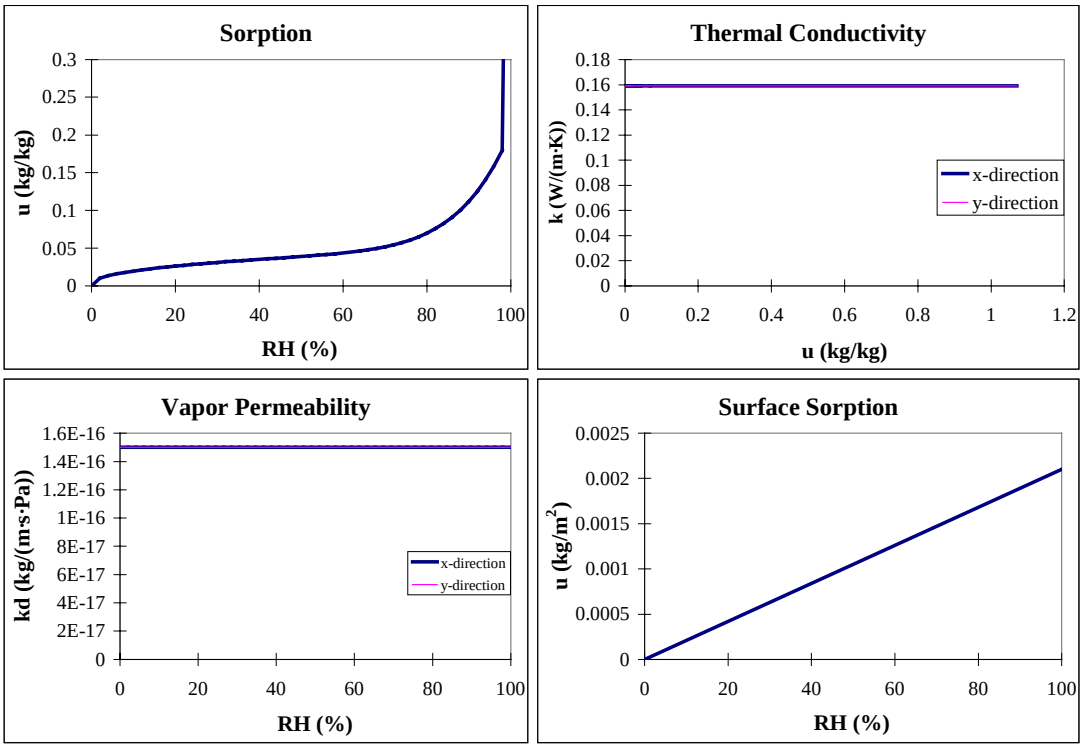

Figure A6. Material properties for 6-mil (0.15 mm) polyethylene.

RED BRICK

ρ =	1670	kg/m^3	Cp =	840	J/(kg·K)

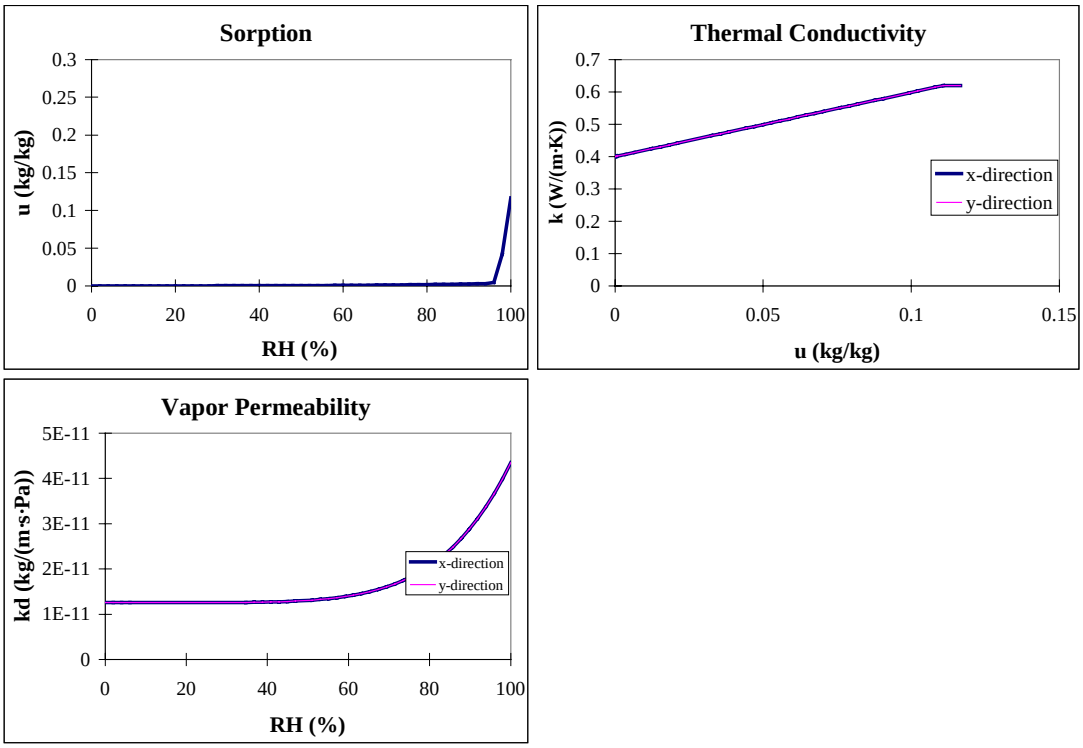

Figure A7. Material properties for brick.

Plaster/Inside (Thickness 3mm)

ρ = 1380 kg/m^3	Cp = 840 J/(kg·K)

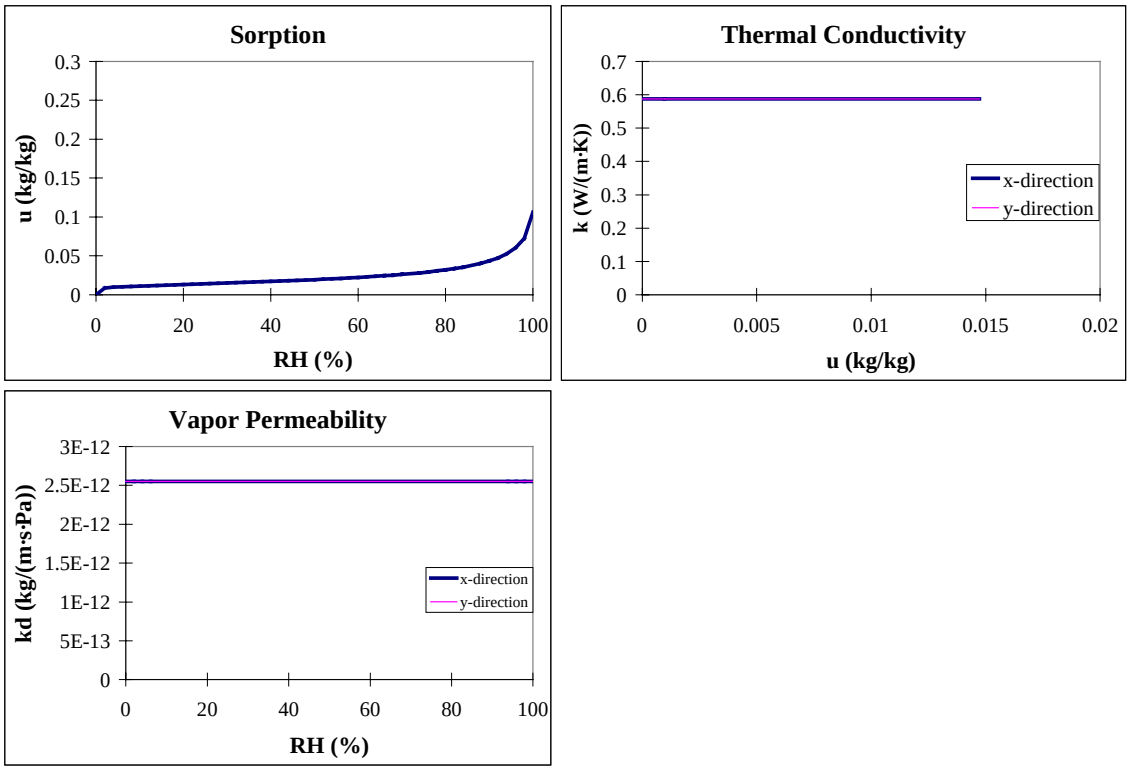

Figure A8. Material properties for plaster.

Published by

Vuorimiehentie 5, P.O.Box 2000, FIN–02044 VTT, Finland
Phone internat. +358 9 4561
Fax +358 9 456 4374

Series title, number and report code of publication

VTT Research Notes 2069
VTT–TIED–2069

Author(s)
Simonson, Carey J.

Title

Moisture, Thermal and Ventilation Performance of Tapanila Ecological House

Abstract

The research presented in this report demonstrates the moisture, thermal and ventilation performance of a recently built ecological house in the Tapanila district of Helsinki, Finland. The single-family house (gross floor area of 237 m^2 including the basement and porch) has a well-insulated (250 mm in the walls and 425 mm in the roof) wooden frame with no plastic vapour retarder. A natural ventilation system provides outdoor ventilation and district heating and a wood-burning fireplace provide space heating. The space heating energy consumption was measured to be 76 kWh/(m^2·a) of which 29% was provided by wood. For comparison, Finnish houses typically consume 120 kWh/(m^2·a) or nearly 60% more energy for space heating. If the building envelope of Tapanila ecological house had been insulated according to the building code, the space heating energy consumption is expected to be 40% higher. The total energy consumption (121 kWh/(m^2·a)) and electricity consumption (28 kWh/(m^2·a)) were quite low. As a result, the total primary energy consumption was only 162 kWh/(m^2·a), while the primary energy consumption in typical Finnish houses is over 40% higher. However, the outdoor ventilation rate provided by the natural ventilation system tended to be lacking (i.e., less than the required value of 0.5 ach) even though the measured CO_2 concentrations were generally below 1000 ppm when the bedroom doors were open. Extrapolating the measured ventilation data shows that the ventilation rate is expected to be about 0.45 ach (10% below the required value) in the winter and about 0.25 ach (50% of required value) in the summer when the windows are closed. When the windows are open in the summer, the outdoor ventilation rate will be higher.

The moisture performance of the building envelope was good and the risk of mould growth low. In addition, the moisture transfer between the envelope and indoor air was measured to significantly influence the indoor humidity. At a ventilation rate of 0.5 ach, the results show that a porous building envelope can decrease the maximum humidity in a bedroom during the night by up to 20% RH, which may double the number of occupants satisfied with thermal comfort and perceived air quality. Furthermore, the minimum indoor humidity in the winter can be increased by about 10% RH, which is also important in cold climates. These results show that it is possible to build a house with a porous and vapour permeable envelope that is moisture physically safe and improves the indoor climate.

Keywords
test houses, residential buildings, ecological houses, moisture, ventilation, indoor climate, heat transfer, small houses, energy consumption, indoor air quality, thermal comfort, space heating, airtightness

Activity unit
VTT Building Technology, Building Physics, Building Services and Fire Technology,
Lämpömiehenkuja 3, P.O.Box 1804, FIN–02044 VTT, Finland

ISBN
951–38–5797–2 (soft back edition)
951–38–5798–0 (URL: http://www.inf.vtt.fi/pdf/

Project number
R7SU00846

Date	Language	Pages	Price
December 2000	English, Finnish abstr.	141 p. + app. 5 p.	C

Name of project
Tapanila Ecological House

Commissioned by
Ministry of the Environment (YM)

Series title and ISSN
VTT Tiedotteita – Meddelanden – Research Notes
1235–0605 (soft back edition)
1455–0865 (URL: http://www.inf.vtt.fi/pdf/)

Sold by
VTT Information Service
P.O.Box 2000, FIN–02044 VTT, Finland
Phone internat. +358 9 456 4404
Fax +358 9 456 4374

Julkaisija

Vuorimiehentie 5, PL 2000, 02044 VTT
Puh. (09) 4561
Faksi (09) 456 4374

Julkaisun sarja, numero ja raporttikoodi

VTT Tiedotteita 2069
VTT–TIED–2069

Tekijä(t)
Simonson, Carey J.

Nimeke

Tapanilan ekotalon ilmanvaihto sekä lämpö- ja kosteustekninen toimivuus

Tiivistelmä

Julkaisussa esitettävässä tutkimuksessa selvitettiin Helsingin Tapanilassa hiljattain rakennetun ekotalon kosteus- ja lämpösuorituskykyä sekä ilmanvaihtoa. Kyseisessä omakotitalossa (kerrosala 237 m^2 mukaan lukien kellarikerros ja kuisti) on hyvin eristetty (250 mm eristettä seinissä ja 425 mm yläpohjassa) puurunko ilman muovista kosteussulkua. Talossa on painovoimainen ilmanvaihtojärjestelmä, se on liitetty kaukolämpöverkkoon ja siinä on takka. Mitattu tilojen lämmitysenergiankulutus oli 76 kWh/(m^2·a), josta energiasta 29 % tuli puusta. Vertailun vuoksi mainittakoon, että suomalaisten talojen tilojen lämmitysenergiankulutus on tavallisesti 120 kWh/(m^2·a) eli lähes 60 % enemmän. Mikäli Tapanilan ekotalon rakennusvaippa olisi eristetty rakentamismääräysten mukaisesti, arvioitu tilojen lämmitysenergiankulutus olisi noin 40 % suurempi. Kokonaisenergiankulutus (121 kWh/(m^2·a)) ja sähkönkulutus (28 kWh/(m^2·a)) olivat melko alhaisia. Tämän takia primäärinen kokonaisenergiankulutus oli vain 162 kWh/(m^2·a), kun primäärinen energiankulutus tavallisessa suomalaisessa talossa on yli 40 % suurempi. Painovoimaisen ilmanvaihtojärjestelmän ilmanvaihtuvuus oli kuitenkin jonkin verran puutteellinen (eli alhaisempi kuin ohjearvo, 0,5 1/h), vaikkakin mitatut CO_2-pitoisuudet olivat yleensä alle 1000 ppm, kun makuuhuoneen ovi oli auki. Mitattujen ilmanvaihtoarvojen ekstrapolointi osoittaa, että ilmanvaihtuvuuden voidaan olettaa olevan noin 0,45 1/h (10 % alle ohjearvon) talvella ja noin 0,25 1/h (50 % ohjearvosta) kesällä ikkunoiden ollessa suljettuna. Ikkunoiden ollessa auki kesällä ilmanvaihtuvuus on suurempi.

Rakennusvaipan kosteussuorituskyky oli hyvä ja homekasvun riski alhainen. Lisäksi mitatulla kosteuden siirtymisellä vaipan ja sisäilman välillä oli huomattava vaikutus sisäilman kosteuteen. Kun ilmanvaihtuvuus on 0,5 1/h, mitatut tulokset osoittavat, että huokoinen rakennusvaippa voi yön aikana alentaa makuuhuoneen maksimikosteutta jopa 20 % r.h., mikä voi kaksinkertaistaa niiden asukkaiden määrän, jotka ovat tyytyväisiä lämmityksen miellyttävyyteen ja havaittuun ilmanlaatuun. Lisäksi, sisäilman minimikosteutta voidaan talvella kasvattaa noin 10 % r.h., mikä on myös tärkeä näkökohta kylmässä ilmastossa. Nämä tulokset osoittavat, että on mahdollista rakentaa talo, jossa on huokoinen, vesihöyryn läpäisevä vaippa ja joka on kosteusteknisesti turvallinen ja sisäilmanlaatua parantava.

Avainsanat
test houses, residential buildings, ecological houses, moisture, ventilation, indoor climate, heat transfer, small houses, energy consumption, indoor air quality, thermal comfort, space heating, airtightness

Toimintayksikkö
VTT Rakennustekniikka, Rakennusfysiikka, talo- ja palotekniikka, Lämpömiehenkuja 3, PL 1804, 02044 VTT

ISBN
951–38–5797–2 (nid.)
951–38–5798–0 (URL: http://www.inf.vtt.fi/pdf/)

Projektinumero
R7SU00846

Julkaisuaika	Kieli	Sivuja	Hinta
Joulukuu 2000	Englanti, suom. tiiv.	141 s. + liitt. 5 s.	C

Projektin nimi
Tapanila Ecological House

Toimeksiantaja(t)
Ympäristöministeriö (YM)

Avainnimeke ja ISSN
VTT Tiedotteita – Meddelanden – Research Notes
1235–0605 (nid.)
1455–0865 (URL: http://www.inf.vtt.fi/pdf/)

Myynti:
VTT Tietopalvelu
PL 2000, 02044 VTT
Puh. (09) 456 4404
Faksi (09) 456 4374